CLEAN WATER

WATER POLLUTION CONTROL RESEARCH SERIES

● DAST-28

14010 _ _ _ 06/69

Oxygenation of Ferrous Iron

U.S. DEPARTMENT OF THE INTERIOR ● FEDERAL WATER POLLUTION CONTROL ADMINISTRATION

OXYGENATION OF FERROUS IRON: THE RATE-DETERMINING STEP IN THE FORMATION OF ACIDIC MINE DRAINAGE

Final Progress Report

Contract PH 36-66-107

Period: April 1, 1966 to December 31, 1968

Sponsoring Agency: Federal Water Pollution Control Administration
United States Department of the Interior

Grantee: Harvard University, Cambridge, Massachusetts 02138

Project Director: Dr. Werner Stumm
Gordon McKay Professor of Applied Chemistry

Progress Reported by: Philip C. Singer and Werner Stumm

ACKNOWLEDGMENTS

This work is based to a large part on research supported by contract PH 86-66-107 between the Federal Water Pollution Administration, Department of the Interior, and Harvard University. In the contract the scope of the work was stated as follows:

Specific Aims:

(1) To determine rates of air oxidation of ferrous iron in the presence of SO_4^{-2} within the pH range 2-5;

(2) To determine rate of ferric iron hydrolysis within the pH range 2-5;

(3) To investigate the colloid-chemical properties of hydrolyzed iron (III) Parameters: (Fe^{+2}), (Fe^{+3}), (H^{+}), (SO_4^{-2}), P_{02};

(4) To investigate specific aims 1, 2, and 3 above under the effect of the following catalysts: Mn^{+2}, Cu^{+2}, $Si(OH)_4$, $SiO_2(S)$, $Fe_2O_3(S)$.

The research effort resulting from this contract has become part of a thesis presented in April, 1969 by Philip Charles Singer to the Division of Engineering and Applied Physics of Harvard University in partial fulfillment of the requirements for the degree of Doctor of Philosophy. In order to accomplish a well rounded research objective, the scope of the work was expanded to include a comprehensive treatment on the chemistry of aqueous iron, and to consider models describing pyrite oxidation.

A good deal of experimental data was collected in order to transform the basic ideas and concepts of this research into the usable conclusions which have been reached. The laboratory assistance of Karlene Spencer, Gay Kunz, and Karl Schneider is an integral part of this report.

Appreciation is also due to Mr. Ronald Hill and Mr. Robert Scott and their staff of the Federal Water Pollution Control Administration who were instrumental in affording the authors opportunity and help to conduct field studies relating to acidic mine drainage. Grateful acknowledgment is also extended to Professors J. Carrell Morris and Ralph Mitchell for their fruitful suggestions and for patiently reading and criticizing this manuscript.

Finally, Philip C. Singer is indepted to the United States Public Health Service for a traineeship that provided financial support during a major part of his graduate studies at Harvard University.

TABLE OF CONTENTS

LIST OF FIGURES

Figure Page

LIST OF TABLES

SYNOPSIS

The rate of oxidation of iron(II) by oxygen conforms to a relationship which is first-order in the concentrations of ferrous iron and oxygen, and second-order in the concentration of hydroxide ion, at pH-values between 6.0 and 7.5. The reaction proceeds relatively rapidly at pH-values greater than 6.5; the half-time of the reaction is 4 minutes at pH 7.0, under a partial pressure of oxygen of 0.20 atmospheres at 25°C. Deferrization processes in water treatment employ the rapidity of the oxidation reaction in order to remove the influent iron(II) as insoluble iron(III) hydroxide. Part of the iron(II) may also be removed as ferrous carbonate ($FeCO_3$), the solubility product of which is 6.0×10^{-11}, as shown by this research.

The dependence of the oxidation rate on $[OH^-]^2$ has been observed, in this study, at pH-values as low as 4.5, where the half-time has increased to approximately 300 days. At lower pH-values, the dependence of the reaction rate on pH (or, more precisely, $[OH^-]$) becomes less marked until at pH-values below 3.5, the oxidation proceeds at a rate which is independent of pH. Here, a half-time of about 2000 days reflects the slowness of the oxidation reaction.

In the acidic drainage waters issuing from coal mines, half of the acidity arises from the oxidation of the sulfide ($S_2(-II)$) of iron pyrite (FeS_2) to sulfate, and half stems from the oxidation of iron(II) to iron(III) by oxygen and the subsequent hydrolysis of the resultant

iron(III). Observations of the rate of oxidation of ferrous to ferric iron in these acidic streams (at pH values close to 3) show it to proceed considerably more rapidly than the laboratory studies at pH 3 would predict.

Several chemical agents which are indigenous to mine drainage waters have been cited in the literature, in various circumstances, as displaying catalytic properties in the oxidation of ferrous iron. These include inorganic ligands, such as sulfate, which coordinate with iron(II) and iron(III), soluble metal ions, such as copper(II), manganese(II), and aluminum(III), suspended material with large surface areas and high adsorptive capacities, such as clay particles, and materials which accelerate the decomposition of peroxides in the presence of iron(II), such as charcoal. An investigation into the catalytic capabilities of these chemical agents in synthetic mine waters demonstrates that clay particles, or their idealized counterparts alumina (Al_2O_3) and silica (SiO_2), exert the greatest influence on the rate of oxidation of iron(II), but only at areal concentrations much larger than those encountered in most natural mine waters. (The reaction proceeds 10-30 times more rapidly in the presence of $8000 m^2/l$ of Al_2O_3 than the uncatalyzed reaction.)

Autotrophic microorganisms have frequently been implicated as the causative agents in the production of acidic mine drainage. These organisms are able to utilize the energy released by the oxidation of ferrous iron for their metabolic processes. A study of the oxidation of iron(II) in natural mine streams near Elkins, West Virginia shows

the reaction to proceed at a rate which is zero-order in iron(II). The field results suggest that the observed rapidity of the reaction in acidic mine waters is apparently the result of microbial catalysis.

Studies of the oxidation of iron pyrite in coal mine drainage have usually considered only oxygen as the specific oxidant, with the potentiality of iron(III) as an oxidant having often been overlooked. Experimental evidence obtained in laboratory systems shows that iron(III) is rapidly reduced by iron pyrite both in the presence and absence of oxygen. There is virtually no difference between the rate of reduction of iron(III) by pyrite, or the rate of change of soluble iron(II), under aerobic or anaerobic conditions indicating that the specific oxidant of iron pyrite is ferric iron.

The time required for the reduction of 50% of the initial iron(III) concentration in contact with 1 gram/liter of pyrite is approximately 250 minutes which is considerably less than the half-time for the oxidation of iron(II) even when accelerated by the chemical catalysts found in natural mine waters. Consequently, the rate-limiting step among the reactions involved in the oxidation of iron pyrite and the production of acidity in mine drainage waters is the oxygenation of ferrous iron.

Based upon the experimental evidence presented, the oxidation of iron pyrite in natural mine waters is shown to be compatible with a cyclical reaction model involving the slow oxygenation of iron(II) to iron(III) followed immediately by the rapid reduction of iron(III) by pyrite, generating in turn more iron(II) and acidity:

$$Fe(II) + O_2 \xrightarrow{\text{slow}} Fe(III)$$

$$Fe(III) + FeS_2 \xrightarrow{\text{fast}} Fe(II) + SO_4^{-2}$$

The oxidation of iron(II) by oxygen is the rate-determining reaction. Oxygen is involved only indirectly in the oxidation of pyrite; it serves to regenerate iron(III) which is itself the specific oxidant of pyrite. Precipitated iron(III) hydroxide within the mine serves as a reservoir for soluble iron(III).

The experimental results and the model are discussed from the standpoint of evaluating the various control measures which have been proposed in order to deal with the costly problem of acidic mine drainage. In view of this research, emphasis needs to be placed upon halting the catalytic oxygenation of iron(II).

CHAPTER 1

INTRODUCTION

Aqueous iron assumes an important role in natural waters in the limnological cycles of several key elements, in water supplies and water purification processes, and in the formation of several types of industrial wastes. Many natural phenomena can be explained and many practical applications can be derived as a result of investigations of the chemical behavior of aqueous iron. An account of the equilibrium and kinetic relationships which describe and control the distribution and activity of aqueous iron in natural waters is reported in this thesis, with special emphasis placed on the kinetics of oxygenation of iron(II), its application to deferrization processes, and its involvement in the formation of acidic coal mine drainage.

The equilibrium relationships which govern the solubilities of ferrous and ferric iron are considered in Chapter 2 in order to gain some insight as to the concentrations of the various species expected in natural waters. Included is a redetermination of the solubility product of ferrous carbonate and an estimate of the stability constant for a possible bicarbonato-complex of Fe(II).

The kinetics of the oxygenation of ferrous iron are discussed in Chapter 3, in both neutral and acidic systems. In the former case, attention is paid to the oxygenation reaction in bicarbonate solutions which are supersaturated with respect to ferrous carbonate. The rate of oxygenation

of ferrous iron over the entire pH-range of interest in natural waters is described, and the results are analyzed in view of modern kinetic theory and the various mechanisms proposed for the reaction.

The pH-dependence of the oxygenation reaction in neutral and slightly acidic systems, where hydrous ferric oxide was observed as the product of the reaction, gave reason to suspect that hydrolysis of ferric iron was directly involved in the oxygenation of ferrous iron. Chapter 4 contains an investigation of the kinetics of hydrolysis of Fe^{+3} in systems oversaturated with respect to ferric hydroxide. The coagulative properties of hydrolyzed ferric iron and phosphate removal by oxygenated ferrous iron are also discussed.

The chemical results obtained in Chapters 3 and 4 are applied in Chapter 5, a study of the chemistry of coal mine drainage. The kinetics of the various reactions involved in the oxidation of iron pyrite and the release of acidity are investigated and their relative rates compared in order to ascertain which of the sequential reactions is rate-limiting. The oxygenation of Fe(II) is considered, subject to the catalytic influences of several agents which are indigenous to natural mine waters, including microorganisms. A model is proposed, incorporating the salient features of the kinetic study, in order to describe the oxidation of iron pyrite in mine drainage waters. The pertinent consequences of the model are examined.

The significant results of the research are summarized in Chapter 6, along with some of the practical applications of these results.

CHAPTER 2

EQUILIBRIUM RELATIONSHIPS OF AQUEOUS IRON

2-1 Introduction

The various species of iron which exist in natural waters are governed by solubility, hydrolysis, complex-formation, and oxidation-reduction relationships. These relationships predict whether or not a given reaction will take place as written, and to what extent, i.e., what concentration of a given species is expected. In contrast, kinetic relationships, which will be considered in Chapters 3 and 4, are needed to predict the rate at which equilibrium is attained.

In order to understand the behavior of iron in natural waters, a theoretical treatment is required in which various equilibria are assumed to be applicable in controlling the different species of iron. Such a theoretical treatment is not intended to provide an all-inclusive chemical description due to the complexity of the natural system, but rather is intended as an oversimplified version to gain some insight as to which equilibria are relevant. The thermodynamic data employed have been obtained in well-defined systems where the individual variables were isolated. The combined investigations of a number of such isolated systems are then compared to the natural system. Deviations between the behavior predicted by thermodynamic considerations and that which actually occurs in the real system can be attributed to the existence of non-equilibrium

conditions where the kinetics of the reactions are limiting, or to an improper description of the system due either to a lack of dependable thermodynamic data or to an oversimplification in predicting which are the controlling equilibrium relationships. The occurrence of such deviations between the "predicted" and the "actual" requires an explanation. A portion of the material presented in this chapter is intended for just this purpose.

The material covered is limited to a discussion of the solubility of iron compounds in natural waters. In the case of ferrous iron, its solubility is governed by the solubility of its respective carbonate, hydroxide, or sulfide, depending upon the composition of the water. The solubility of ferric iron is correspondingly limited by its rather insoluble oxides and hydroxides or, in the presence of high concentrations of phosphate, by ferric phosphate. The equilibrium concentration of Fe(III) may be increased as a result of complex-formation with chloride, sulfate, phosphate, silicate, and organic matter.

Experimental studies of the solubility of iron in natural waters are also presented in this chapter. These studies include a determination of the ill-defined solubility product of ferrous carbonate, $FeCO_3$; an experimental analysis of the relevance of the bicarbonato-complex of Fe(II), $FeHCO_3^+$, in carbonate-bearing waters; and a determination of the stability constant of the sulfato-complex of Fe(III), $FeSO_4^+$, which was essential for consideration of the catalytic effect of sulfate on the hydrolysis of ferric iron, which is discussed in Chapter 4.

Since the relevant features of the chemistry of aqueous iron pertaining to natural waters have previously been discussed by Stumm and Lee (1), only an overall review is presented here, including an up-dating

of their discussion with more recent data. The major portion of the chapter is devoted to the experimental work undertaken to clarify our understanding of the behavior of iron in natural waters.

2-2 Iron(II) Solubility

2-2.1 Solubility in Natural Waters

Under reducing conditions in natural waters, as in the bottoms of lakes under conditions of stagnation, and in most groundwaters, ferrous iron, in the + II oxidation state, is the stable form of iron. In waters free of dissolved carbon dioxide and sulfide, the solubility of Fe(II) is controlled by solid ferrous hydroxide, $Fe(OH)_2$, as shown in Figure 2-1. The equilibria utilized in plotting this solubility diagram and all subsequent diagrams for Fe(II) are given in Table 2-1. (The reader is referred to Sillen's discussion (2) on the graphic representation of equilibrium data for the general principles in the construction of such solubility diagrams.)

In natural groundwaters, alkalinities often exceed 5×10^{-3} eq./l. (7). Figure 2-2 indicates that, for a water containing 5×10^{-3} moles/l. of total carbonic species C_T, the solubility of Fe(II) is markedly influenced by formation of ferrous carbonate, $FeCO_3$. It is immediately evident that at pH-values below 10.5, ferrous carbonate controls the concentration of Fe(II) in solution.

In hypolimnetic waters where the concentration of sulfide species may be appreciable as a result of anaerobic reduction of sulfate, ferrous sulfide, FeS, as shown in Figure 2-3 for a total sulfide content of 10^{-5} moles/l. (8), limits the solubility of Fe(II) over the entire range of pH encountered in natural systems. It should be noted that even in the

Table 2-1. Equilibria Describing Fe(II) Solubility

Equation Number	Reaction	Equilibrium Constant at 25°C	Reference
2-1	$Fe(OH)_{2(s)} = Fe^{+2} + 2OH^-$	8×10^{-16}	3
2-2	$Fe(OH)_{2(s)} = FeOH^+ + OH^-$	4×10^{-10}	3
2-3	$Fe(OH)_{2(s)} + OH^- = Fe(OH)_3^-$	8.3×10^{-6}	4
2-4	$FeCO_{3(s)} = Fe^{+2} + CO_3^{-2}$	2.1×10^{-11}	5
2-5	$H_2CO_3 = H^+ + HCO_3^-$	4.2×10^{-7}	5
2-6	$HCO_3^- = H^+ + CO_3^{-2}$	4.8×10^{-11}	5
2-7	$FeS_{(s)} = Fe^{+2} + S^{-2}$	6×10^{-18}	6
2-8	$H_2S_{(aq)} = H^+ + HS^-$	1.0×10^{-7}	6
2-9	$HS^- = H^+ + S^{-2}$	1.3×10^{-13}	6

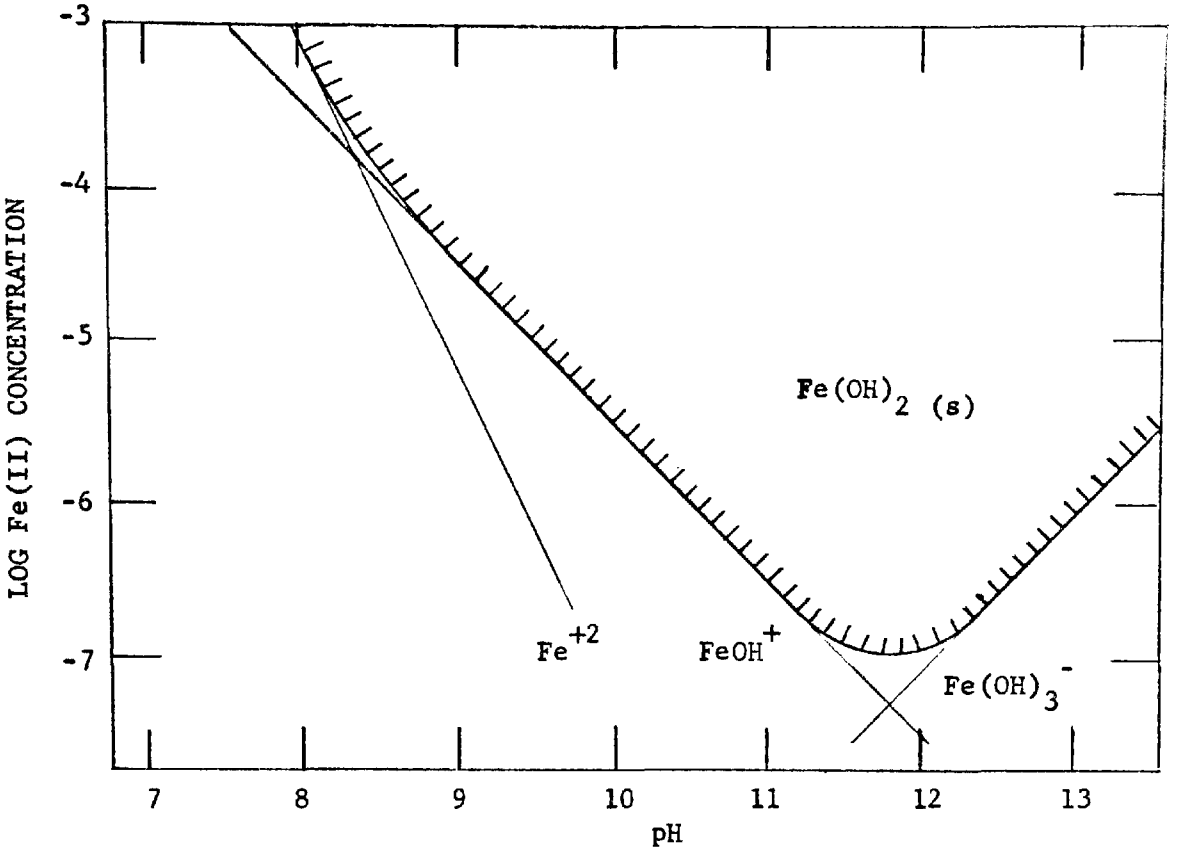

FIGURE 2-1. Solubility of ferrous iron in waters free of appreciable alkalinity and sulfide.

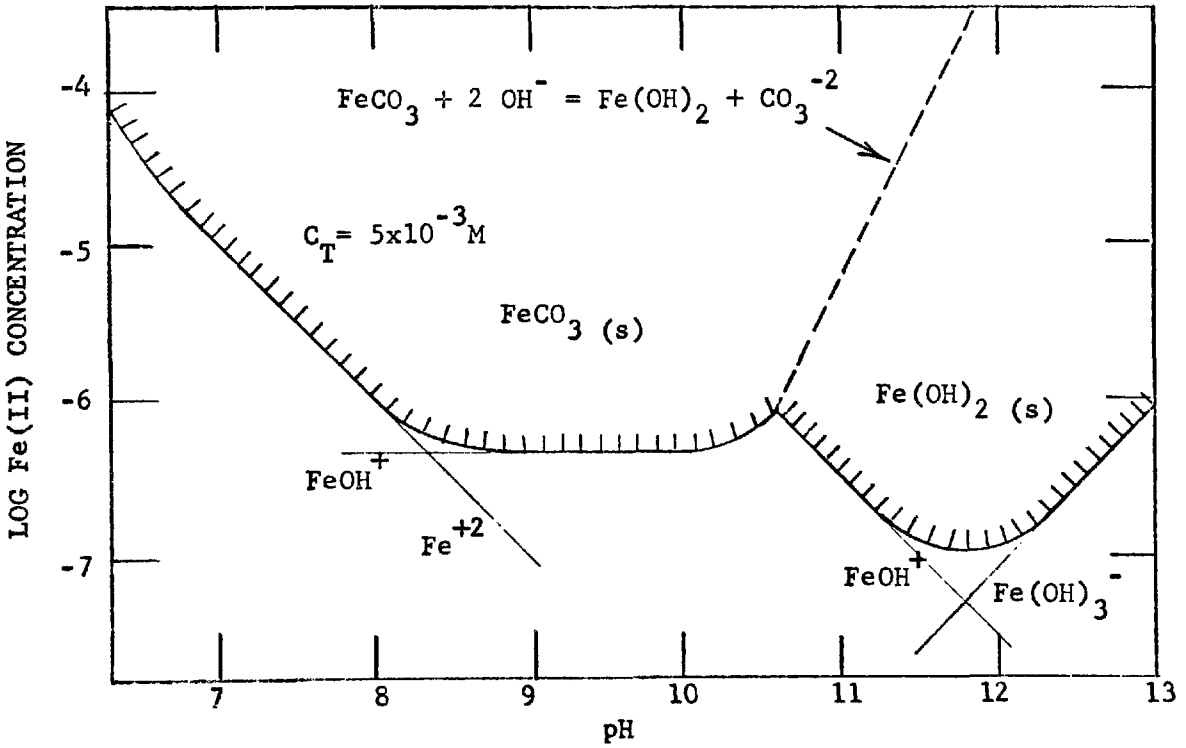

FIGURE 2-2. Solubility of ferrous iron in waters containing 5×10^{-3} M of total carbonate species.

presence of a concentration of 10^{-2}M total carbonic species, ferrous sulfide continues to be the stable solid phase.

If equations 2-4 and 2-7 of Table 2-1 are combined to give

$$FeS_{(s)} + CO_3^{-2} = FeCO_{3(s)} + S^{-2} \qquad (2\text{-}10)$$

where the equilibrium constant for the reaction, as written, is

$$K_{eq} = \frac{K_7}{K_4} = 10^{-6.54} = 3 \times 10^{-7} = \frac{[S^{-2}]}{[CO_3^{-2}]} \qquad (2\text{-}10a)$$

it is seen that $FeCO_3$ becomes the stable solid phase (the reaction proceeds as written) only when the ratio of sulfide to carbonate is smaller than 3×10^{-7}. In other words, the solubility product of ferrous carbonate becomes operative only when the ratio of alkalinity to total sulfide exceeds 2×10^3 at pH 6, or 8×10^3 at pH 7. Hence, at the extremely low concentrations of sulfide found in most groundwaters, ferrous carbonate governs the solubility of ferrous iron, as in Figure 2-2.

2-2.2 Recent Observations of Ferrous Iron Solubility in Carbonate-Bearing Waters

The equilibrium constant for the reaction

$$FeCO_{3(s)} = Fe^{+2} + CO_3^{-2} \qquad (2\text{-}4)$$

given in Table 2-1, was computed from the free energy data tabulated by Latimer (5), and is based upon the experimental work of Smith (9) in 1918 and the calculations of Kelley and Anderson (10). Smith found the solubility product of ferrous carbonate, $K_{so} = [Fe^{+2}]\,[CO_3^{-2}]$, to be 3.45×10^{-11} at 30°C without correcting for activity. Kelley and Anderson modified that value for 25°C and an ionic strength of zero (although their method of correction is not immediately evident) and arrived at a free energy of

solution for reaction 2-4 of 14.54 Kcal./mole, corresponding to a thermodynamic equilibrium constant of $K_{so} = 2.1 \times 10^{-11}$.

More recent reports, however, indicate some discrepancy between field measurements of the solubility of Fe(II) and the solubility predicted using the accepted thermodynamic constant from the literature. Hem (11), in examining twenty groundwaters for equilibrium with calcite (a crystalline form of calcium carbonate) and siderite (the crystalline form of ferrous carbonate), presents a "dual saturation-index" diagram for the two minerals. In general, one would expect a groundwater in equilibrium with calcite to be in equilibrium with siderite, too, if both minerals were present in the same geologic formation. Furthermore, one would expect similar conditions of under- and oversaturation with respect to the two solid phases. Yet, the best straight line through Hem's data does not pass through the origin, although it has roughly a slope of unity indicative of equivalent conditions of saturation (see Figure 2-4). An error in the value of K_{so} would result in such an observation. (The term "measured pH minus computed pH" is equal to the logarithm of the degree of oversaturation.)

Ghosh, O'Connor, and Engelbrecht (7) sampled the influent groundwater at eight water treatment plants in Illinois and reported values of oversaturation with respect to ferrous carbonate of from 20 to 40 times. When these observations were corrected for temperature and activity (12), the oversaturation compared to the accepted value given by Latimer was still on the order of five to ten times.

Larson (13) has suggested that the existence of a bicarbonato-complex of ferrous iron, $FeHCO_3^+$, may serve as an explanation for this reported condition of apparent oversaturation, especially in view of Hem's

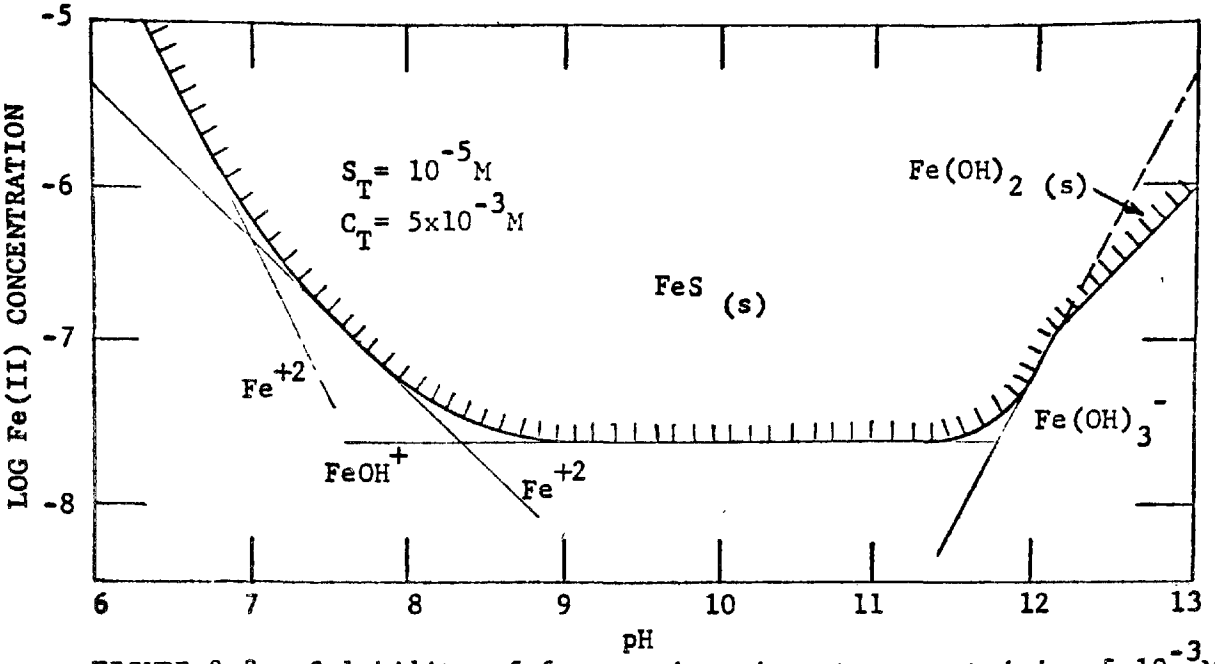

FIGURE 2-3. Solubility of ferrous iron in waters containing 5×10^{-3} M of total carbonate species and 10^{-5} M of total sulfide species.

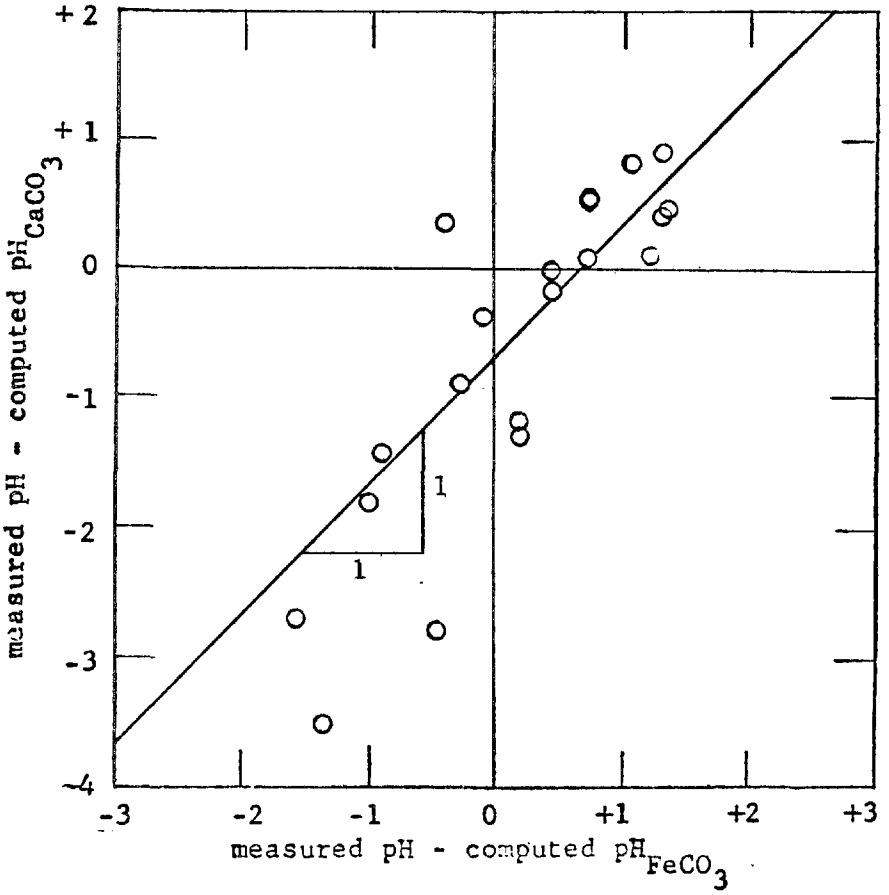

FIGURE 2-4. Dual saturation-index diagram for calcite and siderite in natural waters (after Hem (11)). Measured pH - computed pH is equivalent to the log of the degree of oversaturation.

findings (14) that approximately 35% of the total manganous manganese, Mn(II), is present as the bicarbonato-complex, $MnHCO_3^+$, in a groundwater containing 5×10^{-3} eq./l. of alkalinity.

2-2.3 Experimental Determination of the Solubility Product of Ferrous Carbonate (Siderite)

Since the solubility of ferrous iron in groundwaters has been shown to be limited by the solubility of ferrous carbonate, and since the 50-year-old solubility product cannot account for the high concentrations of Fe(II) found in natural groundwaters, this study was undertaken in order to redetermine the solubility product of ferrous carbonate, and to determine what effect, if any, complexation of Fe(II) by bicarbonate has on the overall solubility of Fe(II).

Experimental Procedures

Ferrous carbonate was prepared directly in the laboratory by precipitation from a solution of excess ferrous perchlorate and sodium bicarbonate. Ferrous perchlorate was added to a pre-determined concentration of perchloric acid in a BOD bottle and the system was flushed with nitrogen to remove all traces of oxygen. (Since conditions for the precipitation of ferrous carbonate were found to be optimal above pH 6.5, the exclusion of oxygen was a prime requirement, Fe(II) being rapidly oxygenated at pH-values greater than 6.0 (15).) Sodium bicarbonate was added and the vessel was immediately stoppered to prevent contamination by oxygen. A series of such bottles were stored under water at constant temperature again to prevent seepage of oxygen into the system, the exclusion of oxygen proving to be the major experimental difficulty.

The preparations of ferrous carbonate were made in a constant ionic medium to insure the constancy of the activity coefficients for each series.

After a period of storage of one to five months, the samples were removed from the water bath and aliquots were taken from each for the determination of alkalinity, soluble ferrous iron, and concentration pH. This latter term, p^cH, is a measure of the concentration of H^+ at a given ionic strength. A combination pH electrode (Beckman Cat. No. 39142) was standardized in a reference solution containing a known concentration of HCl and the same ionic strength as the sample being analyzed. The p^cH of the sample was then measured (Corning Model 12 pH meter) by immediately inserting the pH electrode into the vessel when it was opened. It was feared that rapid evolution of CO_2 upon exposure of the sample to the atmosphere would raise its p^cH, but the measured p^cH was found to remain relatively constant.

Alkalinity was determined by acidimetric titration with 0.1M HCl. Since oxidation of Fe(II) and hydrolysis of the resultant Fe(III) produces acidity which neutralizes a portion of the alkalinity, an aliquot was rapidly titrated to pH 5 with a pre-determined amount of HCl and then slowly titrated to the endpoint at pH 4.3. (Oxidation of Fe(II) below pH 5 is relatively slow, as will be seen in Chapter 3.)

The determination of soluble ferrous iron was carried out by rapidly filtering an aliquot of the sample into a test tube containing dilute acid in order to quench any further reaction. The filtration was performed under an atmosphere of carbon dioxide to prevent oxidation of Fe(II) and dissolution of $FeCO_3$. 100, 220, and 450 mu. filter papers

(Millipore Filter Company) were employed, similar results being obtained for each. Filterable Fe(II) was measured using the colorimetric reagent, bathophenanthroline (4,7-diphenyl-1,10-phenanthroline) (10).

To insure that the precipitate formed was crystalline ferrous carbonate (siderite) and not merely an amorphous intermediate, the sediment was analyzed by X-ray diffraction. The precipitate was collected following filtration and air-dried overnight before determining its crystal structure using a Norelco X-ray diffractometer.

For the analytical determination of the stability constant of the bicarbonato-complex of Fe(II), a specific ion electrode (Orion Research) was employed. The electrode contains a liquid ion-exchange resin having a specificity for various divalent cations, including Fe^{+2}, and is used in conjunction with any standard reference electrode. The selectivity coefficient for Fe^{+2} is high and in the absence of other divalent cations the electrode measures free Fe^{+2} directly.

Various dilutions of a stock solution of ferrous perchlorate were added to oxygen-free samples under one atmosphere of carbon dioxide and containing pre-set concentrations of sodium bicarbonate. Again, exclusion of oxygen was mandatory to prevent oxidation of Fe(II). For a given alkalinity, the greatest concentration of Fe(II) was added such that the solubility product of ferrous carbonate was not exceeded. A constant ionic medium was again maintained to reduce variations in activity coefficients among the different systems.

Following the addition of Fe(II) to the solutions of bicarbonate, the samples were allowed one hour to reach equilibrium. The divalent cation electrode was calibrated using standardized solutions of ferrous

perchlorate, free of CO_2 and at the same ionic strength as the samples. (The solutions of $Fe(ClO_4)_2$ had been standardized with permanganate, which itself had been previously standardized against oven-dried sodium oxalate.) The potentials of the test solutions containing bicarbonate were measured at the same time as the standard solutions, alternating between the unknowns and the standards since the electrode potential is prone to drift with time. The potentials were measured with a Corning Model 12 potentiometer. The p^cH of the samples were recorded and aliquots were analyzed for alkalinity and total ferrous iron, Fe(II), by acidimetric titration and by potentiometric titration with standard permanganate, respectively.

Experimental Results and Discussion

The solubility product of ferrous carbonate was computed utilizing the following chemical equilibria:

$$FeCO_{3(s)} = Fe^{+2} + CO_3^{-2}; \qquad K^c_{so} = [Fe^{+2}][CO_3^{-2}] \tag{2-4}$$

where K^c_{so} is the concentration solubility product of crystalline ferrous carbonate at a known ionic strength and temperature, and

$$HCO_3^- = H^+ + CO_3^{-2}; \qquad K^c_2 = [H^+][CO_3^{-2}]/[HCO_3^-] \tag{2-6a}$$

where K^c_2 is the second acidity constant of carbonic acid at a given ionic strength. It follows that the equilibrium constant for the reaction

$$FeCO_{3(s)} + H^+ = Fe^{+2} + HCO_3^- \tag{2-11}$$

is given by

$$K^c_{eq} = \frac{K^c_{so}}{K^c_2} = \frac{[Fe^{+2}][HCO_3^-]}{[H^+]} \tag{2-11a}$$

Rearranging and taking logarithms, one obtains

$$p^cH + pK^c_{so} - pK^c_2 = -\log([Fe^{+2}][HCO_3^-]) \qquad (2\text{-}12)$$

where p- refers to the negative logarithm of that term. Hence, K^c_{so} can be readily calculated from a knowledge of the experimentally-determined parameters p^cH, soluble Fe(II) (assumed to be equal to $[Fe^{+2}]$), and alkalinity, and the known second acidity constant of carbonic acid under the given experimental conditions.

Equation 2-12 suggests that a plot of p^cH versus $-\log([Fe^{+2}][HCO_3^-])$ will yield a straight line of unit slope having an intercept at $p^cH = 0$ which is equal to $pK^c_{so} - pK^c_2$. Figure 2-5 is such a plot for a series of preparations of ferrous carbonate at 22.5°C and an ionic strength of 0.1. The best straight line of unit slope was fitted to the points resulting in an intercept of $-0.57 \pm .17$, as shown. The majority of the points fall within the p^cH-range 6.5 to 7.5 where precipitation was found to be optimal. The four points at the lower p^cH contain the greatest experimental uncertainty since, due to their low alkalinities, they required only a small amount of titrant before the endpoint was reached. The fact that these four points still approximate the linear plot is gratifying.

The reason for the apparent scatter of the experimental points in the region of p^cH 6.5 to 7.5 is due strictly to the experimental uncertainty in measuring free Fe^{+2}. It has been assumed that filterable Fe(II) is equal to the concentration of free Fe^{+2} in equilibrium with the solid phase. The fact that the concentration of filterable Fe(II) for a given sample was constant for three filters of different pore size (100, 220, and 450 mu.) lends credence to such an assumption in that all solid Fe(II) is retained by the filter, i.e., filterable Fe(II) equals soluble Fe(II).

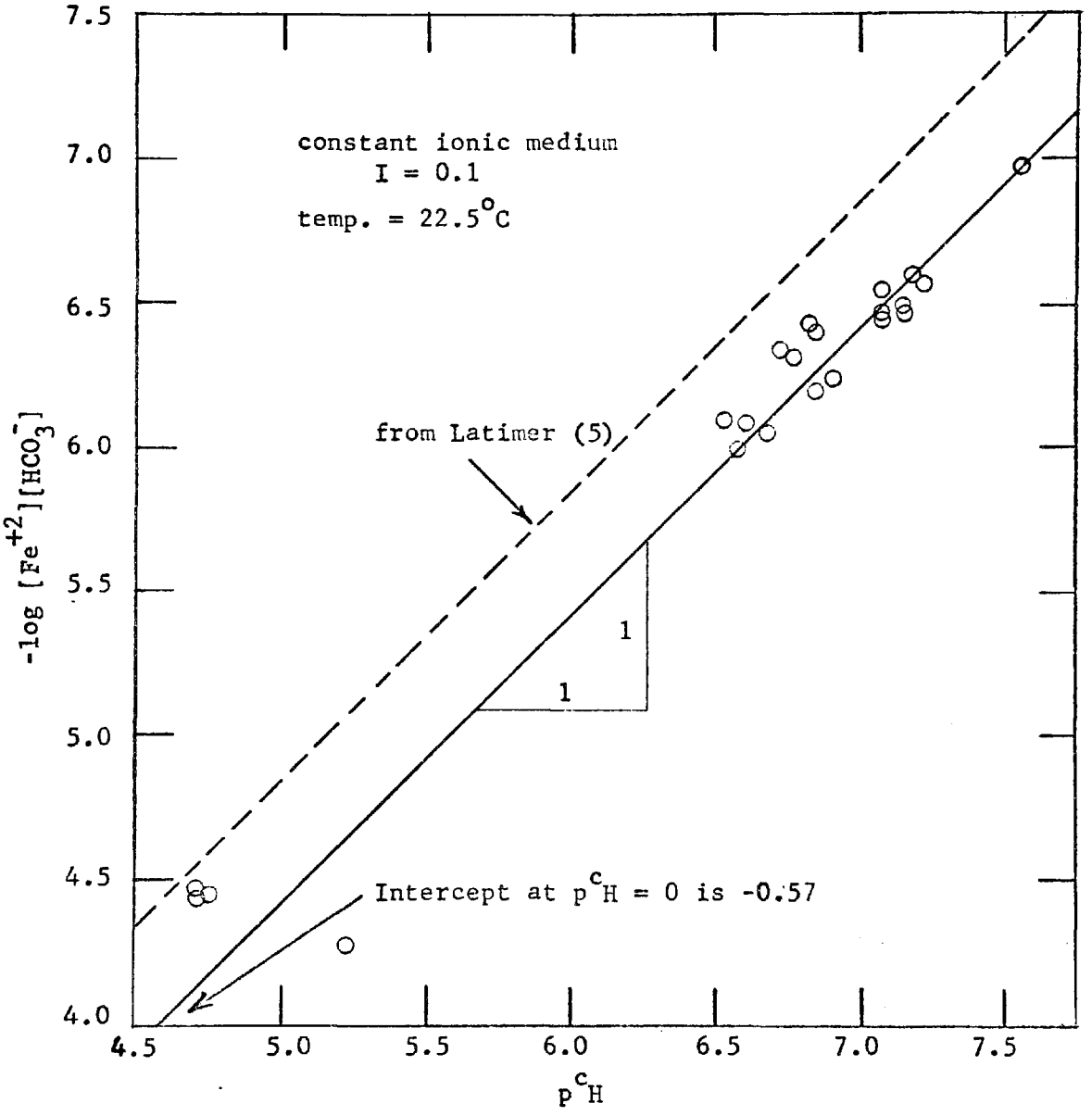

FIGURE 2-5. Experimental data for determination of solubility product of ferrous carbonate (siderite).

On the other hand, it is certainly possible, even probable, that some dissolution of $FeCO_3$ and some oxidation of soluble Fe(II) does occur during filtration. These effects act in opposite directions and tend partially to cancel each other. The extent of such dissolution and oxidation during filtration is manifested in the scatter in Figure 2-5. The experimental uncertainty has been computed on the bases of the greatest degree of scatter in the p^cH-region 6.5 to 7.5.

As shown by equation 2-12, the intercept at $p^cH = 0$ is equal to the quantity $pK^c_{so} - pK^c_2$. If one makes use of the Davies equation to estimate activity coefficients of single ions as suggested by Schindler (17) for carbonates of bivalent metals, the thermodynamic second acidity constant of carbonic acid as a function of temperature as reported by Harned and Scholes (18), and the van't Hoff temperature relationship, the thermodynamic solubility product can be computed as shown in Appendix A. The resulting solubility product, at 25°C and zero ionic strength, is $5.7 \pm 2.3 \times 10^{-11}$ or pK_{so} is 10.24 ± 0.17. The previously-accepted value is 2.1×10^{-11} or $pK_{so} = 10.68$, as shown in Table 2-1.

Using the experimental value of $pK^c_{so} = 10.24 \pm 0.17$, one can compute the free energy of formation of ferrous carbonate as follows (the numbers in parenthesis refer to the presently-accepted values (5)):

$$FeCO_{3(s)} = Fe^{+2} + CO_3^{-2}; \quad K_{so} = 10^{-10.24}(10^{-10.68}) \qquad (2\text{-}4b)$$

$$\Delta F^o = -1.364 \log K_{so} = 14.0 \pm 0.2 \text{ K cal/mole } (14.54) \text{ at } 25^oC$$

$$\Delta F^o = 14.0 = \Delta F^o_{Fe^{+2}} + \Delta F^o_{CO_3^{-2}} - \Delta F^o_{FeCO_3}$$

$$14.0 = -20.3 - 126.2 - \Delta F^o_{FeCO_3}$$

$$\Delta F^o_{FeCO_3} = -160.5 \pm 0.2 \text{ Kcal./mole } (-161.06)$$

(The free energies of formation for Fe^{+2} and CO_3^{-2} have been taken from Latimer (5).) Although the difference of only 0.6 K cal. in 160 K cal. does not appear to be very significant, its importance is magnified when considering the difference between two large numbers as is often done in computing the change in free energy for a given reaction. Such a small error in the change in free energy can result in a much larger error when the equilibrium constant for the reaction is computed.

If the thermodynamic constant given in the literature is modified to the experimental conditions of this study using the same temperature and activity corrections described above, the resulting constant does not fit the experimental data, as Figure 2-5 demonstrates. The new solubility product, however, can be shown to explain adequately the apparent oversaturation described in the literature. If Hem's data (11) for the reaction

$$CaCO_{3(s)} + H^+ = Ca^{+2} + HCO_3^- \qquad (2\text{-}13)$$

is considered, the degree of oversaturation for calcite can be computed to be

$$S_C = \frac{Q_C}{K_C}$$

where Q_C is the actual reaction quotient for 2-13 in the aquifer, and K_C is the thermodynamic equilibrium constant for the same reaction. Q_C is calculated in terms of the measured variables as

$$Q_C = \frac{(Ca^{+2})_m (HCO_3^-)_m}{(H^+)_m} \qquad (2\text{-}15)$$

the subscript m referring to measured quantities, and K_C is given by

$$K_C = \frac{(Ca^{+2})_m (HCO_3^-)_m}{(H^+)_{comp}}$$

where $(H^+)_{comp}$ refers to the computed activity of H^+ in equilibrium with the measured activities of calcium and bicarbonate. Substitution of 2-15 and 2-17 into 2-14 yields

$$S_C = \frac{(Ca^{+2})_m (HCO_3^-)_m / (H^+)_m}{(Ca^{+2})_m (HCO_3^-)_m / (H^+)_{comp}} = \frac{(H^+)_{computed}}{(H^+)_{measured}} \qquad (2\text{-}17)$$

If the degree of oversaturation for siderite is assumed to be the same as that for calcite, one obtains, in similar fashion as with calcite

$$S_C = S_F = \frac{Q_F}{K_F} = \frac{(Fe^{+2})_m (HCO_3^-)_m / (H^+)_m}{K_F} \qquad (2\text{-}18)$$

where Q_F is the reaction quotient for dissolution of siderite as in reaction 2-11, again in terms of the measured parameters, and K_F is the equilibrium constant. It should be noted that

$$K_F = \frac{K_{so}}{K_2} = K_{eq} \qquad (2\text{-}19)$$

as in equation 2-11a. Taking logarithms in equation 2-18, one obtains

$$\log S_C = \log Q_F - \log K_F \qquad (2\text{-}20)$$

If one now uses Hem's data (11) to compute the oversaturation for calcite from 2-17 and the reaction quotient for siderite from 2-18, a plot of log S_C versus log Q_F should result in a straight line with a slope of unity. The intercept at log S_C = 0 should be equal to log K_F which is related to the solubility product of ferrous carbonate by 2-19.

Figure 2-6 is a plot of Hem's data on the log S_C - log Q_F coordinates. Two lines are shown on the graph, A corresponding to the solubility product obtained in this study, and B corresponding to the existing constant

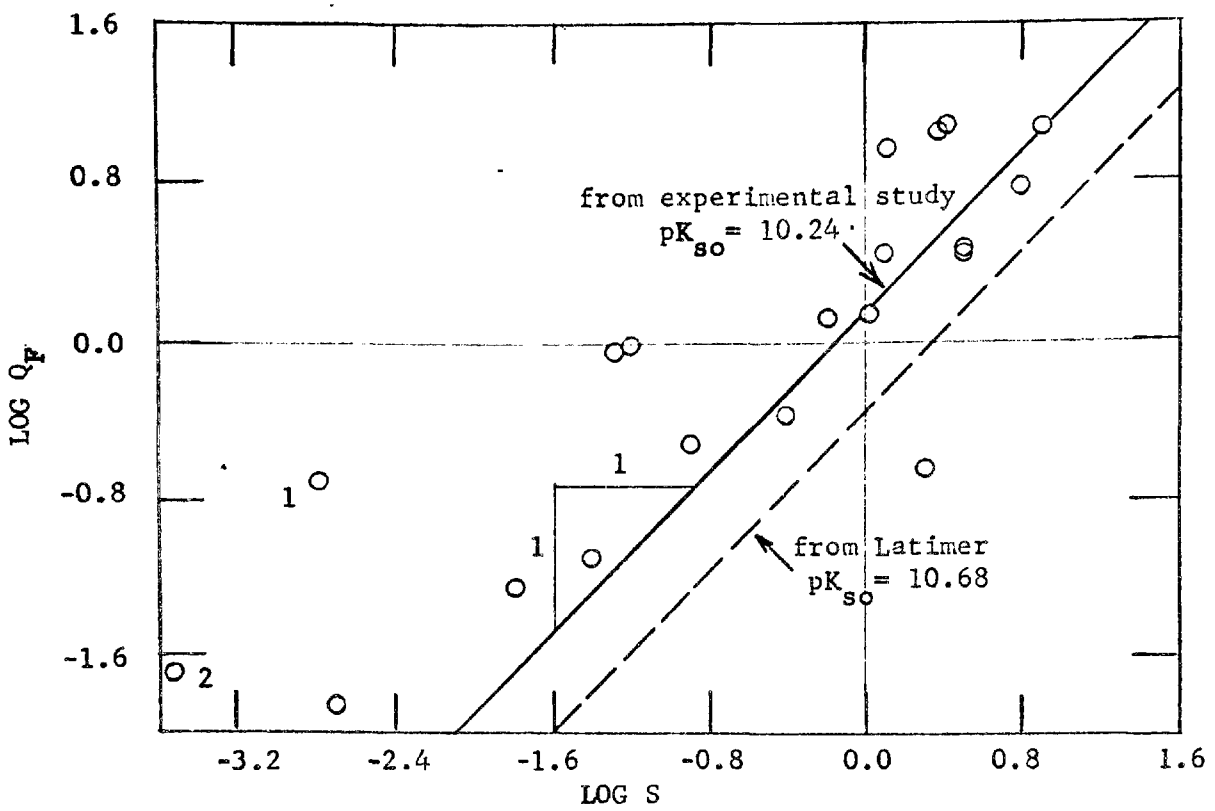

FIGURE 2-6. Conformance of experimental solubility product to data obtained by Hem (11) in natural groundwaters. S is the degree of oversaturation with respect to calcite and Q_F is the reaction quotient for the dissolution of siderite.

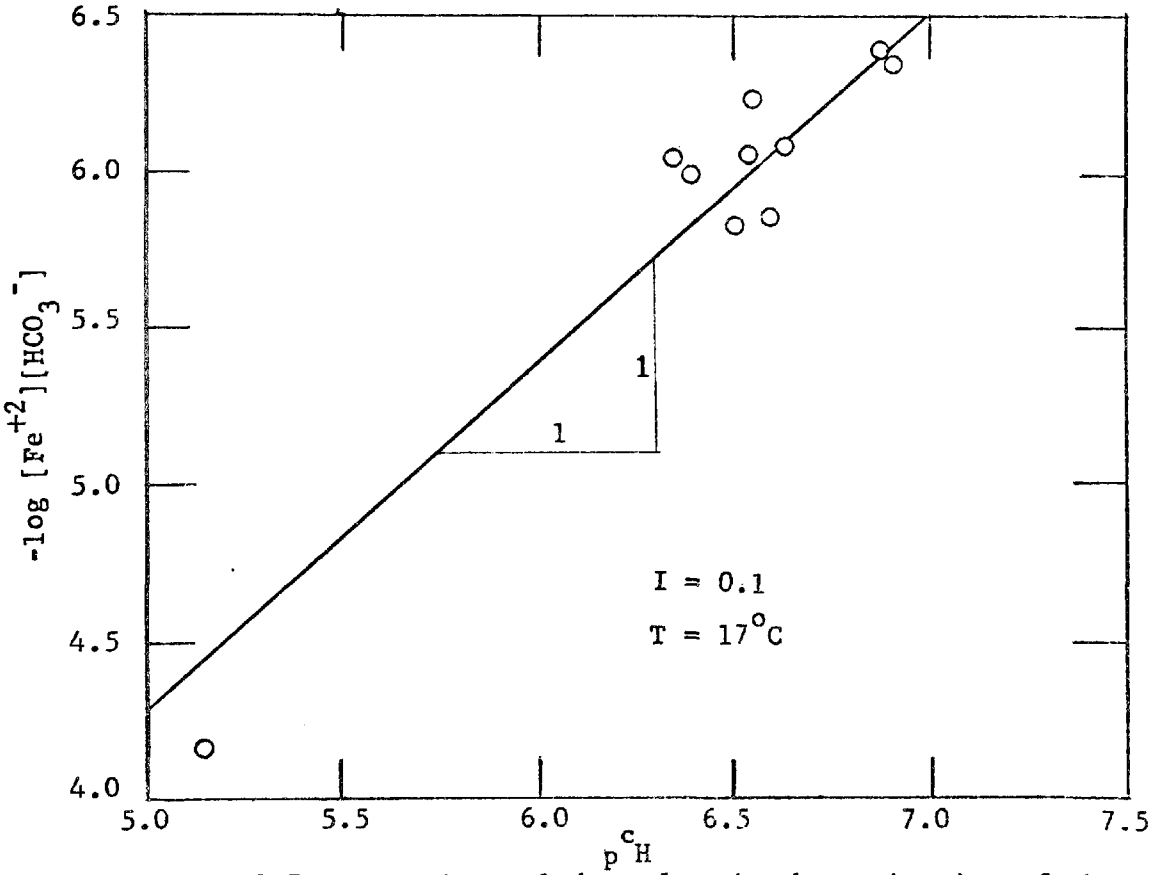

FIGURE 2-7. Experimental data for the determination of the solubility product of ferrous carbonate.

reported in the literature. (In plotting these lines, a value of 10.33 was used for pK_2, at 25°C and zero ionic strength.) Points 1 and 2, which fall considerably off both lines, represent waters in contact with rock formations which are quite low in carbonate content and where pH was not measured directly at the time of collection. Due to the low concentrations of carbonate in these waters, they are weakly buffered with respect to pH so that pH may have changed considerably during storage. (Hem suggests that the initial pH of these two waters could have been half a unit or more higher than the pH which was measured in the laboratory after storage.) It is seen in Figure 2-6 that the experimental solubility product obtained in this study conforms well to Hem's data.

Ghosh, O'Connor, and Engelbrecht (19) have indicated that their apparent oversaturation may partially be explained by their inability to measure the pH in the aquifer at the depths from which the waters were derived. This redetermination of the solubility product additionally explains their observations.

The solubility product of siderite was also determined under different experimental conditions by varying the temperature of the system and the concentration of the constant ionic medium. Figures 2-7 and 2-8 show the results at two other temperatures, and the findings at an ionic strength of 0.05 are presented in Figure 2-9. The data were treated in the same manner as above and the outcome is summarized in Table 2-2. It will be noted that the solubility of $FeCO_3$ increases with decreasing temperature. The solubility products obtained in this study under various experimental conditions are seen to be consistent among themselves and are approximately three times greater than the accepted value reported in the literature.

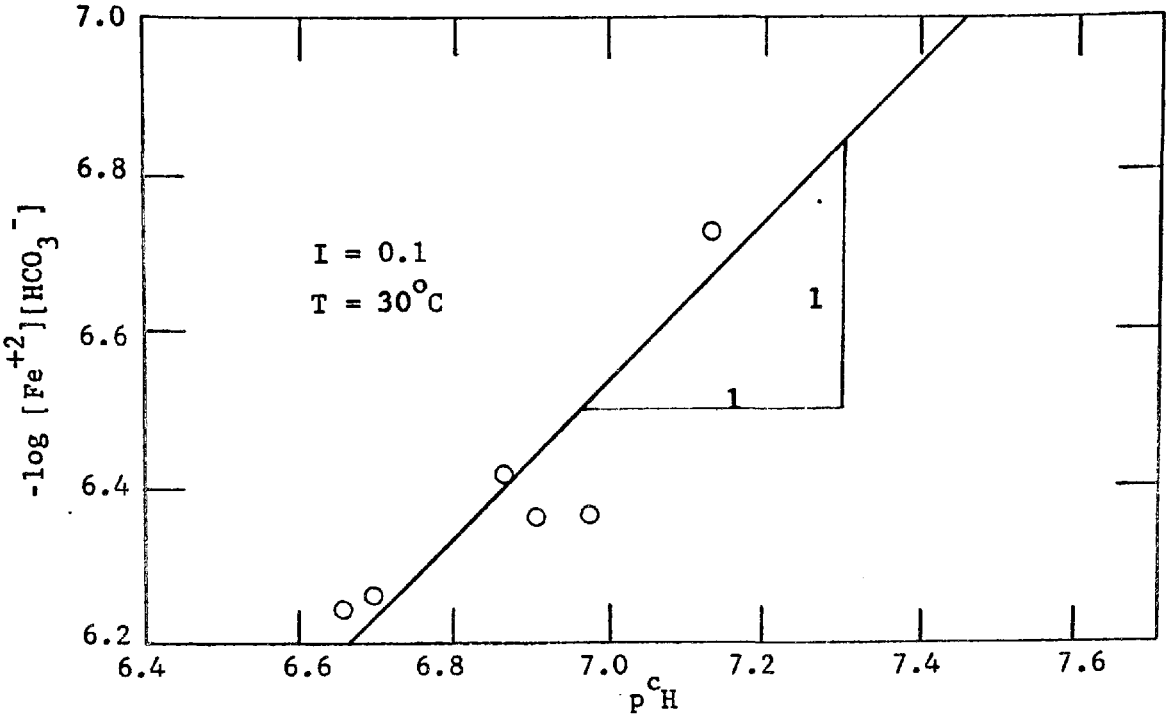

FIGURE 2-8. Experimental data for the determination of the solubility product of ferrous carbonate.

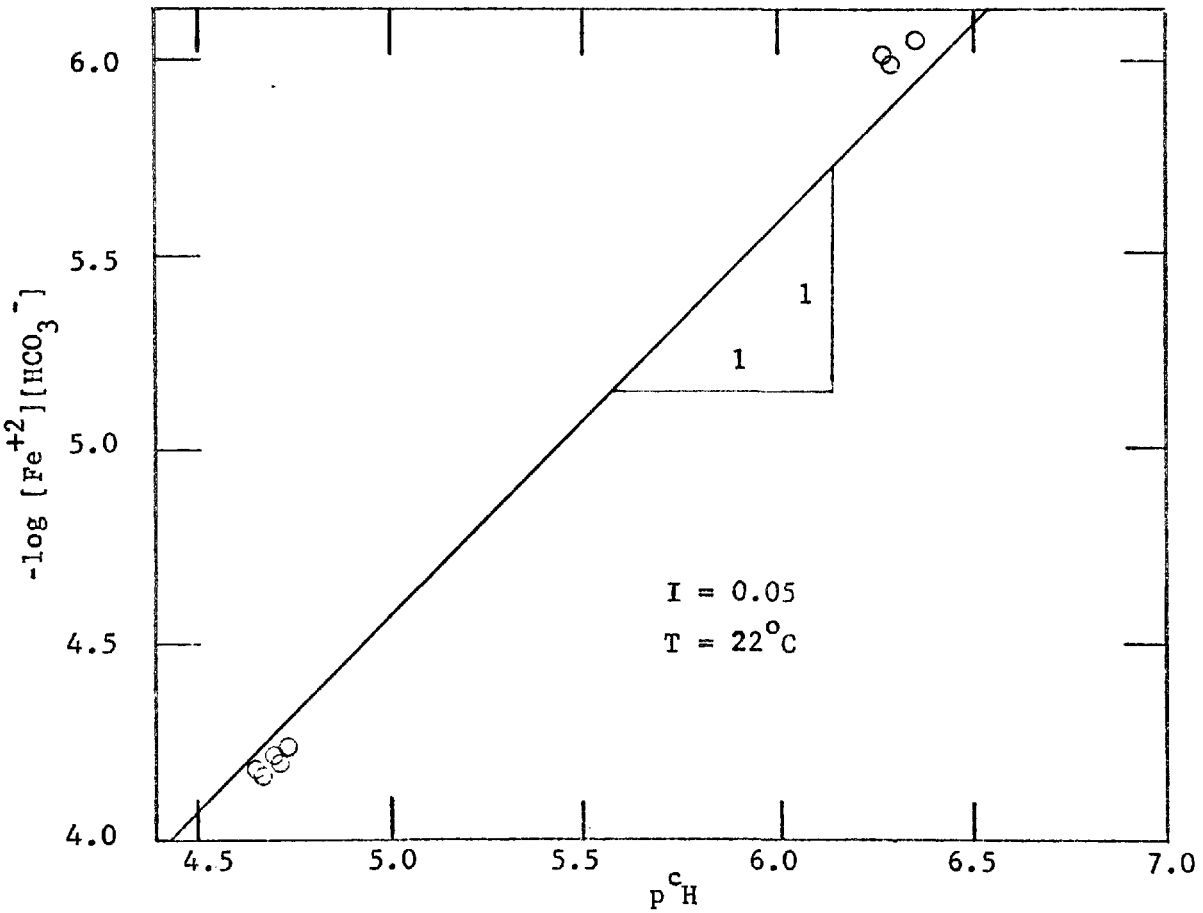

FIGURE 2-9. Experimental data for the determination of the solubility product of ferrous carbonate.

Table 2-2. Experimental Determination of Solubility Product of $FeCO_3$

Temperature °C	Ionic Strength	$pK_1^c eq = pK_{so}^c - pK_2^c$	pK_{so} at Experimental temperature	Thermodynamic Solubility Product* pK_{so} Corrected to 25°C, I = 0.0	K_{so}
17	0.1	-0.72	10.12	10.21	6.2×10^{-11}
22.5	0.1	-0.57	10.21	10.24	5.7×10^{-11}
30	0.1	-0.46	10.25	10.20	6.3×10^{-11}
22	0.05	-0.42	10.28	10.31	4.8×10^{-11}
Accepted Literature Value (5)				10.68	2.1×10^{-11}

*Activity corrections were made using the Davies equation

$$-\log \gamma = Az^2 \left[\frac{\sqrt{I}}{1 + \sqrt{I}} - 0.3I \right]$$

for single ion activity coefficients. The van't Hoff temperature relationship

$$\ln \frac{K_2}{K_1} = \frac{-\Delta H^o}{R} \left(\frac{T_1 - T_2}{T_1 T_2} \right)$$

was used to convert the experimental solubility products to 25°C. (ΔH^o = -4630 cal./mole at 25°C (5).) Sample calculations are given in Appendix A.

X-Ray Analysis of Precipitate

The crystal structure of the precipitate was examined by x-ray diffraction to establish whether the solution was in contact with an amorphous deposit or with crystalline ferrous carbonate, i.e., siderite. The diffraction pattern is shown in Figure 2-10 along with a table describing the standard pattern for siderite given by the American Society for Testing Materials (20). The glancing angle, "θ," corresponds to the interplanar spacing, "d", and I/I_1 is a measure of the relative intensity of any single peak to the largest peak. For example, at $2\theta = 40.6^{\circ}$, the largest peak is obtained so that $I/I_1 = 100\%$, while the intensity of the peak at $2\theta = 68.0^{\circ}$ is only 45% of the intensity at 40.6°. Comparison of the diffraction pattern of the precipitate with the ASTM standard shows definitely that the precipitate was crystalline ferrous carbonate so that the solubility product obtained is the thermodynamic solubility product of siderite.

Stability Constant of $FeHCO_3^+$

Using the divalent cation electrode and standardized solutions of ferrous perchlorate, one obtains a standard curve relating the potential, E_{DCE}, to the concentration of free ferrous iron, Fe^{+2}, in the constant ionic medium. (See Figure 2-11.) At concentrations of Fe^{+2} below 10^{-4}M, E_{DCE} approaches a limiting value due to selective exchange of Na^+ which, at that point, is present at a concentration three orders of magnitude greater than Fe^{+2}. Consequently, in the experimental study in 0.1M $NaClO_4$, a concentration of Fe(II) in excess of 10^{-4}M was always employed.

FIGURE 2-10. X-ray diffraction pattern of experimental ferrous carbonate formed in solubility study. Comparison with diffraction pattern of siderite.

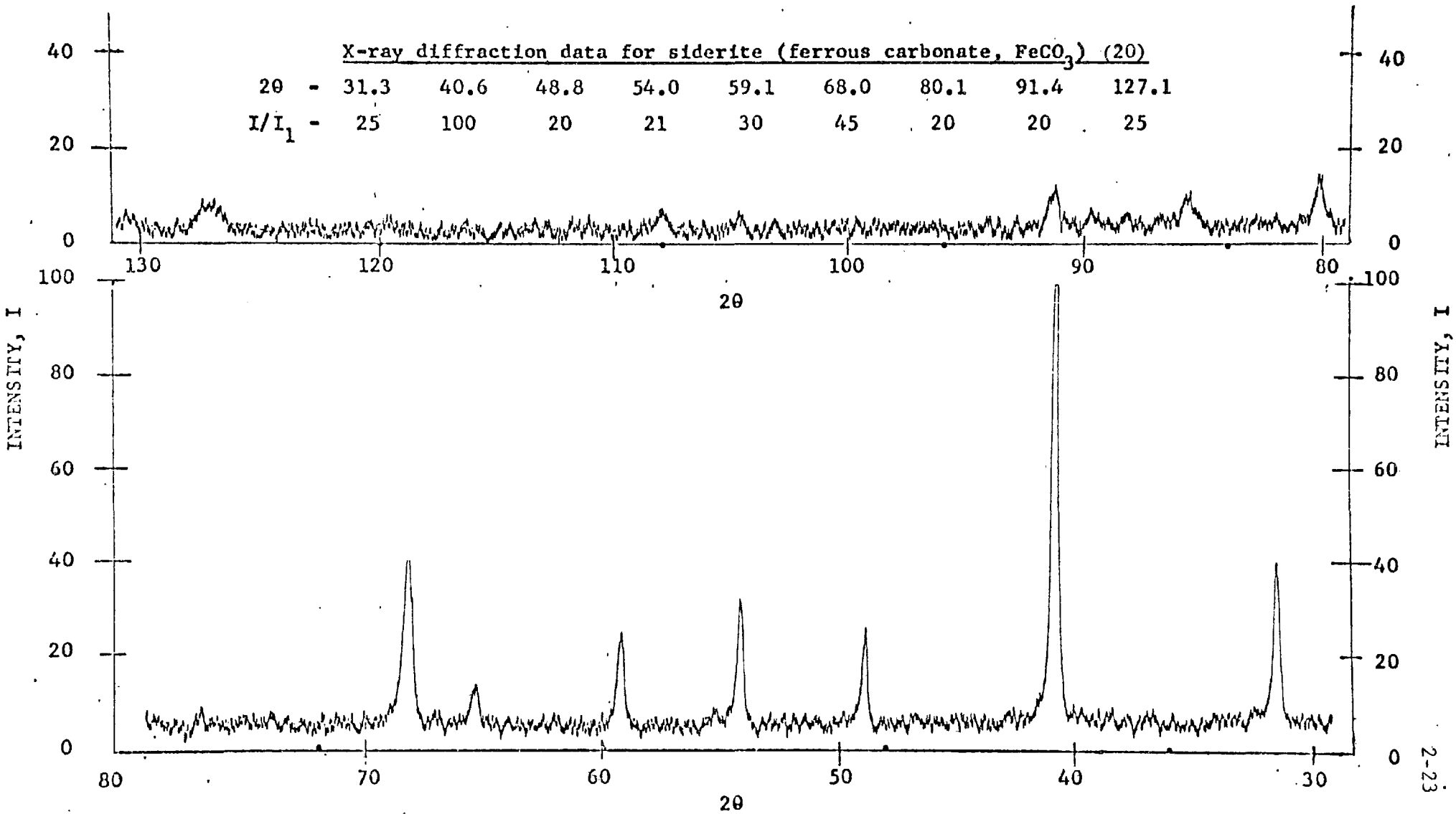

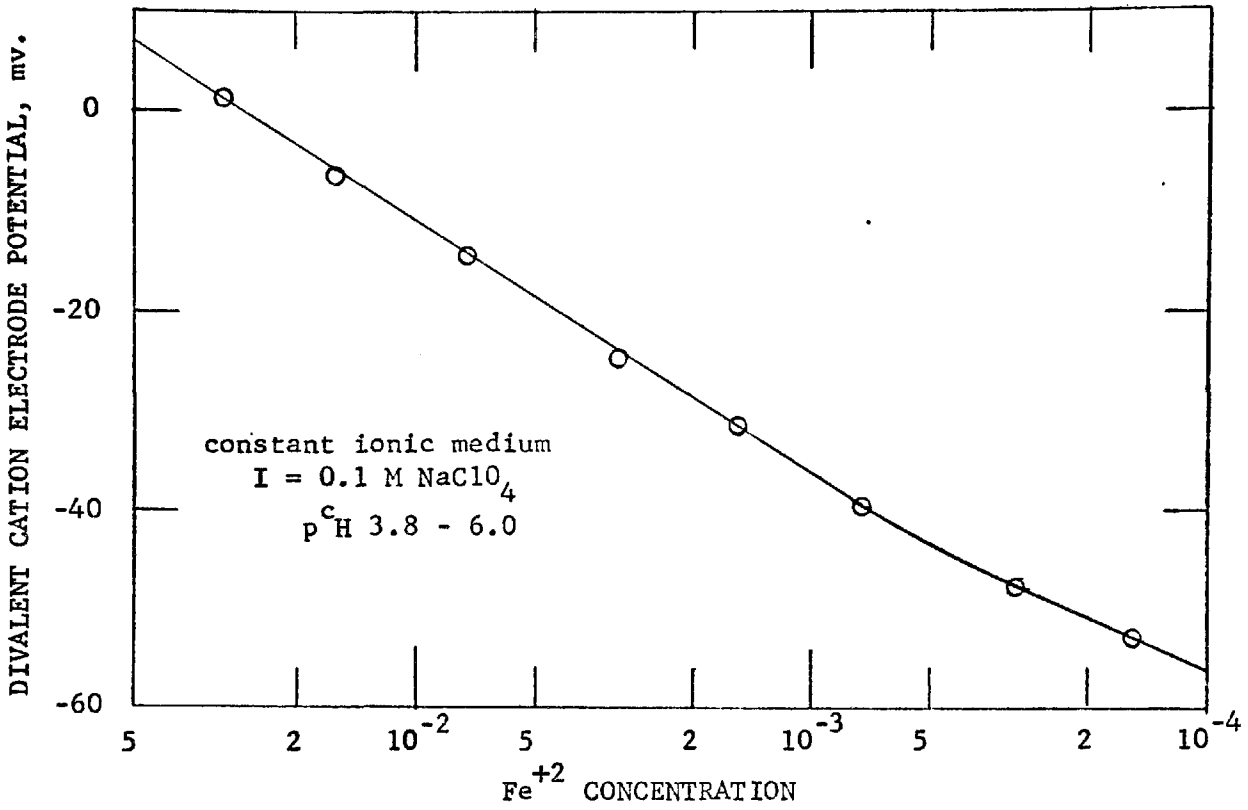

FIGURE 2-11. Standardization curve for divalent cation electrode in ferrous perchlorate solution.

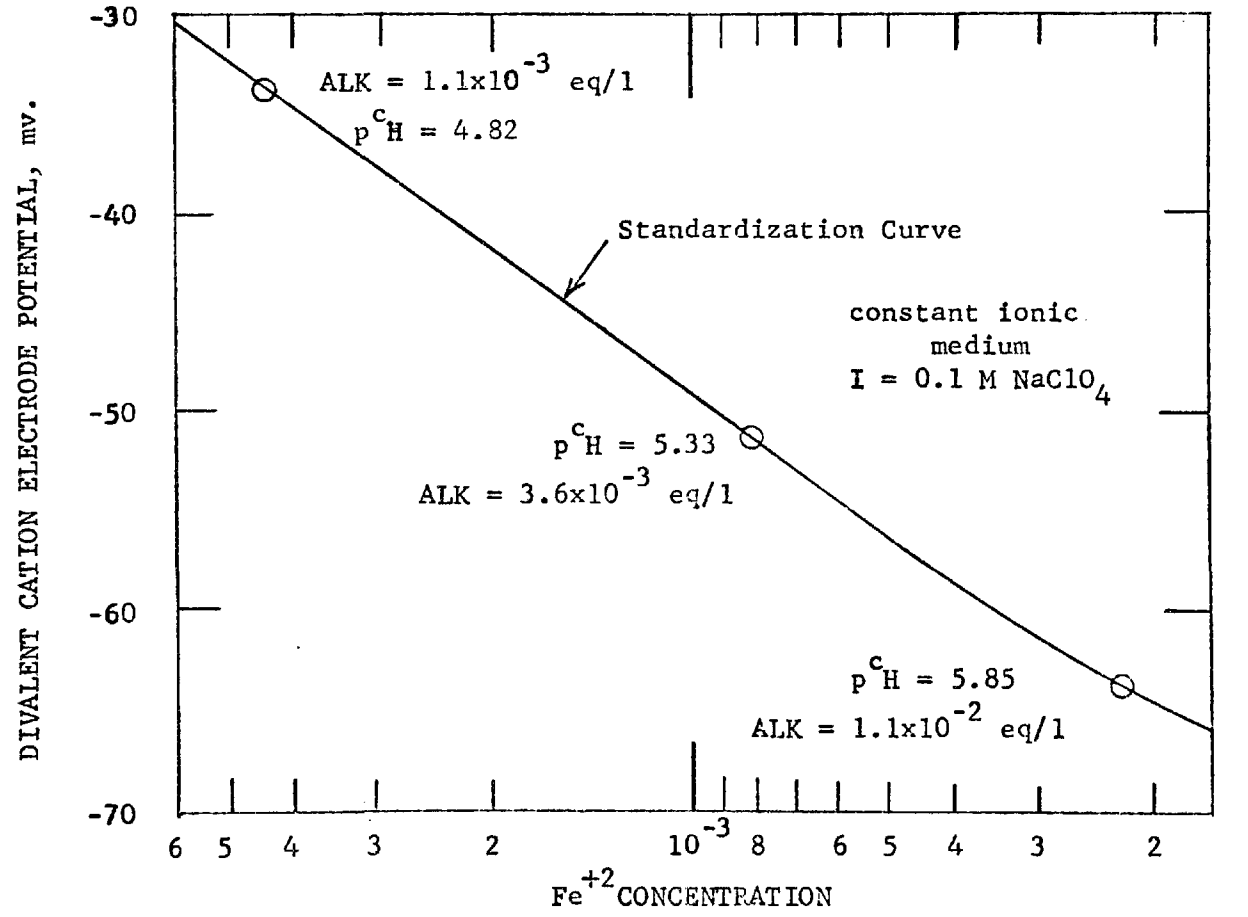

FIGURE 2-12. Determination of free ferrous iron, Fe^{+2}, in bicarbonate solution.

The measured potential of each of the three systems investigated was plotted against the total concentration of Fe(II) for that system, determined independently by titration with permanganate, the points being compared to the calibration curve. The results are presented in Figure 2-12. The standardization curve represents the concentration of free Fe^{+2} corresponding to the given potential, determined in a similar manner as Figure 2-11. It is seen that the total concentration of Fe(II) in the sample is equal to the concentration of Fe^{+2} corresponding to the measured potential. Any deviation between the concentrations of $Fe(II)_T$ and Fe^{+2} would imply formation of $FeHCO_3^+$ or some other soluble complex of ferrous iron and would have been indicated had the three points fallen to the left of the calibration curve, i.e., less free Fe^{+2} for a given Fe(II). For example, the second sample contained 8.3×10^{-4}M of total ferrous iron as determined by titration with permanganate. The potential of the sample was measured as -51.3 mv. But according to the standard curve, this corresponds to a concentration of free Fe^{+2} of 8.3×10^{-4} M. Therefore, all of the total Fe(II) is present as free Fe^{+2}.

Six hours later, the procedure was repeated and with the exception of a slight shift in the calibration curve, the results are identical, i.e., the experimental points fall on the calibration curve. One must conclude that even in the presence of 1.1×10^{-2} eq./l. of alkalinity, there are no other measurable soluble species of Fe(II) besides free Fe^{+2}.

From these results and the limitations imposed by the experimental technique, it may be assumed that the concentration of Fe^{+2} is more than ten times greater than that of $FeHCO_3^+$ at 10^{-2} eq./l. of alkalinity. This

implies that the equilibrium constant (stability constant) is less than 10 and the reaction is of no significance in natural waters. (In more dilute systems, of ionic strength less than 0.1, the stability constant should be even smaller.)

If $FeHCO_3^+$ had been significant, one would have expected curvature in Figures 2-5 and 2-7 to 2-9, the degree of curvature being a function of the concentration of HCO_3^-. As already seen, these data plot well as straight lines.

Hem (14) and Morgan (21) have investigated complex-formation of Mn(II) by bicarbonate and found the solubility of Mn(II) to be influenced by such complexation. For the reaction

$$Mn^{+2} + HCO_3^- = MnHCO_3^+ \qquad (2\text{-}21)$$

Morgan reported an average thermodynamic equilibrium constant of 81, while Hem found an average value of 63, indicating that 35% of the total Mn(II) would be present as $MnHCO_3^+$ in a groundwater containing 5×10^{-3} eq./l. of alkalinity. However, no such complex of bicarbonate with Fe(II) was observed using the direct approach described above employing the ion-sensitive electrode.

Summary of Experimental Study

It can be concluded that the solubility product of ferrous carbonate, which is based upon experimental data obtained 50 years ago, is in error by a factor of 3, Fe(II) being three times more soluble than the accepted value would predict. The re-determined solubility product accounts for the recent reports of apparent oversaturation of natural groundwaters with respect to siderite. The existence of a bicarbonato-complex of ferrous

iron to partially explain increased solubility of Fe(II) has been discounted, the only soluble species of Fe(II) of any significance in carbonate-bearing waters being free ferrous iron, Fe^{+2}.

2-3 Solubility of Ferric Iron

2-3.1 Solubility in Natural Waters

In oxygenated waters, ferric iron, in the + III oxidation state, is the stable form of iron. (Its rate of formation via the oxidation of Fe(II) is discussed in Chapter 3.) Due to its relatively great insolubility, ferric hydroxide, or ferric oxide-hydroxide, controls the concentration of soluble Fe(III) in natural waters. Various structural forms of insoluble ferric hydroxide are known to exist having solubility products ranging from $10^{-35.5}$ to 10^{-44}(22). In the experimental study of the kinetics of hydrolysis of Fe(III) which is presented in Chapter 4, a solubility product of 10^{-38} was determined for freshly-prepared ferric hydroxide. For illustrative purposes, this value will be used here. Figure 2-13 is a solubility diagram for Fe(III) utilizing the equilibrium data presented in Table 2-3. For the sake of convenience, the simple case has been assumed in which $Fe(OH)_3$ is in equilibrium only with its monomeric soluble hydroxo-ferric complexes, the presence of multimers and other complex-formers, such as silicate, sulfate, etc., being neglected for the time being.

In waters containing relatively high concentrations of phosphate, insoluble ferric phosphate, $FePO_4$, becomes operative in limiting the solubility of Fe(III). For a water containing a total concentration of all phosphate species of 10^{-4}M, Figure 2-14 demonstrates that the influence

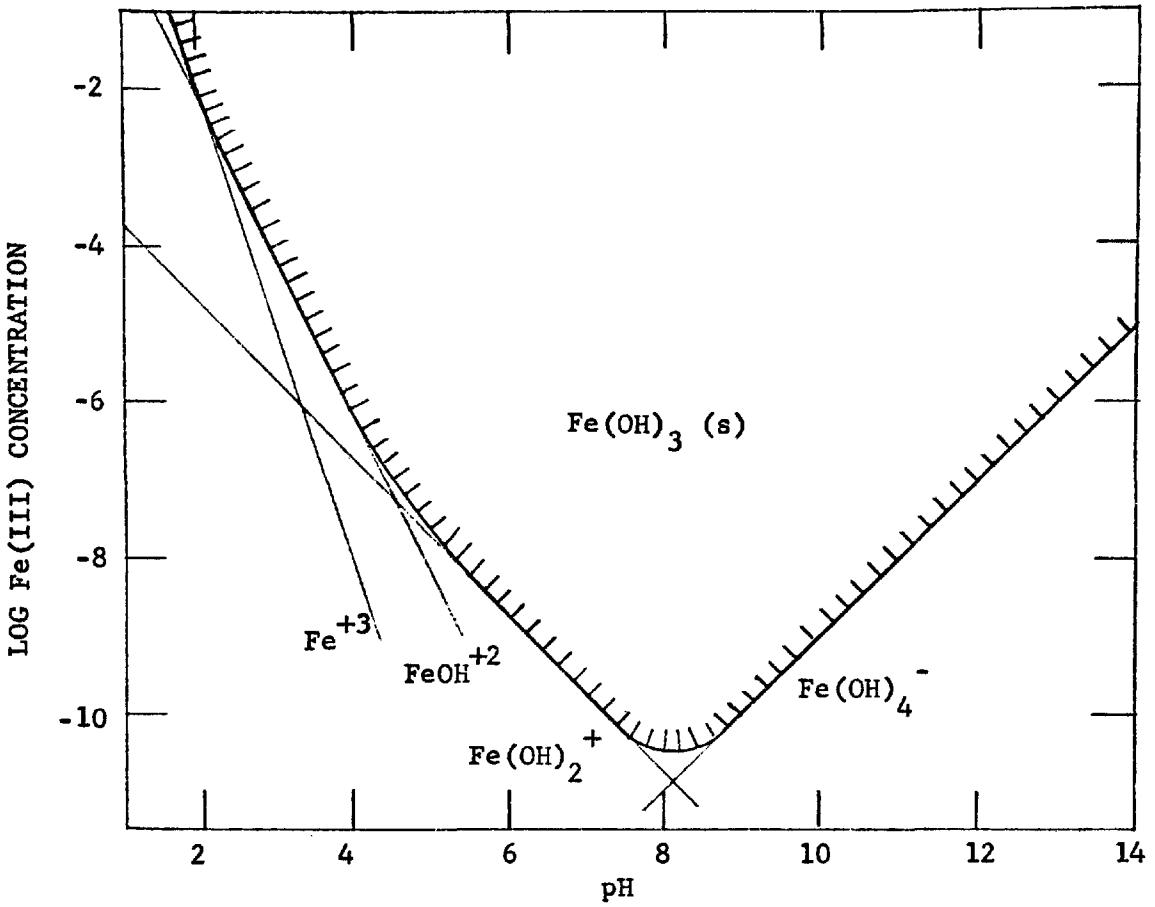

FIGURE 2-13. Solubility of ferric iron.

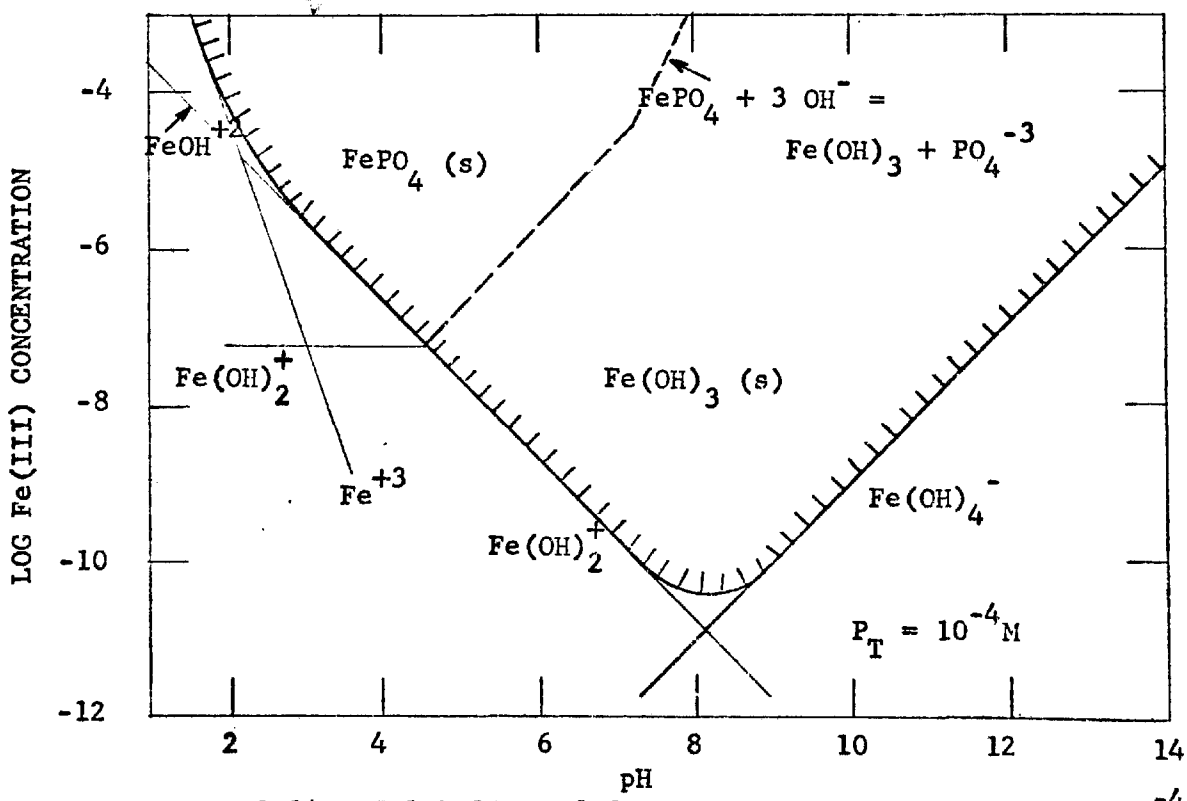

FIGURE 2-14. Solubility of ferric iron in the presence of 10^{-4}M of total phosphate species.

Table 2-3. Equilibria Describing Fe(III) Solubility

Equation No.	Reaction	Equilibrium Constant at 25°C	Reference
2-22	$Fe(OH)_{3(s)} = Fe^{+3} + 3OH^-$	10^{-38}	expt'l, Ch. 4
2-23	$Fe^{+3} + H_2O = Fe(OH)^{+2} + H^+$	6.8×10^{-3}	23
2-24	$FeOH^{+2} + H_2O = Fe(OH)_2^+ + H^+$	2.6×10^{-5}	23
2-25	$Fe(OH)_{3(s)} + OH^- = Fe(OH)_4^-$	10^{-5}	27
2-26	$FePO_{4(s)} = Fe^{+3} + PO_4^{-3}$	10^{-24}	25
2-34	$H_3PO_4 = H_2PO_4^- + H^+$	7.4×10^{-3}	22
2-35	$H_2PO_4^- = HPO_4^{-2} + H^+$	6.4×10^{-8}	22
2-36	$HPO_4^{-2} = PO_4^{-3} + H^+$	5.0×10^{-13}	22

of solid $FePO_4$ is exerted only in the acidic pH-region below pH 5. The solubility product of $FePO_4$ is not a well-known quantity, there being three different values for the constant: $10^{-17.9}$ (computed from the tabulation by Latimer (5)), $10^{-21.9}$(24), and 10^{-24} (25). Again, for illustrative purposes, the value of 10^{-24} determined by Stumm and Galal-Gorchev (25) has been utilized.

One can derive an expression for the conversion of $FePO_4$ to $Fe(OH)_3$ in a similar manner as was done for the system $FeCO_3$ - FeS in equation 2-10. In this case,

$$FePO_{4(s)} + 3\ OH^- = Fe(OH)_{3(s)} + PO_4^{-3} \qquad (2\text{-}27)$$

where the equilibrium constant is

$$K_{eq} = \frac{K_{26}}{K_{22}} = 10^{14} = \frac{[PO_4^{-3}]}{[OH^-]^3} \qquad (2\text{-}27a)$$

For a system at pH 6, the total concentration of phosphate must exceed 2×10^{-3}M in order for solid $FePO_4$ to control the solubility of Fe(III). This is an unlikely situation in most natural systems but under localized conditions where the composition of the water is non-uniform, $FePO_4$ may be influential. Generally, however, the solubility of Fe(III) is controlled by its various oxides and hydroxides.

2-3.2 Effect of Complex Formation on Fe(III) Solubility

The presence of organic and inorganic ligands which are capable of coordinating with Fe(III) to form soluble complexes serves to increase the solubility of Fe(III) in natural waters. In contrast to the case of ferrous iron where the tendency to form complexes is insignificant, ferric iron has a strong affinity for complexing ligands. In the preceding section where the solubility of $Fe(OH)_3$ and $FePO_4$ were considered, the influence of complex-formation was neglected for reasons of simplicity. Since Fe^{+3} has an exceedingly strong affinity for the hydroxide ion, the relative affinities of Fe^{+3} for other ligands must be compared to its affinity for OH^- to evaluate the extent of coordination of Fe(III) by these other ligands. Consequently, the relative concentrations of the various complexes of Fe(III) are pH-dependent. This fact is demonstrated in Appendix B where it is shown that in the presence of phosphate, a rather strong complex-former, the effect of soluble phosphato-complexes of Fe(III) is significant only in the acidic pH-range below pH 4. (It is probable that mixed

hydroxo-phosphato-complexes of Fe(III) exist but there is insufficient thermodynamic data to calculate their relevance.)

It is apparent that, in natural waters, the major effect of ligands other than OH^- is manifested in the acidic pH-range where the concentration of OH^- is inconsequential.

A number of organic agents have a strong tendency to coordinate with Fe^{+3}, examples including EDTA and citrate (22). Again, the existence of mixed organo-hydroxo-complexes is likely. Althougn Figure 2-13 implies that the concentration of soluble Fe(III) cannot exceed 10^{-8}M in the pH-region 6 to 11, significantly higher concentrations of soluble Fe(III) in natural waters have often been reported. Complex-formation with organic material is usually cited as an explanation. Morgan (26) has considered a hypothetical system involving nine metals and nine ligands to demonstrate the significance of complex-formation, and has found that for the types of ligands observed in natural waters, OH^- is the major ligand coordinated with ferric iron. The discrepancy between predicted concentrations of soluble Fe(III) and reported concentrations can be partially explained by the analytical difficulties encountered in distinguishing between soluble Fe(III) and suspended colloidal ferric hydroxide. Lengweiler, Buser, and Feitknecht (27), in order to completely sediment colloidal $Fe(OH)_3$, demonstrated the need to resort to ultracentrifugation. Hence, it is doubtful that conventional methods of filtration are effective in differentiating between soluble and suspended Fe(III).

Furthermore, as Morgan (26) has shown, the concentration of organic matter in natural waters is insufficient to account for significant complexation of Fe(III). However, in view of the extremely high concentrations

of "solubilized" Fe(III) associated with organic color in natural waters, it has been suggested (28) that these color-causing organic agents coordinate with colloidal $Fe(OH)_3$ forming a highly-dispersed peptized colloid.

2-3.3 Experimental Determination of Sulfato-Complex of Fe(III)

As indicated in the previous section, the influence of inorganic ligands other than OH^- in coordinating with Fe(III) is insignificant except in the acidic pH-range, or in the presence of relatively high concentrations of the competing ligand compared to OH^-. In the case of sulfate, both these conditions are fulfilled in the acidic waters draining through coal and copper mines where oxidation of sulfide minerals releases large concentrations of sulfate. (Chapter 5 contains a complete discussion of the chemistry characterizing mine drainage.) In these waters, where concentrations of sulfate exceed 10^{-2}M and pH-values less than 3 are not uncommon, complex-formation of Fe(III) by sulfate appears to be interrelated with the oxidation of ferrous iron and the hydrolysis of ferric iron.

The stability constant for the reaction

$$Fe^{+3} + SO_4^{-2} = FeSO_4^{+}; \qquad K_1 = \frac{(FeSO_4^{+})}{(Fe^{+3})(SO_4^{-2})} \tag{2-28}$$

is fairly well-known (22), having been determined mainly by spectrophotometric techniques. Potentiometry can also be conveniently applied to measure such stability constants (29, 30). Since the rate of hydrolysis of ferric iron (Chapter 4) was to be studied using a potentiometric method, the investigation of complex-formation between sulfate and Fe(III) served as a preparatory exercise in gaining familiarity with the technique.

Furthermore, the experimentally-determined stability constant could then be applied, as needed, in these future studies, some of which were conducted in the presence of sulfate.

Experimental Procedure

The following electrochemical cell was employed in the potentiometric study of complex-formation of Fe(III) by sulfate:

$$Pt \left| Fe(II),\ Fe(III),\ ClO_4^-,\ H^+,\ Na^+,\ SO_4^{-2}, \right| \underset{(sat'd)}{NaCl} \left| Hg_2Cl_2 \right| Hg \quad (2\text{-}29)$$

The cell consisted of a bright platinum spiral indicator electrode and a calomel reference electrode separated by the test solution, contact between the latter two being effected by a solution saturated with NaCl. (NaCl was used in place of KCl to avoid possible precipitation of $KClO_4$ in the event of leakage of K^+ from the calomel electrode.) The redox potential is established by the electroactive Fe(II)-Fe(III) couple in accordance with the Nernst Equation

$$E = E^o - \frac{RT}{f} \ln \frac{(Fe^{+2})}{(Fe^{+3})} \quad (2\text{-}30)$$

A constant ionic medium of 0.1M $NaClO_4$ was maintained and the system kept in a constant-temperature water bath at 25°C so that equation 2-30 can be written as

$$E = E^{o'} - 0.0592 \log \frac{[Fe^{+2}]}{[Fe^{+3}]} \quad (2\text{-}30a)$$

$E^{o'}$ referring to the standard potential at the given ionic strength and temperature.

The study was conducted in the pH-range 1 to 3 in order to avoid formation of higher-order and polynuclear hydroxo-complexes of Fe(III)

other than $FeOH^{+2}$, and to maintain the concentration of Fe(II) constant as free ferrous iron, Fe^{+2}. Ferrous and ferric perchlorate were added to a solution of $NaClO_4$ acidified with $HClO_4$. Nitrogen was bubbled through the system to remove all traces of oxygen and the system was placed on a magnetic stirrer. Measurement of the potential of the Fe(II)-Fe(III) couple was effected using a Heath recording potentiometer (Model number EUA 20-11), and the concentration pH was determined in the same manner as previously described in the study of the solubility of $FeCO_3$, employing a Leeds and Northrup pH meter (Catalog number 7664). After observing constant readings for the potential of the system in the absence of sulfate, 0.5 ml aliquots of a pre-standardized solution of Na_2SO_4 were added from a microburette. Following each addition of sulfate, the potential and p^cH were recorded, stable readings being obtained within three minutes after the ligand was added. The experimental apparatus is shown in Figure 2-15.

Experimental Results and Discussion

The experimental system can be represented by the following chemical equilibria:

$$Fe^{+3} + SO_4^{-2} = FeSO_4^{+}; \qquad K_1 = \frac{[FeSO_4^{+}]}{[Fe^{+3}][SO_4^{-2}]} \qquad (2\text{-}28a)$$

$$HSO_4^{-} = H^{+} + SO_4^{-2}; \qquad K_a = \frac{[H^{+}][SO_4^{-2}]}{[HSO_4^{-}]} \qquad (2\text{-}31)$$

$$Fe^{+3} + H_2O = FeOH^{+2} + H^{+}; \quad Q_h = \frac{[FeOH^{+2}][H^{+}]}{[Fe^{+3}]} \qquad (2\text{-}23a)$$

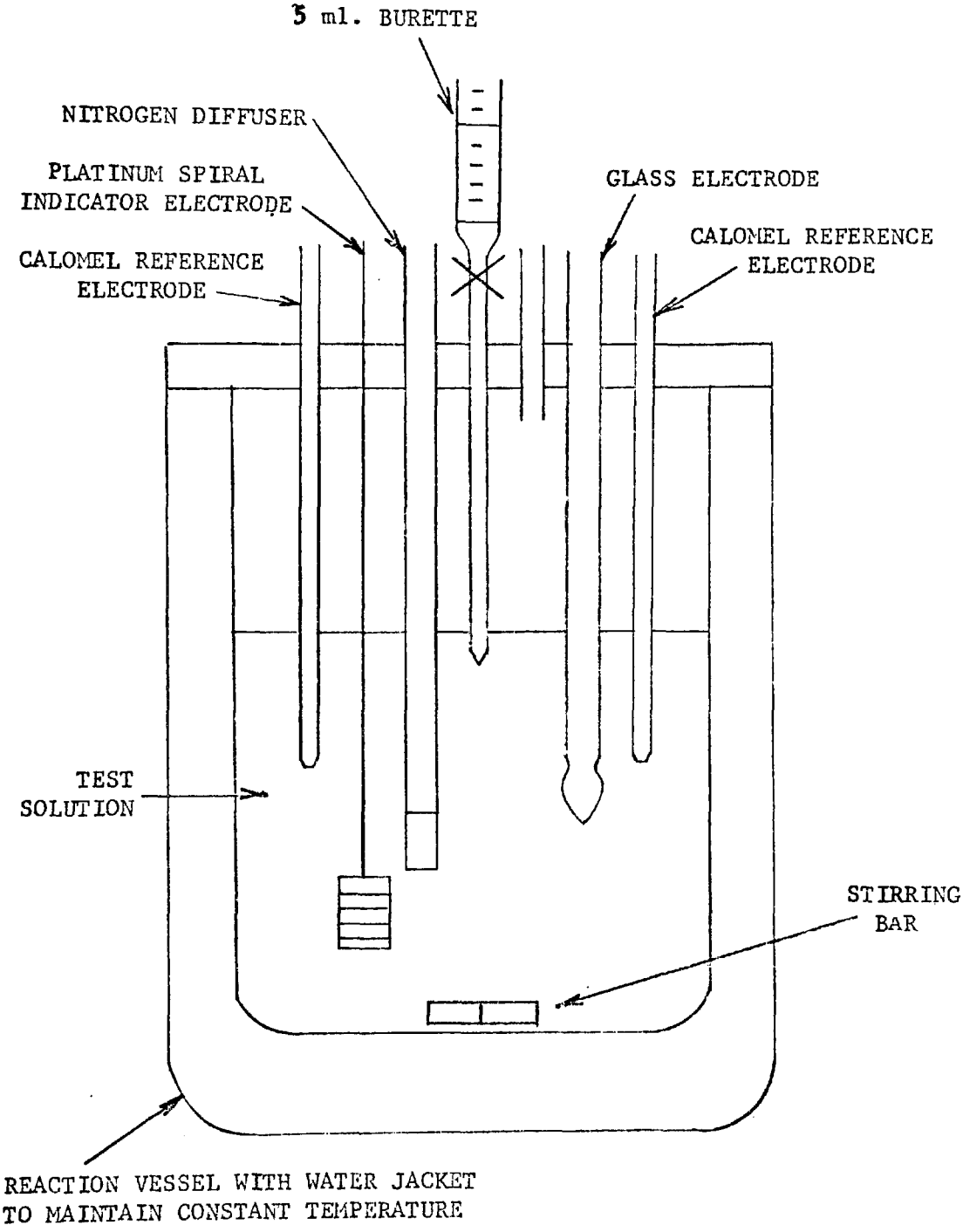

FIGURE 2-15. Experimental apparatus for potentiometric determination of stability constant of sulfato- complex of ferric iron.

The equilibrium constants are defined for 25°C and an ionic strength of 0.1. As derived in Appendix C, the potential can be related to the total concentration of sulfate, S_T, by the equation

$$\left(1 + \frac{Q_h}{[H^+]}\right)\left(\exp \frac{2.3\,\bar{E}}{0.0592} - 1\right) = \frac{K_1 K_a S_T}{[H^+] + K_a} \qquad (2\text{-}32)$$

$\bar{E}$ refers to the difference in potential between the system in the absence of sulfate and that after a given addition of sulfate, S_T. Having measured $\bar{E}$ and $[H^+]$ as a function of S_T, one can compute and plot the left-hand-side of the equation versus S_T, Q_h being the well-known first hydrolysis constant of Fe^{+3}. ($Q_h = 2.89 \times 10^{-3}$ at 25°C and an ionic strength of 0.1 (23).) In the absence of higher order sulfato-ferric complexes other than that given by equation 2-28a, a straight line should result, if $[H^+]$ is assumed to remain relatively constant.

If similar studies are conducted for a series of p^cH-values, the slope of the linear plot in each case should be

$$\text{SLOPE} = n = \frac{K_1 K_a}{[H^+] + K_a} \qquad (2\text{-}33)$$

Rearranging terms, one obtains

$$\frac{K_1 K_a}{n} - K_a = [H^+] \qquad (2\text{-}33a)$$

suggesting that if one plots $\frac{1}{n}$ versus $[H^+]$, the intercept at $[H^+] = 0$ should be equal to $\frac{1}{K_1}$, the reciprocal of the desired stability constant.

Figure 2-16 shows the results of two experiments conducted at $p^cH = 1.02 \pm 0.04$ and 1.39 ± 0.07. The raw data for curve A is presented in Table 2-4. The linearity seems to validate the experimental assumptions

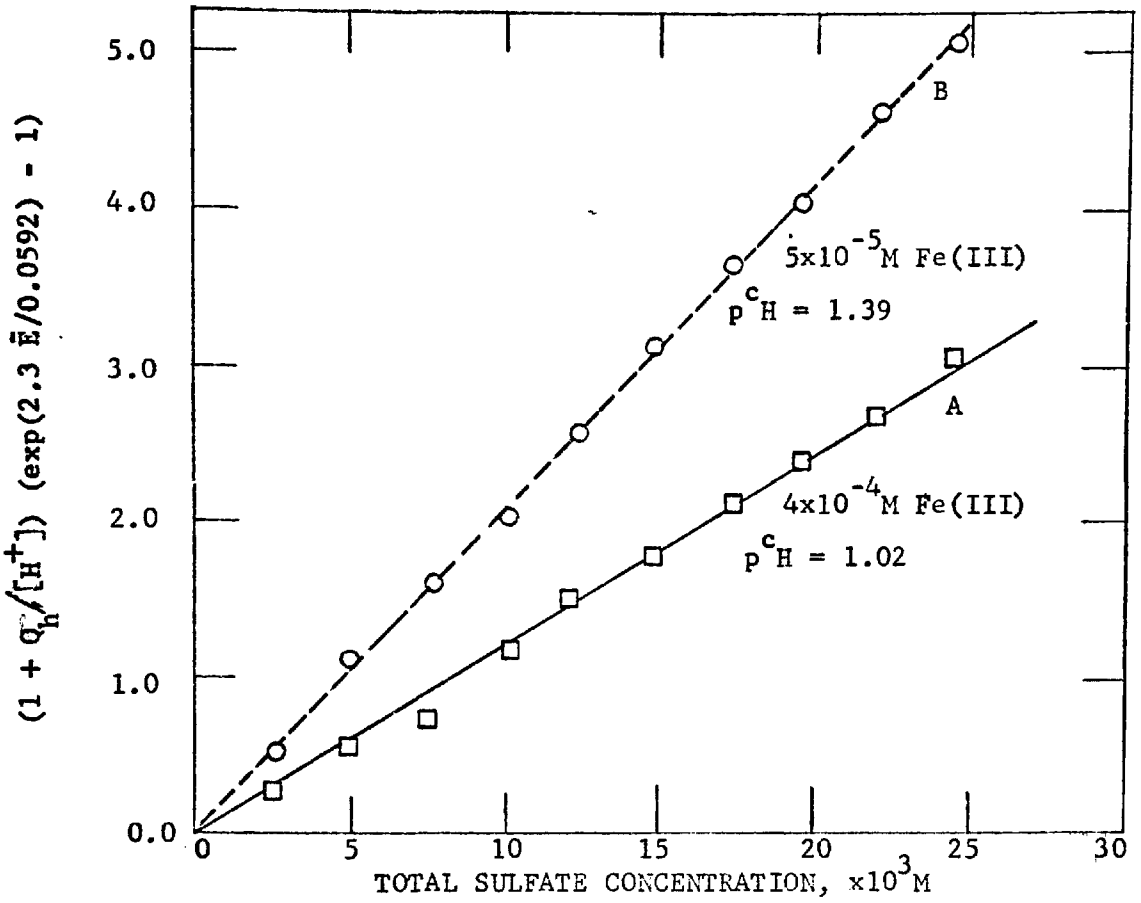

FIGURE 2-16. Experimental data for determination of stability constant of sulfato- complex of Fe(III).

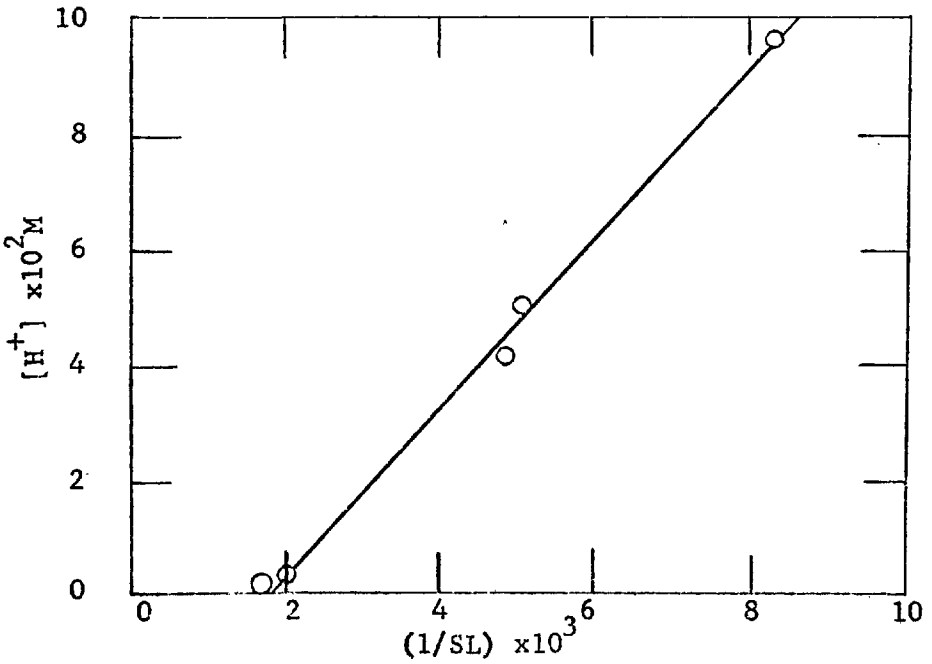

FIGURE 2-17. Determination of stability constant of $FeSO_4^+$.

Table 2-4. Experimental Data and Calculations in Determination of Stability Constant for $FeSO_4^+$

(1) Volume Added, ml	(2) Sulfate Concn., S_T moles/l.	(3) P^cH	(4) Potential,* E, mv.	(5) $E_1-E_2 = \bar{E}^{\ddagger}$	(6) $\exp(\frac{2.3\bar{E}}{59.2})-1$	(7) (6)x$[1 + \frac{Q_h}{[H^+]}]$
0	0	0.98	+513.5	--	--	--
0.5	2.49×10^{-3}		509.0	+4.5	.191	.197
1.0	4.97		503.9	9.6	.452	.466
1.5	7.45		500.2	13.3	.678	.698
2.0	9.91		494.5	19.0	1.10	1.13
2.5	1.233×10^{-2}		490.9	22.6	1.41	1.45
3.0	1.478		487.9	25.6	1.71	1.76
3.5	1.720		485.1	28.4	2.02	2.08
4.0	1.961		483.1	30.4	2.26	2.33
4.5	2.20		480.7	32.8	2.57	2.65
5.0	2.44	1.06	478.1	35.4	2.96	3.05

$[Fe(II)]_T \sim [Fe(III)]_T \sim 4 \times 10^{-4}M$

*Potential readings versus saturated calomel reference electrode.

‡E_1 is the equilibrium potential of the cell in the absence of sulfate. E_2 refers to the potential after the addition of S_T moles/l. of sulfate. (See Appendix C.)

made in deriving equation 2-32. The slopes of a series of such plots at different p^cH-values were calculated and Figure 2-17 has been drawn in accordance with equation 2-33a. As seen from the figure, $\frac{1}{n}$ at $[H^+] = 0$ gives $\frac{1}{K_1} = 1.9 \times 10^{-3}$. Consequently, $K_1 = 5.3 \times 10^2$ or $10^{2.72}$. This agrees quite well with the values reported in "Stability Constants" (22), which range from $10^{2.30}$ (at 25°C and 0.5M $NaClO_4$) to $10^{3.02}$ (at 18°C and 0.066M $NaClO_4$). The two values given for 20°C and an ionic strength of 0.1, conditions which most closely resemble those of this experiment, are $10^{2.62}$ and $10^{2.66}$.

The slope of Figure 2-17 which is equal to K_1K_a is 14.9 If the experimental value for K_1 is used, K_a becomes 2.8×10^{-2} or $10^{-1.55}$. This is an excellent agreement with the value of $10^{-1.59}$ found by Reynolds and Fukushima (31) at 25°C and I = 0.1, and serves to verify further the experimental technique and procedure.

One can now apply this stability constant for $FeSO_4^+$ to the mine-water system using the same technique as that employed for phosphato-complexes of Fe(III) in lakes. At pH-values greater than 2, the magnitude of K_a indicates that most of the sulfate exists as SO_4^{-2}, i.e., $[SO_4^{-2}] = S_T = 10^{-2}M$. If the desired relationships are arranged based upon the previously-discussed equilibria (equations 2-28a and 2-23a), then, for 25°C, I = 0.1, and $S_T = 10^{-2}M$, the extent of coordination is given as

pH	$\frac{[FeSO_4^+]}{[Fe^{+3}]} = K_1S_T$	$\frac{[FeOH^{+2}]}{[Fe^{+3}]} = \frac{Q_h}{[H^+]}$
3	$10^{0.7}$	$10^{0.54}$
2	$10^{0.7}$	$10^{-0.46}$

Hence, it is evident that under conditions of low pH and high concentrations of ligand, as in mine drainage waters, complex-formation can be significant.

2-4 Oxidation-Reduction Reactions of the Iron(II)-Iron(III) System

In oxygenated waters, it is well-known that ferrous iron is thermodynamically unstable, being oxidized to ferric iron. Iron undergoes reversible oxidation and reduction reactions dependent upon given solution conditions. Oxidation-reduction equilibria relate the various oxidation states of a certain element and are characterized by the thermodynamic redox potential, E, in accordance with the classical Nernst Equation. Such a systematization is analogous to that of considering acid-base equilibria as ratios between protonated and deprotonated bases characterized by an acidity potential defined in terms of the change in free energy for the proton transfer reaction. Hence, the electron intensity can be treated in the same manner as the proton intensity or the activity of the hydrogen ion (32). For example,

$$pH = -\log (H^+) = \frac{\Delta F_H}{2.3\ RT} \qquad p\epsilon = -\log (e^-) = \frac{\Delta F_E}{2.3\ RT} \qquad (2\text{-}34)$$

$$pH = -E_G/0.0592 \qquad p\epsilon = -E_R/0.0592$$

The quantity 0.0592 assumes one mole of protons or electrons transferred, at 25°C. E_G refers to the acidity potential, the potential at the glass electrode or some other electrode for measuring pH, E_R refers to the reversible redox potential at an inert electrode, and ΔF_H and ΔF_E refer to the

changes in free energy for the proton and electron transfer reactions, respectively. The term $p\epsilon$ is a convenient measure of electron intensity, and when seen in conjunction with an equivalent measure of proton intensity, ie., pH, its value can be further appreciated.

The distribution of the various species of iron which are stable under given solution conditions can be conveniently summarized with the aid of a $p\epsilon$ - pH diagram in which the predominant species are presented as a function of the two master variables, as shown in Figure 2-18. Such a diagram can be made to be three-dimensional by incorporating a third axis for total concentration of soluble iron, assumed to be 10^{-5}M in Figure 2-18. Actually, the solubility diagrams showing log Fe versus pH which were presented earlier are two-dimensional variations of such a master plot, in which $p\epsilon$ had arbitrarily been made constant.

Since the $p\epsilon$ -pH diagram is a theoretical one based entirely upon reversible Nernstian redox potentials, only well-defined systems where the measured potential is known to be reversible can be interpreted in terms of such a diagram. Due to the complexity of natural systems where several electroactive species exist, mere insertion of an electrode into the water will usually yield a mixed potential and, hence, cannot be related or defined in terms of a $p\epsilon$ -pH diagram. The diagram derives its main value in serving as a guide toward expected behavior under various conditions of pH and $p\epsilon$.

The thermodynamic equilibria diagramatically shown in Figure 2-18 are presented in Table 2-5 together with the corresponding relationship of $p\epsilon$ to pH. The values for the free energy used in these calculations were taken from the tabulation by Latimer (5) and the experimental

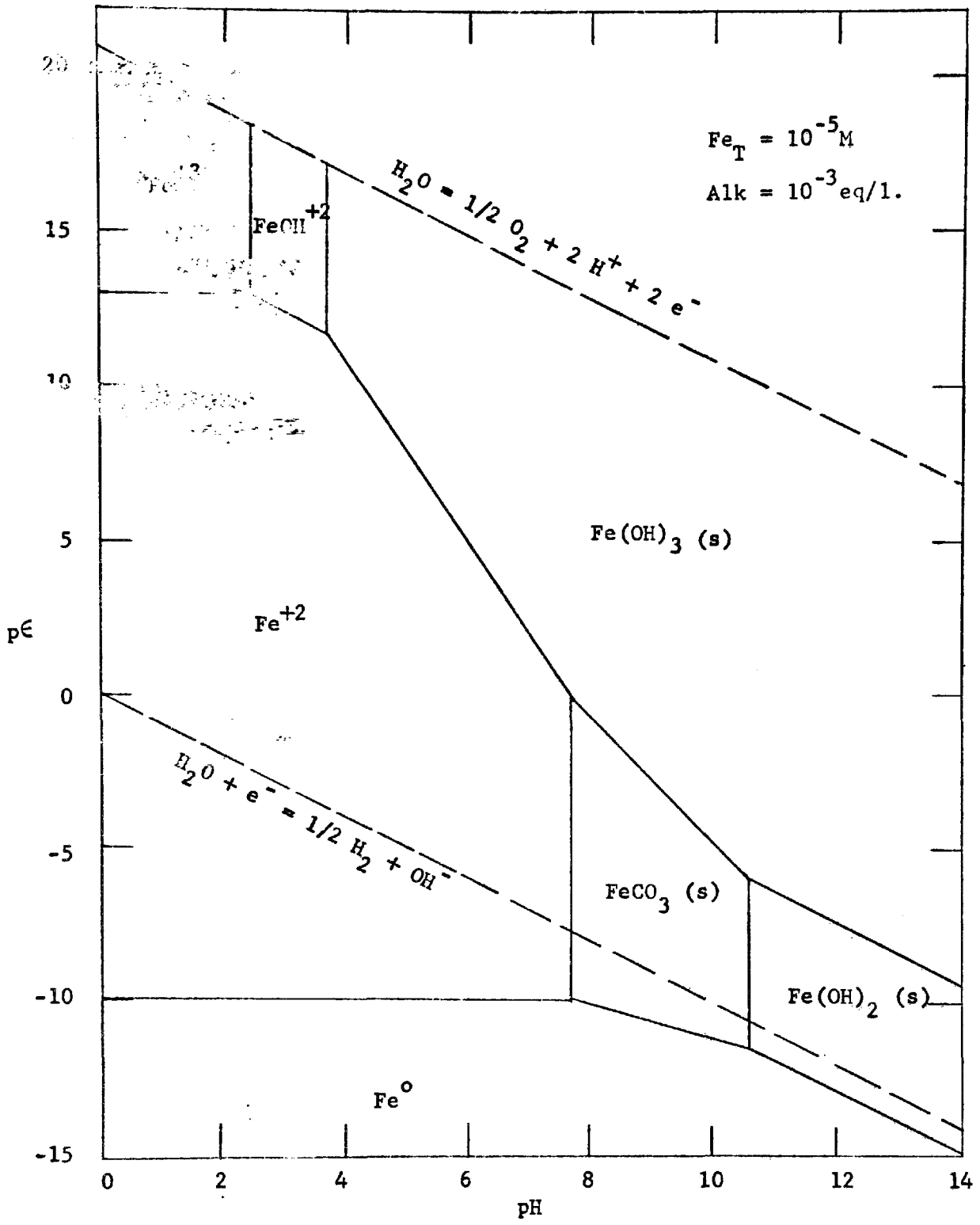

FIGURE 2-18 pE - pH diagram for iron. Concentration of soluble iron species is 10^{-5}M and alkalinity is 10^{-3}eq/1.

Table 2-5. Equilibria for Construction of pε -pH Diagram

Reaction	E^{o*}, volts	pε-pH Relationship
$2H_2O = O_{2(g)} + 4H^+ + 4e^-$	-1.23	$p\varepsilon = 20.8 - pH$
$2H_2O + 2e^- = H_{2(g)} + 2OH^-$	-0.828	$p\varepsilon = -pH$
$Fe^{+2} = Fe^{+3} + e^-$	-0.771	$p\varepsilon = 13.0 - \log \frac{(Fe^{+2})}{(Fe^{+3})}$
$Fe^{+2} + H_2O = FeOH^{+2} + H^+ + e^-$	-0.914	$p\varepsilon = 15.4 - pH - \log \frac{(Fe^{+2})}{(FeOH^{+2})}$
$Fe^{+2} + 2H_2O = Fe(OH)_2^+ + 2H^+ + e^-$	-1.19	$p\varepsilon = 20.1 - 2pH - \log \frac{(Fe^{+2})}{(Fe(OH)_2^+)}$
$Fe^{+2} + 3H_2O = Fe(OH)_{3(s)} + 3H^+ + e^-$	-1.06	$p\varepsilon = 17.9 - 3pH - \log (Fe^{+2})$
$Fe(OH)_{2(s)} + H_2O = Fe(OH)_{3(s)} + H^+ + e^-$	-0.274	$p\varepsilon = 4.63 - pH$
$FeCO_{3(s)} + 3H_2O = Fe(OH)_{3(s)} + HCO_3^- + 2H^+ + e^-$	-1.08‡	$p\varepsilon = 15.3 - 2pH$
$Fe^o = Fe^{+2} + 2e^-$	+0.440	$p\varepsilon = -9.93$
$Fe^o + HCO_3^- = FeCO_{3(s)} + H^+ + 2e^-$	+0.440‡	$p\varepsilon = -5.93 - 1/2\ pH$
$Fe^o + 2H_2O = Fe(OH)_{2(s)} + 2H^+ + 2e^-$	+0.048	$p\varepsilon = -0.97 - pH$

Reaction	pK	pH Relationship
$FeCO_{3(s)} + 2H_2O = Fe(OH)_{2(s)} + H^+ + HCO_3^-$	+13.6‡	$pH = 13.6 + \log(HCO_3^-)$
$Fe^{+3} + H_2O = FeOH^{+2} + H^+$	+2.17	$pH = 2.7 - \log \frac{(Fe^{+3})}{(FeOH^{+2})}$
$FeOH^{+2} + H_2O = Fe(OH)_2^+ + H^+$	+4.6	$pH = 4.6 - \log \frac{(FeOH^{+2})}{(Fe(OH)_2^+)}$
$FeCO_{3(s)} + H^+ = Fe^{+2} + HCO_3^-$	-0.09‡	$pH = 0.09 - \log (Fe^{+2}) - \log (HCO_3^-)$

*Computed from the tabulation of free energies given by Latimer (5).

‡Calculated using $\Delta F^o_{FeCO_3}$ = -160.5 Kcal./mole, determined experimentally in section 2-2.3.

solubility product of $FeCO_3$ (see section 2-2.3). It is clearly seen that in oxygenated natural waters, where $p\epsilon$ -values in the vicinity of the upper dotted line in Figure 2-18 are observed, ferric hydroxide is the predominant form of iron except in the acidic pH-range below 4, where the solubility of Fe(III) increases. In the absence of oxygen, as in hypolimnetic waters, most natural groundwaters, and in anaerobic biological systems such as sludge digesters, ferric iron is readily reduced by organic matter and by sulfide. The extent of the reduction depends upon the $p\epsilon$ and pH of the system, the form of the resultant Fe(II) also depending upon pH. The $p\epsilon$ of such systems is in the region of the lower dotted line in Figure 2-18.

Upon re-exposure to oxygen, Fe(III) again becomes the stable form of iron. The rate at which Fe(III) is formed, however, cannot be inferred from such thermodynamic considerations and requires investigation into the kinetics of oxidation of Fe(II). This is the basis for Chapter 3.

The $p\epsilon$ - pH diagram presented has been simplified in order to demonstrate the underlying principles describing the redox reactions between Fe(II) and Fe(III) in natural waters. For complex systems, however, the various soluble and insoluble species of Fe-S, as well as many of the Fe-organic complexes, should be superimposed on the diagram. Nevertheless, such simplified diagrams help to clarify the chemistry at work in aqueous solutions.

References

1) Stumm, W. and Lee, G. F., "The Chemistry of Aqueous Iron," Schweiz. Zeits. Hydrol., 22, 295 (1960)

2) Sillen, L. G., "Graphical Presentation of Equilibrium Data," Ch. 8, page 227, in Part 1, Volume 1, Treatise on Analytical Chemistry, I. M. Kolthoff and P. J. Elving, editors, Interscience, New York, (1959)

3) Leussing, D. L. and Kolthoff, I. M., "The Solubility Product of Ferrous Hydroxide and the Ionization of the Aquo-Ferrous Iron," Journ. Amer. Chem. Soc., 75, 2476 (1953)

4) Gayer, K. H., and Woontner, L., "The Solubility of Ferrous Hydroxide and Ferric Hydroxide in Acidic and Basic Media at 25°C," J. Phys. Chem., 60, 1509 (1956)

5) Ringbom, A., Solubility of Sulfide, Analytical Section, IUPAC (1953)

6) Latimer, W. E., The Oxidation States of the Elements and Their Potentials in Aqueous Solutions, second edition, Prentice-Hall Inc., Englewood Cliffs, N.J. (1952)

7) Ghosh, M. M., O'Connor, J. T., and Engelbrecht, R. S., "Rate of Precipitation of Iron in Aerated Groundwaters," Journ. San. Eng. Div., Proc. ASCE, 90, 199 (1966)

8) Hem, J. D., "Some Chemical Relationships Among Sulfur Species and Dissolved Ferrous Iron," U. S. Geol. Surv. Water Supply Paper 1459-C, Washington (1960)

9) Smith, H. J., "On Equilibrium in the System: Ferrous Carbonate, Carbon Dioxide and Water," Journ. Amer. Chem. Soc. 40, 879 (1918)

10) Kelley, K. K., and Anderson, C. T., "Contributions to the Data on Theoretical Metallurgy IV Metal Carbonates-Correlations and Applications of Thermodynamic Properties," Bulletin 384, U. S. Bureau of Mines, Washington (1935)

11) Hem, J. D., "Restraints on Dissolved Ferrous Iron Imposed by Bicarbonate, Redox Potential, and pH," U. S. Geol. Surv. Water Supply Paper 1459-B, Washington (1960)

12) Stumm, W., and Singer, P. C., "Precipitation of Iron in Aerated Groundwaters," discussion, Journ. San. Eng. Div., Proc. ASCE, 92 120 (1966)

13) Larson, T. E., "Oxidation of Metals and Ions in Solution," p. 433 in Principles and Applications of Water Chemistry, S. D. Faust and J. V. Hunter, editors, John Wiley and Sons, Inc., New York (1967)

14) Hem, J. D., "Manganese Complexes with Bicarbonate and Sulfate in Natural Water," Journ. Chem. Eng. Data, 8, 99 (1963)

15) Stumm, W., and Lee G. F., "Oxygenation of Ferrous Iron," Ind. Eng. Chem., 53, 143 (1961)

16) Lee, G. F., and Stumm, W., "Determination of Ferrous Iron in the Presence of Ferric Iron," Journ. Amer. Wat. Works Assn. 52, 1567 (1960)

17) Schindler, P. W., "Heterogeneous Equilibria Involving Oxides, Hydroxides, Carbonates, and Hydroxide Carbonates," Ch. 9, p. 196 in Equilibrium Concepts in Natural Water Systems, R. R. Gould, ed., Advances in Chemistry Series 67, Amer. Chem. Soc., Washington (1967)

18) Harned, H. S., and Scholes, S. R., "The Ionization Constant of HCO_3^- from 0 to 50°," Journ. Amer. Chem. Soc., 63, 1706 (1941)

19) Ghosh, M. M., O'Connor, J. T., and Engelbrecht, R. S., "Precipitation of Iron in Aerated Groundwaters," closure of discussion, Journ. San. Eng. Div., Proc. ASCE, 93, 118 (1967)

20) Amer. Soc. Testing Materials, X-Ray Powder Data File, Special Technical Publication No. 48-L, ASTM (1962)

21) Morgan, J. J., "Chemistry of Aqueous Manganese II and IV," Ph.D. Thesis, Harvard University (1964)

22) Sillen, L. G., and Martell, E. A., Stability Constants of Metal-Ion Complexes, Special Publication No. 17, London, The Chemical Society (1964)

23) Milburn, R. M., "A Spectrophotometric Study of the Hydrolysis of Iron III Ion. III Heats and Entropies of Hydrolysis," J. Amer. Chem. Soc., 79, 537 (1957)

24) Zharovskii, F. G., Trudy Kowissii Anolit Khim Akod Nank SSSR, 3, 101 (1951)

25) Galal-Gorchev, H., and Stumm, W., "The Reaction of Ferric Iron with Ortho-Phosphate," Journ. Inorg. Nucl. Chem., 25, 567 (1963)

26) Morgan, J. J., "Metal-Organic Complexes," paper presented at Univ. of Alaska Symposium on Organic Matter in Natural Water, Sept. 2-4, 1968, Fairbanks, Alaska

27) Lengweiler, H., Buser W., and Feitknecht, W., "Die Ermittling Der Loslichkeit von Eisen (III) - Hydroxiden Mit ^{59} Fe," Helv. Chim. Acta, 44, pp. 796 and 805 (1961)

28) Stumm, W., "Metal Ions in Aqueous Solution," p. 520 in Principles and Applications of Water Chemistry, S. D. Faust and J. V. Hunter, editors, John Wiley and Sons, Inc., New York (1967)

29) Willis, R. L. S., "Ferrous-Ferric Redox Reaction in the Presence of Sulfate Ion," Trans. Farod. Soc., 59, 1315 (1963)

30) Matoo, B. N., "Stability of Metal Complexes in Solution. III. Ion Association in Ferric Sulfate and Nitrate Solutions at Low Fe III Concentration," Zeits. for Phys. Chem. Nerre Folge, 19, 156 (1959)

31) Reynolds, W. L., and Fukushima, S., "Iron (II) and Iron (III) Isotope Exchange in Presence of Sulfate Ions," Inorg. Chem., 2, 176 (1963)

32) Stumm, W., "Redox Potential as an Environmental Parameter, Conceptual Significance and Operational Limitations," Proc. Third Intl. Conf. Wat. Poll. Research, Munich, Sept. 1966

CHAPTER 3

KINETICS OF OXYGENATION OF FERROUS IRON

3-1 Introduction

Ferrous iron is thermodynamically unstable in the presence of oxygen. The rate at which Fe(II) is converted to Fe(III) cannot be inferred from thermodynamic data but requires a thorough investigation of the kinetics of the oxidation, i.e., the mechanism by which the reaction occurs and the various factors which influence such a mechanism.

Conventional water treatment for the removal of iron consists of aeration of the raw water followed by sedimentation and filtration. The former process allows for the escape of CO_2, thus raising the pH, and for the introduction of oxygen which oxidizes Fe(II) to Fe(III). The latter hydrolyzes to form a precipitate which is subsequently removed by sedimentation and filtration.

In natural waters, the cycles of phosphorus and sulfur are interrelated with the iron cycle. The rate of oxidation of ferrous to ferric iron during the spring and fall overturn is, therefore, partially responsible for the rate of dissolution and oxidation of sulfide and for the rate of turnover of phosphate.

This chapter is comprised of experimental studies of the rate of oxygenation of ferrous iron in the neutral pH-range encountered in natural groundwaters, of heterogeneous oxygenation in the presence of precipitating

ferrous carbonate, and of oxygenation in the acidic pH-range typical of drainage waters from coal mines. A model is presented depicting the rate of oxidation of Fe(II) over the entire range of pH encountered in natural waters. The model is shown to be compatible with existing theories describing the mechanism by which Fe(II) is oxidized, and its characteristics and implications are explained in accordance with modern kinetic theory.

3-2 Oxygenation of Ferrous Iron at Neutral pH-Values

3-2.1 Oxidation in Natural Groundwaters

The deferrization of iron-bearing waters is customarily accomplished by oxidation of the ferrous iron in the raw water to insoluble ferric hydroxide utilizing dissolved oxygen. The reactions describing the process are

$$Fe^{+2} + 1/4\ O_2 + H^+ = Fe^{+3} + 1/2\ H_2O \qquad (3\text{-}1)$$

$$Fe^{+3} + 3H_2O = Fe(OH)_{3(s)} + 3H^+ \qquad (3\text{-}2)$$

It is well-established that the oxidation of Fe(II) in the neutral pH-range proceeds at a rate which is dependent upon the concentrations of Fe(II), dissolved oxygen, and OH^-, as shown in Table 3-1, in accordance with the rate expression

$$\frac{-d[Fe(II)]}{dt} = k[Fe(II)]\ P_{O_2}\ [OH^-]^2 \qquad (3\text{-}3)$$

The rate constant k is reported by Stumm and Lee(3) to be 8.0 ($\pm$ 2.5) x 10^{13} liter^2 mole^{-2} atm^{-1} min^{-1}; their results were derived for the

Table 3-1. Kinetics of Oxidation of Ferrous Iron

Rate Equation	Reference
$\frac{-d[Fe(II)]}{dt} = \frac{k[Fe(II)][O_2]}{[CO_2]^2}$	Just (1)
$= k'[Fe(II)][O_2][OH^-]^2$	Just (1)
$\frac{d[Fe^{+3}]}{dt} = k[Fe^{+2}][O_2]$	Holluta and Eberhardt (2)
where k = function of pH	
$\frac{-d[Fe(II)]}{dt} = k[Fe(II)][O_2][OH^-]^2$	Stumm and Lee (3)

pH-range 6.0 to 7.5. Just (1) and Stumm and Lee (3) carried out their studies in bicarbonate buffer systems, the latter work being conducted under conditions such that interference by precipitation of ferrous carbonate was precluded. The introduction of Fe(III) at concentrations up to 10^{-4}M had no effect on the rate of oxidation (3). The marked pH-dependence of the reaction rate should be noted; a 100-fold increase in rate was observed for each increase of one pH unit.

Ghosh, O'Connor, and Engelbrecht (4) conducted field studies of the rate of oxidation and removal of Fe(II) from natural groundwaters at eight water treatment plants in Illinois. Their results corroborated the first-order dependence of the reaction rate on [Fe(II)], but only a

remote relationship was observed between the rate and the pH of the system. However, since the reported variation in pH among the eight studies was only 0.3 pH units, one cannot justifiably conclude that pH is insignificant. On the other hand, a definite correlation was noted between alkalinity and rate of oxidation. Stumm and Lee (3) also noticed, in addition to the second-order dependence on $[OH^-]$, that the reaction proceeded at a slower rate in solutions of low alkalinity. This discrepancy was attributed to the slow response of the HCO_3^- - CO_2 buffer system to localized changes in acidity brought about by the oxygenation reaction, or to possible base catalysis by HCO_3^- or CO_3^{-2}. Apparently, higher alkalinities are associated with higher rates of oxidation.

The actual rate of removal of Fe(II) from natural waters (4) was found to be approximately one order of magnitude less than predicted by the studies of oxidation in synthetic systems (3). Ghosh, O'Connor, and Engelbrecht (4) observed removal of Fe(II) both by oxidation to insoluble $Fe(OH)_3$ (reactions 3-1 and 3-2) and by precipitation as $FeCO_3$, in accordance with

$$Fe^{+2} + HCO_3^- = FeCO_{3(s)} + H^+ \qquad (3\text{-}4)$$

Despite the dual mechanism for removal, the rate was still less than the predicted rate. Two explanations were given (5) for the slowness of the reaction in nature. Firstly, the field studies were conducted in waters of alkalinity three to five times less than the laboratory studies. Since the rate of the reaction is apparently accelerated by alkalinity, the reaction should proceed at a slower rate in the Illinois waters. Secondly, the presence of catalysts or inhibitors present in the natural

system could account for variations not only between the field and laboratory studies, but also among the different groundwaters themselves. Organic substances and sulfide compounds, in particular, were cited as inhibitory agents (5) (6) in accordance with the sequence

$$Fe(II) + 1/4\ O_2 + ORG. = Fe(III) - ORG.\ COMPLEX \qquad (3\text{-}5a)$$

$$Fe(III) - ORG.\ COMPLEX = Fe(II) + OXIDIZED\ ORG. \qquad (3\text{-}5b)$$

$$Fe(II) + 1/4\ O_2 + ORG. = Fe(III) - ORG.\ COMPLEX \qquad (3\text{-}5a)$$

In this scheme, the ferrous-ferric system functions as an electron-transfer catalyst for the oxidation of organic material by oxygen. The overall rate of oxidation of Fe(II) may be retarded depending upon the rate of oxygenation of Fe(II) in the presence of organic matter in comparison to the rate of reduction of Fe(III) by the organic matter.

The influence of such factors as these need to be quantitatively evaluated before the actual rate of oxidation of Fe(II) in natural systems can be predicted and before an efficient scheme for iron removal can be designed.

3-2.2 Oxidation of Fe(II) in the Presence of Ferrous Carbonate Oversaturation

It was indicated above that deferrization of iron-bearing waters may be achieved by precipitation of Fe(II) as $FeCO_3$, as well as by its oxidation to $Fe(OH)_3$. In fact, Hale (7) effected satisfactory removal of iron under anoxic conditions by the addition of hydrated lime in a closed system to precipitate $FeCO_3$ along with $CaCO_3$.

For a groundwater previously in equilibrium with siderite ($FeCO_3$, see section 2-2.2), aeration serves a dual purpose. In addition to introducing oxygen for oxidation of Fe(II), aeration allows dissolved carbon dioxide, with which the groundwater is oversaturated, to escape. Consequently, the pH of the system increases and the water becomes progressively oversaturated with respect to ferrous carbonate. If the degree of oversaturation becomes such that the energy barrier to nucleation is overcome, crystallization of $FeCO_3$ takes place and precipitation follows.

In this respect, it should be of interest to measure the rate of oxidation of Fe(II) under the influence of oversaturated conditions favoring precipitation of $FeCO_3$.

Experimental Procedure

A known gas mixture of carbon dioxide and oxygen was bubbled through a series of flasks containing sodium bicarbonate, mounted on magnetic stirrers. The CO_2 - HCO_3^- system buffers the solution with respect to pH. After the attainment of equilibrium, observed by a constancy in pH, various amounts of a stock solution of ferrous perchlorate were added to the bicarbonate solutions. (The stock solution of Fe(II) had previously been equilibrated with the same gas mixture.) The concentration of Fe(II) added was such that the resultant solution was oversaturated with respect to ferrous carbonate. The degree of oversaturation ($S = Q/K$, see section 2-2.2) was computed using the new solubility product for ferrous carbonate determined experimentally in Chapter 2. The rates of oxidation and removal were measured by analyzing the system for total and filterable ferrous iron, respectively.

For the determination of total Fe(II), aliquots were withdrawn from the system at various intervals, and immediately added to 2 ml. of concentrated $HClO_4$ in order to quench the reaction. Solutions of Fe(II) at concentrations greater than 10^{-4}M were analyzed by titration with standardized solutions of permanganate. For concentrations of Fe(II) less than 10^{-4}M, the colorimetric reagent bathophenanthroline was used (8).

Filterable Fe(II) was determined by immediately filtering aliquots of the suspension through 220 mu filter paper (Millipore Filter Corporation, Bedford, Mass.) into 2 ml. of concentrated $HClO_4$, again to stop the reaction. Filtration was rapid (less than 30 seconds for 50 ml. of sample) and was conducted under a partial pressure of CO_2 of one atmosphere in order to prevent additional oxidation and to avoid dissolution of any suspended $FeCO_3$. The filtrate was analyzed for Fe(II) by the same techniques as above.

pH and alkalinity were also measured during the course of the reaction, the latter determined by acidimetric titration to pH 4.3 with standardized HCl.

Experimental Results and Discussion

In discussing oxidation and removal of ferrous iron under conditions favoring precipitation of ferrous carbonate, previous workers have tended to oversimplify the mathematical and chemical formulations of the process. Ghosh, O'Connor, and Engelbrecht (4) combined precipitation of ferrous iron and oxidation of ferrous iron, arriving at a rate of iron removal which was first-order in concentration of Fe(II).

Conversely, in synthetic solutions having an initial oversaturation of 10 with respect to ferrous carbonate, Morgan and Birkner (9) observed that precipitation and removal of Fe(II) did not conform to first-order kinetics. They noted an immediate rapid decrease in filterable Fe(II) in their supersaturated systems, corresponding to concurrent precipitation of $FeCO_3$ and oxidation of Fe(II). Subsequently, the rate of disappearance of Fe(II) was in exact conformance with the first-order relationship observed in parallel studies conducted in the absence of conditions of oversaturation. The latter description and the rate constants reported were in agreement with those of Stumm and Lee (3).

In the experimental study of heterogeneous oxidation described here, no such simple explanation was apparent. Figure 3-1 demonstrates the compliance of both total Fe(II) and filterable Fe(II) to the first-order formulation, despite the fact that the system was 60 times oversaturated with respect to $FeCO_3$. The fact that only a slight increase in total removal of Fe(II) above that by oxidation alone is observed, is indicative of little precipitation of the carbonate. (Precipitation of $FeCO_3$ is manifested by the difference between the two curves.) It would appear that a period of 20 minutes was not sufficient to allow for crystallization of $FeCO_3$ at pH 6.61. The rate of oxidation is seen to agree with that predicted from the rate formulation by Stumm and Lee (3) for equivalent conditions of pH, partial pressure of oxygen, and temperature.

Correspondingly, at pH 6.25, where the rate of oxidation is slower, Figure 3-2 shows precipitation of $FeCO_3$ to become significant, but only after 40 minutes have elapsed. Again, the rate of oxidation

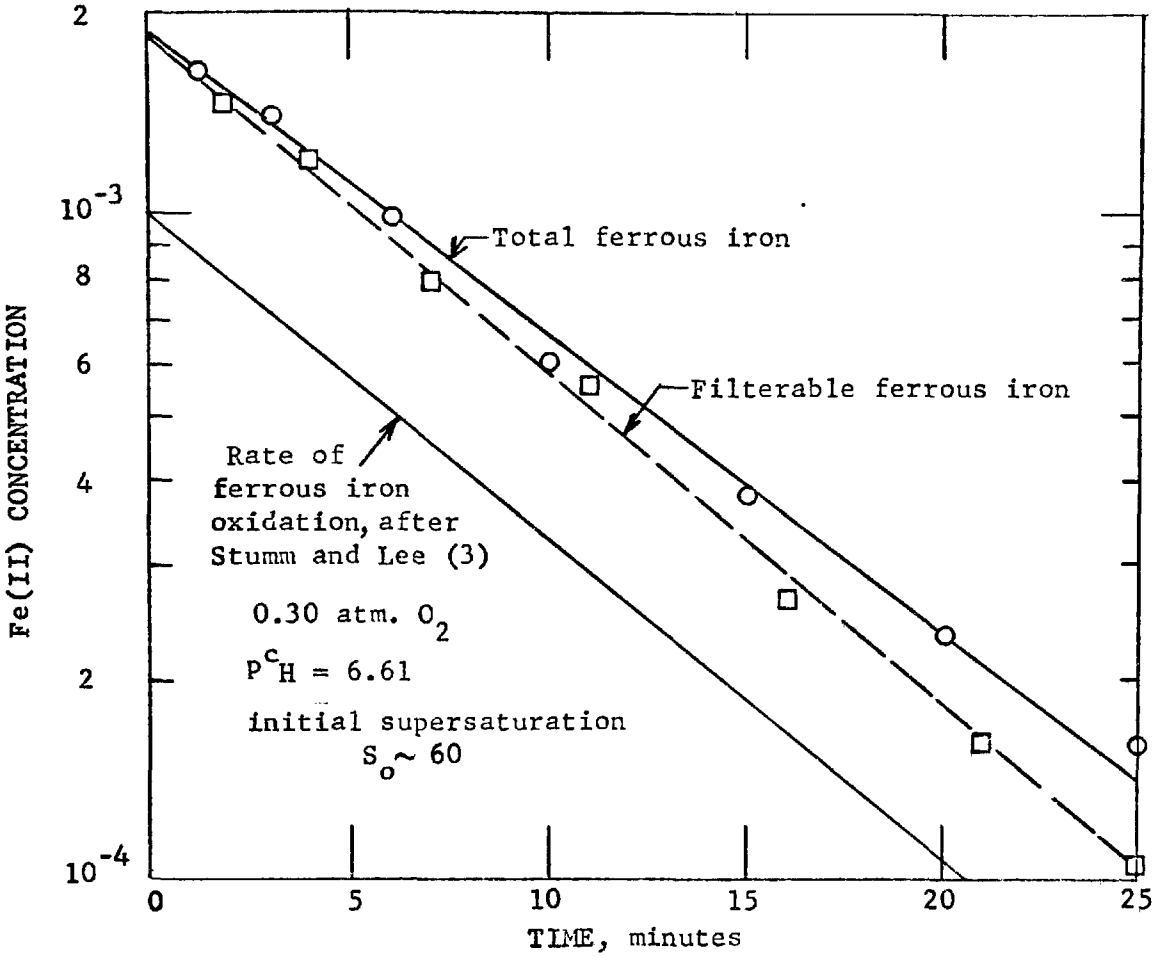

FIGURE 3-1. Oxidation and removal of ferrous iron under conditions favoring precipitation of ferrous carbonate.

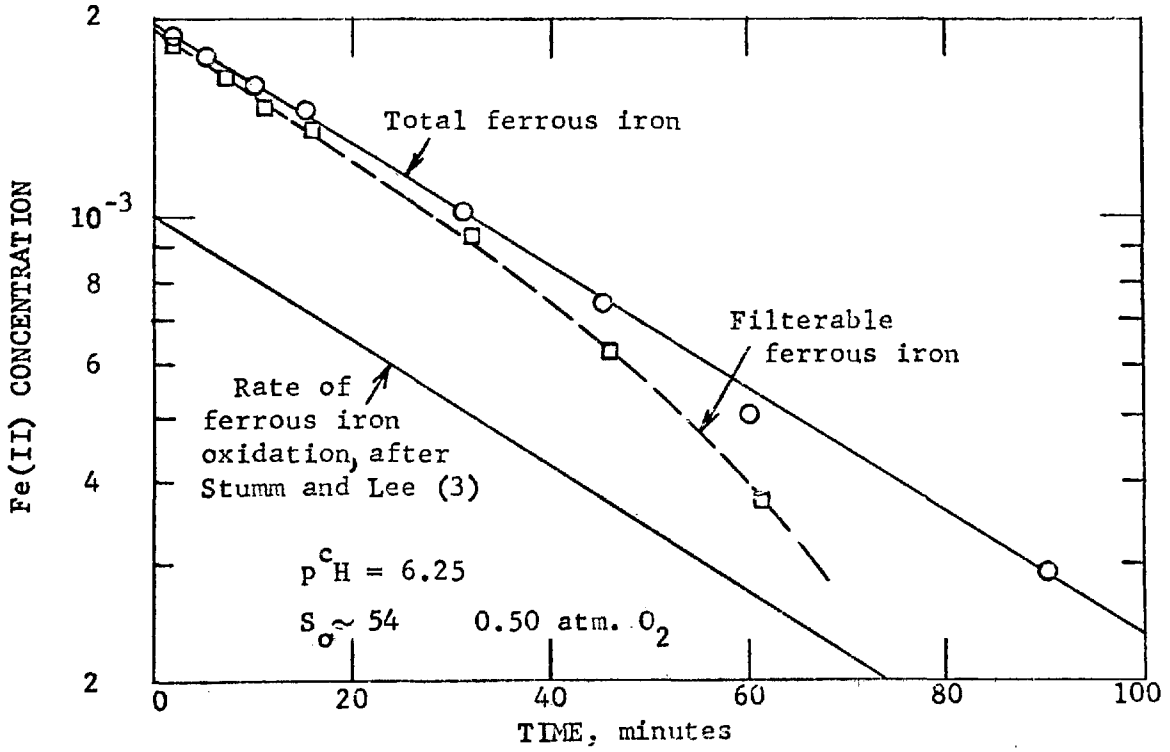

FIGURE 3-2. Oxidation and removal of ferrous iron under conditions favoring precipitation of ferrous carbonate.

of Fe(II) parallels that reported by Stumm and Lee(3) and is apparently unaffected by precipitation of $FeCO_3$.

As the pH is lowered still further, the elapsed time exceeds the induction time required for precipitation of $FeCO_3$ and the precipitate seems to exert a catalytic effect on the rate of oxidation of $Fe(II)_T$ (see Figure 3-3).

To demonstrate that this seemingly autocatalytic response in both the rates of oxidation and removal of Fe(II) is a function of the induction time for nucleation of ferrous carbonate, i.e., the time required to overcome the energy barrier preceding nucleation of the crystalline phase, the studies at higher pH were repeated but the experimental conditions were modified to decrease the rate of the oxidation reaction. Figure 3-4 resembles Figure 3-3, again showing a rapid decay in both total and filterable Fe(II) after their conformance to the accepted first-order relationship for the first 60 minutes.

These studies reflect the complex nature of heterogeneous reactions. For the case in question, the system consists of oxidation of dissolved ferrous iron, precipitation of ferrous iron as the carbonate, heterogeneous oxidation of solid ferrous carbonate, and possible surface-catalysis of the oxidation by ferrous carbonate. To represent such a system by a simple relationship would indeed be a mistake.

Although no conclusions can be drawn from this study, there are some pertinent points worthy of consideration:

i) Supersaturation with respect to some solid phase does not imply that precipitation takes place immediately. The magnitude of the activation energy barrier to the nucleation process is inversely

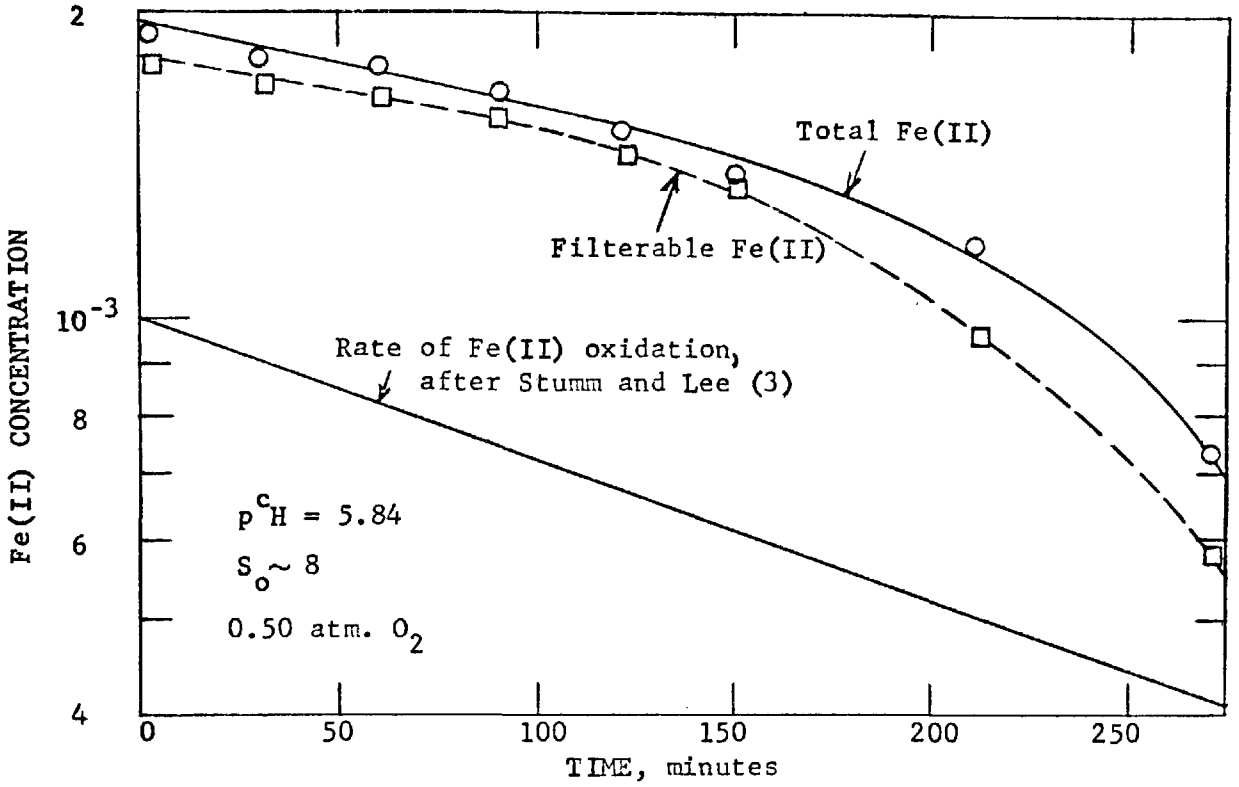

FIGURE 3-3. Effect of $FeCO_3$ precipitation on Fe(II) oxidation and removal.

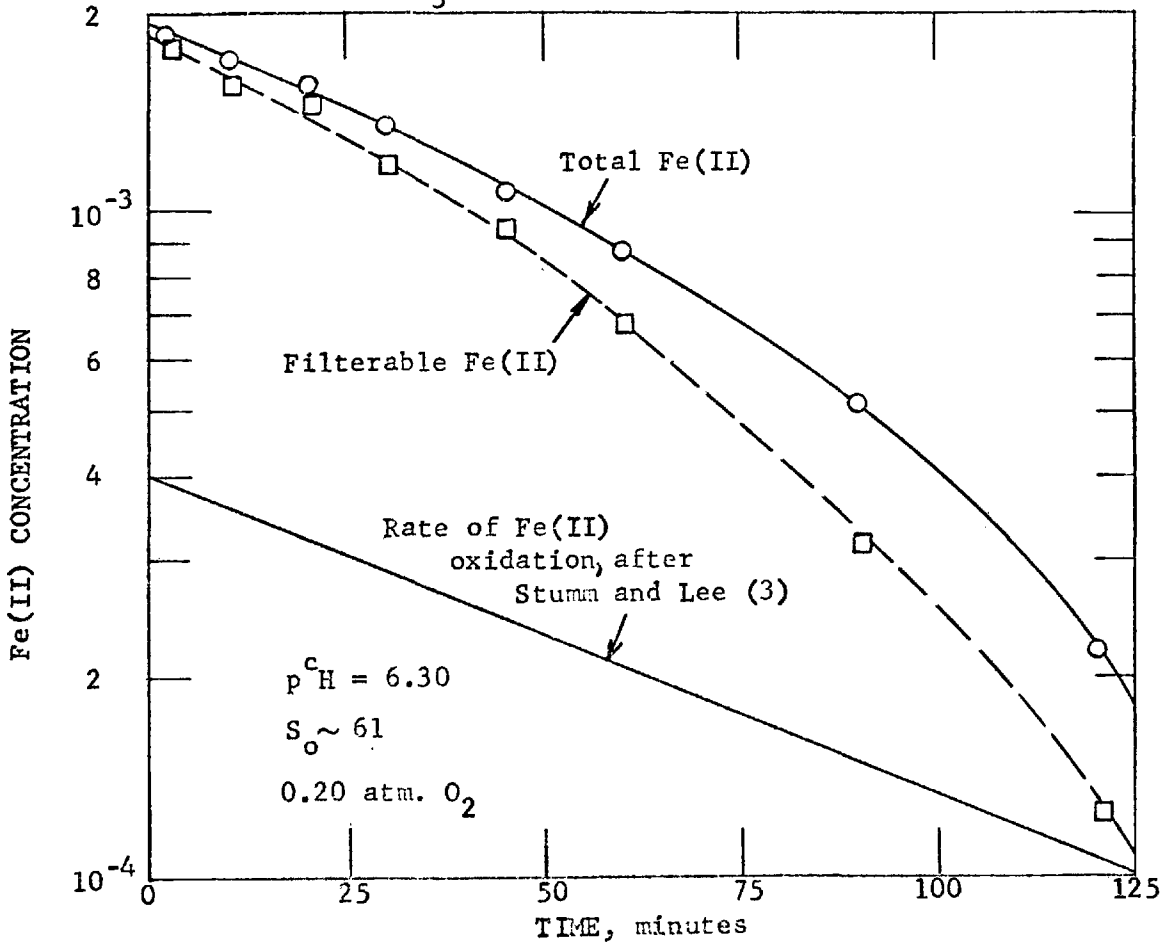

FIGURE 3-4. Effect of $FeCO_3$ precipitation on Fe(II) oxidation and removal.

proportional to the supersaturation, i.e., the activation energy decreases as the supersaturation increases. Consequently, the rate of nucleation is a function of the degree of supersaturation, there being a critical supersaturation value below which nucleation is extremely slow and above which nucleation is rapid. Therefore, the induction time, i.e., the time required for formation of the critical-sized cluster, decreases as the supersaturation increases (10).

ii) Precipitation of ferrous carbonate serves as a mechanism for removal of Fe(II), complementing removal by oxidation and hydrolysis. The rate of removal, however, cannot be described by first-order kinetics.

iii) Ferrous carbonate appears to play a catalytic role in the oxidation of Fe(II). The mechanism for such an effect is uncertain but could conceivably be attributed to a specific surface reaction whereby solid ferrous carbonate provides active sites at which the concentration of Fe(II) is greater than in bulk solution, or sites at which the reaction is favored. Although it has not been demonstrated, one can imagine that precipitation of ferrous carbonate could, under certain circumstances, inhibit the oxidation of Fe(II) by lowering the concentration of free ferrous iron in solution, or by decreasing the available Fe(II) exposed to oxygen with the remainder being incorporated in the interior lattice of the ferrous carbonate crystal. Such inhibition was observed by Morgan (11) in his study of Mn(II) oxygenation in the presence of precipitating manganous carbonate. In any case, even in the event that oxidation is inhibited, the rate of removal of Fe(II) either by oxidation or precipitation should be equally as great in the presence of $FeCO_3$ supersaturation as in its absence.

3-3 Oxygenation of Ferrous Iron in Acidic Systems

3-3.1 Experimental Study of Kinetics of Fe(II) Oxidation at Acidic pH-Values

The kinetic studies of the oxidation of ferrous iron reported above were confined to waters of pH greater than 6. There are a number of instances in nature, however, where iron bearing waters of pH considerably below 6 are encountered. Of special concern are those waters in coal mining regions, where pH-values of 3 are not uncommon (see Chapter 5). It would be of interest to learn if iron oxidation in such acidic systems could be characterized by the same kinetic relationships which describe the reaction in neutral waters.

Experimental Procedure

The rate of oxidation of Fe(II) was followed by measuring the concentration of Fe(III) with time and subtracting this quantity from the initial concentration of Fe(II). An analytical procedure was adopted whereby $[Fe(III)_T]$ (the total concentration of all species of ferric iron) was determined spectrophotometrically at the isosbestic point of an acidified solution where equilibrium had been established between free ferric iron, Fe^{+3}, and monohydroxo-ferric iron, $FeOH^{+2}$, the only soluble species of Fe(III) under the acidic conditions. At the isosbestic point of the system, at a wavelength of 272 mu, both species have identical molar absorptivities so that for a given total concentration of Fe(III), regardless of the ratio of Fe^{+3} to $FeOH^{+2}$, the same absorbance is recorded, independent of pH (see Figure 3-5). Figure 3-6 demonstrates conformance of the absorbance of acidified solu-

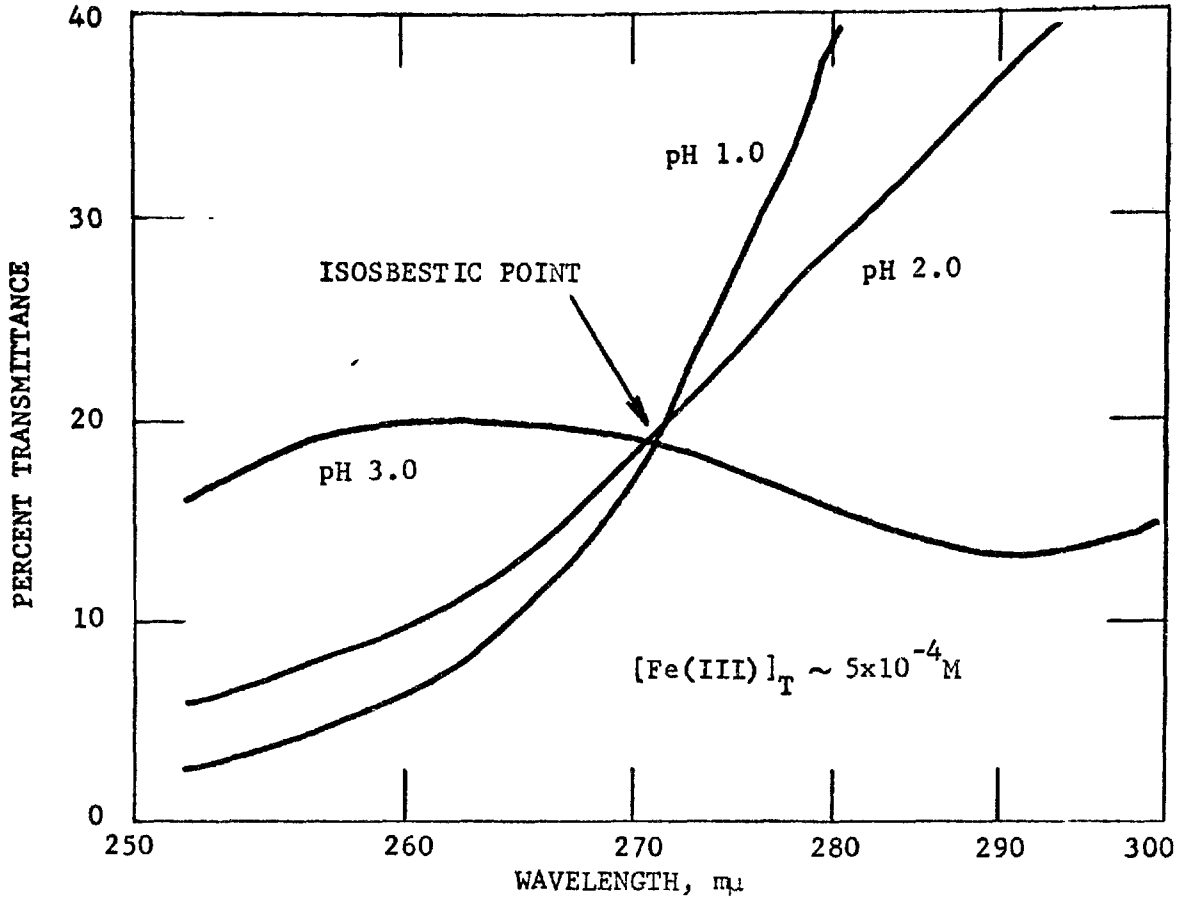

FIGURE 3-5. U-V absorbance spectra of acidified solutions of ferric perchlorate.

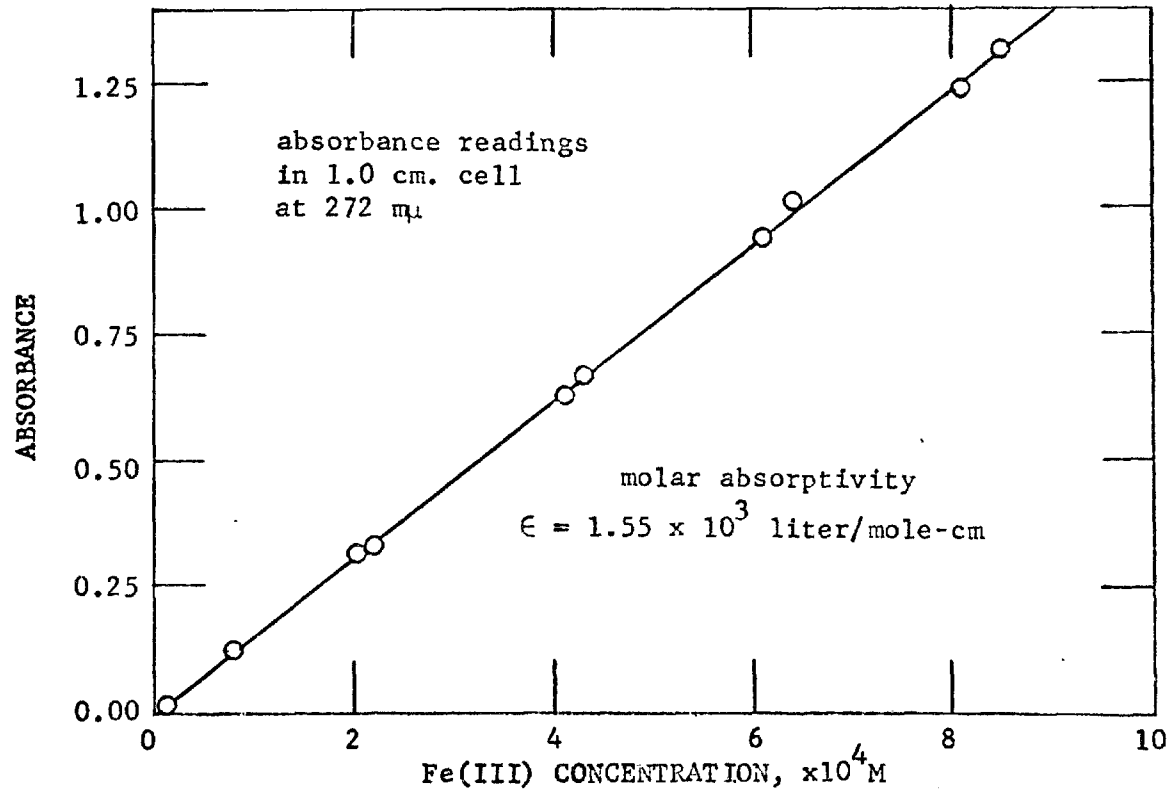

FIGURE 3-6. Relationship between absorbance of acidified solutions of Fe(III) and Fe(III) concentration, at 272 mμ.

tions of Fe(III), at 272 mu, to the Beer-Lambert law. The molar absorptivity is 1.55×10^3 $liter^1\text{-}mole^{-1}\text{-}cm^{-1}$ and is unaffected by the presence of Fe(II).

The samples were prepared containing various dilutions of a stock solution of ferrous perchlorate. In order to determine the dependence of the reaction rate on [Fe(II)], the studies were performed at constant pH and under constant partial pressures of oxygen. The investigations at slightly acidic pH-values were conducted in a CO_2-HCO_3^- buffer system, as in section 3-2.2, in order to maintain constant pH. At pH-values below 5, however, the buffer capacity of the bicarbonate system is insufficient to balance the acidity produced by hydrolysis of the resultant Fe(III) (reaction 3-2), so that the pH of the system tends to be drastically lowered. To combat this effect, smaller initial concentrations of Fe(II) were employed (less than 10^{-4}M) to insure that, for a given percent oxidation, the corresponding change in pH would be slight.

At still lower pH-values, in the vicinity of pH 3, no precautions were necessary since the pH was observed to remain relatively constant. In this range, the pH was adjusted merely by dropwise addition of concentrated $HClO_4$.

The samples were allowed to equilibrate with the oxygen of the atmosphere, or, in the case of the bicarbonate buffer systems, with the gas mixture of oxygen and carbon dioxide. [Fe(III)] was determined by acidifying an aliquot with dilute $HClO_4$ in order to dissolve any hydrous ferric oxide formed and then measuring its absorbance at 272 mu, employing a Beckman Model DU Spectrophotometer. For the smaller range of

concentrations, [Fe(II)] was determined directly using the colorimetric reagent bathophenanthroline (8). After each reading, the solutions were re-equilibrated with their respective atmospheres. The samples were sealed and stored in an incubator at 25°C. (In the lower pH-range, where the rate of oxidation was observed to be slowest, a series of parallel studies was conducted in the dark and exposed to light in order to test for any photochemical effect on the rate of oxidation.)

Experimental Results and Discussion

In order to describe the rate of oxygenation of ferrous iron, an expression similar to that of Stumm and Lee (3) was assumed, of the form

$$\frac{-d[Fe(II)]}{dt} = k\,[Fe(II)]^m[OH^-]^n\,P_{O_2} \qquad (3\text{-}6)$$

where m and n are constants to be determined. In the rate law of Stumm and Lee (3) at pH-values greater than 6, m = 1 and n = 2. Since the studies were conducted at constant pH and constant partial pressure of oxygen, equation 3-6 can be simplified to

$$\frac{-d\,[Fe(II)]}{dt} = k'\,[Fe(II)]^m \qquad (3\text{-}7)$$

where

$$k' = k\,[OH^-]^n\,P_{O_2} \qquad (3\text{-}8)$$

If the reaction were first-order in [Fe(II)], i.e., if m = 1, then

$$\frac{-d\,\log\,[Fe(II)]}{dt} = k'/2.3 = k'' \qquad (3\text{-}9)$$

and a plot of log [Fe(II)] versus time should be linear.

Figure 3-7 presents some of the results obtained in the bicarbonate-buffered system, demonstrating the obedience of the data to equation 3-9. The concentrations of Fe(II) have been carefully selected so that the solubility of ferrous carbonate was not exceeded. Equation 3-9 demands that the slope of the semilog plot be independent of the concentration of Fe(II) at any time, so that parallel lines of slope k" should result regardless of the initial concentration of Fe(II). Figure 3-7 conforms to this requirement, too.

At the lower pH-values where the buffer capacity of the system was low, the pH slowly declined as the reaction proceeded. The accompanying decrease in pH was smallest for the smallest initial concentration of Fe(II), as planned. In these studies, the course of the reaction was followed as long as the pH did not differ greatly from its starting value. Figures 3-8 and 3-9 are plots of log [Fe(II)] with time and also show the corresponding change in pH. Conformance to the first-order expression is demonstrated. When the studies were terminated, approximately 25% of the initial concentration of Fe(II) had been oxidized.

Figures 3-10 and 3-11 depict the rate of oxidation at pH 3 and pH 2, respectively. These results have also been fitted by a first-order rate expression, but this has been done only for convenience and for the sake of comparison both with the above results and with those of Stumm and Lee (3). For a reaction proceeding as slowly as this one does in the low pH-region, where only 5% of the reaction is complete in 150 days, it becomes difficult to characterize the reaction with respect to its kinetic order. The "first-order rate constant" is approximately 1×10^{-4} day^{-1} for both figures, even though the concentration of OH^- differs by

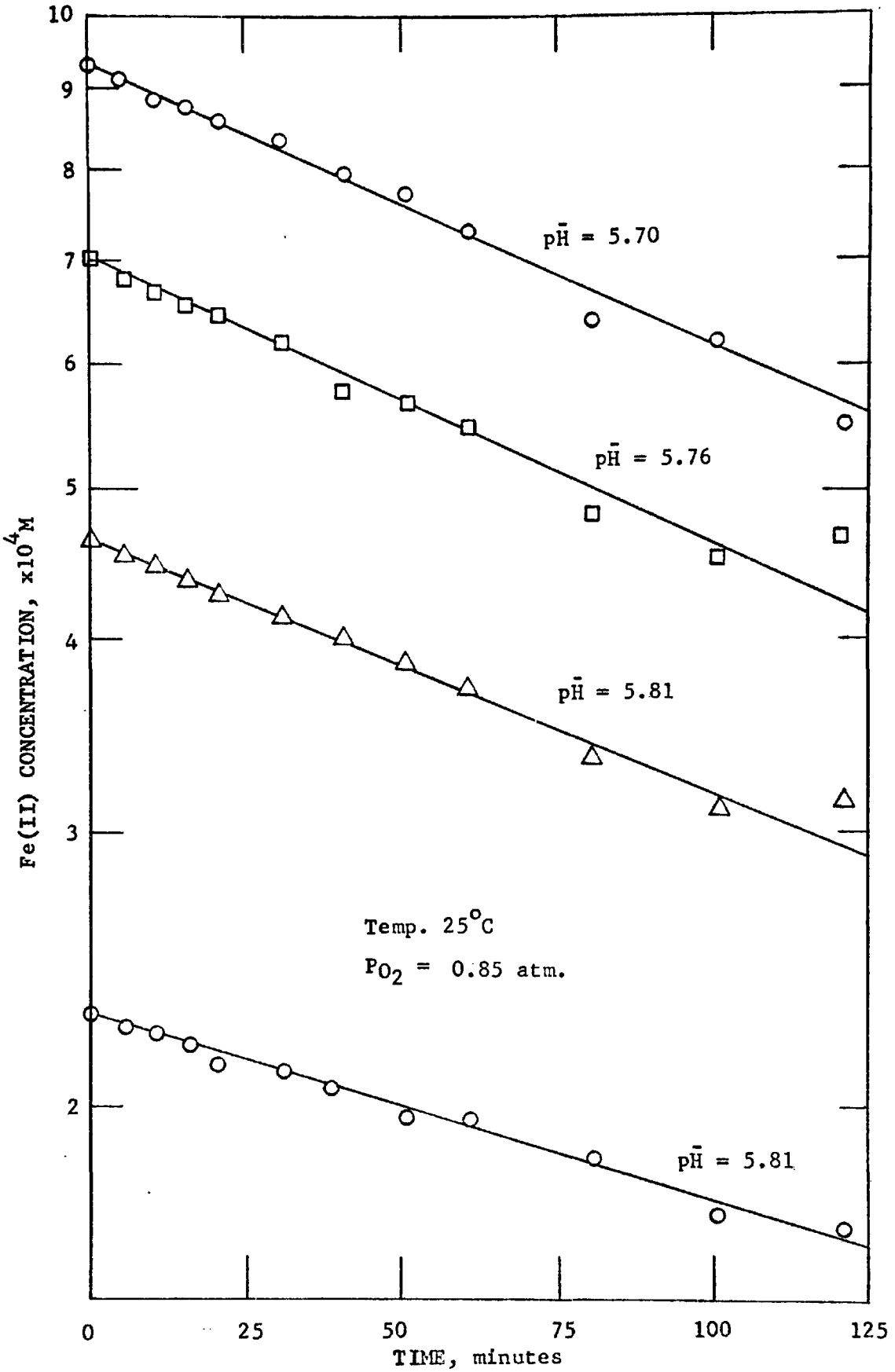

FIGURE 3-7. Rate of oxygenation of Fe(II) in bicarbonate-buffered systems.

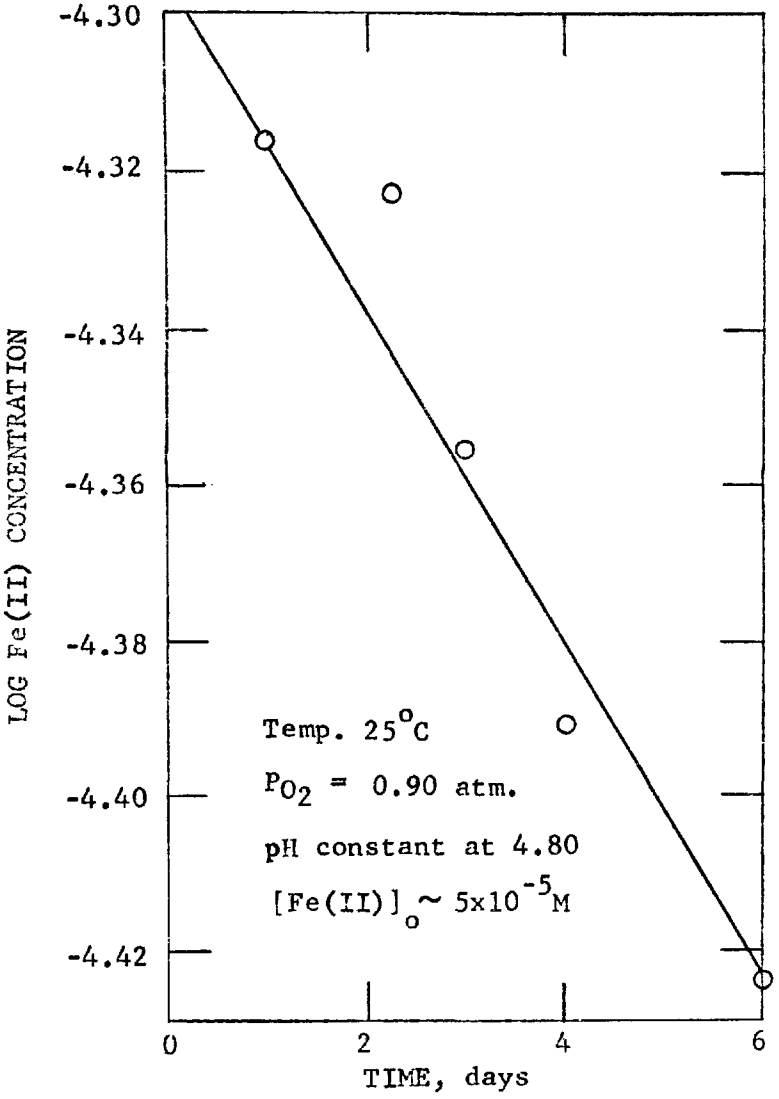

FIGURE 3-8. Rate of oxygenation of Fe(II).

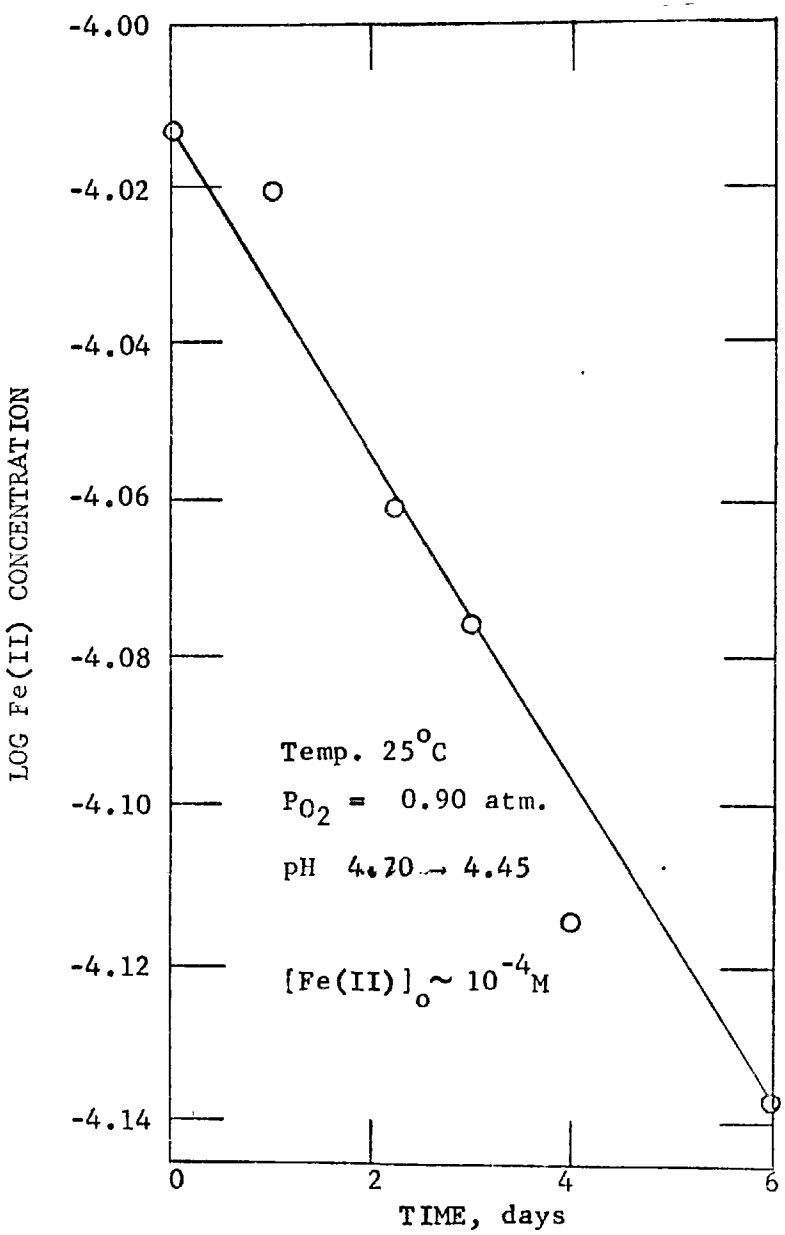

FIGURE 3-9. Rate of oxygenation of Fe(II).

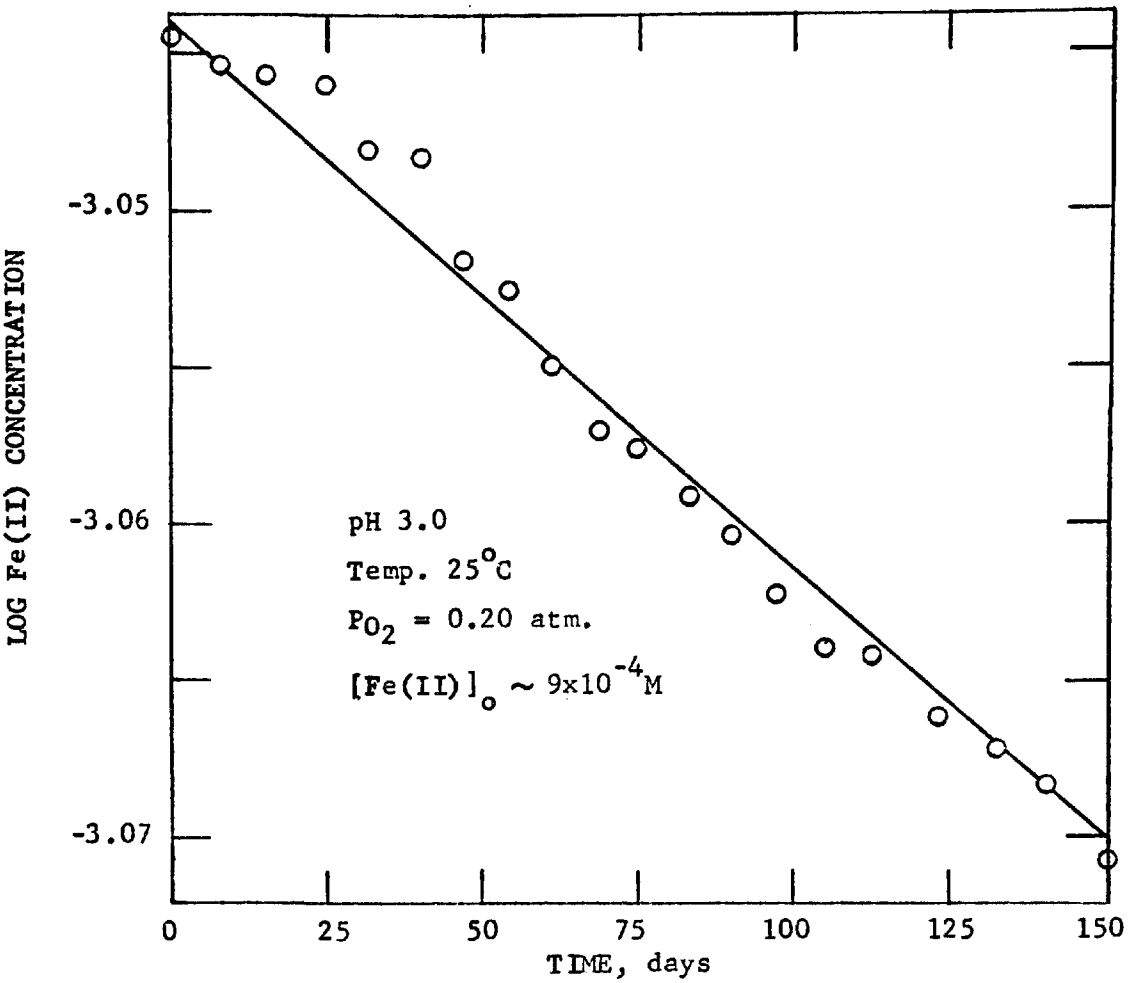

FIGURE 3-10. Oxygenation of Fe(II) at pH 3.

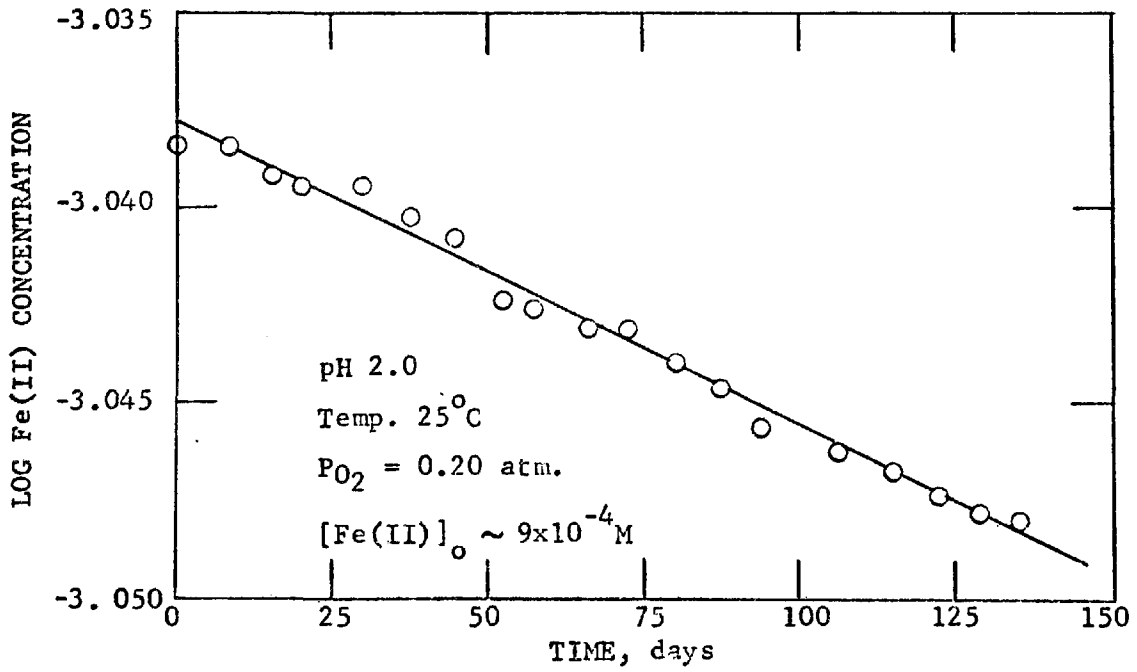

FIGURE 3-11. Rate of oxygenation of Fe(II) at pH 2.

an order of magnitude between them. In fact, additional studies in this acidic pH-range show the rate of oxidation to be relatively independent of pH.

To gain some additional insight as to the order of the reaction rate with respect to [Fe(II)] in this pH-range, further studies were conducted at differing initial concentrations of Fe(II). The parallel slopes in Figures 3-12a through d also imply that the reaction is first-order in [Fe(II)], but this allegation is subject to the same reservations as above.

Because of the slowness of the reaction, the analytical procedure consisting of the spectrophotometric measurement of Fe(III) proved to be the most effective. However, the technique is not amenable for use over a wide range of initial concentrations of Fe(II). At low concentrations, the amount of Fe(III) produced by the oxidation reaction is so small that the measurements of absorbance become less precise. At higher initial concentrations of Fe(II), a sufficient amount of Fe(III) forms that even at pH 3, kinetically irreversible hydrolysis of Fe(III) takes place (see Chapter 4) and it becomes increasingly more difficult to recover all of the Fe(III) as Fe^{+3} or $FeOH^{+2}$. For this reason, the order of the reaction with respect to Fe(II) at this low pH could not be adequately verified by simply varying Fe(II) over a wide range of initial concentrations. Figure 3-12 shows only a three-fold variation in initial concentration of Fe(II). One can conclude from these results only that the reaction is extremely slow and, in this range of concentration, can be represented by a rate expression which is first-order in [Fe(II)].

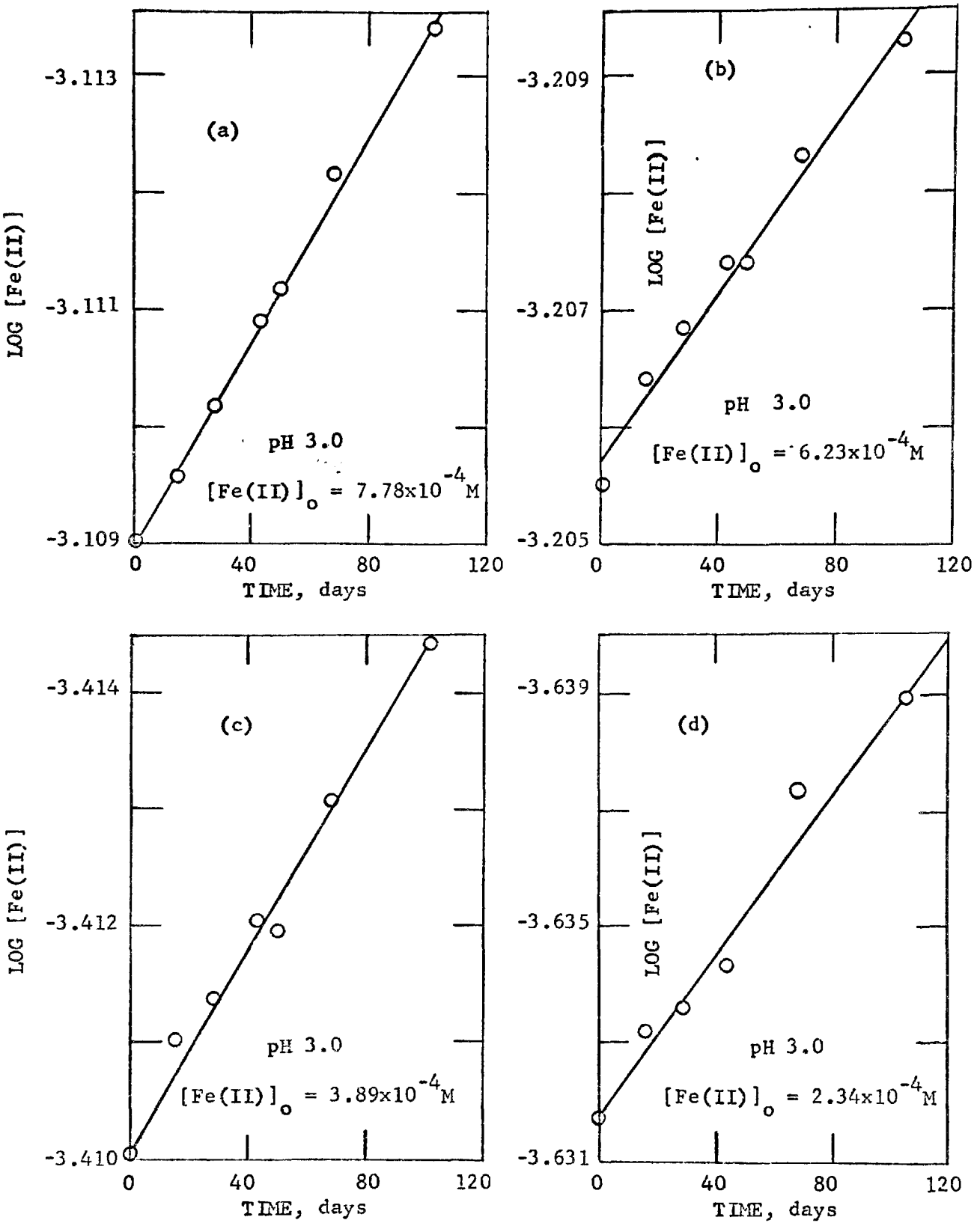

FIGURE 3-12. Oxygenation of ferrous iron at various initial concentrations of Fe(II). Solution conditions are pH 3.0, 25°C, and partial pressure of oxygen of 0.20 atm.

George (12) studied the oxidation of Fe(II) in perchloric acid media and observed a rate law of the form

$$\frac{-d\,[Fe^{+2}]}{dt} = k_{exp}\,[Fe^{+2}]^2[O_2] \qquad (3\text{-}10)$$

where the rate constant, k_{exp}, increased slightly with a decrease in $[H^+]$. The relative insignificance of pH upon the rate (from pH 0 to pH 2) is similar to that obtained in this study, but George has characterized the rate as being dependent upon $[Fe^{+2}]^2$.

Huffman and Davidson (13) have generalized from their own results and those of others that the rate of oxidation is first-order in $[Fe^{+2}]$ in the presence of strong complex-formers, such as pyrophosphate, fluoride, and dihydrogen phosphate. For complexing agents of moderate strength, such as chloride and sulfate, the reaction rate depends upon $[Fe^{+2}]^2$. However, under extreme conditions of temperature and concentration of ligand, the dependence is again first-order. The results of George (12) in perchlorate media are analogous to those in the presence of moderate complex-formers. Although sufficient data are not available, it seems that, in the presence of suitable anions, the relative reaction rates for the bimolecular mechanism (first-order in both $[Fe^{+2}]$ and $[O_2]$) generally parallel the stability constants for association of the ligands with Fe^{+3} (13).

3-4 Oxygenation of Ferrous Iron as a Function of pH

3-4.1 Summary of Experimental Results

By coupling the experimental results obtained for acidic systems with those obtained by Stumm and Lee (3) for neutral waters, one can plot the rate of oxygenation of ferrous iron over the entire pH-range of interest in natural waters, as in Figure 3-13. The rate of reaction has been characterized by the rate constant, $k'' = -d \log [Fe(II)]/dt$, and has been adjusted for the conditions at 25°C and a partial pressure of oxygen equal to 0.20 atm.

If one takes the logarithm of equation 3-8, substituting $k'' = k'/2.3$ (from 3-9) and making use of the ion product of water, one obtains

$$\log k'' = \log C + n \text{ pH} \qquad (3\text{-}11)$$

where C is a constant and n is the order of the reaction with respect to $[OH^-]$. It is readily apparent that the instantaneous slope of the log k'' versus pH curve in Figure 3-13 corresponds to n. The solid line above pH 6 derives from the experimental rate law of Stumm and Lee (3) (equation 3-3) for the given conditions, with n = 2. The dotted portion below pH 6 is an extrapolation of their expression to the acidic pH-region of this study; the rate diminishes by a factor of 100 for each unit decrease in pH. The experimental points are compatible with the formulation of Stumm and Lee at pH-values greater than 4.5, but at lower pH-values, the points sytematically deviate from the extrapolated line. At pH-values below 3, the rate becomes relatively constant and is no longer dependent upon pH, i.e., n = 0.

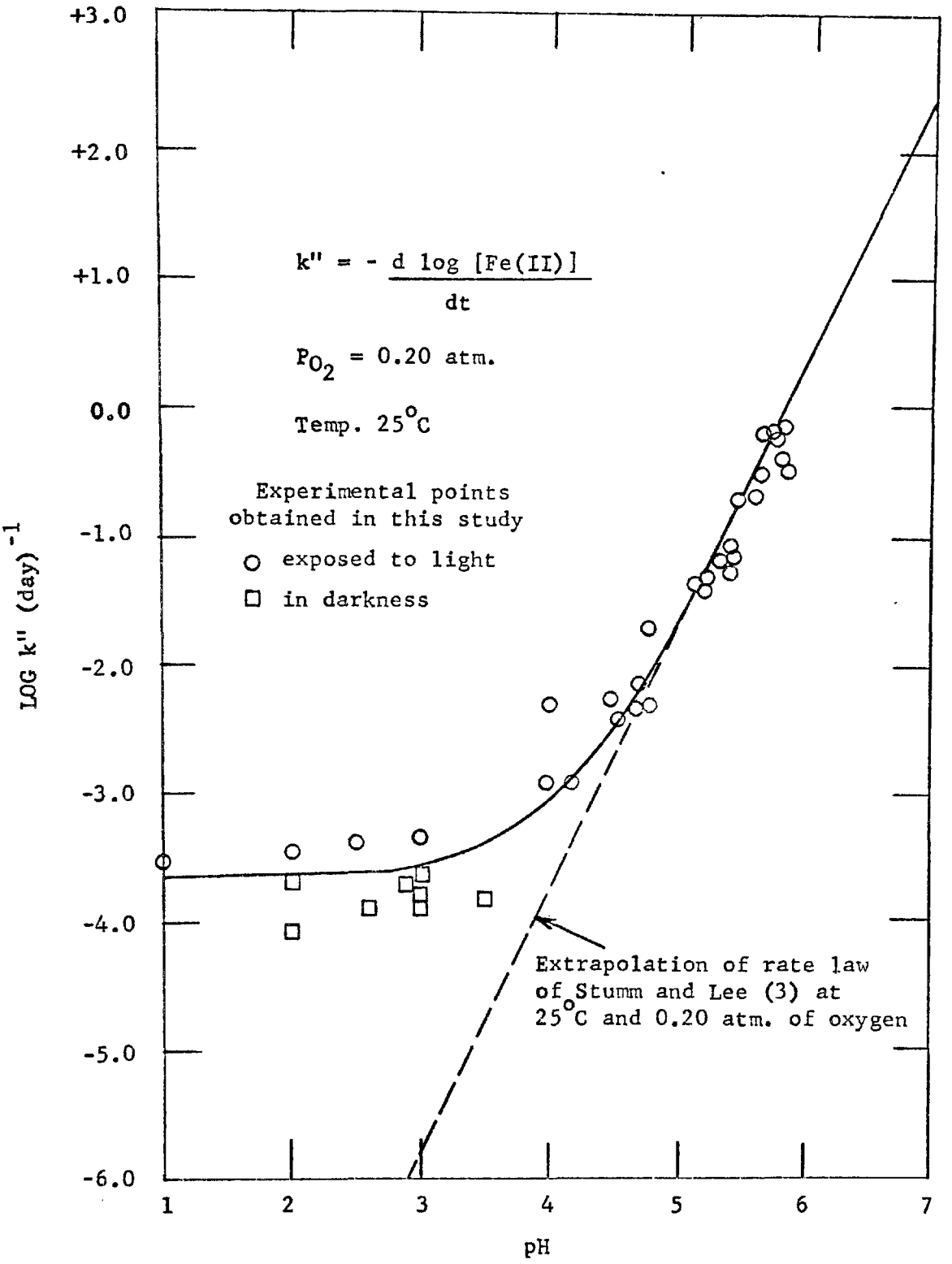

FIGURE 3-13. Oxygenation rate of ferrous iron as a function of pH.

With regard to the relative magnitude of George's results (12) in comparison with those presented in Figure 3-13, one can approximate his rate expression (equation 3-10) by a pseudo-first-order formulation

$$\frac{-d[Fe^{+2}]}{dt} = k'_{exp}[Fe^{+2}] \tag{3-12}$$

where

$$k'_{exp} = k_{exp}\,[Fe^{+2}]_o\,P_{O_2} \tag{3-13}$$

$[Fe^{+2}]$ is essentially constant for only 1% total reaction (the extent of the reaction followed by George) and is equal to $[Fe^{+2}]_o$, the initial concentration of ferrous iron. This approximation is not a mechanistic one but has been made solely for the purpose of comparison. Under a partial pressure of oxygen of 0.2 atm. and at 30^oC and $10^{-2}M$ $HClO_4$, George's results predict that the initial value of k" (k" = -d log [Fe(II)]/dt as in Figure 3-13) would be approximately $1 \times 10^{-4} day^{-1}$ if $[Fe^{+2}]_o = 10^{-2}M$, the concentration used by George. This pseudo-first-order "rate constant" is of the same order of magnitude as that obtained in this study.

The shape of the curve suggests that there are two parallel reaction mechanisms; one operative at higher pH which can be described by the rate law of Stumm and Lee, and the other functioning under more acidic conditions and independent of pH. Previous investigations of the kinetics of oxygenation of Fe(II) in acidic media are in accord with these latter results in that the rate of the reaction is relatively independent of pH. In fact, George (12) observed that his k_{exp} (see equation 3-10) was proportional to $[H^+]^{-0.23}$, increasing only slightly

with an increase in pH. Alternatively, one can consider the reaction to be independent of pH until the concentration of OH^- becomes sufficiently large that OH^- functions as an effective catalyst of the oxidation reaction.

Figure 3-13 also demonstrates that the oxidation of Fe(II) occurs more rapidly in light than in darkness; the reaction proceeds at a rate 2 to 3 times faster in the presence of light. In the acidic region, there appears to be some photooxidation of Fe(II) taking place.

In further studies of the oxidation of Fe(II) under simulated mine conditions (see Chapter 5), the investigations were conducted in the absence of light to avoid such photochemical effects.

3-4.2 Kinetic Implications of Results

Consider first the oxidation of Fe(II) in the acidic region where the reaction proceeds at a rate independent of pH. Weiss (14) proposed a chain mechanism involving one-electron oxidations in order to describe the oxidation of ferrous iron by molecular oxygen. The suggested sequence is:

$$Fe^{+2} + O_2 = Fe^{+3} + \dot{O}_2^- \qquad (k_1,\ k_1') \qquad (3\text{-}14a,b)$$

$$\dot{O}_2^- + H^+ = H\dot{O}_2 \qquad (K_{HO_2}) \qquad (3\text{-}15)$$

$$Fe^{+2} + H\dot{O}_2 = Fe^{+3} + H\dot{O}_2^- \qquad (k_2, k_2') \qquad (3\text{-}16a,b)$$

$$H\dot{O}_2^- + H^+ = H_2O_2 \qquad (K_{H_2O_2}) \qquad (3\text{-}17)$$

$$Fe^{+2} + H_2O_2 \rightarrow Fe^{+3} + OH^- + \dot{O}H \qquad (k_3) \qquad (3\text{-}18)$$

$$Fe^{+2} + \dot{O}H \rightarrow Fe^{+3} + OH^- \qquad (k_4) \qquad (3\text{-}19)$$

The molecules ($\cdot$) are free radicals or reactive intermediates. Reaction 3-14a is believed to be the rate-determining step in the sequence. The rate of oxidation of Fe^{+2} can be derived using steady-state approximations (15) for $H\dot{O}_2$, $\dot{O}H$, and H_2O_2 to give (16)

$$\frac{-d\,[Fe^{+2}]}{dt} = k_1\,[Fe^{+2}]\,[O_2]\,R_1 \qquad (3\text{-}20)$$

where

$$R_1 = \frac{k_2\,[Fe^{+2}]\,[H^+]}{k_2\,[Fe^{+2}]\,[H^+] + k_1'\,K_{HO_2}[Fe^{+3}]} \qquad (3\text{-}20a)$$

Equation 3-20a implies that the oxidation reaction is inhibited by Fe^{+3} due to the back reaction 3-14b. This accounts for the slowness of the reaction in acidic solutions where the resultant Fe(III) is present predominantly as Fe^{+3}. If conditions are such that

$$k_1'\,K_{HO_2}\,[Fe^{+3}] \gg k_2\,[H^+]\,[Fe^{+2}] \qquad (3\text{-}20b)$$

then $R_1 \ll 1$, and the reaction is decelerated because of the relatively rapid reduction of Fe^{+3} by $\dot{O}_2^-$ in comparison to the oxidation of Fe^{+2} by $\dot{O}_2^-$ or $H\dot{O}_2$ (equation 3-16a).

If, on the other hand, anions are present which are capable of forming strong complexes with Fe^{+3}, such complex-formation serves to decrease the concentration of free Fe^{+3} and thus inhibit the back reaction (3-14b). The net effect is to cause the oxidation to proceed more rapidly since

$$k_1'\,K_{HO_2}\,[Fe^{+3}] \ll k_2\,[H^+]\,[Fe^{+2}] \qquad (3\text{-}20c)$$

and R~1. Hence, by equation 3-20

$$\frac{-d\,[Fe^{+2}]}{dt} = k_1\,[Fe^{+2}]\,[O_2] \qquad (3\text{-}20d)$$

One serious drawback of the Weiss mechanism is its unlikelihood from a coulombic standpoint. Zwolinski, Marcus, and Eyring (17) termed the formation of oppositely-charged end-products, as in 3-14a, as highly improbable. In a later paper, Weiss (18) modified his mechanism in accordance with such reasoning to consider that the initial reaction, 3-14a, should be the formation of an ion-pair complex

$$Fe^{+2} + O_2 = (Fe^{+3}\cdot O_2^{-}) \qquad (3\text{-}21)$$

stabilized by coulombic attraction between the oppositely-charged partners. In this scheme, the association does not violate the coulombic restriction imposed by Zwolinski, et al. Again, the back reaction can be inhibited by suitable anions:

$$(Fe^{+3}\cdot O_2^{-}) + X^{-} \rightarrow (X^{-}\cdot Fe^{+3}\cdot O_2^{-}) \qquad (3\text{-}22)$$

where the resultant complex may eventually dissociate

$$(X^{-}\cdot Fe^{+3}\cdot O_2^{-}) \rightarrow (X^{-}\cdot Fe^{+3}) + \dot{O}_2^{-} \qquad (3\text{-}23)$$

The original Weiss scheme continues with reaction 3-15. Under these conditions, the rate is proportional to $[Fe^{+2}]$, $[O_2]$, and $[X^{-}]$, and the anionic complex-former has served in the same capacity as in the original scheme.

In the absence of strong complex-formers, the $(Fe^{+3}\cdot O_2^{-})$ complex can be stabilized by Fe^{+2} (18),

$$(Fe^{+3}\cdot O_2^-) + Fe^{+2} = (Fe^{+3}\cdot O_2^-\cdot Fe^{+2}) = (Fe^{+3}\cdot O_2^{-2}\cdot Fe^{+3}) \quad (3\text{-}24)$$

This would explain the results of George (12) and Huffman and Davidson (13), where the observed rate is proportional to $[O_2]$ and $[Fe^{+2}]^2$. The new complex is again stabilized by coulombic forces and eventually breaks up,

$$(Fe^{+3}\cdot O_2^{-2}\cdot Fe^{+3}) + H^+ \rightarrow 2\ Fe^{+3} + H\dot{O}_2^- \quad (3\text{-}25)$$

followed again by the same sequence as above.

If this were the mechanism describing the oxygenation of Fe(II) and the effect of anionic complex-formers on the rate of reaction, then one should observe a decrease in rate with increasing concentration of Fe^{+3}, as in 3-20. None of the previous workers, however, have observed any inhibitory effects by the addition of Fe^{+3} to their acidic solutions.

The situation can be somewhat clarified by closer scrutinization of 3-20a and b. If the back reaction were relatively rapid and Fe^{+3} were rapidly reduced by $\dot{O}_2^-$, then

$$k_1'\ K_{HO_2}[Fe^{+3}] \gg k_2\ [H^+]\ [Fe^{+2}] \quad (3\text{-}20b)$$

A quantitative comparison of the two terms is called for. For the given experimental conditions ($[H^+] = 10^{-3}M$, $[Fe^{+2}] = 10^{-3}M$, and $[Fe^{+3}] \sim 10^{-5}M$) and using the value approximated by Benson (19) that $pK_{HO_2} = 12 \pm 4$, one obtains $k_1'/k_2 \gg 10^{11}$. Hence, if $k_1'/k_2 \ll 10^{11}$, the back reaction is sufficiently slow that it can be neglected in 3-20a. Barb, et al (20) experimentally measured $k_1'/k_2 = 1.0$ at pH 2.7 in perchlorate media. This implies that reduction of Fe^{+3} by $\dot{O}_2^-$ is signficantly slower than the corresponding oxidation of Fe^{+3} by $\dot{O}_2^-$. Recent experimental evidence

indicates that the value for pK_{HO_2} estimated by Benson is too high and that the proper value should be about $pK_{HO_2} = 5$ (21). Even if this value is utilized, the reverse reaction under these conditions can still be neglected. Therefore, if the Weiss mechanism is valid, one should observe the rate relationship 3-20d, i.e., a reaction rate which is first-order in both $[Fe^{+2}]$ and $[O_2]$. The experimental data presented in Figure 3-13 do obey such a kinetic law in the acidic region.

Another interesting observation with regard to the Weiss mechanism is the hypothesis that the $Fe^{+3} \cdot O_2^-$ complex forms first and is subsequently stabilized by anionic ligands. In view of the rapid nature of simple complex-formation reactions (22), it is more likely that complexation of Fe^{+2} by the ligand occurs first, followed by the reaction with oxygen and, in the termolecular mechanism (13), by another Fe^{+2}. Cher and Davidson(23) have considered that complex-formation serves to make ΔH and ΔF for reaction 3-14a less positive, with the net effect being to lower the activation energy of the reaction.

The possibility of a 2-equivalent electron-transfer has been proposed, largely as a result of the work of Cahill and Taube (24), who postulated $Fe(\dot{I}V)$ to be a reaction intermediate in place of $\dot{H}O_2$ in the single-electron transfer. Such an interpretation would be in accord with

$$Fe(II) + O_2 = Fe(\dot{I}V) + H_2O_2 \qquad (3\text{-}26)$$

$$Fe(II) + Fe(\dot{I}V) = 2\ Fe(III) \qquad (3\text{-}27)$$

$$Fe(II) + H_2O_2 = Fe(\dot{I}V) + 2\ OH^- \qquad (3\text{-}28)$$

$$Fe(II) + Fe(\dot{I}V) = 2\ Fe(III) \qquad (3\text{-}29)$$

The role of anionic complexes with the intermediate $Fe(\dot{IV})$ would be similar to that observed for Fe(III) in the single-electron-transfer mechanism (23).

Conocchioli, et al (25) have begun to investigate the oxidation of Fe(II) by 2-equivalent oxidants, their preliminary data corroborating the proposal of Cahill and Taube with regard to the involvement of $Fe(\dot{IV})$ as an intermediate. Their observation of the Fe(III) dimer as the primary end-product led to their formulation of the mechanism as

$$Fe^{+2} + Ox_2 \xrightarrow{2\ \text{equiv.}} Fe(\dot{IV}) + Red_2 \qquad (3\text{-}30)$$

$$Fe(\dot{IV}) + Fe^{+2} \xrightarrow{\text{rapid}} [Fe(III)]_2 \qquad (3\text{-}31)$$

where $[Fe(III)]_2$ refers to the dimer, represented by $Fe\langle^{OH}_{OH}\rangle Fe^{+4}$. In studies employing HOCl as the 2-equivalent oxidant, the dimer formed was observed to be $Fe\langle^{OH}_{Cl}\rangle Fe^{+4}$, which slowly converted to the dihydroxo-dimer under acidic conditions. In a similar vein, it will be reported in the next chapter that the same inorganic ligands which accelerate the rate of oxidation of Fe(II) by apparently stabilizing the transitory intermediate also accelerate the rate of hydrolysis of Fe^{+3}, which presumably proceeds through the dimer.

The formation of a bridged activated complex, as proposed by Taube (26) to explain the role of complex formers in serving as a bridge between the oxidizing and reducing agents, is unlikely in this situation; its major relevance is in redox reactions between metal ions.

If Figure 3-13 is considered, it is readily apparent that, in the acidic pH-range, the oxidation reaction proceeds relatively slowly, as

predicted by the Weiss mechanism. Whether or not this type of mechanism is valid, one could still postulate that as the pH is increased and [OH^-] increases, the net effect is that the ligand OH^- behaves in the same fashion as the other complexing ligands by coordinating with one of the iron species and stabilizing the transitory complex. If this were the case, then one should not observe other anionic ligands to exert a catalytic effect at the elevated pH-values. Stumm and Lee (3), in a preliminary survey, noted that chloride and sulfate exerted no such accelerative effect at pH-values greater than 6, but $H_2PO_4^-$ did. Formation of mixed hydroxo-ligand complexes of Fe(III) could account for such an observation.

At the higher pH-values investigated, care must be exercised in interpreting the results because of the heterogeneity of the system. The resultant Fe(III) hydrolyzes quite rapidly (see Chapter 4), forming insoluble ferric hydroxide. Although it can be assumed that the catalytic effect of OH^- at higher pH-values is similar to that suggested earlier, one must bear in mind that the previously-mentioned mechanisms have all been derived for homogeneous, one-phase systems.

Abel (27) has proposed that the second-order dependence on [OH^-], exhibited in Figure 3-13, arises from the following scheme:

$$O_2 + OH^- = O_2 \cdot OH^- \qquad (3\text{-}32)$$

$$O_2 \cdot OH^- + OH^- = O_3^{-2} + H_2O \qquad (3\text{-}33)$$

The two equilibria proceed rapidly with the resultant O_3^{-2} slowly reacting with Fe^{+2} to form additional reactive oxo-complexes which propagate the chain.

Wells and Salam (28) have attached special significance to electrostatic considerations in that it is easier to remove an electron (e^-) from Fe^{+2} by decreasing its positive charge through complex-formation.

The second-order dependence on $[OH^-]$ is reminiscent of the second-order dependence on $[H_2PO_4^-]$ observed by Cher and Davidson (23) in their study of the oxidation of Fe(II) in phosphoric acid solution. An explanation was not given for this second-order dependence, but in a later paper King and Davidson (29) proved that it was not due to condensation of $H_2PO_4^-$ to $H_2P_2O_7^{-2}$.

The dependence upon $[OH^-]$ and the conversion of the solution to a two-phase system due to hydrolysis of Fe(III) is suggestive of a kinetic dependence on hydrolyzed species of Fe(III). It is interesting to speculate with regard to such hydroxo-species, especially since the transition region observed in Figure 3-13 occurs near the pK-value for the reaction

$$FeOH^{+2} + H_2O = Fe(OH)_2^+ + H^+ \qquad pK = 4.6 \qquad (3\text{-}34)$$

Beyond pH 4.6, $Fe(OH)_2^+$ becomes the dominant soluble species of Fe(III). The correspondence between the second-order hydroxide-dependence of the rate of oxidation of Fe(II) and the dihydroxo-composition of Fe(III) is striking. However, there is no evidence to indicate that an autocatalytic mechanism is operative, as in the oxygenation of Mn(II) (10); the addition of Fe(III) has no apparent effect on the rate of oxidation of Fe(II). It is also unlikely that hydroxo-species of Fe(II) are involved, since hydrolysis of Fe(II) does not become significant until pH 6.5.

Consequently, with regard to Figure 3-13, one can only emphasize the significance of pH on the rate of oxidation of Fe(II) at pH-values greater than 4.5. At this time, there is insufficient chemical evidence on which to base any conclusive mechanistic interpretation.

References

1) Just, G., "Kinetische Untersuchung der Autoxydation des in Wasser gelosten Ferrobicarbonats," Z. Phys. Chem., 63, 385 (1908)

2) Holluta, J., and Eberhardt, M., "Uber geschlossene Enteisenung durch Schnellfiltration," Vom Wasser, XXIV, 79 (1957)

3) Stumm, W., and Lee, G. F., "Oxygenation of Ferrous Iron," Ind. Eng. Chem., 53, 143 (1961)

4) Ghosh, M. M., O'Connor, J. T., and Engelbrecht, R. S., "Precipitation of Iron in Aerated Groundwaters," Journ. San. Eng. Div., Proc. Amer. Soc. Civil Eng., 92, 120 (1966)

5) Stumm, W., and Singer, P. C., "Precipitation of Iron in Aerated Groundwaters," discussion, Journ. San. Eng. Div., Proc. Amer. Soc. Civil Eng., 92, 120 (1966)

6) Morgan, J. J., and Stumm, W., "The Role of Multivalent Metal Oxides in Limnological Transformations, as Exemplified by Iron and Manganese," Proc. Second Intl. Conf. Water Poll. Res., Tokyo, p. 103 (1964)

7) Hale, F. E., "Iron Removal Without Aeration - The Precipitation of Ferrous Carbonate in a Closed System," J. Amer. Wat. Works Assn. 28, 1577 (1936)

8) Lee, G. F., and Stumm, W., "Determination of Ferrous Iron in the Presence of Ferric Iron," J. Amer. Wat. Works Assn., 52, 1567 (1960)

9) Morgan, J. J., and Birkner, F. B., "Precipitation of Iron in Aerated Groundwaters," discussion, Journ. San. Eng. Div., Proc. Amer. Soc. Civil Eng., 92, 137 (1966)

10) Walton, A. G., The Formation and Properties of Precipitates, Interscience, New York (1967)

11) Morgan, J. J., "Chemistry of Aqueous Manganese (II) and (IV)," Ph.D. thesis, Harvard University (1964)

12) George, P., "The Oxidation of Ferrous Perchlorate by Molecular Oxygen," J. Chem. Soc., 4349 (1954)

13) Huffman, R. E., and Davidson, N., "Kinetics of the Ferrous Iron - Oxygen Reaction in Sulfuric Acid Solution," J. Amer. Chem. Soc., 78, 4836 (1956)

14) Weiss, J., "Elektronenubergangsprozesse im Mechanismus von Oxydations- und Reduktions- Reaktionen in Losungen," Naturwissenschaften, 23, 64 (1935)

15) Frost, A. A., and Pearson, R. G., Kinetics and Mechanism, John Wiley and Sons, New York (1962)

16) Weiss, J., "Electron Transfer Reactions in the Mechanism of Oxidation-Reduction Processes in Solution," J. Chim. Phys., 48, C-6 (1951)

17) Zwolinski, B. J., Marcus, R. J., and Eyring, H., "Inorganic Oxidation-Reduction Reactions in Solution," Chem. Rev., 55, 157 (1955)

18) Weiss, J., "The Autoxidation of Ferrous Ions in Aqueous Solution," Experentia, IX, 61 (1953)

19) Benson, S. W., The Foundations of Chemical Kinetics, McGraw-Hill Book Co., New York (1960)

20) Barb, W. G., Baxendale, J. H., George, P., and Hargrave, K. R., "Reactions of Ferrous and Ferric Ions with Hydrogen Peroxide," Trans. Farad. Soc., 47, 462 (1951)

21) Morris, J. C., Harvard University, Personal Communication

22) Wendt, H., and Strehlow, H., "Schnelle Ionenreaktionen in Losungen. II. Die Bildung Einiger Einfacher Komplexe des Eisen-III- Ions," Z. Elektrochem, 66, 228 (1962)

23) Cher, M., and Davidson, N., "The Kinetics of the Oxygenation of Ferrous Iron in Phosphoric Acid Solution," J. Amer. Chem. Soc., 77, 793 (1955)

24) Cahill, A. E., and Taube, H., "The Use of Heavy Oxygen in the Study of Reactions of Hydrogen Peroxide," J. Amer. Chem. Soc., 74, 2312 (1952)

25) Conocchioli, T. J., Hamilton, E. J., and Sutin, N., "The Formation of Fe(IV) in the Oxidation of Iron (II)," J. Amer. Chem. Soc., 87, 926 (1965)

26) Taube, H., "Mechanisms of Redox Reactions of Simple Chemistry," Advances in Inorganic Chemistry and Radiochemistry,1, 1, Emelius, H. J., and Sharp, A. G., editors, Academic Press, New York (1959)

27) Abel, E., "Uber Autoxydation in Umbelichteter Homogener Wasseriger Losung. Mit Besonderer Berucksichtigung Anorganischer Systeme," Z. Elektrochem., 59, 903 (1955)

28) Wells, C. F., and Salam, M. A., "A Kinetic Approach to the Nature of Ferrous Ions in Aqueous Solution," Nature, 203, 751 (1964)

29) King, J., and Davidson, N., "Kinetics of the Ferrous Iron - Oxygen Reaction in Acidic Phosphate - Pyrophosphate Solutions," J. Amer. Chem. Soc., 80, 1542 (1958)

CHAPTER 4

HYDROLYSIS OF FERRIC IRON

4-1 Introduction

The solubility of ferric iron in natural waters, under most conditions, is controlled by the solubility of its various oxides and hydroxides. Figure 2-13 demonstrated that the concentration of soluble Fe(III) is less than 10^{-6}M at pH 4. When the solubility product of ferric hydroxide is exceeded, a series of hydrolytic reactions takes place as the formation of insoluble ferric hydroxide proceeds through multimeric and polymeric hydroxo-intermediates. These kinetic intermediates tend to be adsorbed at interfaces, thus accounting for the use of Fe(III) as a coagulant in water treatment.

It was also shown (section 2-3.2) that various ligands tend to coordinate with Fe(III) and that the degree of coordination is a function of the relative affinity of Fe(III) for these various ligands versus its affinity for OH^-. The existence of mixed ligand-hydroxo-complexes was assumed to be of relevance in natural waters.

This chapter centers upon the kinetics of hydrolysis of Fe(III) in systems oversaturated with respect to ferric hydroxide. The effect of sulfate on the kinetics of hydrolysis was investigated, especially due to the high concentrations of sulfate found in mine drainage waters. Sulfate also serves as a representative ligand in order to gain some insight as to the rate of hydrolysis of Fe(III) in systems containing

ligands which compete with OH^- for the coordination sites of Fe(III). The coagulative properties of ferric iron are considered, in brief, to demonstrate that it is the hydrolytic intermediates which are responsible for the destabilization of colloidal dispersions. Finally, phosphate removal by ferric iron has been investigated, both by the direct addition of Fe(III) to a system containing phosphate and by the addition of Fe(II) which is subsequently oxidized, in situ, to Fe(III).

4-2 Kinetics of Ferric Iron Hydrolysis

4-2.1 Reactions of Fe^{+3} with Water

Ferric iron in aqueous solution behaves as a multiprotic Brönsted acid, with protons being transferred from the coordinated water molecules of Fe(III) to the solvent water in the following stepwise manner:

$$Fe(H_2O)_6^{+3} + H_2O = Fe(H_2O)_5OH^{+2} + H_3O^+ \qquad (4\text{-}1)$$

$$Fe(H_2O)_5OH^{+2} + H_2O = Fe(H_2O)_4(OH)_2^+ + H_3O^+ \qquad (4\text{-}2)$$

etc.

Such reactions can proceed until all of the coordinated water molecules have been deprotonated, resulting in the formation of anionic hydroxo-ferric species. In addition to these "aquo-acidity" reactions (1) with mononuclear products, these simple hydroxo-ferric complexes tend to polymerize by a condensation process,

$$2\ Fe(H_2O)_5OH^{+2} = Fe_2(H_2O)_8(OH)_2^{+4} + 2\ H_2O \qquad (4\text{-}3)$$

where water is essentially squeezed out of the coordination shell. The resultant dimer has the structural configuration

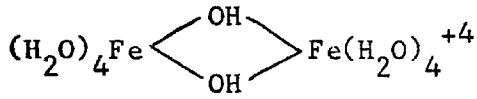

(4-3a)

The dimer is subject to additional hydrolytic reactions, again involving a proton-transfer

$$Fe_2(H_2O)_8(OH)_2^{+4} + H_2O = Fe_2(H_2O)_7(OH)_3^{+3} + H_3O^+ \qquad (4\text{-}4)$$

or additional condensation reactions by which the resultant molecule is further dehydrated

$$2\ Fe_2(H_2O)_7(OH)_3^{+3} = Fe_4(H_2O)_{12}(OH)_6^{+6} + 2\ H_2O \qquad (4\text{-}5)$$

In systems oversaturated with respect to insoluble ferric hydroxide, a series of such hydrolytic and condensation reactions takes place, the multimeric and polymeric hydroxo-species serving as kinetic intermediates in the formation of the solid ferric hydroxide precipitate. (A useful review of the chemistry of metal ions in aqueous solution has recently been presented by Stumm (2).) The solid phase, however, continues to react as the amorphous freshly-precipitated hydroxide generally converts to α-FeOOH. Under special conditions, α-Fe_2O_3, β-FeOOH, and γ-FeOOH can be formed (3). In addition to these crystalline products, an inactive amorphous material is always present, even after prolonged periods of aging. Under certain conditions, a colloidal sol of ferric-oxide hydroxide can be maintained for long periods of time. As previously mentioned (section 2-3.2), it is

analytically very difficult to distinguish between dissolved and suspended ferric iron.

Since the coagulative properties of Fe(III) arise from the tendency of the hydrolyzed polynuclear kinetic intermediates to be adsorbed at interfaces (4), and since $Fe(OH)_3$ and its hydroxo-intermediates are responsible, in part, for the transport of phosphate and organic material in lakes (5), it would be desirable to elucidate the kinetic relationships which govern the hydrolysis of ferric iron.

4-2.2 Experimental Study of the Kinetics of Fe(III) Hydrolysis

Experimental Procedure

The kinetics of hydrolysis of free ferric iron, Fe^{+3}, was studied potentiometrically, employing the ferro-ferri cell

$$Pt/\ Fe(II),Fe(III),Na^+,H^+,ClO_4^-/\ \underset{(sat'd)}{NaCl}\ /\ Hg_2Cl_2/\ Hg \qquad (4\text{-}6)$$

The cell has previously been described in section 2-3.3 and was shown in Figure 2-15. The reversible potential is established by the electroactive ferrous-ferric couple in accordance with the Nernst Equation which, for a constant ionic medium (0.1 M $NaClO_4$) in a constant temperature water bath at 25°C, becomes

$$E = E^{o'} - 0.0592 \log \frac{[Fe^{+2}]}{[Fe^{+3}]} \qquad (4\text{-}7)$$

$E^{o'}$ was determined in a preliminary experiment by measuring the potential of a known system at pH 1.0, where no hydrolysis or oxidation took place, so that $[Fe^{+3}] = [Fe(III)]_T$ and $[Fe^{+2}] = [Fe(II)]_T$. $[Fe(II)]_T$ and $[Fe(III)]_T$ were determined using bathophenanthroline (6).

Solutions containing various concentrations of Fe(II), Fe(III), and H^+ were prepared, under a nitrogen atmosphere, at the same ionic strength and temperature as the standard system. It was noted that the addition of even a weak alkali (dilute $NaHCO_3$) to raise the pH of the system brought about kinetically irreversible hydrolysis. Apparently, localized conditions of high pH (high concentrations of OH^- and a corresponding large degree of oversaturation with respect to ferric hydroxide) were produced in the vicinity of the tip of the burette from which the base was slowly dispensed. Even under conditions of intense mixing, basification of the system containing Fe(II) and Fe(III) resulted in a sharp decline in potential. Therefore, solutions containing Fe(III) had to be maintained under conditions such that the solubility of ferric hydroxide was never exceeded until the time at which the kinetic studies were begun. In most cases, Fe(III) was added directly to the system as the perchlorate salt, at time zero. In those instances where it was desired to begin the study at a higher pH, solutions of Fe(II) were basified with dilute $NaHCO_3$, under a nitrogen atmosphere, and then ozonated (Sanders Ozonator Model No. S-V-106, Triton Aquatics) in order to generate ferric iron <u>in situ</u> (7). Ozone was bubbled through the system and the extent of oxidation of Fe(II) was followed by noting the increase in potential of the ferrous-ferric couple. Generally, one minute was sufficient to oxidize about half of the initial concentration of Fe(II), so that $[Fe(II)]_T \sim [Fe(III)]_T$. Any residual traces of ozone or oxygen were removed by the nitrogen which was continuously bubbled through the solution. $[Fe(II)]_T$ was determined before and after

ozonation, the difference being the total concentration of Fe(III) which was generated.

The solutions were stored under an atmosphere of nitrogen and the pH was kept sufficiently low so that no oxidation of Fe(II) took place, and $[Fe^{+2}] = [Fe(II)]_T$ throughout the duration of the experiment. $[Fe^{+3}]$, the concentration of unhydrolyzed iron (III) species at any time, was calculated from the Nernst Equation (4-7) after measuring the potential of the system to the nearest 0.1 mv., using a Model D Sargent Recording Titrator. The liquid junction potential, E_j, has been shown (7) to be strictly a function of $[H^+]$. Extrapolating the results of Biedermann (7), E_j remains relatively constant during the course of the experiment so that variations in E_j can be neglected. The concentration pH (p^cH) was measured using a Leeds and Northrup Potentiometer (Catalog No. 7664), calibrated in the same manner as previously described in section 2-2.3. The samples were analyzed for $[Fe(II)]_T$ and $[Fe(III)]_T$ using bathophenanthroline.

Experimental Results and Discussion

Due to the acidic nature of the aquo-ferric ion, the pH of the system decreases when ferric salts are placed in solution. The simple proton-transfer reactions by which the mononuclear hydroxo-complexes are formed (reactions 4-1 and 4-2) take place extremely rapidly (8). When the solubility product of $Fe(OH)_3$ is exceeded, the slower hydrolytic and condensation reactions proceed whereby the multinucelar and polynuclear species and, eventually, solid ferric hydroxide are formed. One would expect that the rate of disappearance of free Fe^{+3} would be dependent not only upon the concentration of Fe^{+3}, but also upon pH or,

more precisely, upon the concentration of OH^-. Since hydrolysis tends to decrease $[OH^-]$, the reaction would be expected to decelerate as hydrolysis progresses. Furthermore, the resultant decline in pH also causes a shift in the Fe^{+3} - $FeOH^{+2}$ distribution so that the concentration of Fe^{+3} is partially buffered; on one hand, it is diminished in forming ferric hydroxide, and on the other hand, it is augmented due to conversion of $FeOH^{+2}$ to Fe^{+3}, i.e., the back reaction of 4-1. This effect can be pictured as

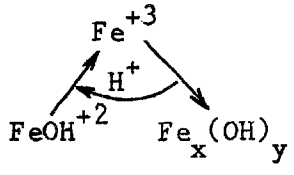

(4-8)

Therefore, in order to derive any useful kinetic information, the system must be maintained at constant pH. Use of a pH-buffer is precluded because of possible kinetic effects the buffering agent might bring about. Alternatively, small concentrations of Fe^{+3} can be employed in order to minimize the pH-decrease accompanying hydrolysis, or one can follow $[Fe^{+3}]$ with time and compute the instantaneous rate of decrease of $[Fe^{+3}]$ at any given pH or in a region of constant pH. These latter two approaches were utilized in treating the experimental data. In this manner, any change in the concentration of Fe^{+3} arises only from hydrolytic reactions.

Figures 4-1 and 4-2 show some of the experimental results. In each case, the data have been plotted assuming either a first- or second-order dependence of the reaction rate on $[Fe^{+3}]$. Rate laws of the form

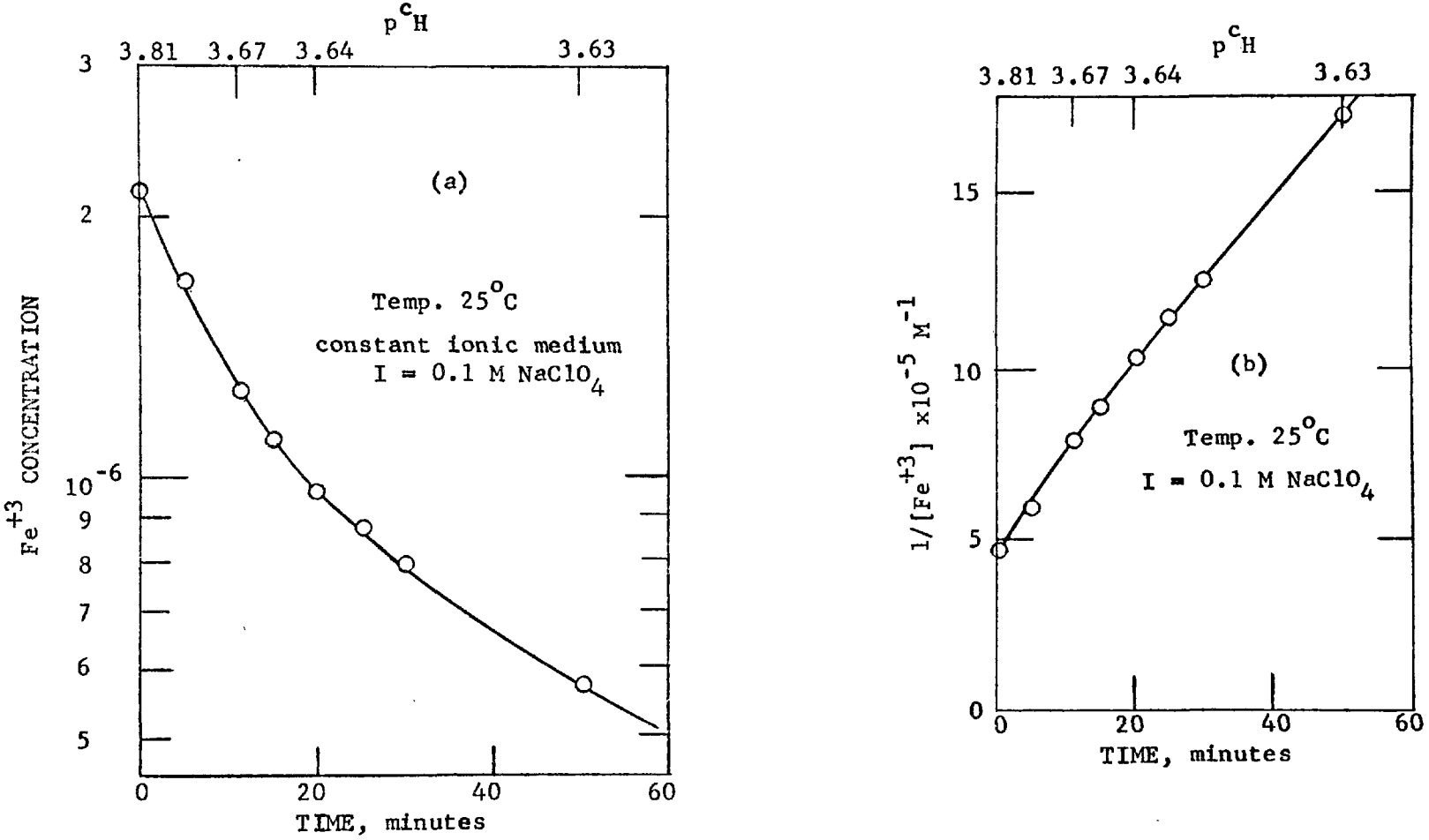

FIGURE 4-1. (a) Logarithmic and (b) reciprocal plots of the rate of hydrolysis of Fe^{+3}. (a) assumes a first-order dependence and (b) a second-order dependence of the reaction rate on the Fe^{+3} concentration.

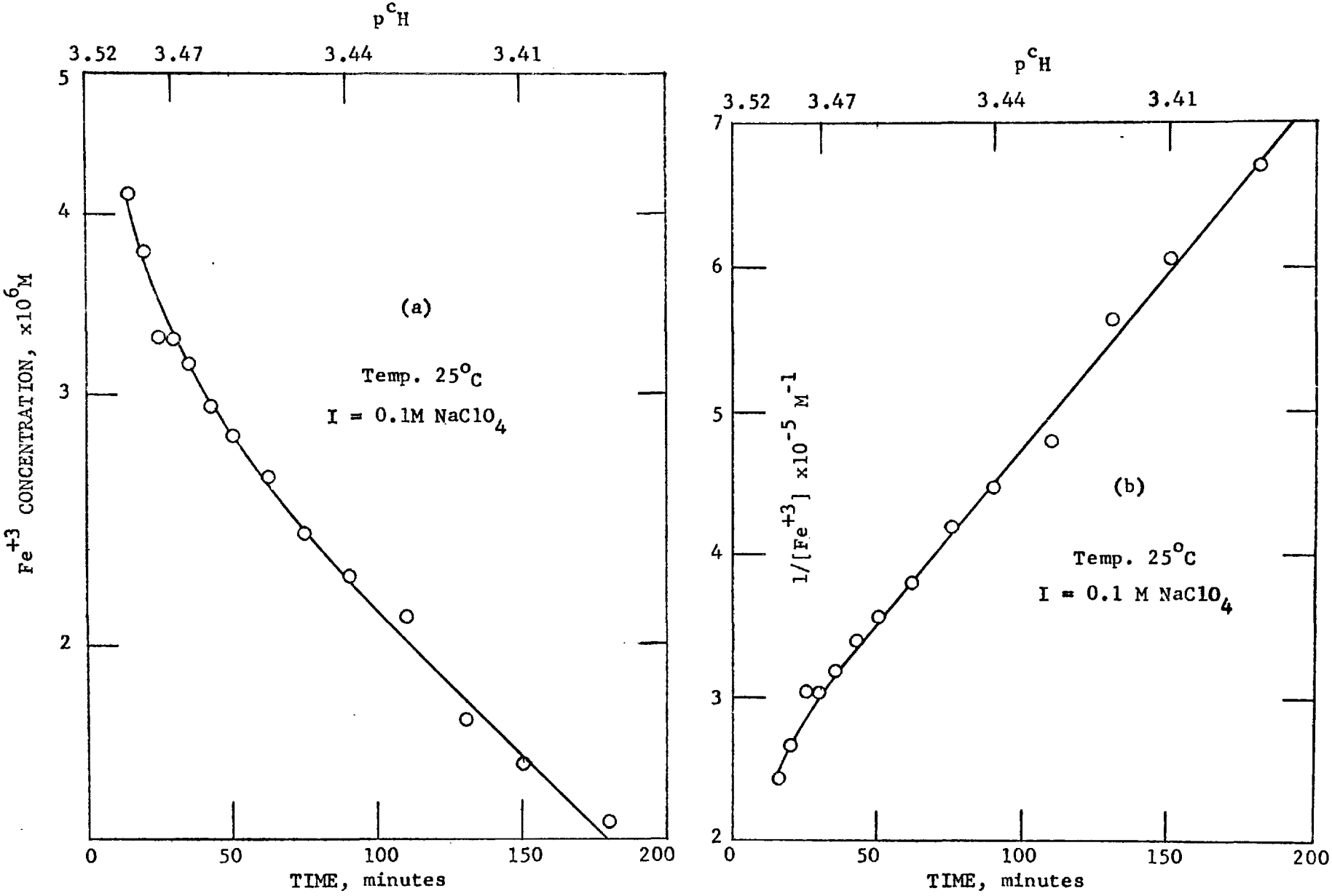

FIGURE 4-2. (a) Logarithmic and (b) reciprocal plots of rate of hydrolysis of the aquo-ferric ion, Fe^{+3}.

$$\frac{-d\,[Fe^{+3}]}{dt} = k_1\,[Fe^{+3}] \qquad (4\text{-}9a)$$

$$\frac{-d\,[Fe^{+3}]}{dt} = k_2\,[Fe^{+3}]^2 \qquad (4\text{-}9b)$$

have been assumed, where k_1 and k_2 are functions of pH. The measured p^cH-values are noted. Kinetic significance of $[OH^-]$ is implied by the decreasing rate of hydrolysis for both the logarithmic and reciprocal plots. If the linear regions of each of the respective logarithmic and reciprocal plots are considered, the instantaneous rate of hydrolysis can be calculated for the p^cH-range over which such linearity is observed to hold. For each sample, the latter portion of the curve is relatively linear for it is in this region that the p^cH remains essentially constant.

The instantaneous slopes of the logarithmic and reciprocal plots are equal to the "rate constants," k_1 and k_2, for the first- and second-order relationships, respectively. If k_1 and k_2 are assumed to be functions of pH of the form

$$k_1 = k_1'\,[OH^-]^n \qquad (4\text{-}10a)$$

$$k_2 = k_2'\,[OH^-]^n \qquad (4\text{-}10b)$$

then a plot of log k_1 or log k_2 versus p^cH should result in a straight line of slope n. Figures 4-3 and 4-4 are plots of the instantaneous slopes of the logarithmic and reciprocal plots (Figures 4-1 and 4-2) against p^cH. A linear regression analysis was performed to compute the best straight line to fit the experimental rate results. The correlation coefficients for Figures 4-3 and 4-4 are 0.76 and 0.97, respectively, indicating that the data conform to a second-order

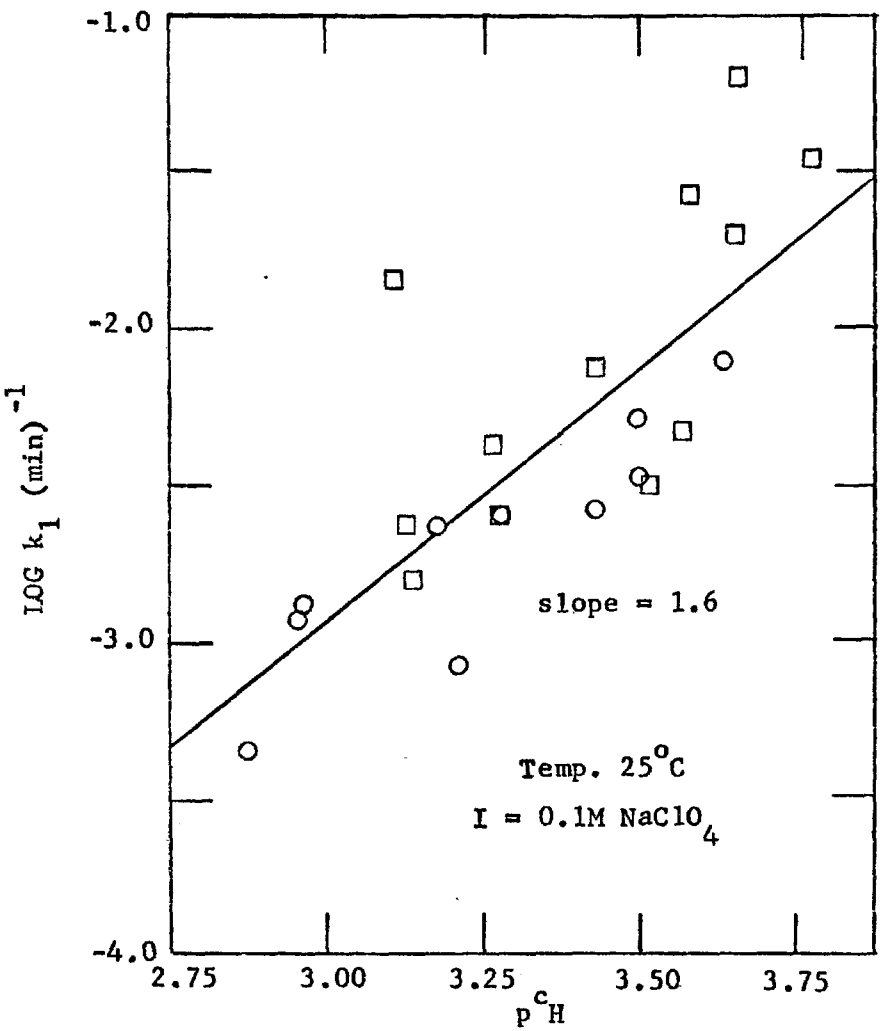

FIGURE 4-3. pH-dependence of "first-order rate constant" for hydrolysis of Fe^{+3}. ○ represent instantaneous slopes in final portion of log plots, where p^cH is constant, and □ represents slopes over a pH-region where linearity of log plots is observed.

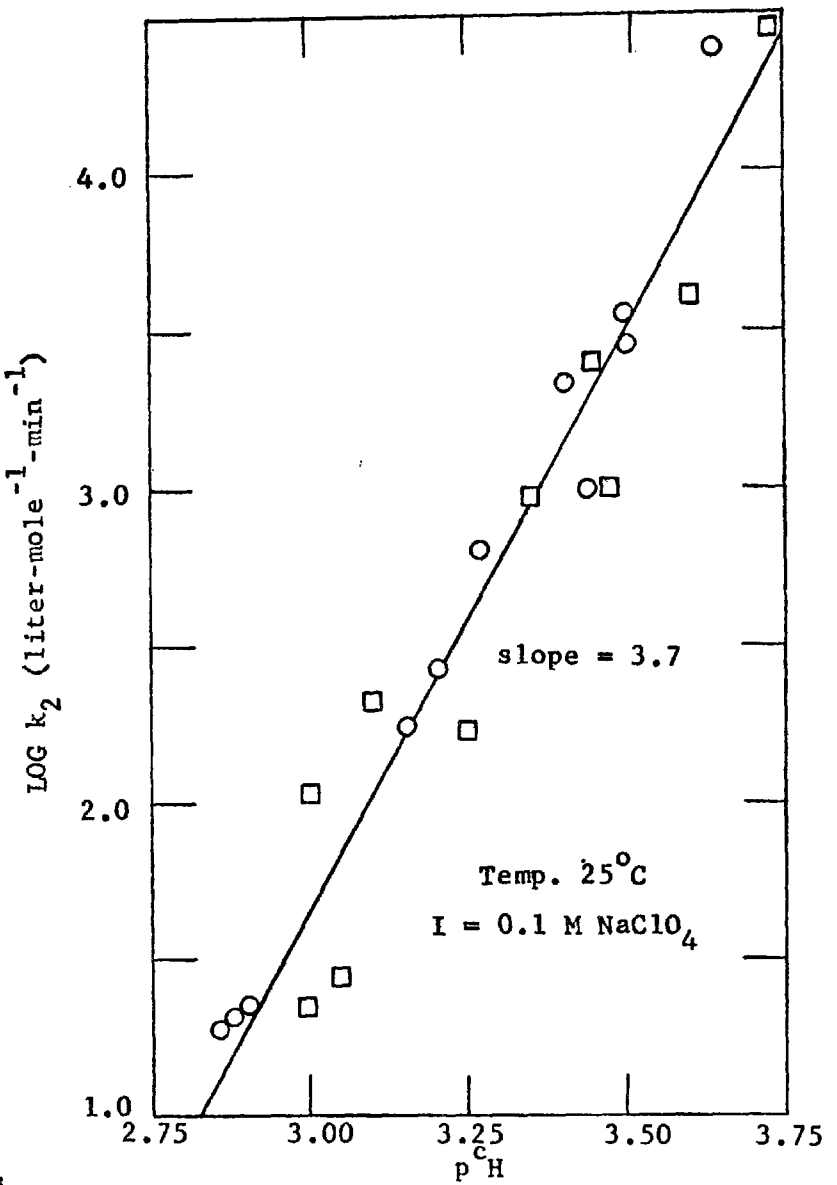

FIGURE 4-4. pH-dependence of "second-order rate constant" for hydrolysis of Fe^{+3}.

dependence on $[Fe^{+3}]$ considerably better than to a first-order dependence. The slope of Figure 4-4 is 3.7, implying that the rate of hydrolysis for the conditions investigated can be reasonably described by a kinetic relationship of the form

$$\frac{-d\,[Fe^{+3}]}{dt} = k_2'\,[Fe^{+3}]^2\,[OH^-]^4 \qquad (4\text{-}11)$$

where the rate constant k_2' is approximately $10^{45.5}$ $mole^3 liter^{-3} min^{-1}$ for the p^cH range 2.8 to 3.8.

The data were also tested for conformance to the von Weimann formulation, whereby the rate of precipitation (hydrolysis) is proportional to the relative degree of oversaturation, i.e.,

$$\frac{-d\,[Fe^{+3}]}{dt} = k\,(Q-K)/K \qquad (4\text{-}12)$$

where Q is the reaction quotient and K is the equilibrium solubility product for the formation of ferric hydroxide. The results might be interpreted in terms of the kinetics of crystal growth but the computations were limited by the lack of a dependable solubility product for $Fe(OH)_3$. A value of $K_{so} = 10^{-38}$ was employed for the calculation (see below), but such treatment of the data met with little success.

It should be emphasized that equation 4-11 is merely a data-fitting relationship. It is not intended to serve in any specific mechanistic way since there are probably numerous other rate expressions which could fit the experimental data. Furthermore, equation 4-11 is applicable only for the experimental conditions investigated; extrapolation of this relationship to other situations might result in serious error.

Wendt observed (9) that the dimerization reaction (4-3) is considerably slower than the simple proton-transfer reaction and that the former is accelerated in the presence of simple anions via a reaction of the form

$$FeX^{(3-n)} + FeOH^{+2} = Fe\langle^{OH}_{X}\rangle Fe^{(5-n)} \qquad (4\text{-}13)$$

Figure 4-5 contains plots of the second-order rate constant for the disappearance of free Fe^{+3} in the presence of sulfate. The figure was developed by treating the experimental data in the same fashion as described above. For the three different concentrations of sulfate analyzed, the average slope is 3.3. The rate of hydrolysis is more rapid in the presence of sulfate than in its absence, as demonstrated in Figure 4-6. These results are especially useful when applied to the mine drainage system considered in Chapter 5.

One could generalize, on the basis of Wendt's findings and those reported here, that anions which coordinate with Fe^{+3} tend to increase the rate of hydrolysis of Fe(III). Hence, hydrolysis would be expected to occur even more rapidly in natural waters under the influence of the many natural anions which are present, such as sulfate, chloride, phosphate, orthosilicate, and the many organic anions. Schenk and Weber (10) reported that silicic acid hindered the hydrolysis of ferric iron, but their results are based upon indirect observations of free Fe^{+3}, such as absorbance of the hydrolytic products at 420 mu, and residual [Fe(III)] following filtration through an 0.45 u membrane filter. It is suggested that the effects of such catalysts

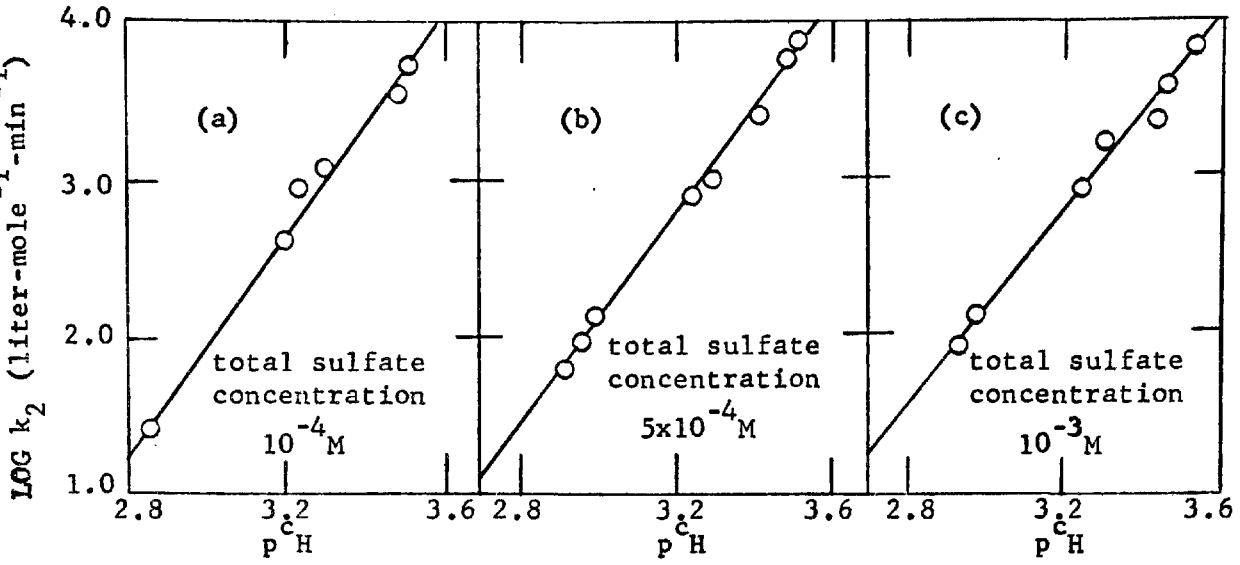

FIGURE 4-5a,b,c. pH-dependence of "second order rate constant" for hydrolysis of Fe^{+3} in the presence of sulfate.

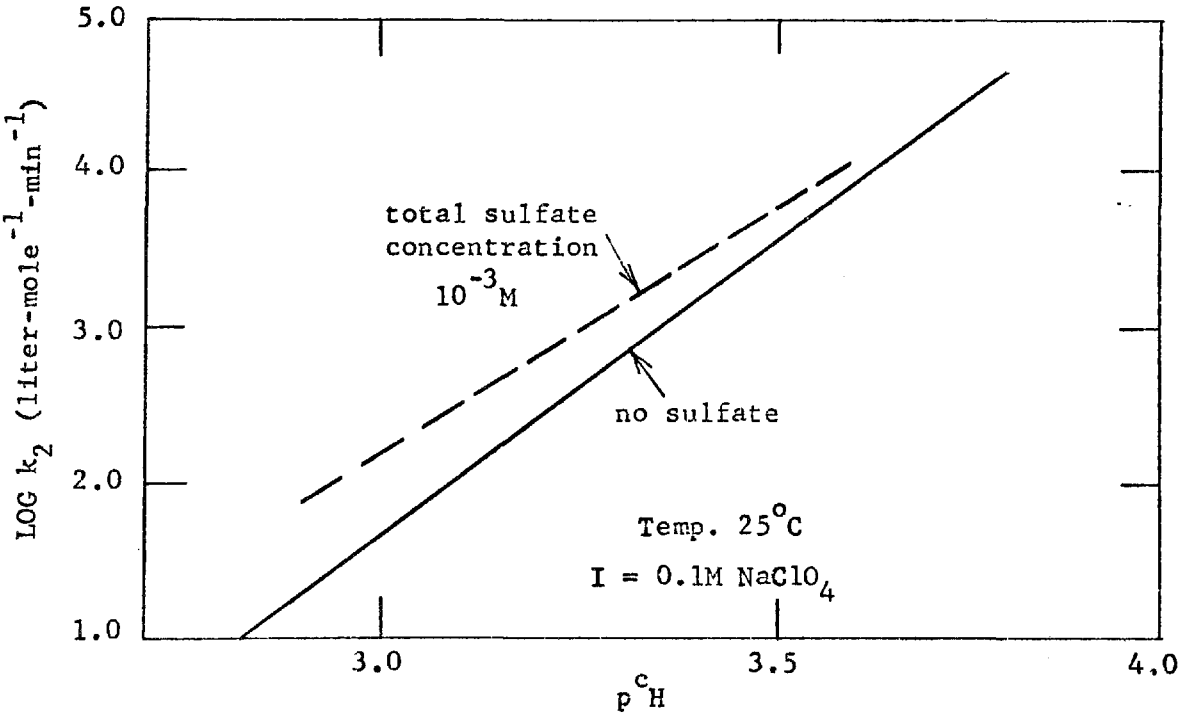

FIGURE 4-6. Comparison between rates of hydrolysis of Fe^{+3} in the presence and absence of sulfate.

or inhibitors be investigated by direct analytical methods such as those employed in this study.

Solubility Product of Amorphous Ferric Hydroxide

Immediately following the investigation of the kinetics of hydrolysis of Fe(III), the remainder of each of the samples was removed from the ferro-ferri cell and placed in a BOD reaction bottle under a nitrogen atmosphere. The BOD bottles were stored under water. After a period of approximately 17 days, the samples were removed from storage and again placed in the ferro-ferri cell. The reversible Nernstian potential, E, p^cH, and $[Fe^{+2}]$ were determined as before, and the solubility of ferric hydroxide was computed. The data and results are summarized in Table 4-1. The pK_{so}-value indicated should not be referred to as the solubility product of ferric hydroxide, since it is probable that equilibrium had not been attained, and the structural form of the end-product was not analyzed. In any case, the average value determined, $pK_{so} = 38.1$, does give some idea as to the magnitude of the solubility product of freshly-precipitated ferric hydroxide. Feitknecht and Schindler (3) report pK_{so}-values for the solubility product of amorphous $Fe(OH)_3$ in 3M $NaClO_4$ of 38 to 39.1, depending upon the age of the precipitate, i.e., the time elapsed following precipitation before the measurements were made.

4-3 Coagulative Properties of Ferric Iron

O'Melia and Stumm (4) have shown that destabilization of colloidal dispersions of silica by Fe(III) is accomplished by the multimeric and polymeric hydroxo ferric species which arise as unstable

Table 4-1. Check on the Solubility Product of Ferric Hydroxide

Sample No.	p^cH	E* mv.	$[Fe^{+2}]$ x 10^4M	$\frac{[Fe^{+2}]}{[Fe^{+3}]}$	$[Fe^{+3}]$ x 10^6M	$[OH^-]^3$ x $10^{33}M^3$	K_{so} x 10^{39}	pK_{so}
14	2.89	403.6	4.52	24.6	18.4	0.468	8.60	38.07
15	2.88	391.8	5.60	39.1	14.3	0.447	6.39	38.19
16	3.00	380.0	5.15	61.7	8.35	1.00	8.35	38.08
17	2.76	416.2	5.46	15.1	36.2	0.191	6.92	38.16
18	3.21	366.9	1.95	103.	1.89	4.27	8.07	38.09
19	3.20	369.2	2.28	93.5	2.44	3.98	9.71	38.01
20	3.31	343.7	2.25	254.	0.886	8.27	7.33	38.14
21	3.20	364.6	2.04	112.	1.82	3.98	7.25	38.14
22	3.20	366.0	2.10	106.	1.98	3.98	7.88	38.10
23	3.22	372.4	1.88	83.0	2.27	4.59	10.42	37.98
24	2.85	387.9	5.64	45.6	12.4	0.355	4.40	38.36

Average pK_{so} =38.1

*Potential readings versus saturated calomel reference electrode

NOTE: $E^{o'}$ = 486.0 mv.

T = 25°C

I = 0.1

Readings taken 17 days after precipitation

kinetic intermediates in the precipitation of ferric hydroxide. The destabilization process is attributed to specific adsorption of these hydroxo-ferric species; this adsorption brings about aggregation either by a bridging effect whereby the hydrolyzed Fe(III) forms linkages between a number of dispersed particles, or by neutralization of the negatively-charged colloidal particles by the positively-charged hydrolyzed Fe(III).

The efficiency of destabilization depends upon the hydrolytic properties of Fe(III) and is, therefore, influenced by pH. Figure 4-7 shows the effect of pH on the concentration of iron (III) required for aggregation of colloidal silica (Ludox SM, E. I. Dupont de Nemours and Co., Wilmington, Delaware) at a surface concentration of 150 m^2/l. The experimental data for Figure 4-7 were obtained in the same manner as those obtained by O'Melia and Stumm (4), using light scattering as an indicator of coagulation.

There are two results of the coagulation study that are directly related to the kinetics of hydrolysis of Fe(III). Firstly, O'Melia and Stumm observed that prolonged thermal aging of solutions of ferric perchlorate, in order to form polymeric hydroxo-ferric species, increased the critical coagulation concentration and the critical restabilization concentration for the colloidal silica dispersion, i.e., greater concentrations of Fe(III) were required for a given degree of coagulation and restabilization, respectively. This was attributed to partial precipitation of $Fe(OH)_3$ and a corresponding reduction in the concentration of active hydrolytic intermediates. Secondly, the plateau between pH 3 and 6 in Figure 4-7 suggests that in this region

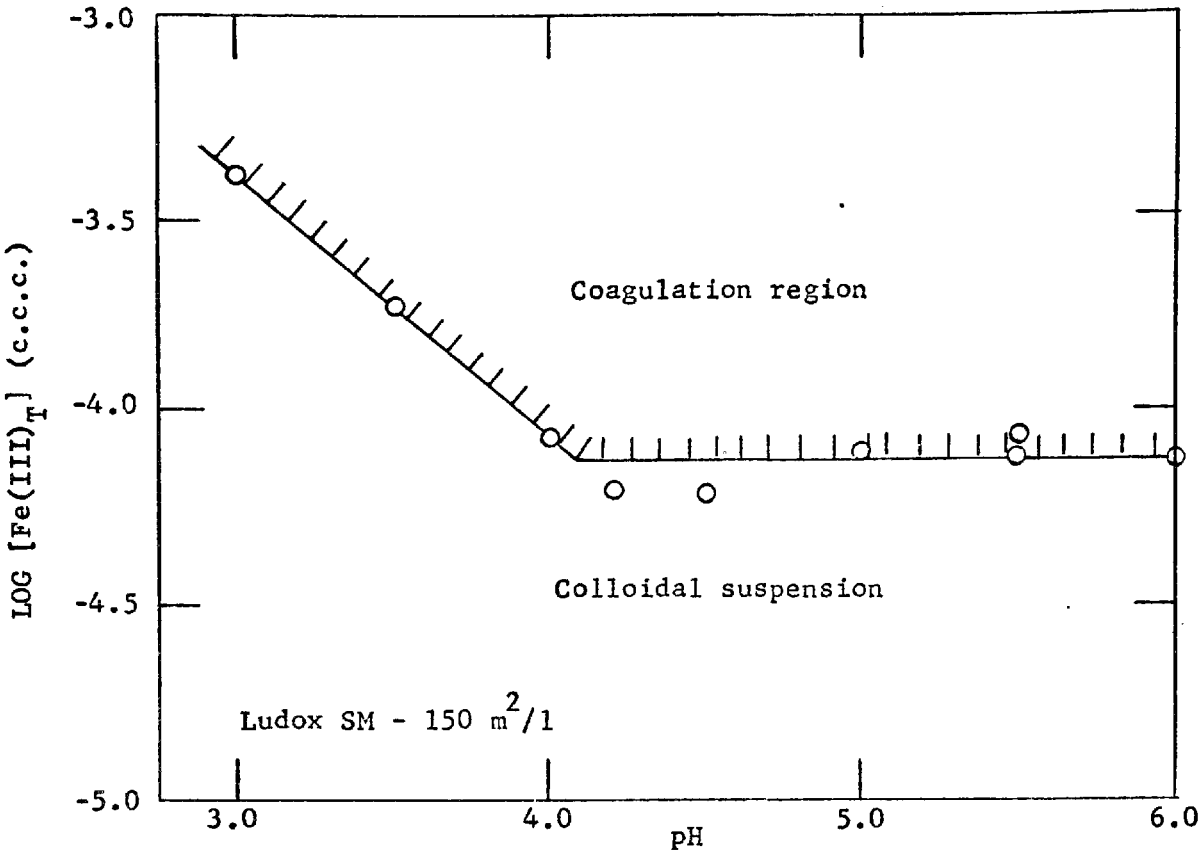

FIGURE 4-7. Aggregation of colloidal silica dispersion by hydrolyzed ferric iron.

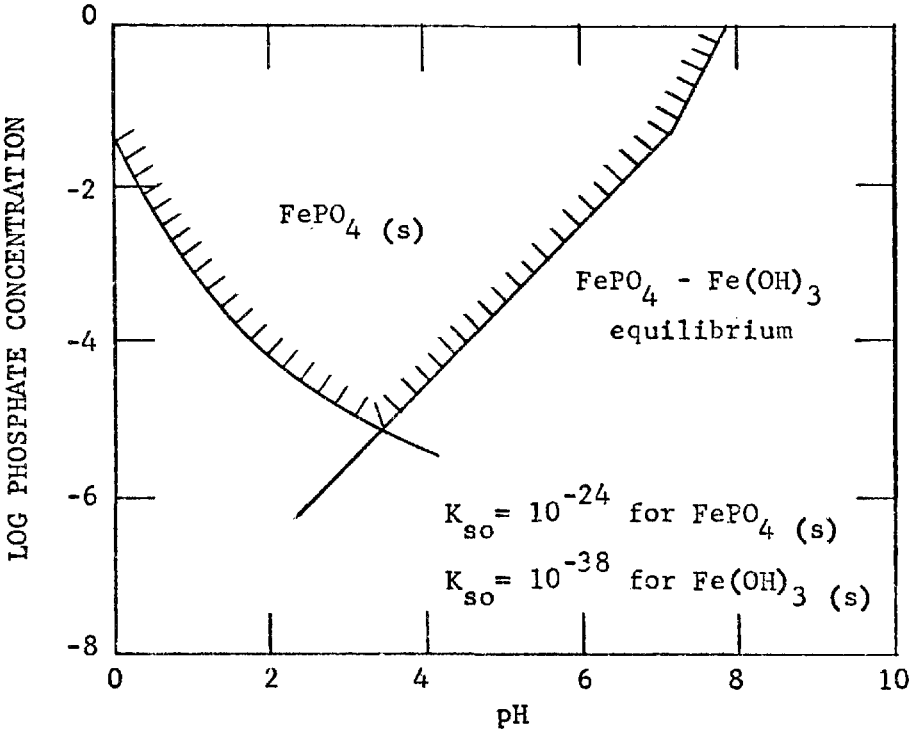

FIGURE 4-8. Solubility of ferric phosphate.

of $Fe(OH)_3$ insolubility, the polynuclear hydroxo-ferric species exhibit equivalent coagulative behavior independent of pH. These studies were conducted in pH-stats where constant pH was maintained by the addition of dilute sodium bicarbonate. However, the localized gradients of high pH which are set up by the external addition of a basifying agent bring about kinetically irreversible hydrolytic reactions. Such effects were observed in the laboratory investigations of the kinetics of Fe(III) hydrolysis (section 4-2.2), and have also been reported by Biedermann and Schindler (11) and by Spiro, et al (12). Since these studies describe the coagulative properties of kinetic intermediates, time of reaction and method of preparation of the hydrolytic reactants should be of significance. Similar comments have been made (13) regarding the coagulative behavior of activated (polymeric) silica. The pertinent variables include polymerization pH, polymerization concentration, polymerization time, and age of diluted polymeric solution. It is hoped that the kinetic studies reported in section 4-2.2 will serve as a guide for further research designed to clarify the mechanism of destabilization by hydrolyzed metal ions, and to identify the parameters which control the destabilization process.

4-4 Removal of Phosphate

It was shown, in section 2-3.1, that the solubility of ferric iron is controlled by the solubility of its oxides and hydroxides, except in waters containing appreciable concentrations of phosphate, at pH-values below 5. In a similar manner, the total concentration of dissolved phosphate is governed by solid ferric phosphate and is lowest

at pH 3.5, where the solubility of $FePO_4$ is at a minimum (see Figure 4-8). The pH at which minimum solubility is exhibited depends upon the solubility products of $FePO_4$ and $Fe(OH)_3$ which are utilized in the computations and the construction of Figure 4-8. The critical pH is not well-defined since neither solubility product is well-known (see section 2-3.1). The boundary below pH 3.5 represents the equilibrium between dissolved phosphate and solid ferric phosphate; the boundary above pH 3.5 corresponds to the control of soluble phosphate by the equilibrium between solid ferric phosphate and solid ferric hydroxide, reaction 2-27. (Soluble phosphato-complexes of ferric iron have been neglected since they do not markedly enhance the solubility of $FePO_4$. In addition, other phosphate minerals, such as $AlPO_4$, $Ca_3(PO_4)_2$, and $Ca_{10}(PO_4)_6(OH)_2$, have been disregarded although their significance in natural systems should not be overlooked.)

Consequently, under certain conditions, Fe(III) can serve as an effective precipitant for the removal of phosphate from waste waters. Figure 4-8 suggests that the efficiency of phosphate removal by Fe(III) is pH-dependent, since OH^- competes with the soluble phosphate species for the metal precipitant. At pH-values greater than 3.5, the efficiency is decreased due to formation of $Fe(OH)_3$ and mixed hydroxo-phosphato-precipitates of Fe(III). However, by the judicious selection of pH and means of addition of Fe(III), the hydrolytic tendency of Fe(III) can be supressed and the quantity of precipitant required for removal of phosphate can be made to be stoichiometric in accordance with the reaction

$$Fe^{+3} + PO_4^{-3} = FePO_{4(s)} \qquad (4\text{-}14)$$

Improvement of phosphate removal by Fe(III) can be achieved by employing the techniques of homogeneous precipitation (14) whereby the precipitant is not added directly to the system in the customary manner, but is generated internally by a homogeneous chemical reaction within the solution. In this way, coprecipitation is minimized and undesirable concentration effects are eliminated. In the case of ferric iron, homogeneous generation can readily be accomplished by the addition of ferrous iron which is subsequently oxidized in situ. The resultant Fe(III) is uniformly distributed throughout the system, promoting direct contact between all of the phosphate and all of the iron.

An experimental study of the removal of phosphate by externally-added and homogeneously-generated ferric iron was undertaken and the results are presented below.

4-4.1 Precipitation of Phosphate by Ferric Iron

Experimental Procedure

Various dilutions of a standardized solution of ferric perchlorate were added to a series of beakers containing 10^{-4}M Na_2HPO_4. (The stock solution of ferric perchlorate had been prepared in dilute perchloric acid to prevent hydrolysis of Fe(III).) Dilute sodium carbonate was simultaneously added in order to achieve and maintain the desired pH. The solutions were flash-mixed and then gently stirred for fifteen minutes. Samples of each were membrane filtered (1.2 u pore diameter) and the residual phosphate in the filtrate was determined employing the method recommended by the AASGP (15).

In the study of phosphate removal by homogeneous precipitation, acidified ferrous perchlorate and dilute Na_2CO_3 were added to a similar series of beakers containing 10^{-4}M Na_2HPO_4. The solutions were flash-mixed and gently stirred while the ferrous iron was oxidized, in situ, by atmospheric oxygen. At pH-values below 6 where the oxygenation reaction is slow (see section 3-4.1), ozone was bubbled through the system. (Ozone was generated by passing a stream of oxygen through a Sanders ozonator, Model No. S-V-106, Triton Aquatics.) Aliquots were removed from each of the precipitating systems at various time intervals and were analyzed for residual phosphate and Fe(II), using the AASGP (15) and bathophenanthroline (6) procedures, respectively. The concentration of Fe(III) at any given time was calculated as the difference between the initial concentration of Fe(II) and [Fe(II)] at that time.

Results and Discussion

Figure 4-9a shows the residual concentration of phosphate for various concentrations of ferric iron applied directly from solutions of ferric perchlorate. The efficiency of Fe(III) as a precipitant of phosphate appears to improve as the pH of the system is lowered, confirming the predictions made in connection with Figure 4-8. Stoichiometric removal is approached at pH 5.

Removal of phosphate by homogeneously-generated ferric iron is presented in Figure 4-9b. Here again, removal is improved as the pH decreases. Comparison of Figures 4-9a and b demonstrates that, with the exception of the results at pH 7.0, the degree of removal is enhanced by utilization of the homogeneous precipitation technique.

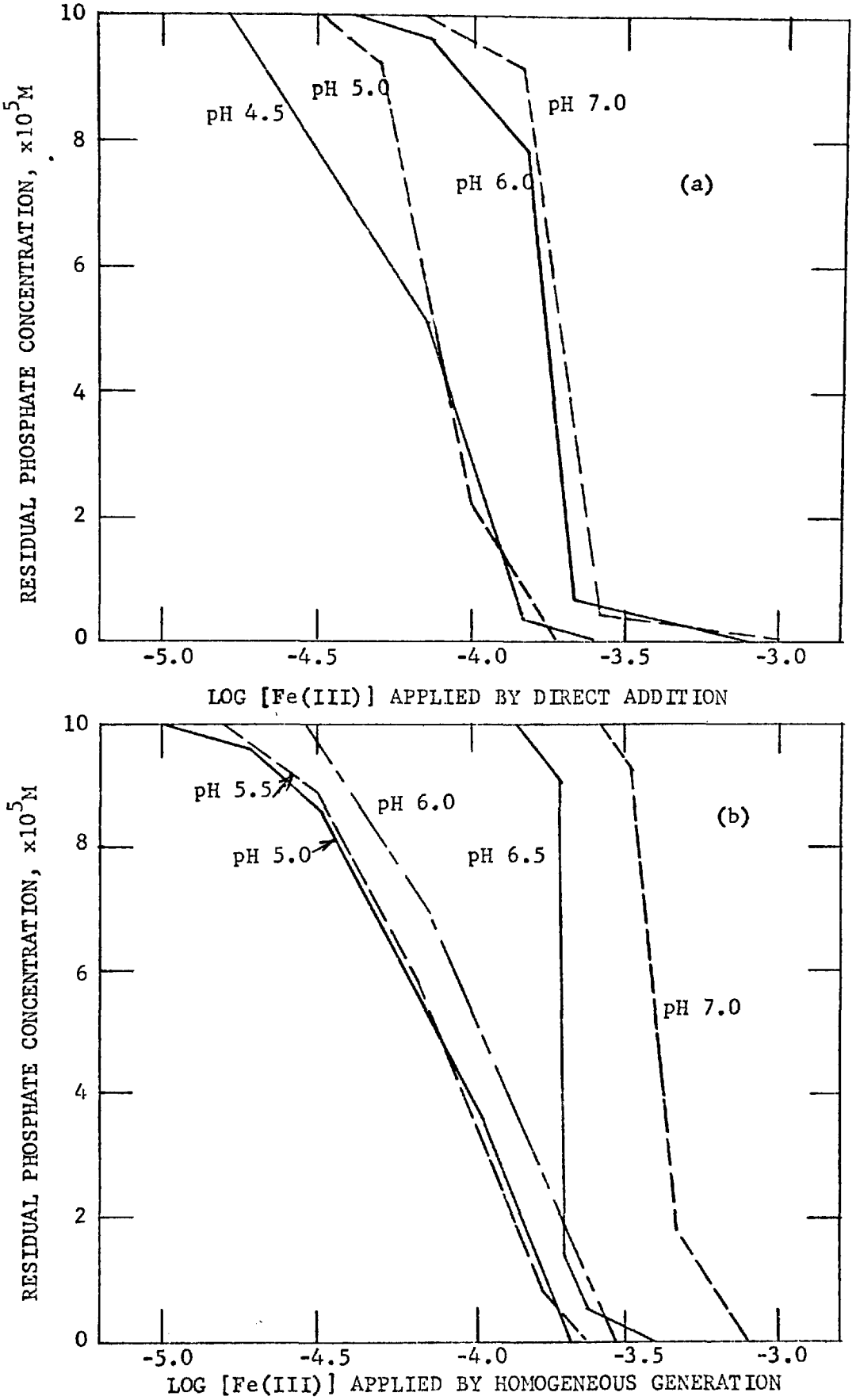

FIGURE 4-9. Precipitation of phosphate by (a) direct addition of Fe(III) and by (b) homogeneous generation of Fe(III).

The improvement is exhibited most clearly at the lower pH-values studied. Stoichiometric removal is again observed in the lower pH-range, where partial removal is exhibited even at applied concentrations of Fe(III) considerably below 10^{-4}M. It should be noted, however, that perfect stoichiometric removal is not effected; approximately 3×10^{-5}M of phosphate still remains, even after the application of 10^{-4}M Fe(III).

A distinction must again be made between equilibrium and kinetics. The problem at-hand deals with a non-equilibrium situation and, although equilibrium considerations can serve as a guide, kinetic considerations are required. Phosphate may be removed from solution in two ways: by formation of insoluble ferric phosphate, or by incorporation in the ferric hydroxide network. The latter is, by definition, a less efficient process. Conditions which favor direct iron-phosphate interactions over hydrolytic reactions should lead to a more effectual removal of phosphate. At lower pH-values, hydrolysis is decelerated and precipitation of phosphate is enhanced. However, given sufficient time, the possibility of conversion of $FePO_4$ to $Fe(OH)_3$ cannot be discounted under conditions where the latter is the thermodynamically stable solid phase. The results reported in Figure 4-9 reflect removal of phosphate after only fifteen minutes. With longer periods of time, phosphate might be released if such a solid conversion were to occur.

The improvement in the removal of phosphate by homogeneous precipitation can also be attributed, in part, to the catalytic influence which phosphate exerts on the oxidation of ferrous iron. In Chapter 3, it was indicated that the apparent catalytic effect of

phosphate may arise from its coordination with Fe^{+2}, in which case it would remain bound to the product Fe(III), thus increasing its chances of removal from solution.

4-5 Summary

The rate of hydrolysis of ferric iron was shown to be an influential parameter in coagulation and precipitation phenomena in natural systems. Two important features of the hydrolytic reactions were emphasized, namely the decided dependence of the reaction rate on $[OH^-]$, and the kinetic irreversibility of the reactions. Consequently, the creation of concentration gradients, such as those which arise by the addition of a basifying agent, may cause an undesirable effect in the system under investigation. The techniques of homogeneous precipitation are recommended as one means of overcoming such irreversible interferences.

References

1) Sillen, L.G., "Quantitative Studies of Hydrolitic Equilibria," Quart. Revs., Chem. Soc. London, 13, 146 (1959)

2) Stumm, W., "Metal Ions in Aqueous Solution," page 520 in Principles and Applications of Water Chemistry, S. D. Faust and J. V. Hunter, eds., John Wiley and Sons, Inc., New York (1967)

3) Feitknecht, W., and Schindler, P., "Solubility Constants of Metal Oxides, Metal Hydroxides, and Metal Hydroxide Salts in Aqueous Solution," Pure Appl. Chem., 6, 132 (1963)

4) O'Melia, C. R., and Stumm, W., "Aggregation of Silica Dispersions by Iron (III)," Journ. Coll. Inter. Sci., 23, 437 (1967)

5) Morgan, J. J., and Stumm, W., "The Role of Multivalent Metal Oxides in Limnological Transformations, as Exemplified by Iron and Manganese," Proc. 2nd Intl. Wat. Poll. Res. Conf., page 103, Tokyo (1964)

6) Lee, G. F., and Stumm, W., "Determination of Ferrous Iron in the Presence of Ferric Iron," J. Amer. Wat. Works Assn., 52, 1567 (1960)

7) Biedermann, G., and Chow, J. T., "The Hydrolysis of the Iron (III) Ion and the Solubility Product of $Fe(OH)_{2.70}Cl_{0.30}$ in 0.5M $(Na^+)Cl^-$ Medium," Acta Chem. Scand., 20, 1376 (1966)

8) Wendt, H., and Strehlow, H., "Schnelle Ionenreaktionen in Losungen. II. Die Bildung einiger einfacher Komplexe des Eisen-III-ions," Z. Elektrochem., 66, 228 (1962)

9) Wendt, H., "Schnelle Ionenreaktionen in Losungen. III. Die Kinetik der Bildung des binuklearen Eisen-III-hydroxokomplexes $Fe(OH)_2Fe^{+4}$," Z. Elektrochem., 66, 235 (1962)

10) Schenk, J. E., and Weber, W. J., "Chemical Interactions of Dissolved Silica with Iron (II) and Iron (III)," J. Amer. Wat. Works Assn., 60, 199 (1968)

11) Biedermann, G., and Schindler, P., "On the Solubility Product of Precipitated Iron (III) Hydroxide," Acta Chem. Scand., 11, 731 (1957)

12) Spiro, T. G., Allerton, S. E., Renner, J., Terzis, A., Bils, R., and Saltman, P., "The Hydrolytic Polymerization of Iron (III)," J. Amer. Chem. Soc., 88 2721 (1966)

13) Stumm, W., Huper, H., and Champlin, R. L., "Formation of Polysilicates as Determined by Coagulation Effects," Environ. Sci. Tech., 1, 221 (1967)

14) Gordon, L., Salutsky, M. L., and Willard, H. H., Precipitation from Homogeneous Solution, John Wiley and Sons, Inc., New York (1959)

15) Association of American Soap and Glycerine Producers, "Determination of Orthophosphate, Hydrolyzable Phosphate, and Total Phosphate in Surface Waters," J. Amer. Wat. Works Assn., 50, 1563 (1958)

CHAPTER 5

OXIDATION OF IRON PYRITE: POLLUTION OF NATURAL WATERS BY COAL MINE DRAINAGE

5-1 Introduction

Pollution by coal mine drainage arises from the exposure of sulfur-bearing minerals present in the coal strata to the natural weathering process. Mine drainage waters are characterized by low pH, high acidity, and large concentrations of sulfate and iron as well as other dissolved metals. Various measures have been proposed to cope with this problem, ranging from treatment of the ensuing wastewater to abatement methodology in which the weathering process is inhibited. However, before considering such corrective measures, attention must first be focused on the chemical reactions which occur and upon the kinetics which govern these reactions.

Despite previous creditable efforts, no unambiguous answer has been found as to which of the steps in the production of acid mine drainage determines the overall rate of dissolution of the sulfuritic agglomerates. To date, a didactical approach toward evaluating the individual factors controlling the kinetics of the overall reaction has been lacking. This chapter describes such an approach. The relative rates of the consecutive reactions involved have been considered, as well as the importance of each as it contributes to the problem of mine drainage. The rate-determining step of the overall sequence has

been ascertained and the physical, chemical, and biological factors influencing this step have been quantitatively evaluated. A model is presented to describe the mechanism by which the sulfide minerals are oxidized, and the consequences of the model are discussed from the standpoint of the various control methods which have been suggested.

5-2 Thermodynamics and Stoichiometry of Reactions

The mine-water system can be characterized by the following overall stoichiometric reactions:

$$FeS_2(s) + \frac{7}{2} O_2 + H_2O = Fe^{+2} + 2\ SO_4^{-2} + 2\ H^+ \qquad (5\text{-}1)$$

$$Fe^{+2} + \frac{1}{4} O_2 + H^+ = Fe^{+3} + \frac{1}{2} H_2O \qquad (5\text{-}2)$$

$$Fe^{+3} + 3\ H_2O = Fe(OH)_3(s) + 3\ H^+ \qquad (5\text{-}3)$$

$$FeS_2(s) + 14\ Fe^{+3} + 8\ H_2O = 15\ Fe^{+2} + 2\ SO_4^{-2} + 16\ H^+ \qquad (5\text{-}4)$$

The sulfur-bearing minerals predominant in coal seams are the iron sulfide ores, pyrite and marcasite. Both have the same ratio of sulfur to iron, but their crystallographic properties are quite different. Marcasite has an orthorhombic structure while pyrite is isometric (1). Marcasite is less stable and more easily decomposed than pyrite. The latter is the most widespread of all sulfide minerals and, as a result of its greater abundance in the eastern United States (2), pyrite is recognized as the major source of acid mine drainage.

During coal mining operations, pyrite is exposed to air and water with atmospheric oxygen oxidizing the sulfide of the pyrite to sulfate (5-1), releasing dissolved ferrous iron and acidity into the water. The dissolved ferrous iron undergoes oxygenation to ferric iron (5-2) which subsequently hydrolyzes to form insoluble ferric hydroxide (5-3), releasing more acidity to the stream and coating the stream bed. Ferric iron can also be reduced by pyrite itself, as in reaction 5-4, where sulfide is again oxidized and acidity is released along with additional ferrous iron which may re-enter the reaction cycle via 5-2.

The concentration of sulfate or acidity in the water can be directly correlated to the amount of pyrite which has been dissolved. The introduction of acidity into the stream arises from the oxidation of S_2(-II) of the iron pyrite (reactions 5-1 and 5-4) and from the oxygenation of Fe(II) and the ensuing hydrolysis of the resulting Fe(III) (reactions 5-2 and 5-3). There is a stoichiometry which should not be overlooked: the dissolution of one mole of iron pyrite leads ultimately to the release of four equivalents of acidity--two equivalents from the oxidation of S_2(-II) and two from the oxidation of Fe(II). The decomposition of iron pyrite is among the most acidic of all weathering reactions owing to the great insolubility of Fe(III) (3).

Pyritic agglomerates are thermodynamically unstable upon exposure to atmospheric oxygen, as demonstrated by calculating the change in free energy for reaction 5-1 as given in Appendix D. The exclusion of oxygen from the system may not be a practical solution to the problem from the standpoint of economics, technology, and, as will be seen

below, chemistry. Hence, efforts must be aimed at retarding the kinetics which control the dissolution of the pyritic material.

5-3 Previous Investigations of the Kinetics and Mechanism of Pyrite Dissolution

5-3.1 Physical and Chemical Studies

As a result of the complexity of the reactions and the failure of many previous observers to properly identify, isolate, and control the rate-determining variables, much of the data reported previously is difficult to interpret. The complex nature of pyrite itself, the variety of forms that sulfur may take as an intermediate, and the failure to single out the oxidizing agent all contribute to the complexity of the system.

Stokes (4) studied the oxidation of pyrite and marcasite by Fe(III) and, by analyzing the end products, concluded that the reaction proceeded by a two-step mechanism

$$FeS_2(s) + Fe_2(SO_4)_3 = 3\ FeSO_4 + 2\ S^o \qquad (5\text{-}5)$$

$$2\ S^o + 6\ Fe_2(SO_4)_3 + 8\ H_2O = 12\ FeSO_4 + 8\ H_2SO_4 \qquad (5\text{-}6)$$

Nelson and Snow (5) observed that the rate of oxidation of pyritic sulfur in coal by oxygen was markedly influenced by the degree of fineness of the coal, the rate being inversely proportional to the average diameter of the coal particles. The addition of ferric sulfate was found to hasten the oxidation process.

Instead of looking at the overall reaction and the kinetic variables affecting it, Sato (6) employed a technique by which electrode

potentials of sulfide minerals were measured in order to elucidate the oxidation mechanism by which the minerals dissolve. When both the oxidation potential of the sulfide test electrode and the oxidation potential of the solution with which it is in contact are identical, equilibrium has been reached, i.e., the potential corresponds to the equilibrium potential between the mineral and its dissolved oxidizing ions. Consequently, the equilibrium potential is controlled by the first-step reaction: the heterogeneous reaction whereby the sulfide dissolves. By measuring the electrode potential of the mineral and comparing it to the oxidation potentials of the various possible half-cell reactions of the sulfide using independent thermodynamic data, Sato found the oxidation reaction for pyrite which best fits the measured electrode potentials to be

$$FeS_2(s) = Fe^{+2} + S_2(g) + 2\ e^- \qquad (5\text{-}7)$$

for pH values below 2. This technique, although it does not describe the kinetics of the oxidation of pyrite, does give some insight as to the mechanism by which pyrite is oxidized. If the reduction reaction could be identified then, by summation of the two half-reactions, one would have the first step in the dissolution of iron pyrite. As Sato explains, once the heterogeneous reaction is established, the other consecutive reactions for the oxidation of sulfur and ferrous iron can be treated individually.

Garrels and Thompson (7) studied the rate of reduction of Fe(III) by iron pyrite at pH values below 2 and observed that the instantaneous rate of reduction of Fe(III) decreased as the ratio of ferric to ferrous

iron decreased. The rate was assumed to be proportional to differential adsorption of ferric and ferrous iron on the surface of pyrite, i.e., to the fraction of pyrite surface occupied by Fe(III). In each case, fifty percent of the ferric iron was reduced by two grams of crushed pyrite in less than one day.

A number of hydrometallurgical studies have been conducted dealing with the oxidation of iron sulfide minerals at elevated temperatures and under pressure to further understand the kinetics of the pressure-leach process employed in the treatment of pyritic ores. McKay and Halpern (8) investigated the oxidation of iron pyrite at temperatures of 100 to 130°C and at partial pressures of oxygen of 0 to 4 atmospheres. The reaction was found to be first order in surface area of pyrite and first order in the partial pressure of oxygen. An attempt was made by McKay and Halpern to study the effect of Fe(III) on pyrite in the absence of oxygen in which they found that, although FeS_2 was oxidized and leached, the quantity of FeS_2 oxidized was small compared to that amount oxidized by oxygen under similar conditions. However, since the concentration of Fe(III) was limiting, i.e., 10^{-1}M Fe(III) was completely reduced by 0.33M FeS_2 within two hours, one should not expect more than $\frac{1}{14} \times 10^{-1}$M of pyrite to be leached according to the stoichiometry of the reaction (5-4). Hence, the inability of Fe(III) to compete with oxygen as an effective oxidant of iron pyrite was not justifiably demonstrated.

Pressure-leaching of pyrite was also investigated by Gerlach, et al (9) over a wider range of temperatures and partial pressures of oxygen. Their results are similar to those of McKay and Halpern (8)

with regard to the observed dependencies of the rate law and the proposed mechanism for the reaction.

Neither study, however, considered in adequate detail the oxidation of pyrite by ferric iron which is inevitably produced by the process. Barnes and Romberger (10) also fail to place ferric iron in its proper perspective when they consider the concentration of dissolved Fe(III) to be so small in acid mine drainage that its significance as an oxidant is unlikely. However, in view of the vast amount of Fe(II) oxidized to Fe(III), there certainly is a significant supply of Fe(III) readily available as an oxidant of pyrite. Even though the standing concentration of Fe(III) may be small, its reactivity in terms of its rate of turnover is relatively high. Smith, Svanks, and Shumate (11) noted the significance of ferric iron after observing a similarity between the rates of aerobic and anaerobic oxidation of iron pyrite, and postulated that the ultimate oxidant for both aerobic and anaerobic oxidation is ferric iron.

5-3.2 Microbiological Studies

Since the first recorded isolation from acid mine waters of bacteria capable of influencing the oxidation of ferrous iron to ferric iron (12), numerous biological reports dealing with microbial catalysis of the oxidation of ferrous iron and various sulfide minerals have flooded the literature. Temple and Colmer (13) named their "iron-oxidizing" autotroph Thiobacillus ferrooxidans, it being capable of autotrophic growth at the expense of ferrous iron or thiosulfate. This bacterium differs from the autotroph Thiobacillus thiooxidans

which also has been isolated from acid mine streams but which derives its energy by catalyzing the oxidation of elemental sulfur. After summarizing the known facts regarding autotrophic bacteria and the dissolution of iron pyrite, Temple and Delchamps (14) postulated the overall sequence describing the formation of acid in coal mines as follows:

The sulfide of finely-divided iron pyrite or marcasite is chemically oxidized by oxygen to sulfate

$$FeS_2(s) + H_2O + 3\ 1/2\ O_2 = Fe^{+2} + 2\ SO_4^{-2} + 2\ H^+ \qquad (5\text{-}8)$$

Ferrous iron is oxygenated, under the catalytic influence of the autotroph Thiobacillus ferrooxidans, to ferric iron

$$Fe^{+2} + 1/4\ O_2 + H^+ = Fe^{+3} + 1/2\ H_2O \qquad (5\text{-}9)$$

As rapidly as it is formed, ferric iron is chemically reduced by the finely-divided iron pyrite

$$2\ Fe^{+3} + FeS_2(s) = 3\ Fe^{+2} + 2\ S^o \qquad (5\text{-}10)$$

The elemental sulfur liberated may be oxidized by ferric iron

$$2\ S^o + 12\ Fe^{+3} + 8\ H_2O = 12\ Fe^{+2} + 2\ SO_4^{-2} + 16\ H^+ \qquad (5\text{-}11)$$

or by oxygen, in which case the reaction is catalyzed by the autotroph Thiobacillus thiooxidans

$$S^o + 1\ 1/2\ O_2 + H_2O = 2\ H^+ + SO_4^{-2} \qquad (5\text{-}12)$$

The ferrous iron resulting from the oxidation of pyrite by ferric iron is then subject to further microbial action by Thiobacillus ferrooxidans, as in reaction 5-9. A cycle is established involving formation

of Fe(III) from Fe(II) by microbial catalysis, and chemical oxidation of iron pyrite by the resultant Fe(III).

This significant piece of work was obscured by later developments which questioned some of the physiological properties of T. ferrooxidans, in particular its ability toward mediating the oxidation of thiosulfate and not elemental sulfur. Two additional autotrophic organisms were proposed, confusing the issue regarding autotrophic oxidation of ferrous iron and its role in acid mine drainage: Ferrobacillus ferrooxidans (15), which was able to grow on ferrous iron but not on thiosulfate or elemental sulfur, and Ferrobacillus sulfoxidans (16), which could utilize either ferrous iron or elemental sulfur as an energy source. Unz and Lundgren (17) concluded that the organisms were all nutritionally similar and called for a re-evaluation of the current classification procedure.

This controversy also hindered verification that the oxidation of Fe(II) was a direct microbial effect and not an indirect one, i.e., whether or not the organisms were true chemo-autotrophs which derived their energy from the direct oxidation of Fe(II). Little quantitative evidence correlating the rate of growth of the organisms and the rate of oxidation of ferrous iron was available until Silverman and Lundgren (18) showed that the change in the logarithm of the concentration of F. ferrooxidans paralleled the increase in the logarithm of the concentration of Fe(III) produced by the oxidation of Fe(II). They also observed (19) that the quantity of carbon assimilated was in accordance with the thermodynamic free energy available from the oxidation of Fe(II). Schnaitman (20) demonstrated that microbial mediation of the oxidation of ferrous iron by F. ferrooxidans conformed to Michaelis-

Menton enzyme kinetics, and that the rate of oxidation was proportional to the relative concentration of bacterial cells.

Numerous reports persist in the literature concerning the nature of the influence these chemo-autotrophic microorganisms exert on the oxidation of pyrite and marcasite, as well as other sulfide minerals encountered especially in the copper mines in the western United States. Brynner, et al (21) have attributed leaching of chalcopyrite ($CuFeS_2$), covellite (CuS), chalcocite (Cu_2S), bornite ($CuFeS_4$), and tetrahedrite ($Cu_8Sb_2S_7$) to direct biological oxidation. Molybdenite (MoS_2) (22) and orpiment (As_2S_3) (23) have also been reported to be subject to direct oxidation. Silverman and Ehrlich (24) reviewed the subject of microbial catalysis of mineral transformations and indicated that the action of autotrophic microorganisms may be two-fold: to regenerate ferric iron from ferrous iron which then chemically oxidizes the mineral sulfide; and to directly attack and oxidize the sulfide minerals independent of the action of ferric iron. Ehrlich (25) has testified to the likelihood of such a direct effect, but no mechanism has yet been proposed.

5-4 Purpose of Experimental Study

Since "at-source" control of coal mine drainage must depend upon retardation of the kinetics controlling the oxidation of pyrite, it is necessary to know which of the sequential reactions involved controls the overall rate of the reaction. This study was undertaken to investigate the relative rates of the various reactions producing acid mine drainage, to ascertain which of the steps is rate-limiting,

and to suggest measures for controlling this particular reaction in natural waters.

5-5 Oxygenation of Ferrous Iron

The oxidation of ferrous iron was discussed in Chapter 3 and it was seen that, in the acidic pH-range corresponding to conditions encountered in mine drainage waters, the reaction proceeds relatively slowly and is independent of pH. However, the composition of actual mine waters may be such that oxidation is accelerated, i.e., physical conditions or chemical and biological agents may be present which influence the rate of oxidation of Fe(II). Examples of these include inorganic ligands, such as sulfate, which complex ferrous and ferric iron, soluble metal ions such as copper(II), aluminum, and manganese(II), suspended material with large surface areas and high adsorptive capacities, such as coal and clay particles, and microorganisms. All have been implicated in the literature, in various circumstances, as being capable of accelerating the rate of oxidation of Fe(II). Consequently, the oxidation was investigated in the presence of many of these chemical catalytic agents to observe their effect on the rate of oxidation under synthetic mine conditions and to compare the observed catalytic rate with the actual rate of oxidation of ferrous iron in natural mine waters.

The studies were initially conducted in the absence of microorganisms in order to characterize the kinetics of the reaction in purely chemical terms.

5-5.1 Experimental Procedure

The experimental procedure and analytical techniques were similar to those employed in Chapter 3 to follow the oxidation of ferrous iron with time. For the slower long-term studies, the absorbances of acidified aliquots of the samples were measured at the isosbestic point of the system (where Fe^{+3} and $FeOH^{+2}$ have the same molar absorptivity) as an indication of the quantity of ferrous iron oxidized. Figure 5-1 shows that the molar absorptivity of the acidified solution containing Fe^{+3} and $FeOH^{+2}$, at 272 mu, is unaffected by concentrations of sulfate as high as 10^{-3}M.

For the short-term, more rapid catalytic studies, ferrous iron was determined directly by titration with permanganate, or by chelation by the colorimetric reagent bathophenanthroline (4,7-diphenyl-1,10-phenanthroline) (26). In the surface-catalytic studies, aliquots of the heterogeneous suspension were acidified with dilute perchloric acid and filtered. The solid material recovered was rinsed with dilute acid to remove all traces of ferrous iron that might have been adsorbed on the surfaces of the particles.

Samples were prepared containing various dilutions of a standardized solution of ferrous perchlorate and different concentrations of the catalytic agents. The effects of sulfate, aluminum, manganese(II), copper(II), powdered charcoal, alumina, silica, aged ferric hydroxide, crushed iron pyrite, and the natural clays bentonite and kaolinite were examined. The pH was adjusted with concentrated perchloric acid and the samples were allowed to equilibrate with the oxygen of the atmosphere. After removing aliquots for the above-mentioned analyses, the solutions

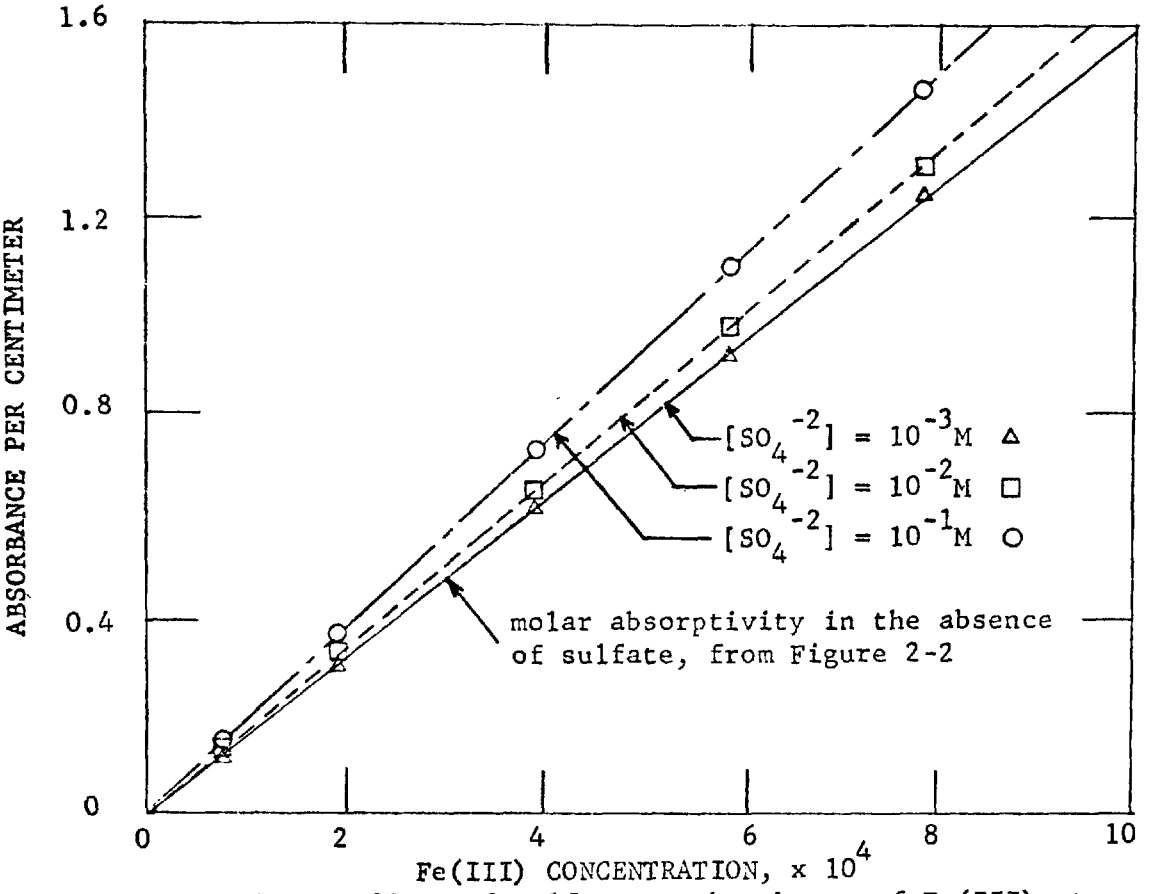

FIGURE 5-1. Effect of sulfate on absorbance of Fe(III) at 272 mμ.

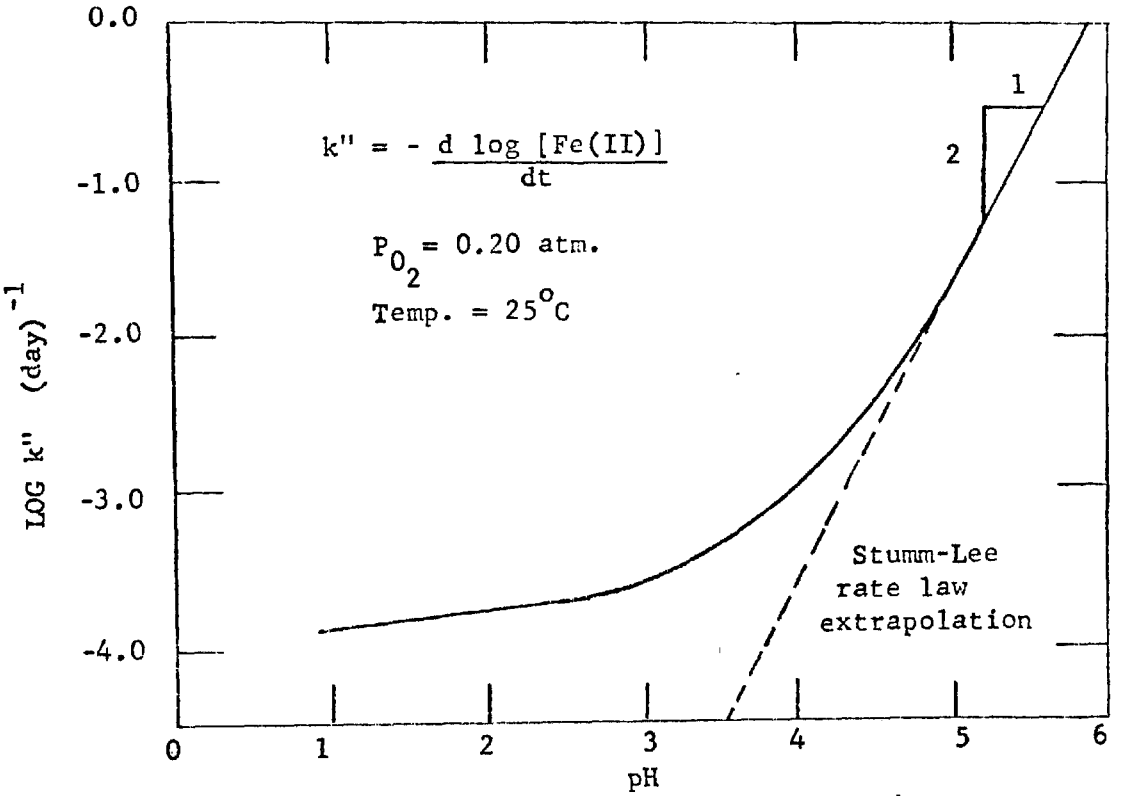

FIGURE 5-2. Rate of oxygenation of ferrous iron as a function of pH.

were re-equilibrated with the atmosphere. The samples were sealed and stored, quiescently, in an incubator at 25°C in the dark to avoid any photochemical interference. In the investigations involving heterogeneous catalysis (clays, pyrite, and powdered charcoal), the suspensions were stored on magnetic stirrers and shielded from light. One study was conducted under sterile conditions to preclude the influence of microbial catalysis which may have been accidentally effective through contamination.

5-5.2 Experimental Results and Discussion

Figure 5-2 summarizes the results reported in Chapter 3 for the uncatalyzed rate of oxidation of ferrous iron. This figure serves as the basis for comparison with the catalyzed rates.

Effect of Sulfate

The rate of oxidation of ferrous iron in the presence of sulfate can be satisfactorily fitted to a rate relationship which is first-order in the concentration of ferrous iron, as shown in Figure 5-3. The rate constant $k'' = -d \log_{10} [Fe(II)]/dt$ is of the same order of magnitude and is quite similar to the rate constant for the uncatalyzed reaction. To magnify the effect of any catalytic dependence of the oxidation on the concentration of sulfate, the study was repeated at 50°C where the change in Fe(II) per unit time is greater. Figure 5-4 demonstrates more vividly the catalytic effect of sulfate.

Huffman and Davidson (27) investigated the oxidation of Fe(II) in solutions of sulfuric acid, at 30.5°C and 1 M H_2SO_4, and observed the reaction to be second-order in Fe(II) according to the rate law

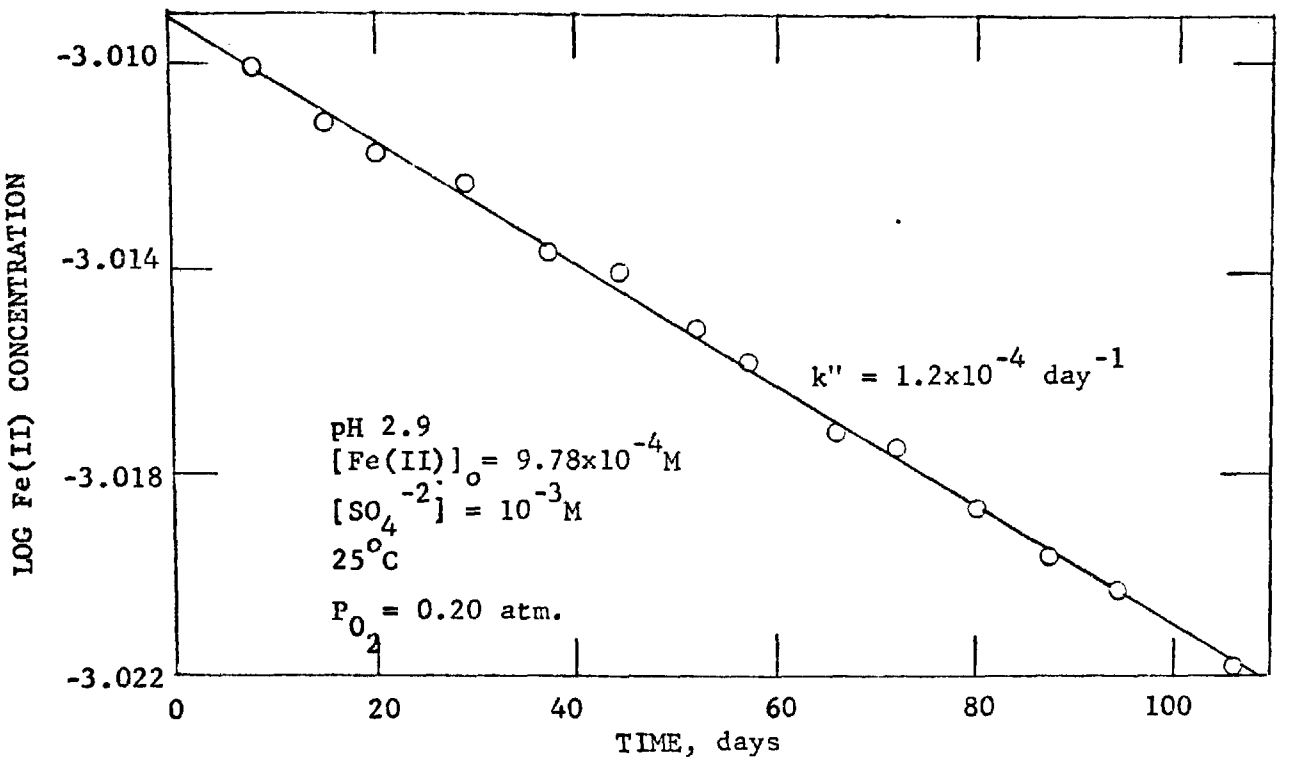

FIGURE 5-3. Rate of oxidation of ferrous iron in the presence of sulfate.

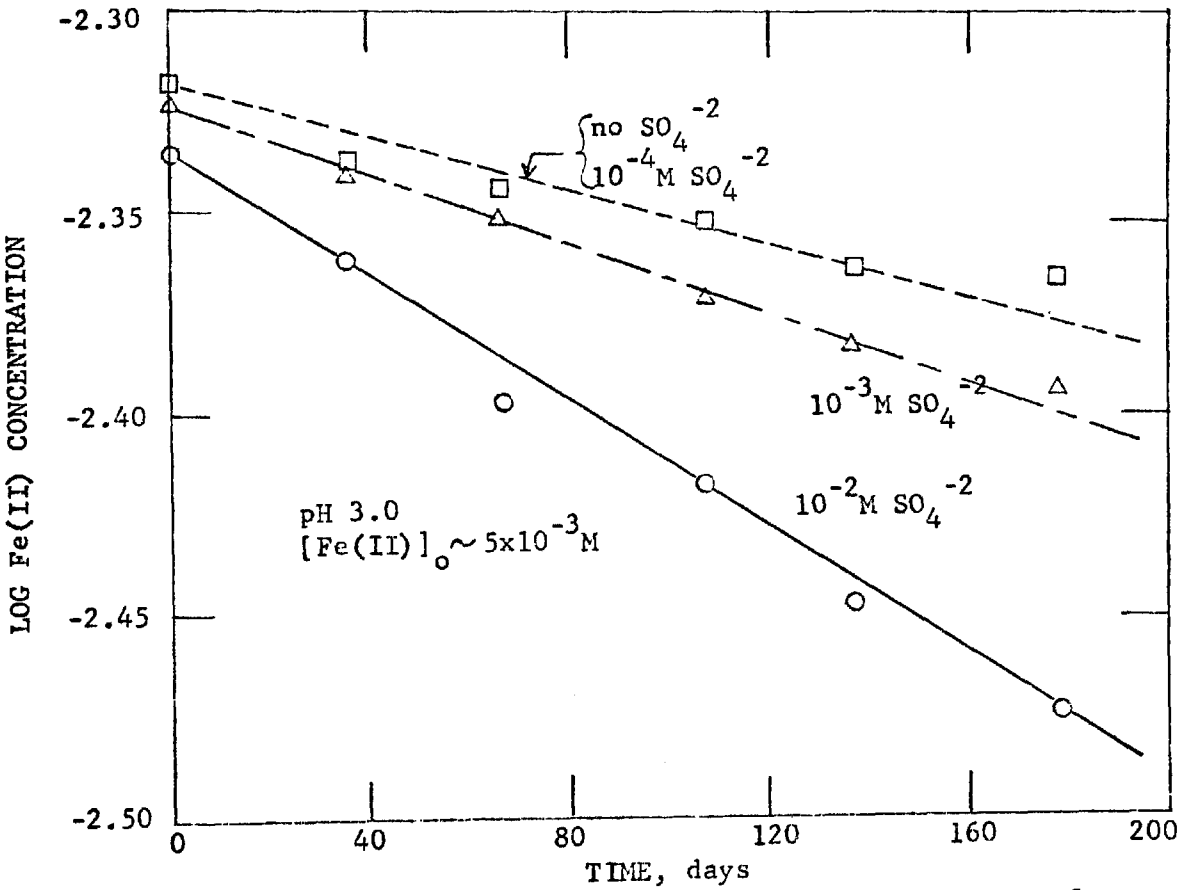

FIGURE 5-4. Effect of sulfate on the oxidation rate of ferrous iron at 50°C.

$$\frac{-d\,[Fe(II)]}{dt} = k_t\,[Fe(II)]^2\,P_{O_2} \qquad (5\text{-}13)$$

where the termolecular rate constant $k_t = 2.8 \times 10^{-6}$ liter mole $^{-1}$ atm^{-1}sec^{-1}. Under a partial pressure of oxygen of 0.2 atm. and an initial concentration of Fe(II) of 10^{-3}M, and converting the units of time, the initial rate "constant" of Huffman and Davidson can be approximated as $k' = 4.8 \times 10^{-5}$ day^{-1} ($k' = k_t[Fe(II)]_o P_{O_2} = -d \ln [Fe(II)]_o/dt$) or $k'' = 2.0 \times 10^{-5}$ day^{-1}. This pseudo-first-order rate "constant" can now be compared with the rate constants obtained in this study.

The observations of Huffman and Davidson in sulfuric acid show the oxidation to occur more rapidly in a solution containing sulfate than in a medium of perchlorate as investigated by George (28). The latter conducted his study of the oxidation of Fe(II) in perchloric acid and also observed the reaction to be second-order in Fe(II). (See Section 3-3.1.) Performing a similar calculation as above, the pseudo-first-order rate "constant" obtained by George is $k'' = 1.0 \times 10^{-5}$ day^{-1} at 30°C and approximately 10^{-2}M $HClO_4$.

The results both of Huffman and Davidson and of George are of the same order of magnitude as the results obtained in this study, except that these authors have characterized the oxidation as being second-order in Fe(II). For such an investigation, where the reaction proceeds so slowly that only 2-3% of the reaction is complete after three months, it becomes difficult to classify the reaction with respect to its order, as previously discussed in Chapter 3. The agreement among the pseudo-first-order rate constants is gratifying in itself. George and Huffman and Davidson also observed the rate of oxidation to increase only slightly with an increase in pH.

Figure 5-4, and a comparison of the results of Huffman and Davidson to those of George suggest that the oxidation of ferrous iron takes place more rapidly in the presence of sulfate than in perchlorate alone, the magnitude of the catalysis, however, being not very great.

Catalysis by Dissolved Metal Ions

Of the dissolved heavy metals which are normally present in natural mine waters, copper(II) exerted the strongest catalytic influence as shown in Figure 5-5. For the sake of convenience, and since the data fit the formulation fairly well, the rate has been plotted as a reaction which is first-order in Fe(II). The pseudo-first-order rate constant of $k'' = 4 \times 10^{-4} day^{-1}$ indicates that 10^{-4}M Cu(II) accelerates the rate of oxidation of Fe(II) approximately four-fold.

The cupric ion has been reported to be an efficient catalyst in the oxidation of Fe(II) in solutions of phosphoric acid (29), sulfuric acid (27), hydrochloric acid (30), and in the neutral pH-range corresponding to natural waters (31). Cher and Davidson (29) account for the catalytic effect of copper(II) by the following mechanism whereby Cu(II) serves as an electron-transfer catalyst:

$$Fe(II) + Cu(II) = Fe(III) + Cu(I) \qquad (5\text{-}14)$$

$$Cu(I) + O_2 = Cu(II) + \dot{H}O_2 \qquad (5\text{-}15)$$

The free radical $\dot{H}O_2$ reacts further with additional Fe(II) as in the Weiss scheme (32) previously discussed in Chapter 3.

The rate law for the oxidation of Fe(II) in solutions of sulfuric acid containing Cu(II) was reported by Huffman and Davidson (27) to be

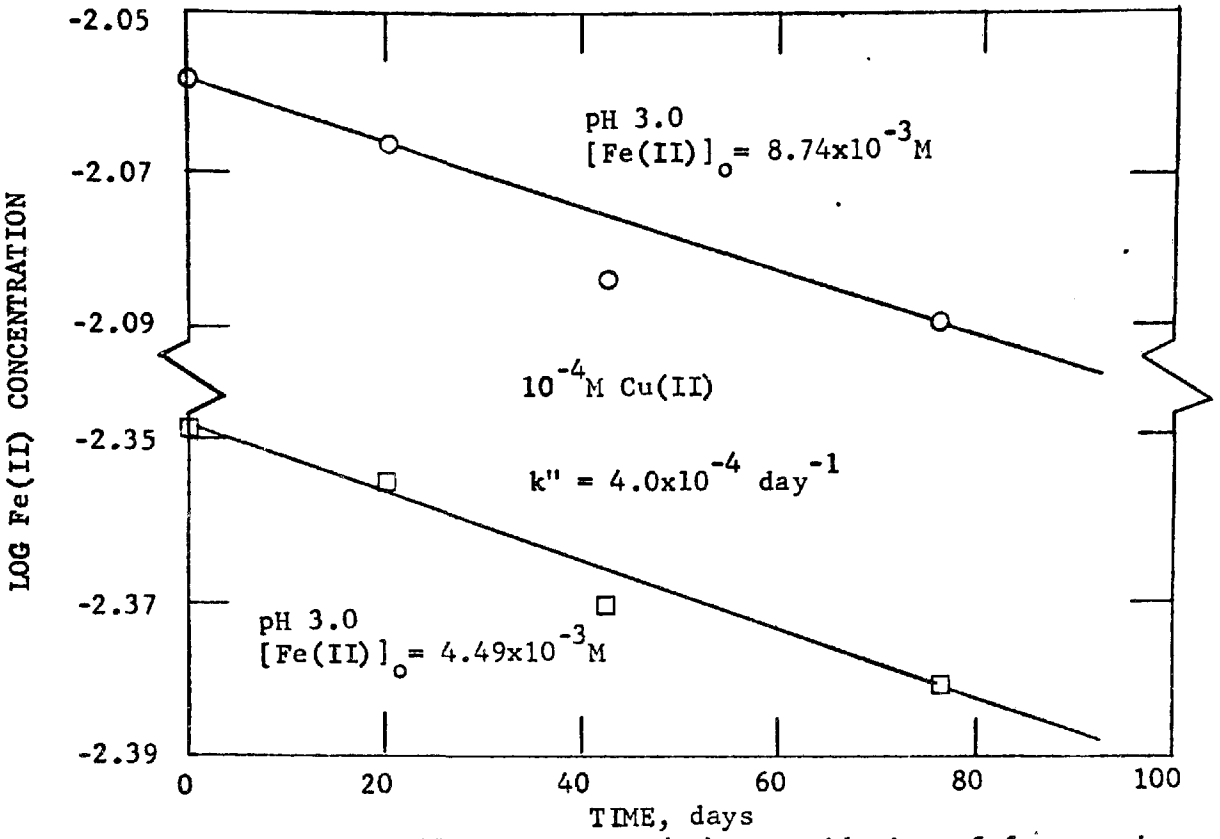

FIGURE 5-5. Effect of copper(II) on oxidation of ferrous iron.

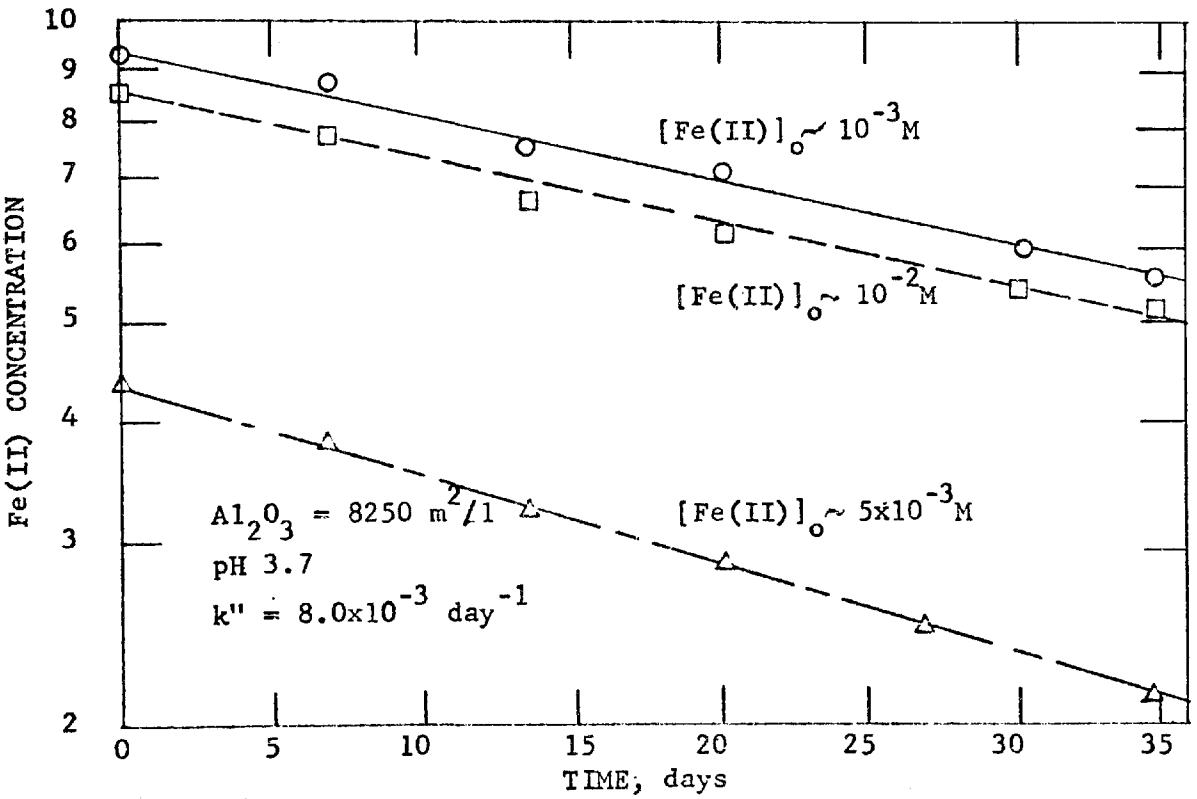

FIGURE 5-6. Rate of oxidation of ferrous iron in the presence of suspended aluminum oxide.

first-order in the concentrations of Fe(II) and Cu(II), Figure 5-5 conforming to such a description. The magnitude of the rate constant obtained in this study, however, cannot be compared with that of Huffman and Davidson in sulfuric acid since, in contrast to solutions containing no Cu(II), the rate of oxidation increases markedly with increasing concentration of acid (33). Indeed, the results of Huffman and Davidson, in 0.11M (H^+) and a total activity of sulfate of 0.58M, show the rate of oxidation of Fe(II) in the presence of 10^{-4}M Cu(II) to be about 100 times greater than depicted by Figure 5-5.

Although Stumm and Lee (31) observed other heavy metal ions (Mn^{+2}, Co^{+2}) to exhibit similar catalytic effects on the rate of oxidation of Fe(II) at neutral pH values, it was found that Mn^{+2} and Al^{+3} showed no measurable acceleration of the reaction rate for the acidic conditions of this study.

The Effect of Clays

On the premise that surfaces of clays play a significant role in the oxidation of ferrous iron in natural mine waters, a study of the catalytic effect of silica, SiO_2, and alumina, Al_2O_3, was undertaken. Silica and alumina, which are the basic building blocks of all clays (clays being composed of two dimensional arrays of silicon-oxygen tetrahedra and aluminum or magnesium-oxygen-hydroxide octahedra (34)), were selected as idealized representatives of natural clays. Hydration of the surface of the clay results in the formation of silanol, Si-OH, and aluminol, Al-OH, groups. Since the rate of oxidation of ferrous iron at higher pH-values is dependent upon $[OH^-]^2$ (see Chapter 3), it was believed that the hydroxo-metal groups of the

hydrated clay surface played a specific catalytic role due to the apparent localized high pH (high concentration of OH groups) at the particle surface. Furthermore, since clays are strongly adsorptive and exhibit ion-exchange properties, a general catalytic influence was thought to occur as a result of adsorption of the reactants and localized increased concentrations of reactants at the particle surface. In addition, Schenk and Weber (35) observed orthosilicic acid, H_4SiO_4, with which natural clays are in equilibrium, to increase the rate of oxidation of Fe(II) at pH-values greater than 5 in much the same manner as other inorganic ligands, such as phosphate, chloride, and sulfate.

Of the clay surfaces investigated, aluminum oxide (Baymal colloidal alumina, manufactured by E. I. DuPont de Nemours and Co., Wilmington, Delaware) exhibited the strongest catalytic properties. Figure 5-6 shows that, for a given pH and concentration of alumina, the surface-catalytic oxidation can be described by a rate equation which is first-order in concentration of Fe(II). The slope of the first-order plots (which is, by definition, the rate constant) is independent of the initial concentration of Fe(II) which further confirms the order of the reaction with respect to Fe(II). The rapidity of the surface-catalytic reaction compared to the uncatalyzed oxidation is demonstrated by noting the half-time of the former (the time required for 50% of the initial concentration of ferrous iron to be oxidized) to be only about 40 days, in contrast to about 500 days for the latter. Table 5-1 compares the surface-catalytic rate constants for alumina with the uncatalyzed rate constants for the oxidation of Fe(II), and it is seen that in the presence of about 8000 m^2/l of

Table 5-1. Comparison of Surface-Catalytic Rate Constants with Uncatalyzed Rate Constants

pH	log k''	
	Uncatalyzed Reaction	Al_2O_3* 8000 m^2/l
3.5	-3.6	-2.52
3.8	-3.4	-2.05
4.0	-3.3	-1.80

$$k'' = \frac{-d \log [Fe(II)]}{dt}$$

*Baymal Colloidal Alumina - manufactured by E. I. DuPont de Nemours and Co., Wilmington, Delaware.

Al_2O_3 surface, the catalyzed reaction is 10-30 times faster than the uncatalyzed reaction.

Figure 5-7 demonstrates further the direct catalytic dependence on Al_2O_3, showing the rate of oxidation of Fe(II) to increase as the areal concentration of the idealized clay is increased. The oxidation rate in the presence of alumina is also dependent upon pH as seen in Figure 5-8, with a regular increase in rate with increasing pH being observed.

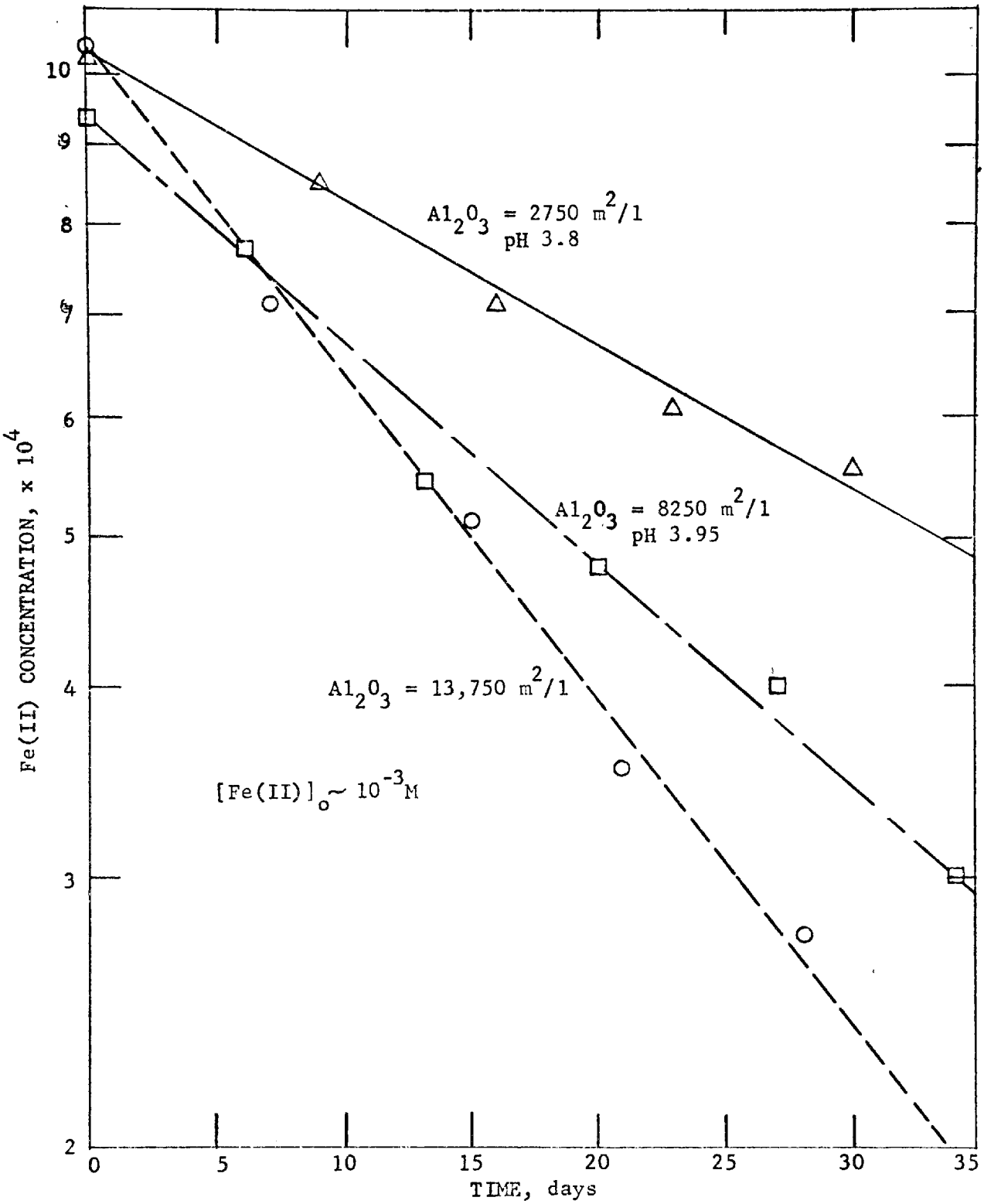

FIGURE 5-7. Oxidation of Fe(II) as a function of Al_2O_3 concentration.

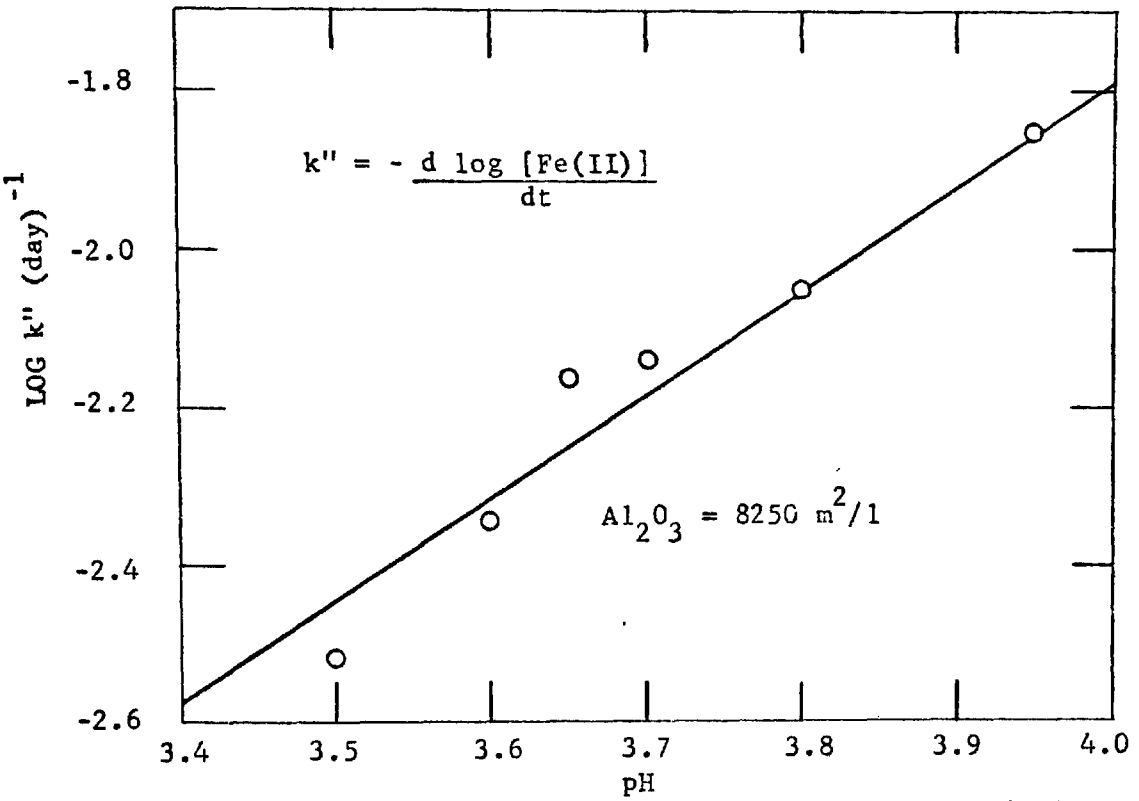

FIGURE 5-8. Effect of pH on surface-catalytic oxidation of ferrous iron.

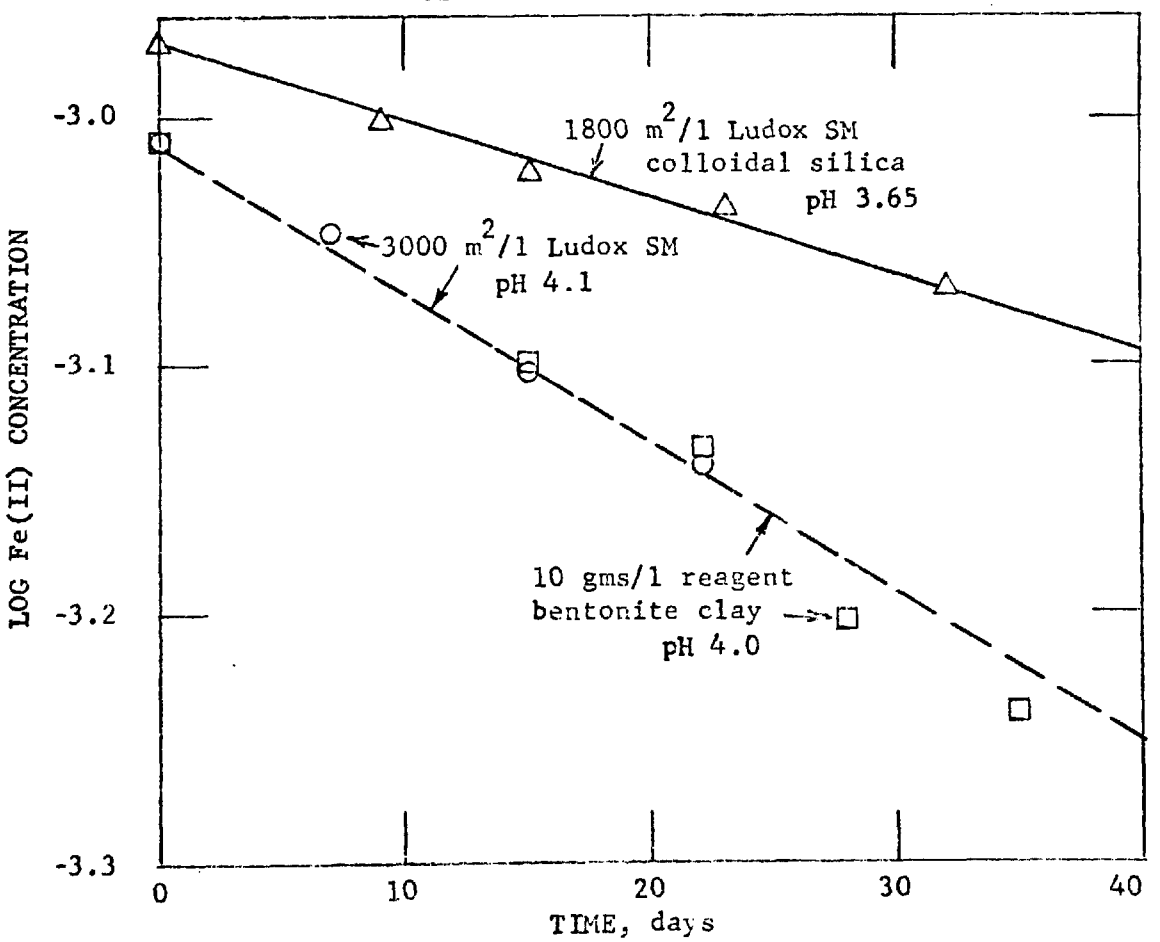

FIGURE 5-9. Rate of oxidation of ferrous iron in the presence of colloidal silica and bentonite clay.

(The catalytic effect of Al_2O_3 cannot be attributed to specific catalysis by dissolved Al(III) in equilibrium with the solid since it was previously shown that dissolved Al(III) had no measurable effect on the rate of oxidation of ferrous iron.)

Ludox colloidal silica (Ludox SM is a colloidal silica manufactured by E. I. DuPont de Nemours and Co., Wilmington, Delaware) and bentonite, a natural montmorillonite clay (Bentonite Powder, U.S.P., Fisher Scientific Co., Fair Lawn, New Jersey) were also found to catalyze the oxidation (Figure 5-9) but to a slightly lesser degree than the alumina. Kaolinite, another natural clay, demonstrated no catalytic properties although it gradually neutralized the acidity.

Colloidal ferric hydroxide, prepared by allowing a solution of Fe(III) oversaturated with respect to the hydroxide to hydrolyze, showed no tendency toward catalyzing the oxidation of Fe(II).

Catalysis by Powdered Charcoal

Lamb and Elder (33) reported that granular, steam-activated coconut charcoal markedly accelerated the rate of oxygenation of ferrous iron. This phenomenon was attributed to the ability of charcoal to greatly enhance decomposition of hydrogen peroxide in the presence of Fe(II), generating in turn the active free radicals which oxidize Fe(II) according to the Weiss mechanism (32).

In this study, reagent-grade sugar charcoal(purified reagent, Fisher Scientific Co., Fair Lawn, New Jersey) displayed no apparent catalytic tendency toward the oxygenation of Fe(II). Again, however, the catalytic properties of charcoal described by Lamb and Elder increased considerably as the concentration of acid increased, thus

accounting in part for the discrepancy between their results and those reported here. Furthermore, Lamb and Elder followed the oxidation of Fe(II) using an electrochemical technique whereby the change in electrochemical potential was correlated to a change in the Fe^{+2}/Fe^{+3} ratio by a modified Nernst equation. In the heterogeneous system containing suspended charcoal, the reliability of such measured potentials as indicators of the total concentration of Fe(II), both in solution and associated with the surface of charcoal, must be questioned especially when the rate of change of Fe(II) is so small. The presence of impurities in the charcoal also tend to cast doubt on the experimental reliability.*

Effect of Iron Pyrite

To complete the investigation of all natural chemical catalytic agents which may be responsible for acceleration of the rate of oxidation of ferrous iron in mine waters, the effect of iron pyrite itself was studied. It has been suggested by Smith, et al (11) that the surface of pyrite acts as a catalyst to greatly increase the rate of oxidation of adsorbed ferrous ions.

Mineral iron pyrite (Ward's Natural Science Establishment, Rochester, New York) was ball-milled and a portion of the 200-250 mesh fraction was suspended in a solution of ferrous iron at pH 3.0. The system was left open to the atmosphere and treated in the same fashion as the suspensions containing clays, aliquots being removed, acidified, millipore-filtered, and titrated with permanganate. The solid material recovered was rinsed with dilute acid to remove any adsorbed ferrous iron. No significant decrease in Fe(II) was observed after

* Researchers at Bituminous Coal Research, have found that some activated carbons have catalytic properties for ferrous iron oxidation while others do not.

several days although in some instances the concentration of Fe(II) increased slightly. Upon placing the system under an atmosphere of nitrogen, a similar small increase in ferrous iron was observed, indicative of a gradual dissolution of the pyrite itself.

Effect of Microorganisms

No microbial contaminations was observed in any of the above systems as evidenced by similar rates of oxidation in both sterile and nonsterile samples. The sterile samples gave, in every case, analogous results to those conducted under nonsterile conditions. The above findings are, therefore, the same as those obtained under sterile conditions.

Summary

Table 5-2 summarizes the results of the catalytic studies with the various chemical agents. The greatest influence on the rate of oxidation of Fe(II) was exhibited by the clay particles or their idealized counterparts, alumina and silica. The areal concentrations, however, are extremely large and are probably much greater than those encountered in most natural waters.

5-6 Field Investigations of Pyrite Oxidation in Natural Mine Waters

In order to compare these experimental results describing the kinetics of oxidation of ferrous iron in synthetic mine waters with the rate of oxidation in natural mine drainage waters, field investigations were conducted in the bituminous coal region of West Virginia. The Federal Water Pollution Control Administration has established a demonstration project in the Norton-Coalton area in north-central West

Table 5-2. Chemical Catalysis of Oxidation of Ferrous Iron

pH	log k''					
	Uncatalyzed	Catalysis By				
		10^{-2}M SO_4^{-2} at 50°C	10^{-4}M Cu^{+2}	Al_2O_3* 8000 m^2/1.	SiO_2‡ 3000 m^2/1.	Bentonite# 10 gms/1.
3.0	-3.8	-3.1	-3.4	--	--	--
3.5	-3.6	--	--	-2.5	--	--
3.8	-3.4	--	--	-2.1	--	--
4.0	-3.3	--	--	-1.8	-2.2	-2.2

$$k'' = \frac{-d \log [Fe(II)]}{dt}$$

*Baymal colloidal alumina, E. I. DuPont de Nemours and Co., Wilmington, Delaware

‡Ludox SM colloidal silica, E. I. DuPont de Nemours and Co., Wilmington, Delaware

#Fisher Scientific Company, U.S.P., Fair Lawn, New Jersey

Virginia, near Elkins, where various methods of pollution abatement technology are being examined. These attempts include air-sealing of mines and surface reclamation.

5-6.1 Collection and Analyses of Samples

Three sites were selected for the field investigation. Figure 5-10a shows an abandoned strip (surface) mine which is scheduled for

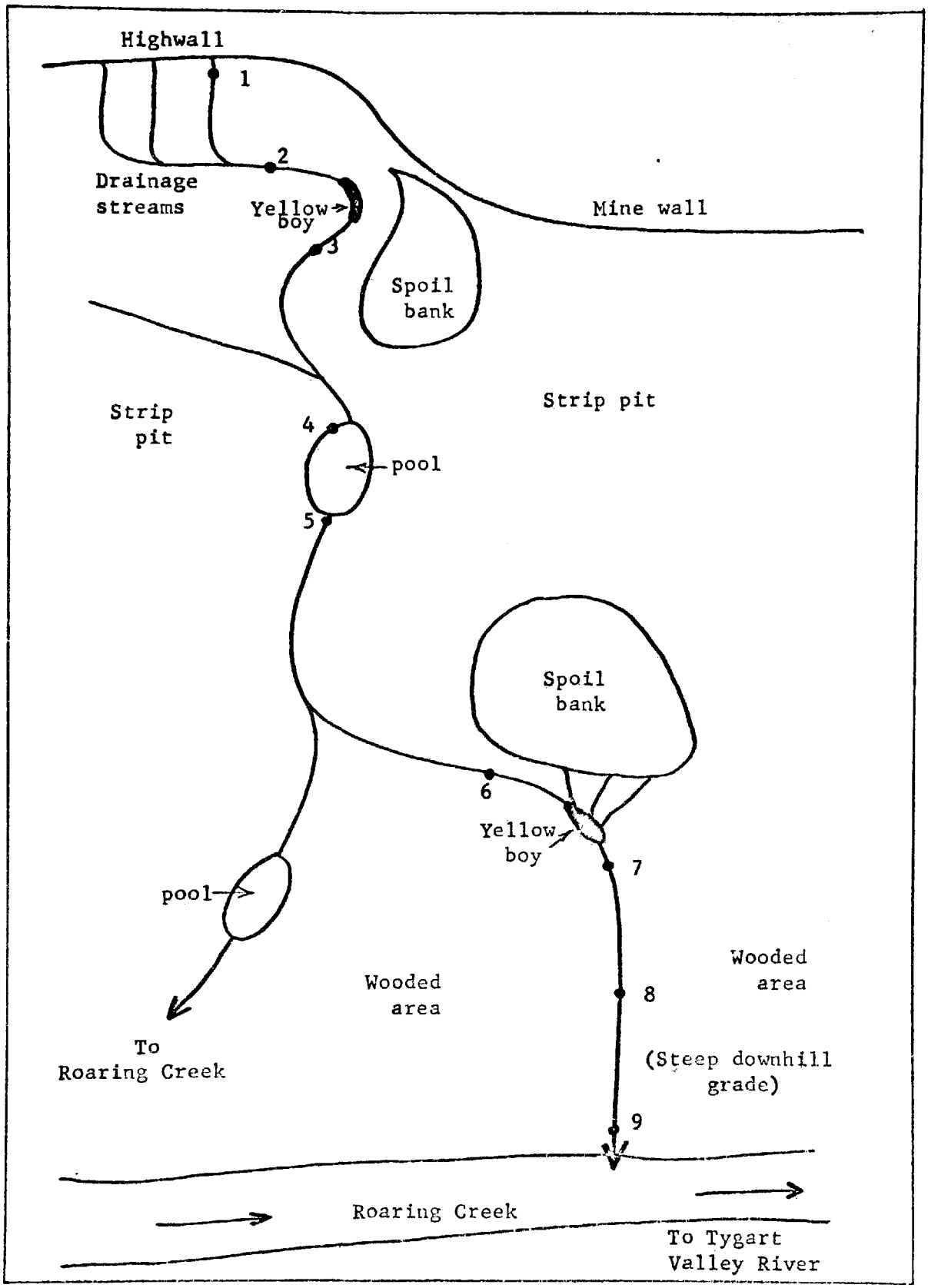

FIGURE 5-10a. Aerial view of drainage through a strip (surface) mine in the Mercer seam near Elkins, West Virginia. The points (•) refer to locations at which samples were collected for laboratory analyses.

reclamation. Surface runoff flows through a vegetated area, over a high-wall, and into the abandoned mine. In mining terminology, this worked-out mine is designated as a "strip pit"; the piles of waste material previously dug out are termed "spoil banks"; and the precipitated ferric hydroxide or sulfato-hydroxo intermediate is referred to as "yellow boy." Drainage water flowing through the mine deposits thick sediments of yellow boy at each juncture with drainage water from the spoil banks which are laden with pyritic material. The water exits the strip pit at site 7 and flows rapidly downhill through a wooded area to Roaring Creek, the main interceptor for this mining region.

Figure 5-10b represents a contour strip mine where drainage water passes between the mine wall and a spoil bank. Water which has drained through the underground mine trickles out of the mine opening at site 2.

The third sampling location, Figure 5-10c, is a mine entrance which has been sealed with concrete blocks and urethane foam to exclude air in an attempt to inhibit oxidation of pyrite inside the underground mine. Measurements by the FWPCA indicate that the partial pressure of oxygen behind the wall has been reduced to 7% (36). Drainage water flows out of the mine over a weir, and is exposed to oxygen of the atmosphere. After leaving the mine tunnel, the water enters a reclaimed area which has been limed in preparation for future vegetation. Deposits of yellow boy are abundant behind the weir and on the floor of the tunnel.

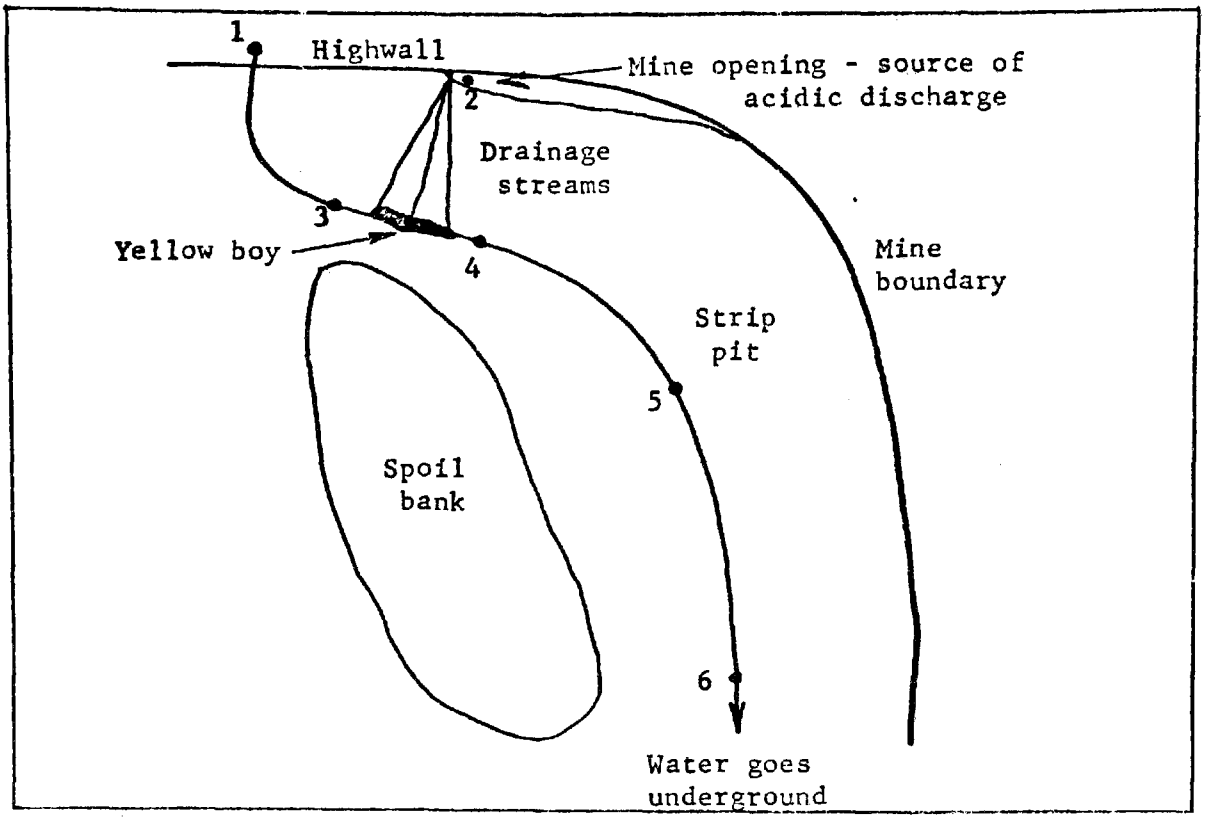

FIGURE 5-10b. Aerial view of surface mine near Elkins, West Virginia (Site GT 7-2). The points refer to sampling locations.

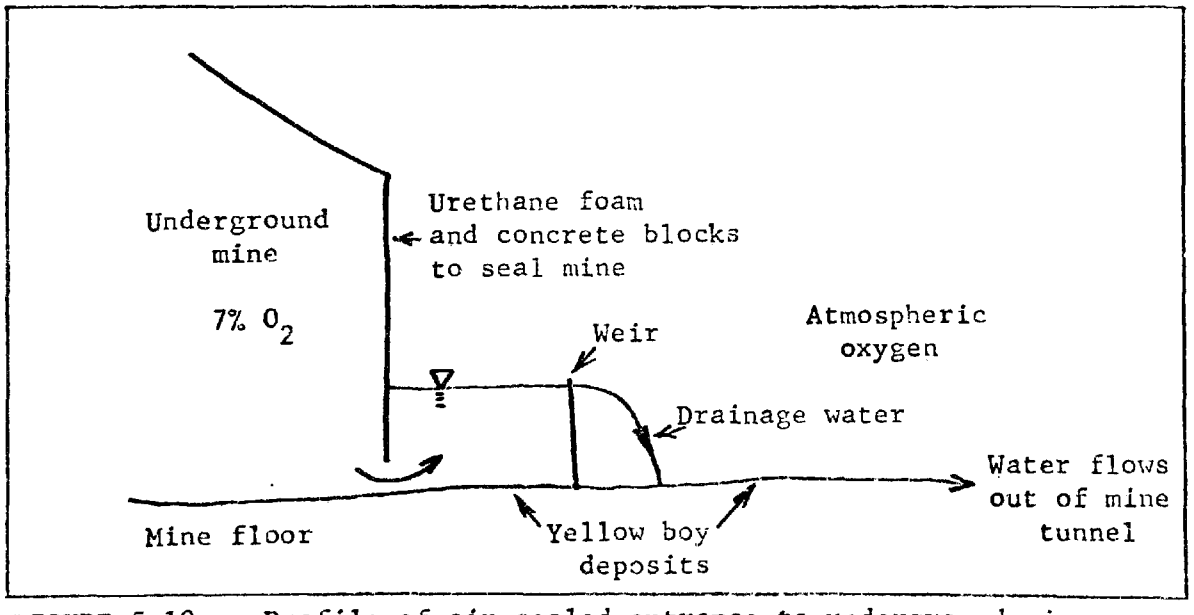

FIGURE 5-10c. Profile of air-sealed entrance to underground mine near Elkins, West Virginia (Site RT 9-11).

Samples from the three mining areas were analyzed for ferrous and total iron, sulfate, and acidity; temperature and pH were recorded in the field at the time of collection. Those samples taken for iron analyses were acidified with dilute acid upon collection, to quench any further reaction. Ferrous and total iron were determined utilizing bathophenanthroline (26). The burbidimetric procedure described in Standard Methods for the Examination of Water and Wastewater (37) was employed in the analysis for sulfate, the percent transmittance of the suspension of barium sulfate being measured using a Bausch and Lomb spectrophotometer (Model #340). The method of Salotto, et al (38), in which the sample is rapidly titrated to pH 7.3 with standard sodium hydroxide, after addition of hydrogen peroxide, was employed for the determination of acidity.

5-6.2 Results of Field Investigation

Stoichiometric Relationship Between Sulfate Concentration and Acidity

It was indicated in section 5-2 that the stoichiometry accompanying the dissolution of iron pyrite should conform to a definite pattern, the oxidation of one mole of pyrite causing the release of two moles of sulfate and four equivalents of acidity. Therefore, if sulfate and acidity were to behave in a conservative manner in mine waters, the change in either one or both of these products could be directly correlated to the quantity of pyrite dissolved.

A summary of the data obtained by analysis of the field samples is given in Table 5-3. For site GT7-2, a large increase in acidity, sulfate, and iron is seen at sampling site 4 after water from the mine

Table 5-3. Summary of Field Data

Sample Number	Distance, Feet	Temp., ^{o}C	pH	$FeII_T$ x 10^5M	Fe_T x 10^5M	SO_4^{-2} x 10^4M	Acidity x 10^4 eq/l
GT 7-2 1	0	13	5.2	0.12	0.22	0.76	1.8
3	50	16	4.2	0.15	0.25	0.86	2.0
4	75	17	3.7	1.74	4.07	2.49	4.7
5	300	18	3.7	1.67	2.71	4.44	5.0
6	500	15	3.8	0.80	1.67	4.32	4.5
2	-	12	2.8	7.92	98.9	29.0	41.7
MS - 1	0	14	3.9	0.07	0.12	7.1	7.5
2	100	19	3.6	3.49	5.68	19.9	24.8
3	300	20	3.4	5.63	13.8	25.8	26.0
4	425	--	3.4	6.50	10.7	33.8	21.7
5	550	18	3.4	8.54	11.3	34.3	22.4
6	800	20	3.3	5.94	11.9	33.7	23.1
7	1000	18	3.2	15.5	42.1	57.8	56.5
8	1200	15	3.5	11.3	38.4	49.0	48.5
9	1400	16	3.3	7.90	34.3	56.8	60.0
RT 9 -11	-	--	3.2	78.6	132.	78.0	49.8

opening has drained into the stream. The same observation can be made in the drainage from the Mercer Seam immediately downstream from the spoil bank. The low pH of the surface runoff upstream from the mines should be noted. Due to the low buffer capacity of the water, the mere introduction of organic acids from the soil and vegetation is sufficient to significantly lower the pH of the raw water.

Figure 5-11 is an attempt to correlate acidity to concentration of sulfate, the lines drawn representing the theoretical 2/1 ratio. As shown, the field data do not conform to such a correlation, the acidity being too low. Some of the acidity is apparently being neutralized by clays which are invariably present in the drainage waters and coal strata. The presence of dissolved aluminum in the acidic waters is indicative of decomposition of the clays and neutralization of acidity by the clay-water interaction. Hence, sulfate alone may be considered to behave in a conservative fashion in acid mine waters, in contrast to acidity and iron, and therefore it may be used, by itself, as an indicator of the quantity of pyrite dissolved.

Rate of Oxidation of Ferrous Iron

Of the mining areas sampled, RT 9-11 and the Mercer Seam proved to be the most informative. RT 9-11 served as a source of mine water having a high concentration of ferrous iron, while drainage from the Mercer Seam provided an opportunity by which the change in concentration of Fe(II) could be followed through a strip mine and downstream in an attempt to deduce the rate of oxidation of iron.

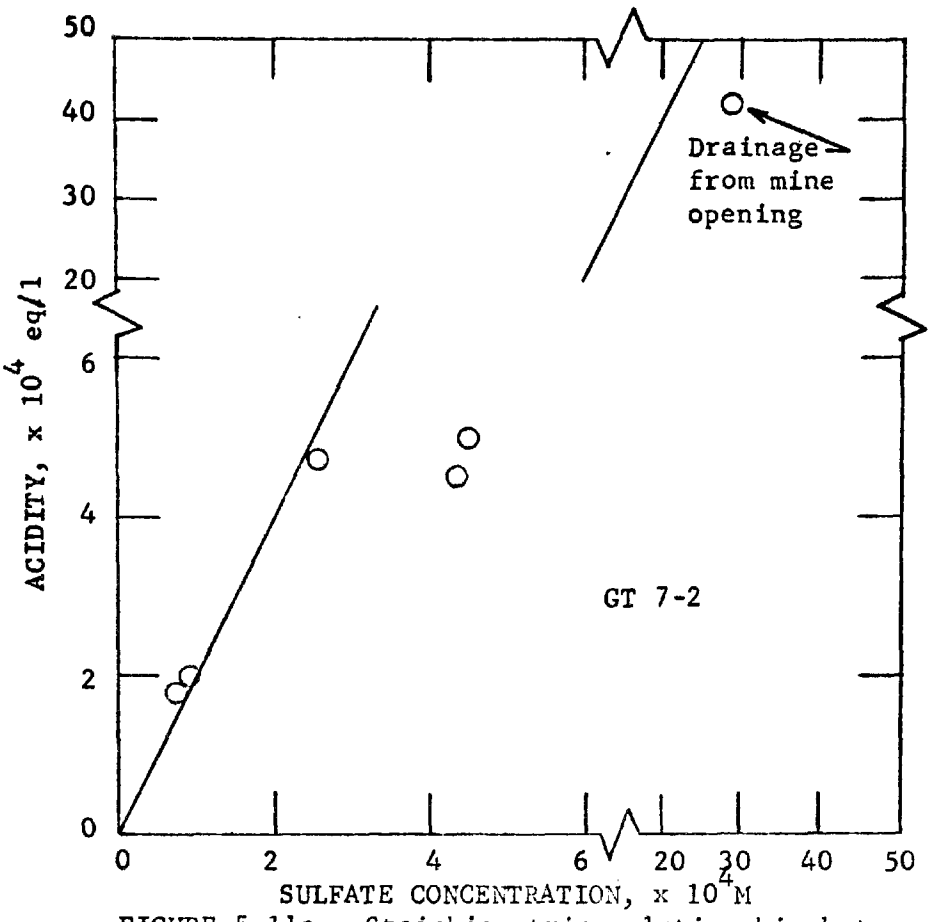

FIGURE 5-11a. Stoichiometric relationship between acidity and sulfate concentration in drainage water at location GT 7-2.

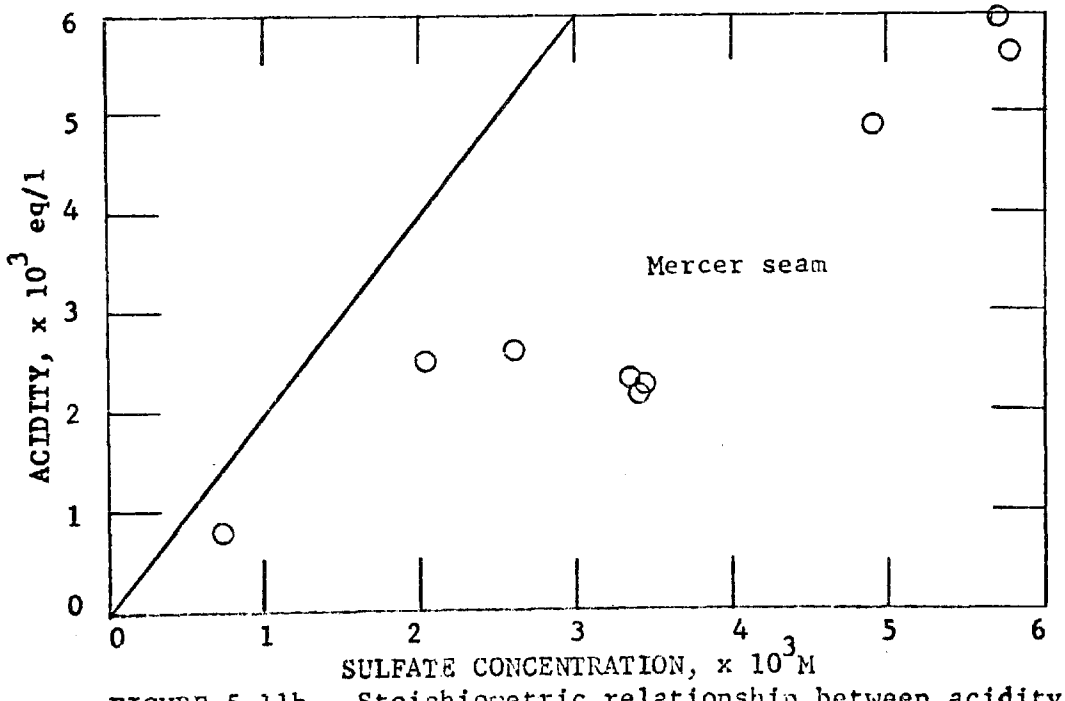

FIGURE 5-11b. Stoichiometric relationship between acidity and sulfate concentration in drainage through strip mine in Mercer seam.

Comparison with Laboratory Results

The data from Table 5-3 are plotted in Figure 5-12 showing the change in chemical composition of a drainage stream flowing through the Mercer mine and downstream before entering Roaring Creek. For the initial 1000 feet, the water continues to collect leachate from the spoil banks and from the pyrite with which it is in contact. The increase in the concentration of sulfate from 0 to 400 feet is about 3×10^{-2}M. This implies that the corresponding input of ferrous iron would increase by approximately 1.5×10^{-2}M bearing in mind the stoichiometry that one mole of pyrite releases two moles of sulfate and one mole of ferrous iron. However, most of this Fe(II) is apparently oxidized quite rapidly as evidenced by the abundant deposition of yellow boy and by the low concentration of Fe(II) observed in the stream (only 8×10^{-5}M at 550 feet).

Beyond 1000 feet, the drainage stream flows outside the mine and is no longer subject to continuous pyritic discharges, or to dilution from additional drainage streams. Figure 5-13 shows the oxidation of Fe(II) in the non-pyritic wooded area to be essentially first-order in Fe(II) with distance. If one assumes a constant velocity of flow over this distance in the range of 1 ft. per min. to 100 ft. per min., the range of the first-order rate constant, k", is 7.4×10^{-4} to 7.4×10^{-2} min.$^{-1}$, where $k'' = -d \log [Fe(II)]/dt$. This corresponds to $k'' \sim 1 \times 10^{1}$ day^{-1} which is orders of magnitude greater than the laboratory experiments at pH 3.3 would predict. The velocity of flow is probably not constant but for the sake of comparison, in order to underscore the rapidity of the reaction in natural mine waters, it is a useful approximation.

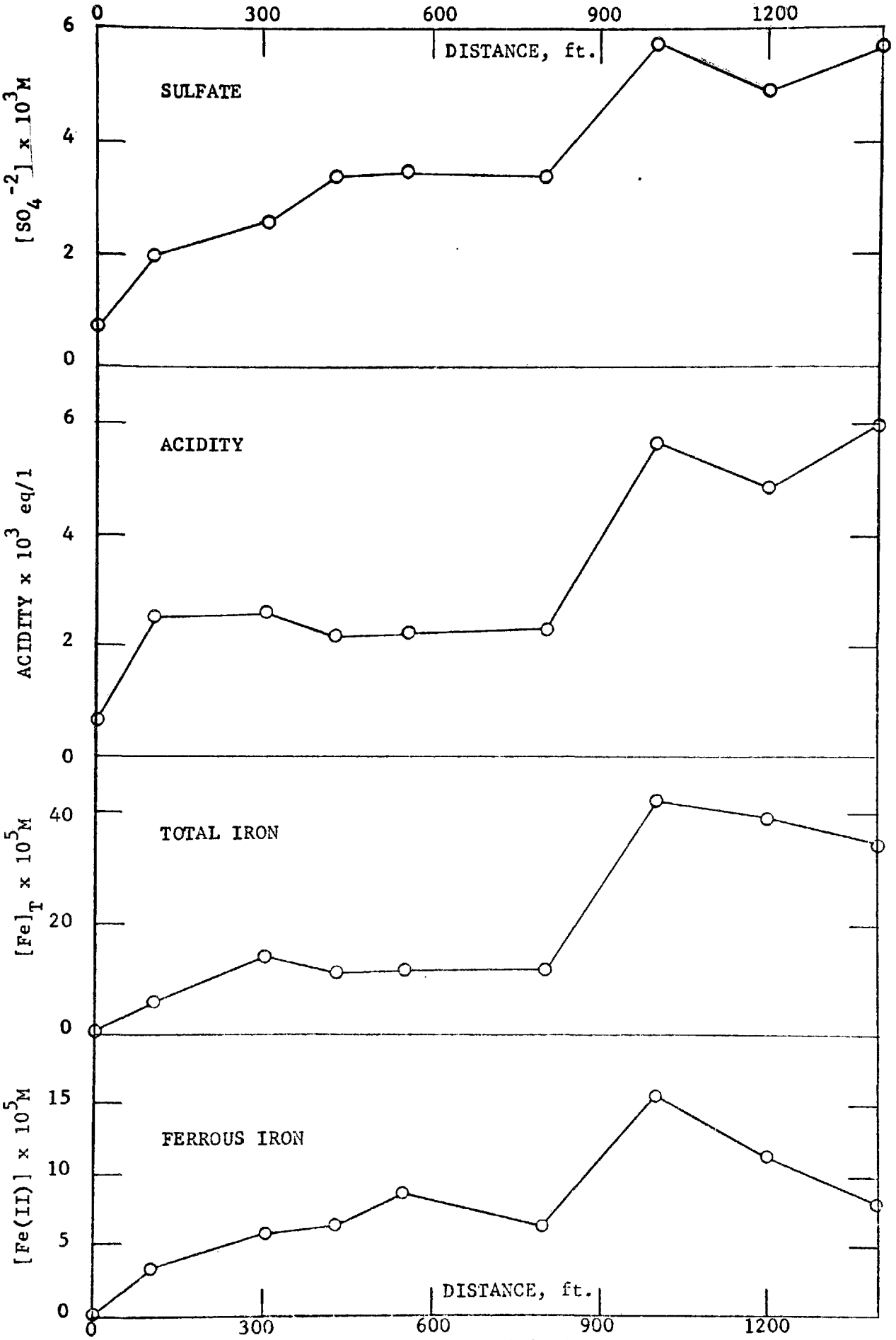

FIGURE 5-12. Chemical composition of drainage water through strip mine in Mercer seam.

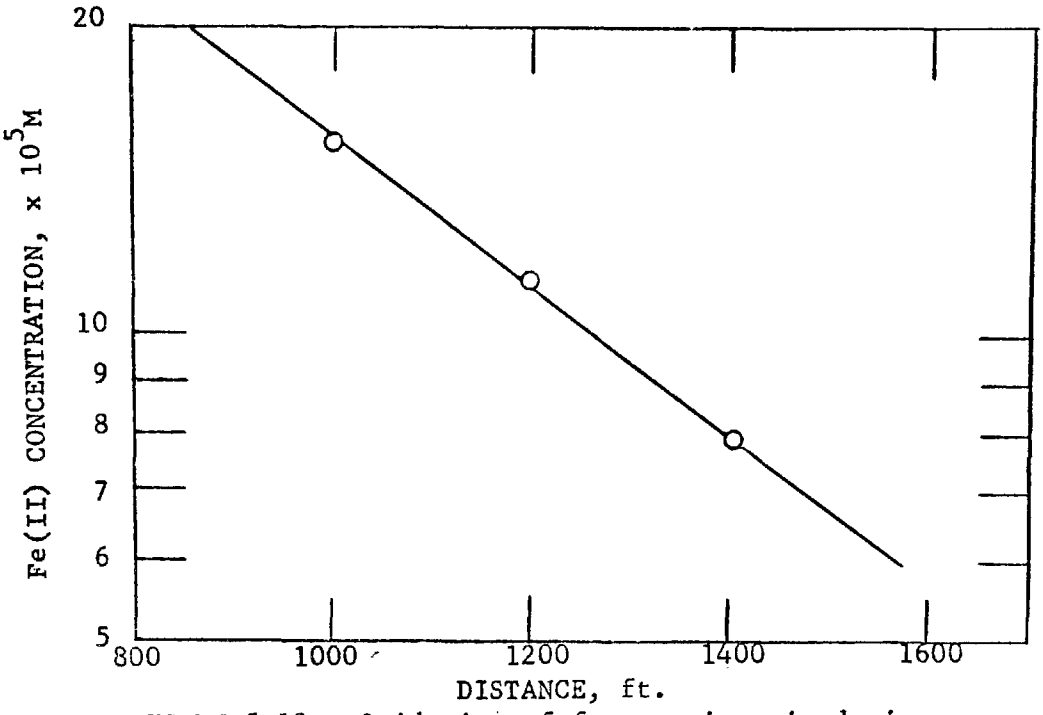

FIGURE 5-13. Oxidation of ferrous iron in drainage water after leaving strip mine.

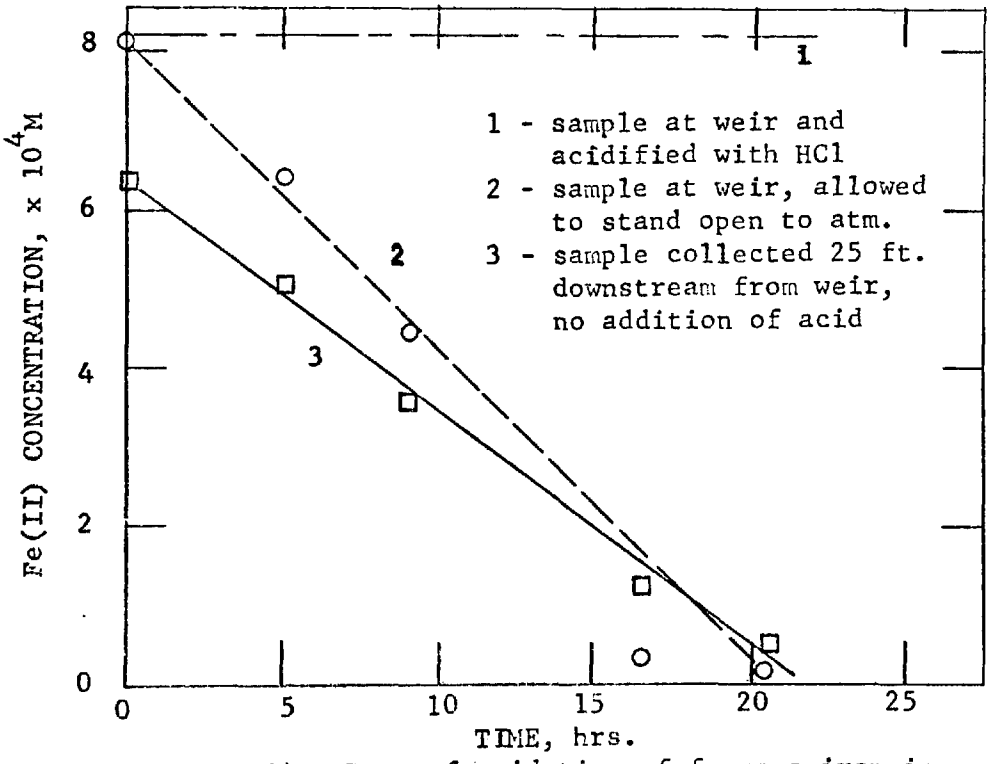

FIGURE 5-14. Rate of oxidation of ferrous iron in water collected from air-sealed underground mine at RT 9-11.

Figure 5-14 presents the results obtained at the air-sealed mine opening at RT 9-11. Curves 2 and 3 show the decrease in Fe(II) by oxidation after collection of the samples and allowing them to stand back in the laboratory exposed to the atmosphere. Aliquots were removed at various intervals and titrated with permanganate, sample number 1 being acidified at the time of collection to serve as a control. Samples 2 and 3 were not acidified.

The linearity of the arithmetic plot indicates the oxidation of Fe(II) in its native solution to be zero-order in Fe(II), i.e., the instantaneous rate is independent of the concentration of ferrous iron. The rate of reaction is dramatic when compared to the previous laboratory investigation.

Implications of Field Results

The zero-order nature of the oxidation reaction is suggestive of a biological reaction in which substrate is non-limiting and in which the concentration of microorganisms remains relatively constant. The rate equation for such conditions has been derived in Appendix E as

$$\frac{-dS}{dt} = \frac{\mu_{max} B}{y} = \text{constant} \qquad (5\text{-}16)$$

where S is the concentration of substrate (source of energy), in this case ferrous iron, μ_{max} is the maximum specific growth rate for the microorganisms, y is the yield of microorganisms per unit of substrate utilized, and B is the instantaneous concentration of microorganisms, assumed here to be constant. Figure 5-14 satisfies equation 5-16 and therefore the results imply that the oxidation is being catalyzed by microorganisms which are utilizing the energy derived from the

oxidation of ferrous iron for cellular metabolism, i.e., catalysis by autotrophic bacteria is taking place.

Microbial catalysis, however, is not the only explanation for the zero-order nature of the observations. A heterogeneous reaction mechanism could be invoked, involving complete saturation of the solid phase with the reactant, Fe(II), in order to account for the zero-order dependence on Fe(II). However, for the additional reasons described below, the autotrophic explanation is an extremely plausible one.

As shown in Appendix F, a thermodynamic free energy balance appears to negate the existence of such autotrophic iron bacteria; only 1 gram of organic carbon is synthesized for every 250 gms of ferrous iron oxidized. In fact, the autotrophic nature of these organisms and their ecological significance was initially doubted due to the meager amount of free energy available from the oxidation of Fe(II).

Since the energy released is so small, one would not expect the oxidation of 10^{-3}M Fe(II) to significantly change the bacterial concentration if a sufficient number of microorganisms were present in the mine water at RT 9-11, i.e., $\underline{B}$ should remain constant. Figure 5-14 reflects such reasoning. Kim (39), of the Pittsburgh Mining Research Center of the Bureau of Mines, has obtained similar zero-order plots of oxidation of Fe(II) in natural mine waters.

If, however, the concentration of bacteria were diminished, as by filtration of the mine water, $\underline{B}$ would be expected to increase logarithmically (see equation E-13 in the Appendix) as the substrate, Fe(II), is utilized. A sample of mine water from RT 9-11 was millipore-filtered (0.8 u pore diameter) and the resultant degree of oxidation of

Fe(II) was markedly reduced due to removal of a significant fraction of the bacteria. The unfiltered sample was completely oxidized within 20 hours, while the filtered sample displayed a lag before significant oxidation began (see Figure 5-15). If $\underline{B}$ is not constant during the course of the reaction, then

$$\frac{-dS}{dt} = \frac{\mu_{max}}{y} B_o \, e^{\mu_{max} t} \tag{5-17}$$

and, as derived in Appendix E

$$S_o - S = \frac{B_o}{y} \, e^{\mu_{max} t} \tag{5-18}$$

where $\underline{B_o}$ is the initial concentration of bacteria, and $\underline{S_o}$ is the initial concentration of substrate, Fe(II). Taking logs of both sides one obtains

$$\log (S_o - S) = \log \frac{B_o}{y} + \frac{\mu_{max} t}{2.3} \tag{5-19}$$

Figure 5-16 is a semilogarithmic plot of the change in concentration of Fe(II) with time, the linear nature of the plot confirming the logarithmic change in $\underline{B}$ in accordance with equations 5-17 and 5-19. Equation 5-19 indicates that the slope of the semilog plot is equal to $\mu_{max}/2.3$. Consequently, μ_{max} is 0.076 hrs^{-1} for the experimental conditions. The generation time, the time required for the concentration of bacteria to double, is, by definition, equal to $\ln 2/\mu$ or 9.1 hours. Silverman and Lundgren (18) observed generation times of about 7.0 hours in their laboratory under ideal experimental conditions.

To further substantiate biological significance, sterile solutions of ferrous sulfate were inoculated with various amounts of acid

mine drainage. Two sterile controls were maintained: one in which aseptically filtered mine water (220 mu pore diameter) was added to sterile solutions of ferrous sulfate; and another containing sterile ferrous sulfate alone. Aliquots were removed aseptically and analyzed for residual Fe(II) by titration with permanganate. Figure 5-17 shows a linear decrease in Fe(II) for the arithmetic plot, as in Figures 5-14, but only for the specimen containing microorganisms. The slowness of the oxidation reaction in the laboratory samples compared to that in the field samples (Figure 5-17 compared to Figure 5-14) may have resulted from a decrease in the concentration of some essential growth factor in the course of the dilution.

Therefore, the oxidation of ferrous iron occurs more rapidly in natural mine waters than in any of the synthetic solutions investigated in the laboratory subject to the various chemical catalytic additives. The rapidity of the reaction in nature is apparently the result of microbial catalysis, as evidenced by Figures 5-14 to 5-17.

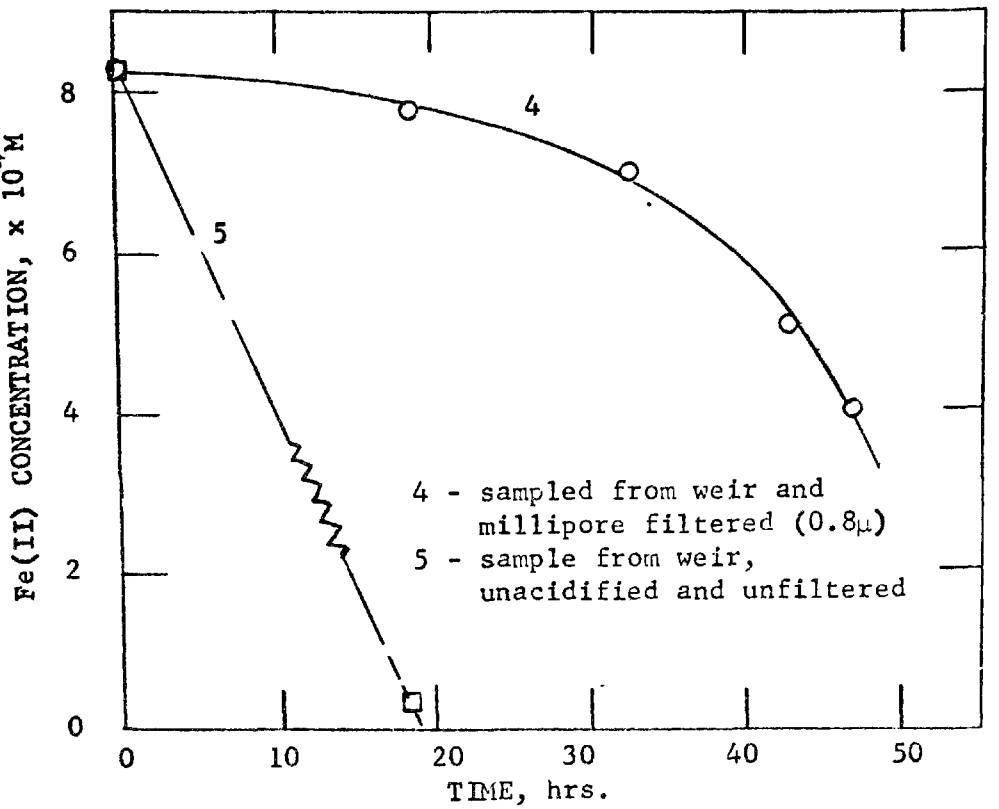

FIGURE 5-15. Oxidation of ferrous iron in water collected from air-sealed mine.

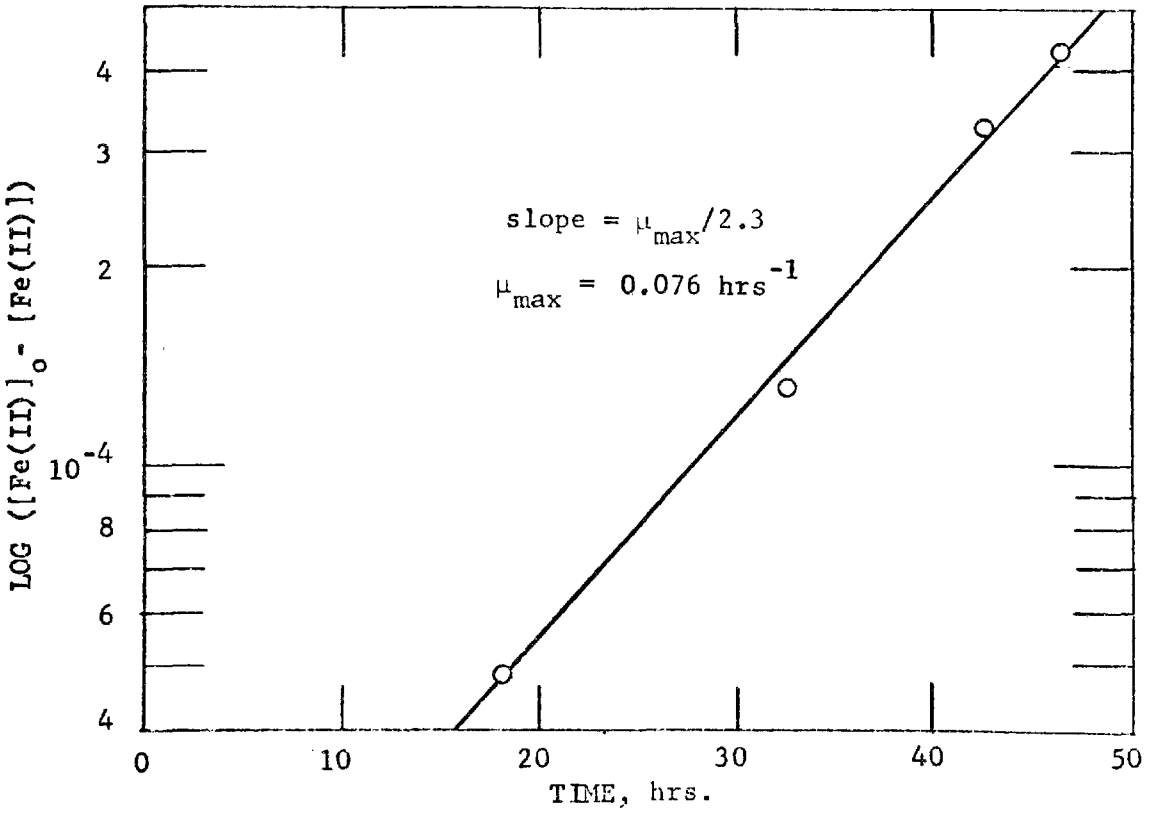

FIGURE 5-16. Change in ferrous iron concentration in millipore filtered water collected from air-sealed mine.

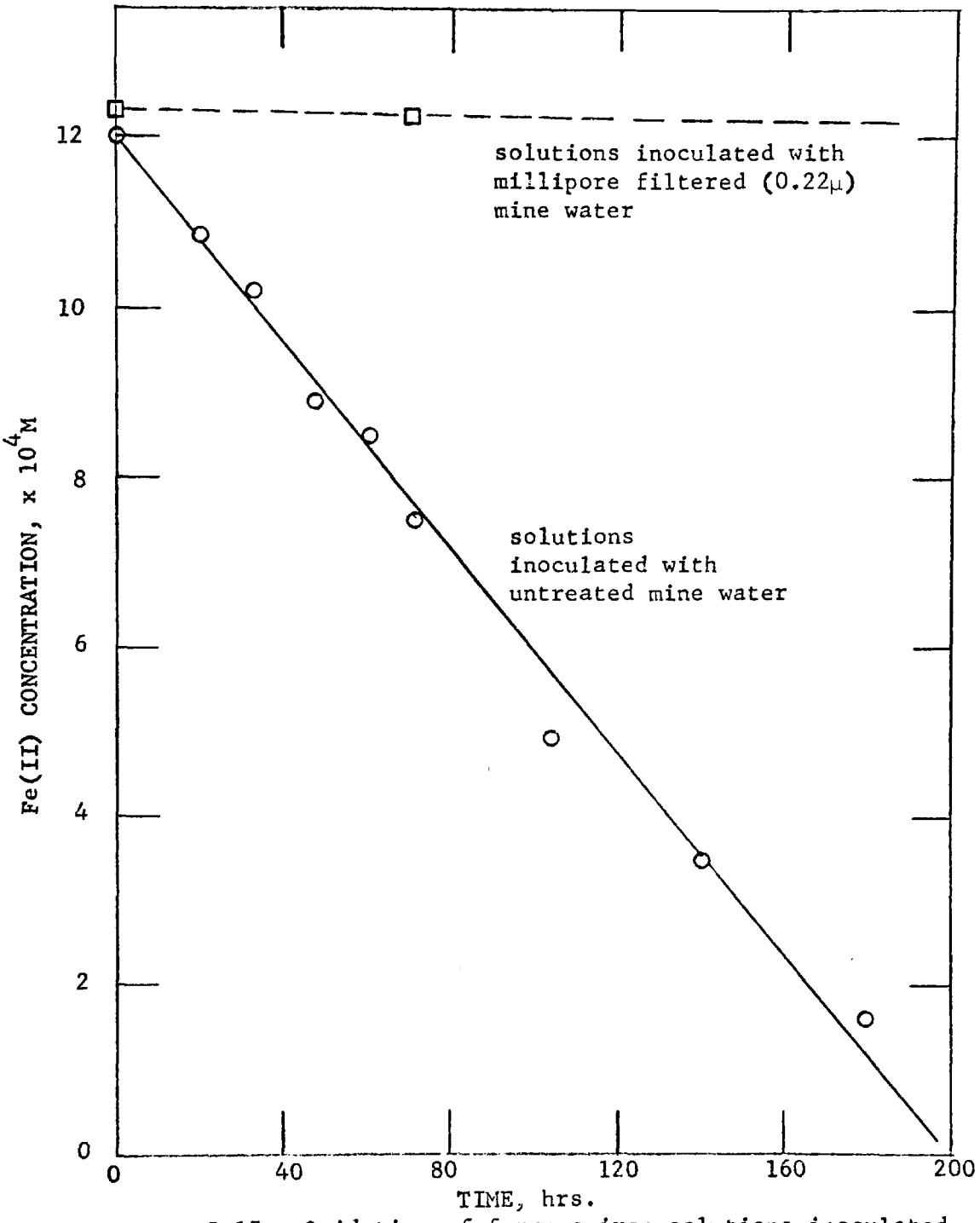

FIGURE 5-17. Oxidation of ferrous iron solutions inoculated with mine water from RT 9-11.

5-7 Oxidation of Iron Pyrite

The kinetics of oxidation of ferrous iron in the mine water system (sections 5-5 and 5-6) and the kinetics of hydrolysis of ferric iron (Chapter 4) having been studied, the final step in the sequence of chemical reactions describing the dissolution of pyritic agglomerates is the oxidation of pyrite itself, both by oxygen and by ferric iron. With the exception of the study by Garrels and Thompson (7), prior investigations of the oxidation of pyrite have been concerned almost entirely with oxygen as the oxidant. In many cases, the potentiality of ferric iron as an oxidant has been overlooked. It was desired to obtain some idea as to the rate of oxidation of pyrite by ferric iron relative to that by oxygen.

5-7.1 Experimental Procedures

Several dilutions of a stock solution of ferric perchlorate were prepared and adjusted to pH 1.0 with perchloric acid. (Sato (6) and Garrels and Thompson (7) noted the oxidation of pyrite to be independent of pH below 2.0.) Nitrogen was bubbled continuously through the solution to remove all traces of oxygen, any oxidation of pyrite then being attributable only to the action of ferric iron. Iron pyrite from Rico, Colorado (Ward's Natural Science Establishment, Rochester, New York) was ball-milled and screened, and the 200-250 mesh fraction was selected for the experiment. At time zero, various amounts of the finely-divided pyrite were added to the solution of ferric iron, the solid phase being uniformly dispersed by means of a magnetic stirrer. The electrochemical potential of the system was measured at various

intervals using a platinum spiral indicator electrode and a calomel reference electrode saturated with NaCl, as described in section 2-3.3. A Leeds and Northrup potentiometer (Cat. No. 7664) was employed for the potential measurements.

The procedure adopted was similar to that used in Chapter 4. In a well-defined system such as this, the reversible potential is established by the electroactive Fe^{+2} - Fe^{+3} couple in accordance with the Nernst Equation

$$E = E^{o} - .0592 \log \frac{(Fe^{+2})}{(Fe^{+3})} \quad \text{at } 25^{o}C \qquad (5\text{-}20)$$

At pH 1.0, since $[Fe^{+2}] = [Fe(II)]_T$ and $[Fe^{+3}] = [Fe(III)]_T$, E^{o} can easily be computed in a constant ionic medium by measuring the potential, E, and independently determining the total concentrations of ferrous and ferric iron. By conducting all future studies under the same experimental conditions of constant ionic strength and temperature (to insure that the activity coefficients remain constant), this value for the equilibrium potential, E^{o}, can be utilized to compute the ratio $[Fe^{+2}]/[Fe^{+3}]$ by simply measuring the potential of the system.

After the potential was recorded, aliquots of the suspension were removed and filtered. The concentration of total iron in the filtrate was determined using the bathophenanthroline procedure in which 10% hydroxylamine is utilized to reduce all ferric iron to the ferrous state. The individual concentrations of Fe(II) and Fe(III) were calculated knowing the concentration of total iron and the $[Fe^{+2}]/[Fe^{+3}]$ ratio from the potential measurements.

5-7.2 Results and Discussion

Rate of Oxidation in Absence of Oxygen

The rate of disappearance of ferric iron in the presence of finely-divided iron pyrite is remarkably rapid. Since the rate of oxidation of pyrite is independent of pH below pH 2.0 (6) (7), a simple rate law dependent upon the two reactants can be assumed, of the form

$$-\frac{d\,[Fe(III)]}{dt} = k\,[Fe(III)]^m[FeS_2]^n \qquad (5\text{-}21)$$

If the concentration of pyrite is large compared to that of Fe(III), $[FeS_2]$ will remain relatively constant during the course of the reaction. (Note also, from the stoichiometry of the reaction (equation 5-4), that the oxidation of one mole of pyrite consumes fourteen moles of ferric iron.) Therefore, under these conditions, the rate of oxidation can be approximated by

$$-\frac{d\,[Fe(III)]}{dt} = k_1\,[Fe(III)]^m \qquad (5\text{-}22)$$

where

$$k_1 = k\,[FeS_2]^n \qquad (5\text{-}23)$$

and is constant. Furthermore, if m = 1 and the reaction is first-order in the concentration of Fe(III), a plot of log [Fe(III)] versus time should be linear. Figure 5-18 shows that the decrease in Fe(III) conforms to such a formulation. It is also seen that the rate of decrease of Fe(III) is a function of the concentration of pyrite, presumably the surface concentration; for the same initial concentration of Fe(III), the half-time is about 250 minutes in the presence of

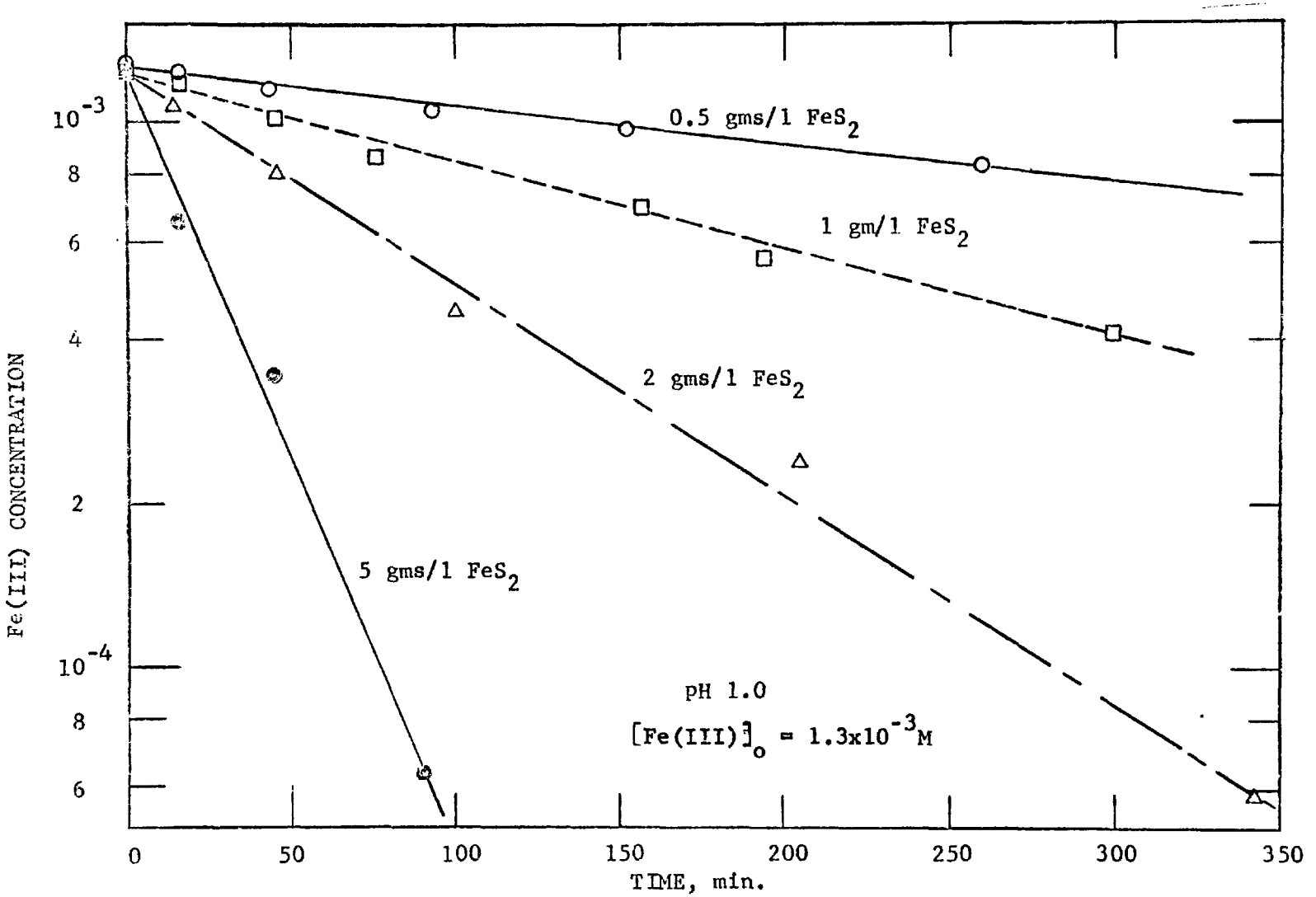

FIGURE 5-18. Reduction of ferric iron by iron pyrite (200-250 mesh) in the absence of oxygen.

1 gm/l of FeS_2, and only 25 minutes when 5 gms/l of pyrite are present.

Taking the logarithm of equation 5-23, one obtains

$$\log k_1 = \log k + n \log [FeS_2] \qquad (5\text{-}24)$$

A log-log plot of the pseudo-first-order rate constants (computed from the slopes of the straight lines in Figure 5-18) against the concentration of pyrite should yield a straight line of slope n, the order of the rate-dependence on FeS_2, if the assumed rate law, equation 5-21, is valid. Two such plots are shown in Figure 5-19 for two different initial concentrations of Fe(III). The order, n, is seen to be about 1.3 and 1.1, implying a first-order-dependence of the rate on the concentration of iron pyrite.

If the assumed rate law is valid and the first-order-dependence upon Fe(III) is correct, as demonstrated in Figure 5-18, the rate constant k_1 should be independent of the initial concentration of Fe(III). This is not the case, however, as seen in Figure 5-20. In fact, the slope of the semilog plot increases as the initial concentration of Fe(III) decreases, implying an inverse dependence of the rate on Fe(III). An understanding of the kinetics of the reaction is further complicated by the findings of Garrels and Thompson (7) that the instantaneous rate of reduction of Fe(III) decreases with time (implying direct kinetic dependence on Fe(III)), but the average rate of reduction is independent of the initial concentration of Fe(III) (suggestive of zero-order dependence on Fe(III)). Furthermore, they present a figure similar to Figure 5-20, showing essentially a logarithmic decrease in

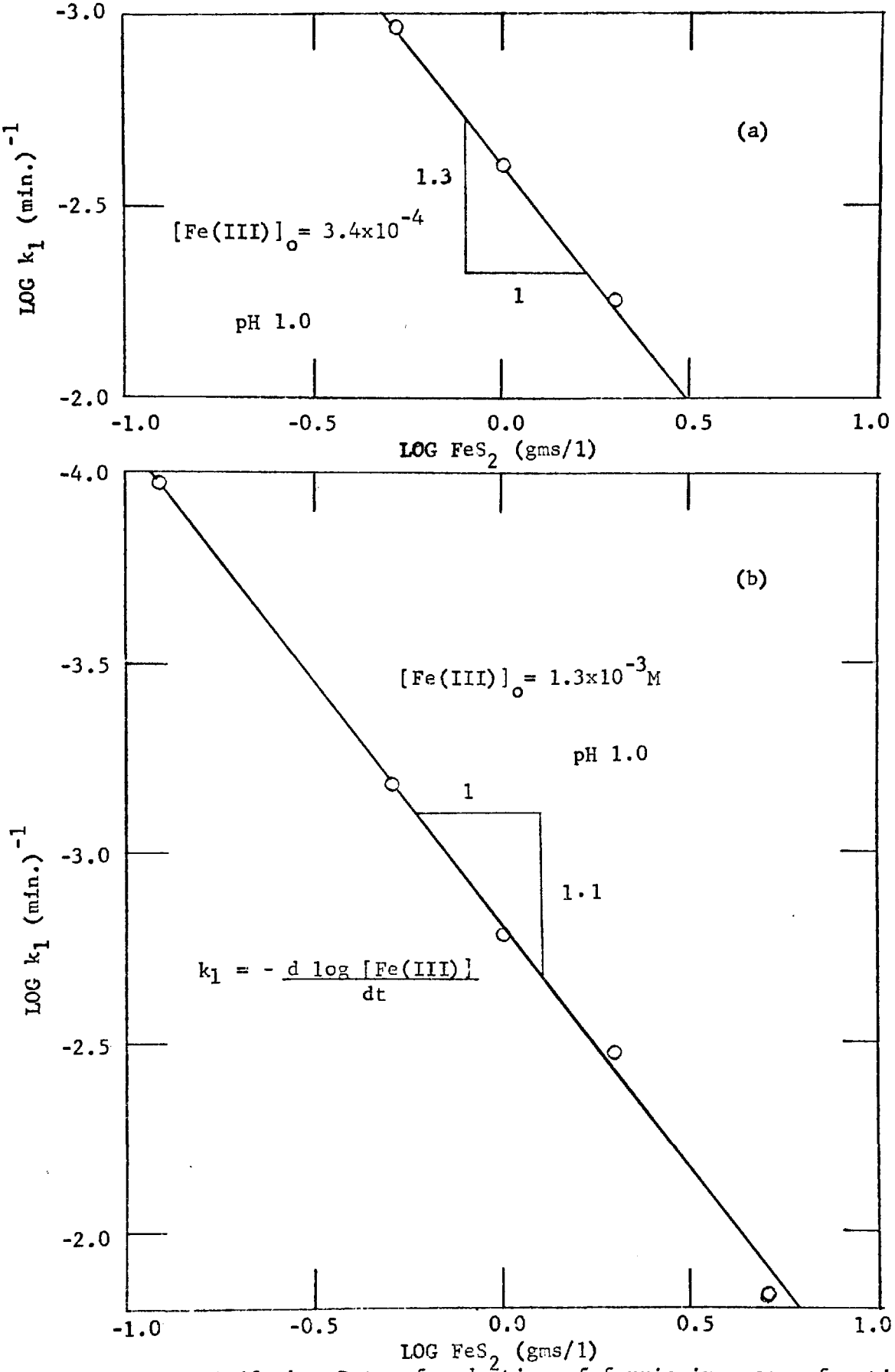

FIGURE 5-19a,b. Rate of reduction of ferric iron as a function of pyrite concentration.

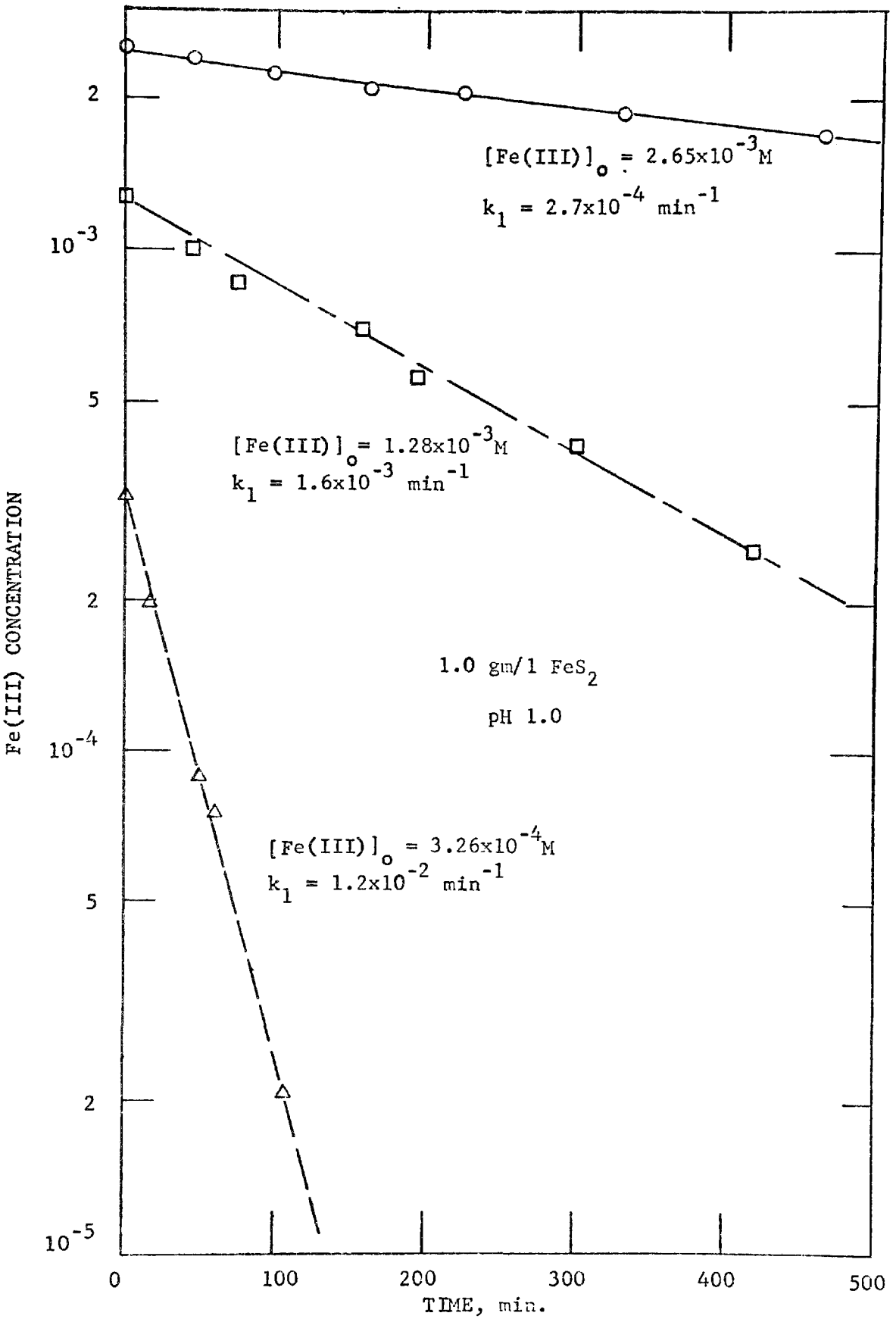

FIGURE 5-20. Effect of initial concentration of ferric iron on rate of reduction of Fe(III) by pyrite, in the absence of oxygen.

Fe(III) with time, with the rate of decrease becoming steeper as the initial concentration of Fe(III) decreases.

(The stoichiometry of the reaction (equation 5-4) was verified by noting a 7% increase (15/14) in the concentration of total dissolved iron (Fe(II) and Fe(III)), using the bathophenanthroline procedure.)

Since the mechanism of the oxidation of pyrite by Fe(III) was not the primary purpose of this study, but rather the relative rate of the reaction as compared to that of the oxidation of Fe(II) was of major concern, it will be sufficient to note the rapidity by which Fe(III) is reduced by pyrite. Even for the slowest case observed, where $[Fe(III)]_o \sim 10^{-3}M$ and $[FeS_2] = 0.12$ gms/l ($\sim 10^{-3}M$), the half-time is approximately 2 days which is considerably less than that for the oxidation of Fe(II) even when accelerated by any of the experimental chemical catalysts found in natural waters.

Oxidation Rate in Presence of Oxygen

After finding that there is no appreciable adsorption of dissolved Fe(II) on iron pyrite, and that Fe(II) is not catalytically oxidized in the presence of FeS_2 (see section 5-5.2), the rate of reduction of Fe(III) by pyrite in the presence of oxygen was investigated. The experimental procedure was identical to that in the preceding section except that the system was left open to the atmosphere. The results are shown in Figure 5-21, indicating that there is virtually no difference between the rate of reduction of Fe(III) by pyrite, or the rate of change of soluble Fe(II), under aerobic or anaerobic conditions. Hence, the implication is that even in the presence of a partial pressure of oxygen of 0.2 atm. the oxidant of iron pyrite is ferric iron. Fe(III) at pH = 1 oxidizes FeS_2 faster than O_2.

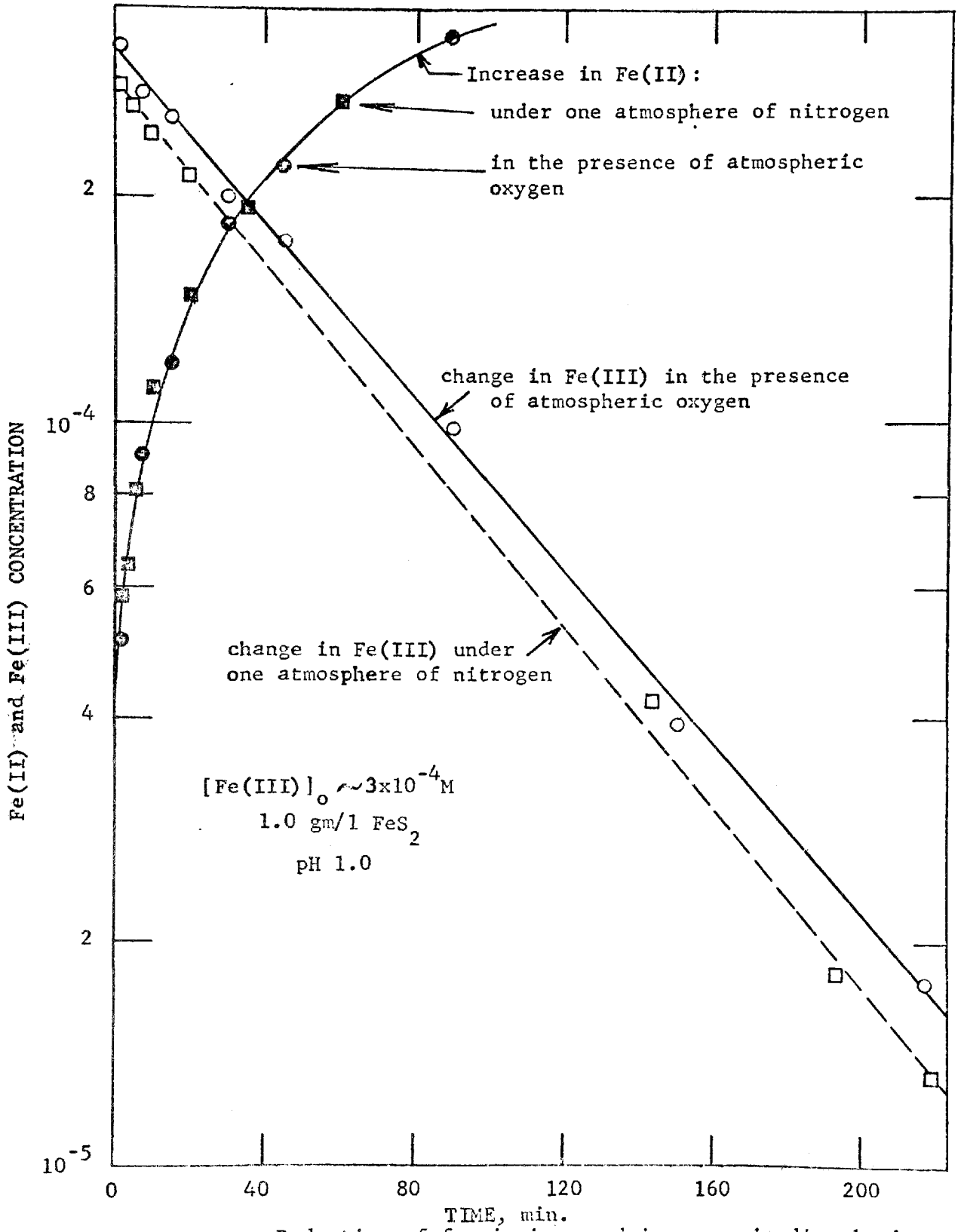

FIGURE 5-21. Reduction of ferric iron and increase in dissolved ferrous iron in the presence and absence of oxygen.

5-8 Conclusions

5-8.1 Model Describing Pyrite Oxidation and Pollution by Coal Mine Drainage

In accordance with the experimental results presented in this chapter, the following model is proposed to describe the oxidation of iron pyrite in natural mine waters:

Initiation Reaction: $FeS_2(s) \xrightarrow{(+\ O_2)} Fe(II) + S\text{ - compound}$ (5-24a)

Propagation Cycle:

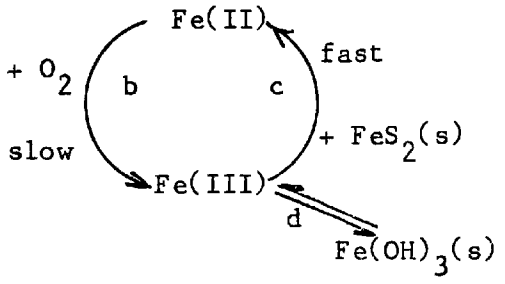

(5-24b,c)

(5-24d)

The reactions shown are schematic and do not represent the exact mechanistic steps. The model is similar to and carries with it the same overall consequences as that suggested by Temple and Delchamps (14). In this model, the rate-determining step is a reactive step in the specific oxidation of ferrous iron, reaction 5-24b. As this investigation has demonstrated, the rate of oxidation of ferrous iron under chemical conditions analogous to those found in mine waters is very slow, indeed considerably slower than the oxidation of iron pyrite by ferric iron, reaction 5-24c. At pH 3, half-times for the oxidation of Fe(II) are on the order of 1000 days while in the case of oxidation of pyrite by Fe(III), half-times on the order of 20 to 1000 minutes were observed.

Reaction 5-24a serves only as an initiator of the overall reaction: ferrous iron may be released by simple dissociation of the pyrite, or by oxidation of the pyrite by oxygen. Once the sequence has been initiated, a cycle is established in which ferric iron rapidly oxidizes pyrite and is slowly regenerated through the oxygenation of the resultant ferrous iron, reactions 5-24b and c. Oxygen is involved only indirectly, in the regeneration of Fe(III).

Precipitated ferric hydroxide deposited in the mine and the streams serves as a reservoir for soluble Fe(III), by reaction 5-24d. If the regeneration of Fe(III) by 5-24b is halted so that the concentration of soluble Fe(III) decreases, it will be replenished by dissolution of the solid $Fe(OH)_3$ and will be free to act again should it come in contact with additional FeS_2.* The presence of sulfate in solution increases the concentration of dissolved Fe(III) in equilibrium with the precipitate, by complex formation (see section 2-3.3). Barnes and Romberger's argument (10) that there is insufficient Fe(III) available for the reaction appears fallacious.

Smith, et al (13) investigated the effect of pH on the rate of oxidation of pyrite by oxygen and observed the reaction rate to be relatively independent of pH below pH 4, while the rate increased rapidly in a pH-dependent manner above pH 7. Since this parallels the pH-dependence of the rate of oxidation of ferrous iron (Figure 5-2), this writer contends that Smith, et al actually observed the oxidation of pyrite by Fe(III). At higher pH-values, the rate of oxidation of FeS_2 increases because the rate of formation of Fe(III), via oxidation of Fe(II), increases with increasing pH. These results lend further support to the proposed model.

* The contact with Fe(III) however may be small if the pyrite lies on the ceiling or on walls.

The following pertinent consequences of this model need to be emphasized:

1) Ferric iron cannot exist for long in contact with pyritic agglomerates. Fe(III) is rapidly reduced by iron pyrite.

2) The elimination of oxygen is of no consequence with regard to the specific oxidation of iron pyrite. However, the exclusion of oxygen does inhibit regeneration of Fe(III) through the oxidation of Fe(II), and will be of significance once the supply of available Fe(III) is exhausted.

3) The overall rate of dissolution of pyrite is independent of its surface structure. Interference with the surface of pyrite, such as the application of inhibitors which are adsorbed at the solid-solution interface, is inconsequential since the oxidation of pyrite is not the rate-limiting step. If, on the other hand, such a technique could make the rate of oxidation of pyrite less than the rate of oxidation of Fe(II), then such a control measure may have merit.

4) Microorganisms can only be influential by mediating the oxidation of ferrous iron since it, alone, is the rate-determining step. Catalysis of the specific oxidation of iron pyrite by microorganisms, even if it could be unequivocally demonstrated, can have no effect on the overall rate of dissolution of iron pyrite.

It is probably this same cycle which is responsible for the dissolution and leaching of other mineral sulfides as found in copper and uranium mines. Microbial leaching of these other minerals has always been demonstrated in the presence of iron, pyrite being the most abundant and widespread of all mineral sulfides (2). Until it

can definitely be proven otherwise, cycle 5-24 adequately accounts for the observed microbial leaching of other mineral sulfides, and direct microbial oxidation must be discounted.

The solution to the problem of acid mine drainage, therefore, appears to rest with methods of controlling the oxidation of ferrous iron. Due to the cyclical nature of the process describing dissolution of pyrite, mere treatment of the resulting drainage water will allow the problem to compound and magnify itself. Hence, at-source control measures are preferred. One such method might involve the inhibition of natural catalysts which are of significance in accelerating the rate of oxidation of Fe(II) in mine waters. It is of primary concern to discover which of these catalysts causes the oxidation to proceed as rapidly as it does in nature. From the preliminary analysis presented in this chapter, the major chemical catalysts appear to be alumino-silicate clays, but only at considerably larger surface concentrations than would be expected in natural mine waters. Microbial catalysis, as by the autotrophic iron-bacteria Thiobacillus and Ferrobacillus ferrooxidans, seems to be ecologically significant as evidenced by the few field investigations conducted. Numerous accounts of autotrophic iron oxidation prevail, but only few quantitative reports of their actual activity in nature have appeared. Tuttle, Randles, and Dugan (40) observed only 10^2 to 10^3 iron-oxidizers per ml. in an acid mine stream, using an MPN technique.* This is not a significant concentration when one considers the limited amount of iron which can be oxidized by these few microorganisms (see Appendix F). However, there may be considerable surface growth of

* These counts are probably not representative of the concentration near the pyrite surface.

these microorganisms associated with the available solid material suspended or deposited in the drainage streams. It is important to know the actual concentration of these autotrophic microorganisms found in mine waters in order to assess their relevance regarding the rate of oxidation of ferrous iron. Once the role of all catalytic agents has been evaluated, methods can then be devised to control the oxidation of ferrous iron and, hence, the dissolution of iron pyrite and the introduction of acidity into natural mine waters.

References

1) Palathe, C., Berman, H., and Frondel, C., Dana's System of Mineralogy, 7th ed., vol. 1, John Wiley and Sons, Inc., New York, 1944.

2) Clark, C. S., "Oxidation of Coal Mine Pyrite," Journ. San. Eng. Div., Proc. Amer. Soc. Civil Eng., 92, 127 (1966).

3) Krauskopf, K. B., Introduction to Geochemistry, Ch. 18, McGraw-Hill Book Company, New York, 1967.

4) Stokes, H. N., "On Pyrite and Marcasite," U. S. Geol. Surv. Bull. 186 (1901).

5) Nelson, H. W., Snow, R. D., and Keyes, D. B., "Oxidation of Pyritic Sulfur in Bituminous Coal," Ind. Eng. Chem., 25, 1335 (1933).

6) Sato, M., "Oxidation of Sulfide Ore Bodies. II. Oxidation Mechanisms of Sulfide Minerals at 25°C," Econ. Geol., 55, 1202 (1960).

7) Garrels, R. H., and Thompson, M. W., "Oxidation of Pyrite by Iron Sulfate Solutions," Amer. Journ. Sci., 258-A, 57 (1960).

8) McKay, O. R., and Halpern, J., "A Kinetic Study of the Oxidation of Pyrite in Aqueous Suspension," Trans. Met. Soc. AIME, 212, 301 (1958).

9) Gerlach, J., Hähne, H., and Pawlek, F., "Beitrag zur Drucklangung von Eisensulfiden. II. Zur Kinetik der Drucklangung von Pyrit," Zeit. Erzb. Metall., 19, 66 (1966).

10) Barnes, H. L., and Romberger, S. B., "Chemical Aspects of Acid Mine Drainage," Journ. Wat. Poll. Contr. Fed., 40, 371 (1968).

11) Smith, E. E., Svanks, K., and Shumate, K., "Sulfide to Sulfate Reaction Studies," Proc. 2nd Symp. on Coal Mine Drainage Research, Coal Industry Advisory Committee to ORSANCO, Pittsburgh, May 1968.

12) Colmer, A. R., and Hinkle, M. E., "The Role of Microorganisms in Acid Mine Drainage: A Preliminary Report," Science, 106, 253 (1947).

13) Temple, K. L., and Colmer, A. R., "The Autotrophic Oxidation of Iron by a New Bacterium: Thiobacillus Ferrooxidans," J. Bact., 62, 605 (1951).

14) Temple, K. L., and Delchamps, E. W., "Autotrophic Bacteria and the Formation of Acid in Bituminous Coal Mines," Appl. Microbiol., 1, 255 (1953).

15) Leathen, W. W., Kinsel, N. A., and Braley, S. A., "Ferrobacillus Ferrooxidans: A Chemosynthetic Autotrophic Bacterium," J. Bact., 72, 700 (1956).

16) Kinsel, N. A., "New Sulfur-Oxidizing Iron Bacterium: Ferrobacillus Sulfooxidans SP.N." J. Bact., 80, 628 (1960).

17) Unz, R. F., and Lundgren, D. G., "A Comparative Nutritional Study of Three Chemoautotrophic Bacteria: Ferrobacillus Ferrooxidans, Thiobacillus Ferrooxidans, and Thiobacillus Thiooxidans," Soil Science, 92, 302 (1961).

18) Silverman, M. P., and Lundgren, D. G., "Studies on the Chemoautotrophic Iron Bacterium Ferrobacillus Ferrooxidans: I. An Improved Medium and Harvesting Procedure for Securing High Cell Yields," J. Bact., 77, 642 (1959).

19) Silverman, M. P., and Lundgren, D. G., "Studies on the Chemoautotrophic Iron Bacterium Ferrobacillus Ferrooxidans. II. Manometric Studies," J. Bact., 78, 325 (1959).

20) Schnaitman, C. A., "A Study of the Mechanism of Iron Oxidation by Ferrobacillus ferrooxidans," Ph.D. Thesis, Syracuse University (1965).

21) Brynner, L. C., Beck, J. V., Davis, D. B., and Wilson, D. G., "Microorganisms in Leaching Sulfide Minerals," Ind. Eng. Chem., 46, 2587 (1954).

22) Brynner, L. C., and Anderson, R., "Microorganisms in Leaching Sulfide Minerals," Ind. Eng. Chem., 49, 1721 (1957).

23) Ehrlich, H. L., "Bacterial Action on Orpiment," Econ. Geol., 58, 991 (1963).

24) Silverman, M. P., and Ehrlich, H. L., "Microbial Formation and Degradation of Minerals," Advances in Appl. Microbiol., 6, 153 (1964).

25) Ehrlich, H. L., "Observation on Microbial Association with Some Mineral Sulfides," p. 153 in Biogeochemistry of Sulfur Isotopes, M. L. Jensen, ed., Nat'l Sci. Found. Symp., Yale Univ., New Haven, Conn. (1962).

26) Lee, G. F., and Stumm, W., "Determination of Ferrous Iron in the Presence of Ferric Iron," Journ. Amer. Wat. Works Assoc., 52 1567 (1960).

27) Huffman, R. E., and Davidson, N., "Kinetics of the Ferrous Iron-Oxygen Reaction in Sulfuric Acid Solution," Journ. Amer. Chem. Soc., 78, 4836 (1956).

28) George, P., "The Oxidation of Ferrous Perchlorate by Molecular Oxygen," Journ. Chem. Soc., p. 4349 (1954).

29) Cher, M., and Davidson, N. "The Kinetics of the Oxygenation of Ferrous Iron in Phosphoric Acid Solution," Journ. Amer. Chem. Soc., 77, 793 (1955).

30) Crabtree, J. H., and Schaefer, W. P., "The Oxidation of Iron (II) by Chlorine," Inorg. Chem., 5, 1348 (1966).

31) Stumm, W., and Lee, G. F., "Oxygenation of Ferrous Iron," Ind. Eng. Chem., 53, 143 (1961).

32) Weiss, J., "ElektronenÜbergangsprozesse in Mechanismus von Oxydations - und Reduktions-Reaktionen in Lösungen," Naturwissenschaften, 23, 64 (1935).

33) Lamb, A. B., and Elder, L. W., "The Electromotive Activation of Oxygen," Journ. Amer. Chem. Soc., 53, 137 (1931).

34) Van Olphen, H., An Introduction to Clay Colloid Chemistry, Interscience Publ., New York (1963).

35) Schenk, J. E., and Weber, W. J., "Chemical Interactions of Dissolved Silica with Iron (II) and (III)," Journ. Amer. Wat. Works Assn., 60, 199 (1968).

36) Scott, Robert, Personal Communication, Project Engineer, Federal Water Pollution Control Administration, Elkins, West Virginia (1968).

37) Standard Methods for the Examination of Water and Wastewater, 11th ed., American Public Health Assn., Inc., New York (1960).

38) Salotto, B. V., Barth, E. F., Ettinger, M. B., and Tolliver, W. E., "Determination of Mine Waste Acidity," submitted to Environ. Sci. and Tech. (1967)

39) Kim, A. G., Personal Communication, Pittsburgh Mining Research Center, U. S. Bureau of Mines, Pittsburgh, Pa. (1968).

40) Tuttle, J. H., Randles, C. I., and Dugan, P. R., "Activity of Microorganisms in Acid Mine Water," Journ. Bact., 95, 1495 (1968).

CHAPTER 6

CONCLUSIONS

Information concerning the chemistry of aqueous iron can be applied to natural water systems in order to cope with the vast and costly problem of acid mine drainage, for the design of efficient deferrization processes, and to provide for a better understanding of the limnological cycles of a number of key elements. This chapter summarizes the relevant results realized in this research, and discusses the practical consequences of these results.

6-1 Principal Findings

1) Ferrous iron is thermodynamically unstable in the presence of oxygen. The rate at which it is oxidized to ferric iron is compatible with a rate law which is first-order in both [Fe(II)] and [O_2], and second-order in [OH^-] at pH-values above 4.5. At lower pH-values, the rate of oxidation is independent of pH. The reaction proceeds extremely slowly in the acidic region, but is catalyzed by inorganic and organic ligands capable of forming complexes with Fe(II) and Fe(III), heavy metal ions, clay particles, and bacteria.

2) The oxidation of ferrous iron is the specific rate-determining step in the oxidation of iron pyrite and the subsequent discharge of acidity into mine drainage waters. The chemical oxygenation of Fe(II) at pH-values less than 4 takes place very slowly, even in the presence of the many chemical catalysts which are operative in

nature. The direct oxidation of iron pyrite by ferric iron is quite rapid and Fe(III) serves as the prime oxidant of iron pyrite. A cycle is established involving the rapid oxidation of pyrite by Fe(III), and the slow regeneration of Fe(III) through the oxygenation of Fe(II), in the following schematic way:

$$FeS_2 + Fe(III) \xrightarrow{\text{fast}} Fe(II) + SO_4^{-2}$$

$$Fe(II) + O_2 \xrightarrow{\text{slow}} Fe(III)$$

$$FeS_2 + Fe(III) \xrightarrow{\text{fast}} Fe(II) + SO_4^{-2}$$

Microorganisms, presumably the autotrophic "iron bacteria," markedly enhance the rate of oxidation of Fe(II), and, therefore, accelerate the overall rate of pyrite oxidation. Oxygen participates in the cycle only in the regeneration of spent ferric iron.

6-2 Practical Consequences and Implications Resulting From This Research

1) The proposed cycle to describe the oxidation of iron pyrite and the acidification of mine drainage waters can be utilized in evaluating some of the methods recommended for the prevention of acid mine drainage, and should serve as a guide to indicate the direction in which future control measures should be aimed.

Mine-sealing and the application of bactericides are two proposals, both directed at the retardation of the oxidation of ferrous iron. The former involves the elimination of air and/or water from the mine and is intended to stop the reaction entirely. The latter is aimed at destroying the catalytic agent which is responsible for the

rapid rate at which Fe(II) is oxidized in mine drainage. Previous assertions that oxygen serves as the specific, direct oxidant of iron pyrite are unjustified in view of this research which indicates that oxygen is involved only indirectly, producing ferric iron which is, itself, the primary oxidant of FeS_2. Furthermore, this research has shown that in the absence of microbial catalysis, the oxygenation of Fe(II) is sufficiently slow that it is essentially halted. The regeneration of Fe(III) proceeds so slowly that its effect on pyrite is of little consequence.

Both mine-sealing and the application of bactericides, however, are subject to similar limitations. Firstly, neither will result in the immediate cessation of acidic discharges. Ferric iron must first be flushed out of the mine, or rendered inactive, before any beneficial effects could be realized. Reports of previous mine-sealing operations demonstrate that in spite of significant reductions in the concentration of oxygen, there was not always a marked change in the quantity of acid released although the discharge had a higher concentration of ferrous iron (1). In the few successful mine-sealing operations, often little improvement in the quality of the effluent from the mine was observed for several years (2).* These observations can readily be interpreted in view of the proposed scheme; the elimination of oxygen stops the oxidation of ferrous iron but the pyrite is still subject to oxidation by the vast quantity of Fe(III) available in the mine. Only after the active Fe(III) is depleted should one observe a decrease in the acidity of the drainage water.

---

* There are instances where mine sealing was followed by reduced acidity. For a recent review see R. D. Hill, Acid Mine Water Control, presented before the Mining Environmental Conference, University of Missouri, Rolla, Missouri. April, 1969.

Secondly, from a practical standpoint, both methods are of doubtful applicability. Total exclusion of oxygen is unlikely due to the many fractures and minute cracks in the mine wall and the frequent collapses experienced in the mine itself. Application of a bactericide requires continual injection of the agent into the system at a suitable location where the entire inflow could be treated. In most mining areas, such a location is non-existent. There are some situations, however, where a bactericide could be employed. Although it is not feasible to treat the mine itself, the various spoil banks exposing pyrite previously dug out of the mine are amenable to such treatment as they can be reached rather easily. It is conceivable, also, that strip mines would yield to such treatment since the influent water can usually be located.

Another proposal concerns the addition of an alkali to the system in order to raise the pH of the environment within the mine, thus inhibiting the microorganisms which catalyze the oxidation of ferrous iron. Here again, a suitable location for treatment is required. Furthermore, if the pH is raised appreciably, this study has shown that the chemical oxygenation of Fe(II) will proceed sufficiently fast by itself.

The introduction of organic material to chemically reduce ferric iron and sulfate has also been suggested in order to promote precipitation of ferrous sulfide. The continuous addition of organic material is necessary and the elimination of oxygen is mandatory so that Fe(II) and S(-II) are maintained in their reduced states.

Inactivation of the pyrite surface through the application of chemical inhibitors which are adsorbed at the solid-solution interface is unfeasible and inconsequential. Since the specific oxidation of pyrite is not the rate-determining step, partial coverage of the pyritic surface would not affect the overall rate of pyrite oxidation. In addition, constant exposure of new pyritic surfaces would be expected as a result of the frequent collapses inside the mine.

This discussion has considered only control methods for the abatement of pollution by coal mine drainage. Proposals for the treatment of effluent waters from these mines include acid neutralization by the addition of lime, reverse osmosis, and ion exchange. Each produces a voluminous or a concentrated waste which must ultimately be disposed of.

This research suggests that treatment of acid mine drainage requires treatment of the cycle by which such acidic discharges arise. Although no specific schemes for such treatment are proposed as a result of this study, it is emphasized that the catalytic oxidation of ferrous iron need to be halted. Because of the inaccessibility of the pyrite oxidation site, it is difficult to convert this theoretical suggestion into a practical treatment. (Catalytic oxidation of ferrous iron, however, is an asset, where mine drainage is treated for iron removal.)

2) This research has shown that the concentration of ferrous iron in natural groundwaters can often be predicted from considerations of solubility relationships, specifically the solubility product of ferrous carbonate which was obtained in this study, i.e., $pK_{so} = 10.24$ at $25^{\circ}C$ and zero ionic strength. The expected concentration of Fe(II)

can be calculated if the pH and alkalinity of the groundwater are monitored. The kinetic relationships describing the oxygenation of Fe(II) have also been derived. If the solubility and kinetic relationships are coupled, they can be applied to the design of an efficient iron-removal facility in order to bring the raw water into conformance with the Public Health Service drinking water standards for iron (0.3ppm) (3). This assumes an efficient filtration system for the actual removal of the resultant hydrous ferric oxide. For example, a groundwater at pH 6.5 containing 5×10^{-3} eq/l alkalinity should contain approximately 1.7 ppm of dissolved Fe(II) (approximately 3×10^{-5}M), and would therefore require 85% oxidation of the Fe(II) in order to provide an acceptable finished water having 0.3 ppm of iron. At a partial pressure of oxygen of 0.20 atm. and at 25°C, a detention time of about 60 minutes would be necessary ($t_{85} = \log (85/15)/k''$) if the oxidation were to proceed at pH 6.5. Furthermore, iron-removal may be aided by precipitation of Fe(II) as ferrous carbonate.

In addition, this study has demonstrated the capability of many elements in natural waters to accelerate the oxidation of Fe(II). Retardation of the oxidation of ferrous iron in the presence of oxygen can, therefore, be attributed almost entirely to the presence of reducing agents in natural systems, notably organic matter. Ferric iron is a potent oxidant of organic material, getting reduced to Fe(II) in the process. The net effect appears as an inhibition of the rate of oxidation of Fe(II), whereas in fact, the Fe(II)-Fe(III) reaction serves as an electron-transport mechanism between oxygen and the organic material. The stability of ferrous iron in the epilimnion

of lakes and reservoirs, in the presence of oxygen, can, in a similar manner, only be interpreted in terms of a steady-state condition maintained by the two concurrent oxidations: the oxidation of Fe(II) by oxygen and the oxidation of the organic matter by Fe(III).

References

1) Scott, R., Project Engineer, Federal Water Pollution Control Administration, Elkins, West Virginia, Personal Communication (1968)

2) Moebs, N. N., "Mine Air Sealing: A Progress Report," Proc. Second Symp. Coal Mine Drainage Res., Coal Industry Advisory Committee to ORSANCO, Pittsburgh, May, 1968

3) United States Public Health Service Drinking Water Standards, Publication No. 956, Washington (1962)

APPENDIX A

Correction of Experimental Solubility Data for Temperature and Activity

The experimental equilibrium relationship, given by equation (2-11a), is

$$\frac{[Fe^{+2}]\,[HCO_3^-]}{[H^+]} = K^c_{eq} = \frac{K^c_{so}}{K^c_2} \tag{A-1}$$

the superscript c referring to equilibrium constants at a given ionic strength. The corresponding thermodynamic equilibrium constant for the reaction, at 25°C and zero ionic strength is

$$\frac{(Fe^{+2})\,(HCO_3^-)}{(H^+)} = K_{eq} = \frac{K_{so}}{K_2} \tag{A-2}$$

The two equilibrium constants are related by the equation

$$\frac{K^c_{eq}\,\gamma_{Fe^{+2}}\,\gamma_{HCO_3^-}}{\gamma_{H^+}} = K_{eq} \tag{A-3}$$

where the γ's are single ion activity coefficients. Schindler (1) has suggested that for carbonates of bivalent metals in a constant ionic medium similar to 0.2M $NaClO_4$, the Davies equation

$$-\log \gamma = Az^2\left[\frac{\sqrt{I}}{1+\sqrt{I}} - 0.3I\right] \tag{A-4}$$

should be applied for the computation of activity coefficients. I is the ionic strength of the system, z is the charge of the specific ion under consideration, and A is a constant equal to 0.509 for water at 25°C.

Taking logarithms of equation A-3, one obtains

$$pK^{c}_{eq} - \log \gamma_{Fe^{+2}} - \log \gamma_{HCO_3^-} + \log \gamma_{H^+} = pK_{eq} \qquad \text{(A-5)}$$

where p- refers to the negative logarithm of that term. Substitution of the Davies equation into A-5 gives

$$pK^{c}_{eq} + 0.509 \left[\frac{\sqrt{I}}{1 + \sqrt{I}} - 0.3I \right] (z^2_{Fe^{+2}} + z^2_{HCO_3^-} - z^2_{H^+}) = pK_{eq} \qquad \text{(A-6)}$$

If the proper charges for the ionic species are used, the equation describing the experimental system at 0.1M $NaClO_4$ reduces to

$$pK^{c}_{eq} + 0.107\ (4 + 1 - 1) = pK_{eq} \qquad \text{(A-6a)}$$

or

$$pK^{c}_{eq} + 0.428 = pK_{eq} \qquad \text{(A-6b)}$$

Taking logarithms of the right-hand equality in equation A-2, one obtains

$$pK_{eq} = pK_{so} - pK_2 \qquad \text{(A-7)}$$

Substitution of this quantity into A-6b gives, after rearrangement

$$pK_{so} = pK^{c}_{eq} + 0.428 + pK_2 \qquad \text{(A-8)}$$

From the plot of p^cH versus $-\log[Fe^{+2}][HCO_3^-]$ in accordance with equation 2-12, the intercept at $p^cH = 0$ is equal to pK^{c}_{eq}. Figure 2-5 shows the desired intercept to be -0.57. In the determination of pK_2 as a function of temperature, by Harned and Scholes (2), it is found that, at 22.5°C, $pK_2 = 10.35$. Substitution into A-8 gives

$$pK_{so} = -0.57 + 0.43 + 10.35 \qquad \text{(A-8a)}$$

$$pK_{so} = 10.21 \qquad \text{at } 22.5^{\circ}C \qquad \text{(A-8b)}$$

or $$K_{so} = 6.1 \times 10^{-11}$$

The solubility product can readily be converted to 25°C utilizing the van't Hoff temperature relationship

$$\ln \frac{K_2}{K_1} = \frac{-\Delta H^{\circ}}{R} \left(\frac{T_1 - T_2}{T_1 T_2} \right) \qquad \text{(A-9)}$$

where K_2 and K_1 are the equilibrium constants at the absolute temperatures T_2 and T_1, respectively. R is the ideal gas constant, equal to 1.987 cal./mole-°K, and ΔH° is the change in enthalpy for reaction 2-4, equal to -4639 cal./mole at 25°C (3). (The literature value for ΔH° was employed since the experimental temperature-dependence was not sufficiently precise to extract a usable change in enthalpy for the reaction. Only three experimental points were available for such a calculation, giving $\Delta H^{\circ}_{experimental} = 1800 \pm 1200$ cal./mole.)

Substitution of these values into A-9 yields

$$K_{25^{\circ}C} = K_{22.5^{\circ}C}/1.068 \qquad \text{(A-9a)}$$

which, combined with A-8b, gives

$$K_{so} = 5.7 \times 10^{-11} \qquad \text{(A-10)}$$

$$pK_{so} = 10.24 \quad \text{at } 25^{\circ}C$$

the desired thermodynamic solubility product.

References

1) Schindler, P. W., "Heterogeneous Equilibria Involving Oxides, Hydroxides, Carbonates, and Hydroxide Carbonates," Ch. 9, p. 196 in Equilibrium Concepts in Natural Water Systems, R. F. Gould, ed., Advances in Chemistry Series 67, Amer. Chem. Soc., Washington (1967)

2) Harned, H. S., and Scholes, S. R., "The Ionization Constant of HCO_3^- from 0 to 50°," Journ. Amer. Chem. Soc., 63, 1706 (1941)

3) Latimer, W. E., The Oxidation States of the Elements and Their Potentials in Aqueous Solutions, 2nd ed., Prentice-Hall Inc., Englewood Cliffs, N.J., (1952)

APPENDIX B

Relative Significance of Soluble Phosphato-Complexes of Fe(III)

Consider the following equilibria, the equilibrium constants of which were taken from Stability Constants (1):

$$Fe^{+3} + H_2O = FeOH^{+2} + H^+ \qquad K_1 = 10^{-2.2} \qquad \text{(B-1)}$$

$$Fe^{+3} + 2H_2O = Fe(OH)_2^+ + 2H^+ \qquad K_1K_2 = 10^{-6.8} \qquad \text{(B-2)}$$

$$H^+ + HPO_4^{-2} = H_2PO_4^- \qquad K_{12} = 10^{7.2} \qquad \text{(B-3)}$$

$$Fe^{+3} + HPO_4^{-2} = FeHPO_4^+ \qquad \beta_1 = 10^{8.3} \qquad \text{(B-4)}$$

$$Fe^{+3} + H_2PO_4^- = FeH_2PO_4^{+2} \qquad \beta_2 = 10^{3.5} \qquad \text{(B-5)}$$

$$FeHPO_4^+ + H^+ = FeH_2PO_4^{+2} \qquad \frac{K_{12}\beta_2}{\beta_1} = 10^{2.4} \qquad \text{(B-6)}$$

$$FePO_{4(s)} = Fe^{+3} + PO_4^{-3} \qquad K_{so} = 10^{-24} \qquad \text{(B-7)}$$

Figures B-1 and B-2 show pH-log concentration diagrams for phosphate, and for Fe(III) in the absence of phosphate, respectively.

Using equation B-6

$$\frac{[FeH_2PO_4^{+2}]}{[FeHPO_4^+]} = [H^+]\, K_{12}\, \frac{\beta_2}{\beta_1} = 10^{2.4}[H^+] \qquad \text{(B-8)}$$

one sees that at pH-values greater than 2.4, $FeHPO_4^+$ is the predominant soluble phosphato-complex of Fe(III). The following relationships should also be noted:

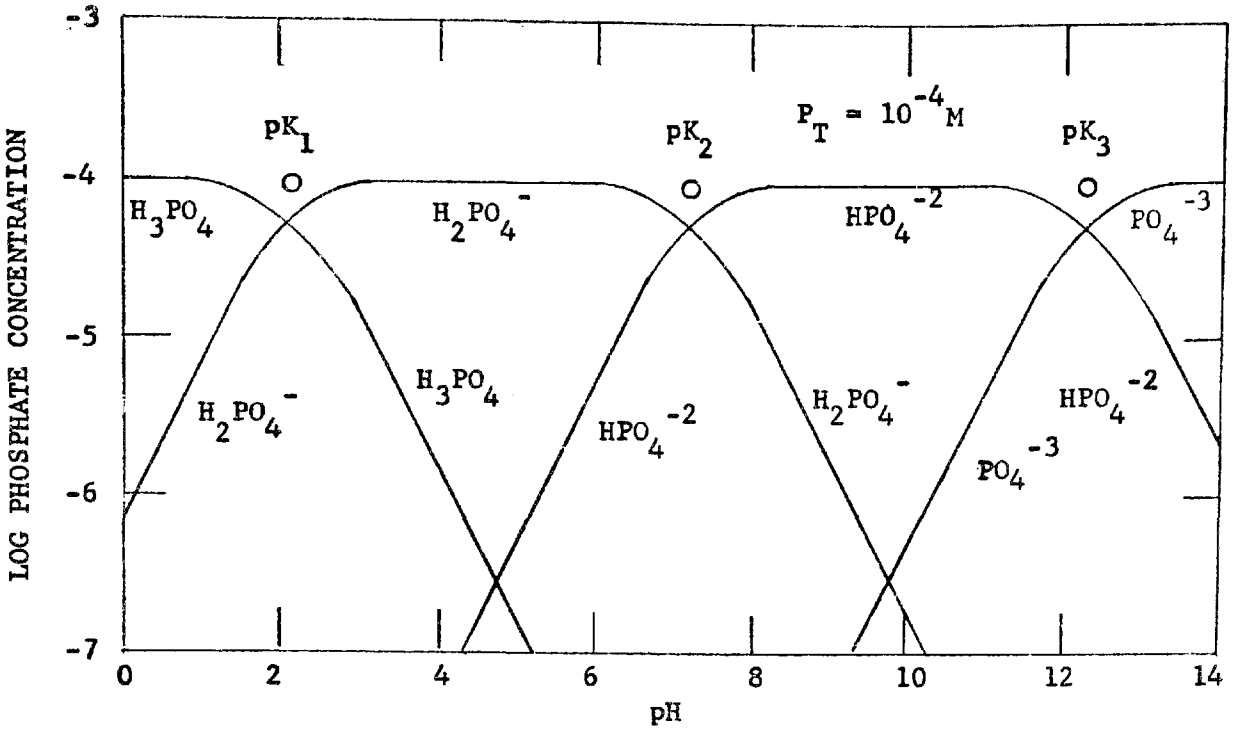

FIGURE B-1. Log concentration diagram for phosphoric acid.

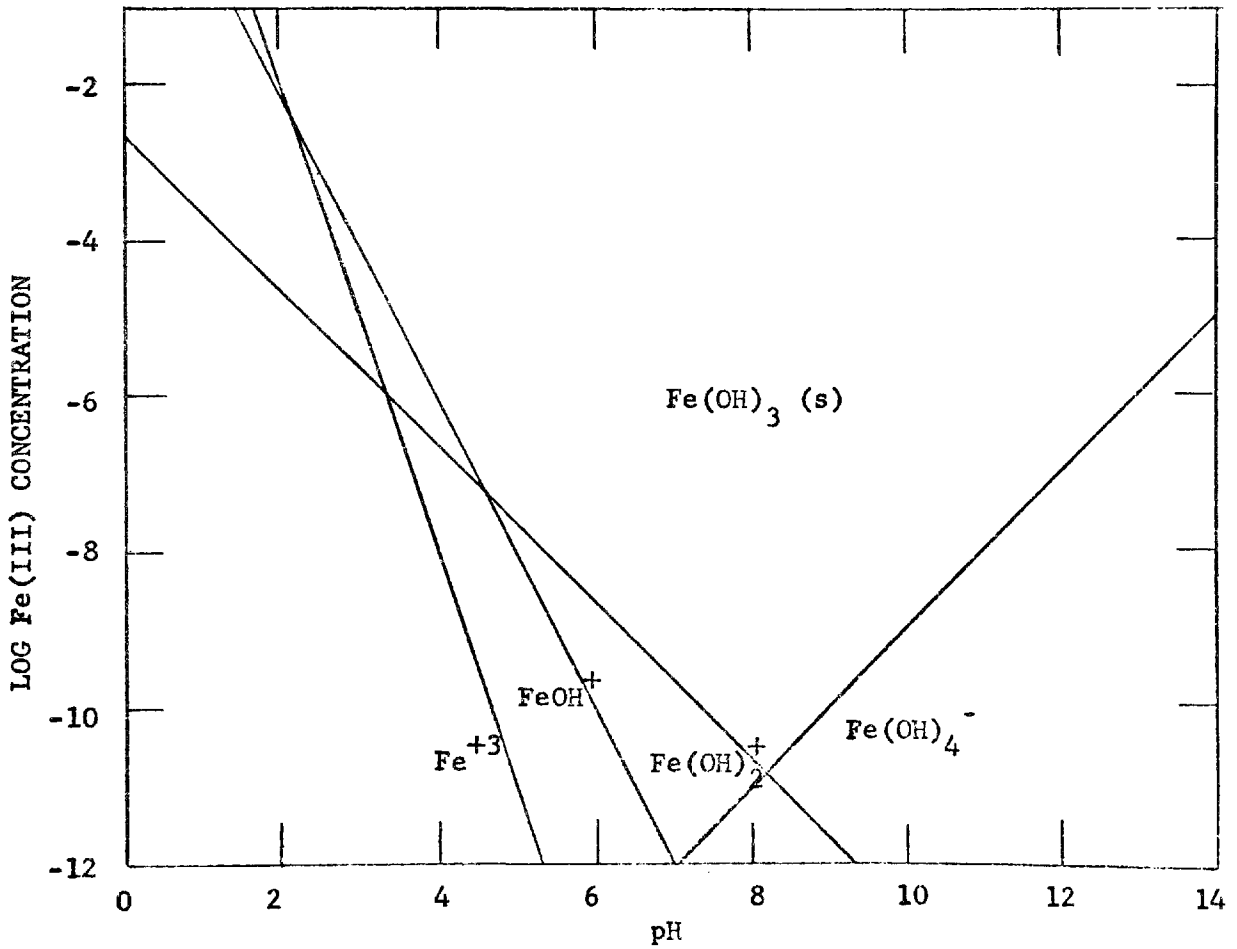

FIGURE B-2. Distribution diagram for soluble monomeric hydroxo-species of ferric iron.

A) At pH$>$ 5, $Fe(OH)_2^+$ is the predominant soluble species of Fe(III). Hence, by equation B-2,

$$\frac{[Fe(OH)_2^+]}{[Fe^{+3}]} = \frac{K_1K_2}{[H^+]^2} = \frac{10^{-6.8}}{[H^+]^2} \qquad \text{(B-9)}$$

B) In the pH-range 2.5 to 4.5, $FeOH^{+2}$ predominates. Using equation B-1,

$$\frac{[FeOH^{+2}]}{[Fe^{+3}]} = \frac{K_1}{[H^+]} = \frac{10^{-2.2}}{[H^+]} \qquad \text{(B-10)}$$

C) At pH$>$ 7.5, $[HPO_4^{-2}] \sim P_T$, the total concentration of dissolved phosphate. By equation B-4,

$$\frac{[FeHPO_4^{+2}]}{[Fe^{+3}]} = \beta_1 P_T = 10^{8.3} \times P_T \qquad \text{(B-11)}$$

D) In the pH-range 2 to 7, using equation B-3,

$$[HPO_4^{-2}] = \frac{P_T}{[H^+]K_{12}}, \quad \text{since } [H_2PO_4^-] \sim P_T. \qquad \text{(B-12)}$$

Hence, by equation B-4,

$$\frac{[FeHPO_4^{+2}]}{[Fe^{+3}]} = \frac{\beta_1 P_T}{[H^+]K_{12}} = 10^{1.1} \frac{P_T}{[H^+]} \qquad \text{(B-13)}$$

Making use of relationships (B-9) through (B-13), one can prepare the following table showing the relative abundance of the various soluble complex species (assuming $P_T = 10^{-4}$M):

pH	$\frac{[Fe(OH)_2^+]}{[Fe^{+3}]}$	$\frac{[FeOH^{+2}]}{[Fe^{+3}]}$	$\frac{[FeHPO_4^+]}{[Fe^{+3}]}$
8	$10^{9.2}$	--	$10^{4.3}$
7	$10^{7.2}$	--	$10^{4.1}$
6	$10^{5.2}$	--	$10^{3.1}$
5	$10^{3.2}$	$10^{2.6}$	$10^{2.1}$
4	$10^{1.2}$	$10^{1.6}$	$10^{1.1}$
3	--	$10^{0.6}$	$10^{0.1}$

It is, therefore, apparent that the known soluble phosphato-complexes of Fe(III) become influential only below pH 4, but to a very limited extent.

References

1) Sillén, L. G., and Martell, E. A., Stability Constants of Metal-Ion Complexes, Special Publication No.17, London, The Chemical Society (1964)

APPENDIX C

Derivation of Relations Between Redox Potential and Sulfate Concentration for Determination of Stability Constant for $FeSO_4^+$

The reactions pertaining to this study are

$$Fe^{+3} + SO_4^{-2} = FeSO_4^+ \qquad K_1 \qquad \text{(C-1)}$$

$$HSO_4^- = H^+ + SO_4^{-2} \qquad K_A \qquad \text{(C-2)}$$

$$Fe^{+3} + H_2O = FeOH^{+2} + H^+ \qquad Q_h \qquad \text{(C-3)}$$

In a system containing ferrous and ferric iron at 25°C and a constant ionic medium of 0.1M $NaClO_4$, the redox potential is defined by the Nernst Equation

$$E = E^o - 0.0592 \log \frac{[Fe^{+2}]}{[Fe^{+3}]} \qquad \text{(C-4)}$$

It will be convenient to refer to the system in the absence of sulfate as cell 1 so that

$$E_1 = E^o{}_1 - 0.0592 \log \frac{[Fe^{+2}]_1}{[Fe^{+3}]_1} \qquad \text{(C-5)}$$

If the pH is maintained below 3, the total concentration of ferric iron is given by

$$[Fe(III)_T]_1 = [Fe^{+3}]_1 + [FeOH^{+2}]_1 = [Fe^{+3}]_1\left(1 + \frac{Q_h}{[H^+]}\right) \qquad \text{(C-6)}$$

and that of ferrous iron is

$$[Fe(II)_T]_1 = [Fe^{+2}]_1 \qquad \text{(C-7)}$$

Upon addition of sulfate, let us refer to the system as cell 2, where

$$E_2 = E^\circ_2 - 0.0592 \log \frac{[Fe^{+2}]_2}{[Fe^{+3}]_2} \qquad (C\text{-}8)$$

In the presence of sulfate,

$$[Fe(III)_T]_2 = [Fe^{+3}]_2 + [FeOH^{+2}]_2 + [FeSO_4^{+}]_2 \qquad (C\text{-}9)$$

or, substituting equations C-1 and C-3,

$$[Fe(III)_T]_2 = [Fe^{+3}]_2(1 + \frac{Q_h}{[H^+]} + K_1[SO_4^{-2}]) \qquad (C\text{-}10)$$

where only the monosulfato-complex of Fe(III) is assumed, and

$$[Fe(II)_T]_2 = [Fe^{+2}]_2 \qquad (C\text{-}11)$$

Sulfate, however, reacts with water in the acidic pH-range, so that

$$[SO_4^{-2}]_{ADDED} = S_T = [SO_4^{-2}] + [HSO_4^{-}] + [FeSO_4^{+}] \qquad (C\text{-}12)$$

If it is assumed that $[FeSO_4^{+}] \ll [SO_4^{-2}] + [HSO_4^{-}]$, then, using C-2, equation C-12 becomes

$$S_T = [SO_4^{-2}](1 + \frac{[H^+]}{K_A}) \qquad (C\text{-}13)$$

Rearranging C-13

$$[SO_4^{-2}] = \frac{K_A S_T}{K_A + [H^+]} \qquad (C\text{-}13a)$$

and substituting into C-10, one obtains

$$[Fe(III)_T]_2 = [Fe^{+3}]_2(1 + \frac{Q_h}{[H^+]} + \frac{K_1 K_A S_T}{K_A + [H^+]}) \qquad (C\text{-}14)$$

The difference in potential between the cell before and after sulfate is added can be obtained by subtracting equation C-8 from C-5 to give

$$E_1 - E_2 = \bar{E} = 0.0592 \log \frac{[Fe^{+2}]_2[Fe^{+3}]_1}{[Fe^{+2}]_1[Fe^{+3}]_2} \qquad \text{(C-15)}$$

since the standard potentials are equal, i.e., $E^o_1 = E^o_2$. It is seen also in this step that the liquid junction potentials for the two cells cancel out. The experiment has been designed such that $[Fe^{+2}]_2 = [Fe^{+2}]_1$. Hence,

$$\bar{E} = 0.0592 \log \frac{[Fe^{+3}]_1}{[Fe^{+3}]_2} \qquad \text{(C-15a)}$$

or

$$\frac{[Fe^{+3}]_1}{[Fe^{+3}]_2} = \exp\left(\frac{2.3\bar{E}}{0.0592}\right) \qquad \text{(C-15b)}$$

Furthermore, by experimental design, $[Fe(III)_T]_1 = [Fe(III)_T]_2$ so that equation C-6 can be set equal to C-14,

$$[Fe^{+3}]_1\left(1 + \frac{Q_h}{[H^+]}\right) = [Fe^{+3}]_2\left(1 + \frac{Q_h}{[H^+]} + \frac{K_1K_AS_T}{K_A + [H^+]}\right) \qquad \text{(C-16)}$$

assuming the concentration of H^+ to remain constant with the addition of sulfate. Equation C-16 can be rearranged and set equal to C-15b so that

$$\frac{[Fe^{+3}]_1}{[Fe^{+3}]_2} = \frac{1 + \frac{Q_h}{[H^+]} + \frac{K_1K_AS_T}{K_A + [H^+]}}{1 + \frac{Q_h}{[H^+]}} = \exp\left(\frac{2.3\bar{E}}{0.0592}\right) \qquad \text{(C-17)}$$

Considering the equality on the right, after rearranging and simplifying, we obtain

$$\left[1 + \frac{Q_h}{[H^+]}\right] \exp\left(\frac{2.3\bar{E}}{0.0592}\right) - \left(1 + \frac{Q_h}{[H^+]}\right) = \frac{K_1 K_A S_T}{K_A + [H^+]} \qquad \text{(C-17a)}$$

$$\left[1 + \frac{Q_h}{[H^+]}\right]\left(\exp\left(\frac{2.3\bar{E}}{0.0592}\right) - 1\right) = \frac{K_1 K_A S_T}{K_A + [H^+]} \qquad \text{(C-17b)}$$

Equation C-17b is now in a usable form. If the potential and pH are measured as a function of the sulfate added, and it is known that $Q_h = 2.89 \times 10^{-3}$ at 25°C and 0.1M $NaClO_4$ (1), the left-hand side can be plotted against S_T, the slope of the resultant straight line being $\frac{K_1 K_A}{K_A + [H^+]}$. Knowing K_A, the second acidity constant of sulfuric acid, and the pH at which the study was conducted, one can compute the stability constant for the monosulfato-complex of Fe(III).

References

1) Milburn, R. M., "A Spectrophotometric Study of the Hydrolysis of Iron (III) Ion. III. Heats and Entropies of Hydrolysis," J. Amer. Soc., 79, 537 (1957)

APPENDIX D

Thermodynamic Stability of Iron Pyrite

The change in free energy for the oxidation of iron pyrite by oxygen, using the data available in Latimer (1), is

$$FeS_{2(s)} + \frac{7}{2}O_2 + H_2O = Fe^{+2} + 2SO_4^{-2} + 2H^+ \quad (D\text{-}1)$$

$$\Delta F^\circ \quad (-39.84) \quad \frac{7}{2}(0) \quad (-56.7) \quad (-20.3) \quad 2(-177.34) \quad 2(0)$$

$$\Sigma \Delta F^\circ = -278.4 \text{ kcal.}$$

The reaction should take place spontaneously, iron pyrite being thermodynamically unstable in the presence of oxygen.

References

1) Latimer, W. M., The Oxidation States of the Elements and Their Potentials in Aqueous Solutions, second ed., Prentice-Hall, Inc., Englewood Cliffs, New Jersey (1952)

APPENDIX E

Kinetics of Microbial Growth (1)

The change in concentration of microorganisms, B, with time is first-order in concentration of microorganisms,

$$\frac{dB}{dt} = \mu B \tag{E-1}$$

where μ is the specific growth-rate constant. For an enzymatic process, the growth-rate is given by the Michaelis-Menton equation,

$$\mu = \frac{\mu_{max} S}{K_m + S} \tag{E-2}$$

where S is the concentration of substrate (source of energy), μ_{max} is the maximum growth-rate, and K_m is the Michaelis-Menton constant. The change in concentration of microorganisms upon utilization of the substrate is

$$\frac{-dB}{dS} = Y \tag{E-3}$$

where Y is defined as the yield. Equations E-1, E-2, and E-3 can be combined to give the change in substrate with time as

$$\frac{-dS}{dt} = \frac{\mu_{max} S}{(K_m + S)\, Y} B \tag{E-4}$$

If the concentration of substrate is large compared to the Michaelis-Menton constant, i.e., if substrate is non-limiting, the specific growth-rate is constant and equal to the maximum growth-rate, so that E-4 simplifies to

$$\frac{-dS}{dt} = \frac{\mu_{max} B}{Y} \tag{E-5}$$

the number of the microorganisms increasing logarithmically in accordance with equation E-1. If B remains relatively constant during the course of the oxidation reaction, then

$$\frac{-dS}{dt} = \text{constant} \tag{E-6}$$

If, on the other hand, the concentration of microorganisms changes considerably, then equation E-1 can be integrated

$$\int_{B_o}^{B} \frac{dB}{B} = \mu \int_{o}^{t} dt \tag{E-7}$$

$$B = B_o e^{\mu t} \tag{E-8}$$

where B_o is the initial concentration of microorganisms at time zero. E-5 then becomes

$$\frac{-dS}{dt} = \frac{\mu_{max} B_o e^{\mu_{max} t}}{Y} \tag{E-9}$$

in the growth region where substrate is non-limiting. Integrating equation E-9, we get

$$\int_{S_o}^{S} dS = \frac{\mu_{max}}{Y} B_o \int_{o}^{t} e^{\mu_{max} t} dt \tag{E-10}$$

$$S_o - S = \frac{B_o}{Y} e^{\mu_{max} t} - \frac{B_o}{Y} = \frac{B_o}{Y} (e^{\mu_{max} t} - 1) \tag{E-11}$$

If $e^{\mu_{max} t}$ is much greater than unity, then

$$S_o - S = \frac{B_o}{Y} e^{\left(u_{max} t\right)} \qquad \text{(E-12)}$$

or, taking logarithms of both sides of the equation, one obtains

$$\log (S_o - S) = \log \frac{B_o}{Y} + \frac{u_{max} t}{2.3} \qquad \text{(E-13)}$$

These equations (E-6 and E-13) can now be used from a biological viewpoint as models to account for the fate of Fe(II) in natural waters.

References

1) Monod, J., Recherces sur la Croissance des Cultures Bacteriennes, Hermann and Cie, Paris (1942)

APPENDIX F

Autotrophic Iron Bacteria - Ratio of Ferrous Iron Oxidized to Organic Carbon Synthesized

The free energy released by the oxidation of ferrous iron, using the data available in Latimer (1), is

$$4\ Fe^{+2} + O_2 + 4\ H^+ = 4\ Fe^{+3} + 2\ H_2O \qquad \text{(F-1)}$$

ΔF° 4(-20.3) (0) 4(0) 4(-2.53) 2(-56.7)

$\sum \Delta F^\circ$ = -42.4 K cal. or

-10.6 K cal./mole of Fe(II) oxidized.

At pH 3, since

$$\Delta F = \Delta F^\circ + RT \ln Q \qquad \text{(F-2)}$$

where Q is the reaction quotient, the free energy released per mole is

$$\Delta F = -10.6 + 1.364 \log \frac{1}{10^{-3}} = -6.5 \text{ K cal./mole} \qquad \text{(F-2a)}$$

For synthesis of cell material from CO_2 (assuming the assimilated end product to be glucose), the free energy required is

$$6\ CO_2 + 6\ H_2O = C_6H_{12}O_6 + 6\ O_2 \qquad \text{(F-3)}$$

ΔF° 6(-92.3) 6(-56.7) (-217.0) 6(0)

$\sum \Delta F^\circ$ = + 677 K cal./mole of glucose or

+115 K cal./mole of carbon synthesized.

Assuming a 36% efficiency for microbial conversion of energy as is common in autotrophic processes (2), the stoichiometry of the

autotrophic oxidation of ferrous iron is

$$\frac{6.5 \text{ K cal./55.8 gms. Fe(II) oxidized}}{115 \text{ K cal./12 gms. carbon assimilated}} \times 0.36 = \frac{1}{250} \qquad \text{(F-4)}$$

Hence, one gram of organic carbon is synthesized for every 250 gms of Fe(II) oxidized.

If one considers the thermodynamic relationships in another way,

$$1 \text{ mole of Fe(II) oxidized} = \frac{6.5 \text{ K cal.}}{115 \text{ K cal./mole of carbon}} \times 0.36 \times \frac{12 \text{ gms}}{\text{mole of carbon}} \qquad \text{(F-5)}$$

$$= 0.25 \text{ gms of carbon synthesized}$$

Lamanna and Mallette (3) approximate that 1 gm. of bacteria contains 10^{12} to 10^{13} bacterial cells. Therefore, 1 mole of Fe(II) yields approximately 10^{12} bacterial cells or

$$Y = \frac{-dB}{dS} = 10^{12} \text{ cells/mole of Fe(II) oxidized} \qquad \text{(F-6)}$$

References

1) Latimer, W. M., The Oxidation States of the Elements and Their Potentials in Aqueous Solutions, second ed., Prentice-Hall, Inc., Englewood Cliffs, New Jersey (1952)

2) McCarty, P. L., "Thermodynamics of Biological Synthesis and Growth," in Advances in Water Pollution Research, J. K. Baars, ed., vol. 2, Pergamon Press, New York (1965)

3) Lamanna, C., and Mallette, M. F., Basic Bacteriology, third ed., The Williams and Wilkins Co., Baltimore (1965)